



**SEISMIC HAZARD ASSESSMENT AND  
SITE RESPONSE ANALYSIS  
PART 1: SEISMIC HAZARD ASSESSMENT AND  
GROUND MOTION DEVELOPMENT**

Doyle Drive Replacement Project  
San Francisco, California

*Submitted to:*

**ARUP PB Joint Venture, San Francisco, California**

*Submitted by:*

**AMEC Geomatrix, Inc., Oakland, California**

February 2010

Project 14450.000 Task 4



February 26, 2010

Project 14450.000

Mr. John E. Karn, Project Manager  
ARUP PB Joint Venture  
560 Mission Street, Suite 700  
San Francisco, CA 94105

**Subject: Final Report**  
**Seismic Hazard Assessment and Site Response Analysis**  
Doyle Drive Replacement Project  
San Francisco, California

Dear Mr. Karn:

Enclosed is the final report describing the results of the seismic hazard assessment and site response analysis performed for the Doyle Drive Replacement Project. The work was performed under Subconsultant Agreement No. 131558/17 between AMEC Geomatrix, Inc. (Subconsultant) and Arup PB Joint Venture dated September 29, 2008. The work was performed in accordance with the scope of work defined in the Subconsultant Agreement dated September 29, 2008. Site-specific seismic hazard assessment and development of the site-specific rock response spectra were performed by Dr. Norman Abrahamson, subconsultant to AMEC Geomatrix. Mr. Roupen Donikian of PB and Messrs. Francis R. Greguras and Terrence Carroll of Arup reviewed the draft version of the report and provided review comments. The report incorporated these review comments.

This report consists of following three parts:

PART 1: SEISMIC HAZARD ASSESSMENT AND GROUND MOTION DEVELOPMENT

PART 2: SITE RESPONSE ANALYSES

PART 3: FLING EFFECTS ON SOIL MOTIONS

We appreciate the opportunity to be of service to Arup PB Joint Venture, on this important project. If you have any questions on the report, please contact us.

Sincerely yours,  
AMEC Geomatrix, Inc.

Tawat Anantanavanich, PhD, PE  
Staff Engineer II

C.-Y. Chang, PhD, GE  
Principal Engineer

TA/CYC/LDU  
\\Oad-fs1\doc\_safe\14000s\14450.000\3000 REPORT\Doyle Drive\cvrltr, Cvrsl\Cover Letter\_022610.doc

Enclosure

AMEC Geomatrix, Inc.  
2101 Webster Street, 12th Floor  
Oakland, California  
USA 94612-3066  
Tel (510) 663-4100  
Fax (510) 663-4141  
www.amecgeomatrixinc.com

**AMEC Geomatrix**

## TABLE OF CONTENTS

		Page
1.0	INTRODUCTION .....	1
1.1	SCOPE OF WORK .....	1
1.2	PROJECT DESCRIPTION.....	2
1.3	REPORT ORGANIZATION.....	3
1.4	LIMITATIONS .....	3
2.0	SITE-SPECIFIC SEISMIC HAZARD ASSESSMENT .....	4
2.1	APPROACH FOR PROBABILISTIC GROUND MOTION ANALYSIS .....	4
2.2	ATTENUATION RELATIONSHIPS .....	5
2.3	RESULTS OF PROBABILISTIC SEISMIC HAZARDS ANALYSIS .....	6
2.4	DETERMINISTIC RESPONSE SPECTRA .....	7
2.5	SEE AND FEE RESPONSE SPECTRA .....	7
3.0	SELECTION OF SEED TIME HISTORIES.....	14
4.0	DEVELOPMENT OF SPECTRUM-COMPATIBLE TIME HISTORIES OF ROCK MOTION .....	15
4.1	SPECTRUM MATCHING PROCESS .....	15
4.2	ANALYSIS OF CHARACTERISTICS OF SPECTRUM-COMPATIBLE TIME HISTORY.....	15
5.0	MODIFICATION OF FAULT PARALLEL COMPONENTS OF THE SEE FOR FLING EFFECTS .....	18
5.1	GROUND MOTION DUE TO PERMANENT TECTONIC DEFORMATION .....	18
5.2	DEVELOPMENT OF FAULT-PARALLEL ACCELERATION TIME HISTORIES .....	19
	5.2.1 Input Parameters for SEE .....	19
	5.2.2 Method .....	20
	5.2.3 Results for SEE .....	20
6.0	REFERENCES .....	21

## LIST OF TABLES

Table 1:	Site-specific SEE Response Spectra (5% damping in g's) for Fault-normal (FN), Fault-parallel (FP), and Vertical (Z) Components for the Doyle Drive Replacement Project.....	8
Table 2:	Site-specific FEE Response Spectra (5% damping in g's) for Fault-normal (FN), Fault-parallel (FP), and Vertical (Z) Components for the Doyle Drive Replacement Project.....	9
Table 3:	Seed Time Histories for Spectral Matching.....	14
Table 4:	Summary of ground motion parameters of spectrum-compatible time histories, SEE and FEE criteria at $V_{S30} = 3000$ ft/sec .....	16
Table 5:	Summary of ground motion parameters of spectrum-compatible time histories, SEE and FEE criteria at $V_{S30} = 5000$ ft/sec .....	17
Table 6:	Recommended range of PGV (cm/sec) at $V_{S30} = 3000$ and 5000 ft/sec .....	17

**TABLE OF CONTENTS**  
(Continued)

**LIST OF FIGURES**

Figure 1: Acceleration Response Spectra (5 % Damping in g's) for SEE Scenario.....	10
Figure 2: Acceleration Response Spectra (5 % Damping in g's) for FEE Scenario.....	11
Figure 3: Displacement Response Spectra (5 % Damping in cm's) for SEE Scenario.....	12
Figure 4: Displacement Response Spectra (5 % Damping in cm's) for FEE Scenario.....	13
Figure 5: Acceleration and Displacement Response Spectra. Seed Motion: 1990 Manjil Earthquake, Abbar Station, T Component. Target: Fault Normal, SEE $V_{S30} = 3000$ ft/sec. ....	22
Figure 6: Acceleration, Velocity, and Displacement Time Histories. Seed Motion: 1990 Manjil Earthquake, Abbar Station, T Component. Target: Fault Normal, SEE $V_{S30} = 3000$ ft/sec. ....	23
Figure 7: Acceleration and Displacement Response Spectra. Seed Motion: 1990 Manjil Earthquake, Abbar Station, L Component. Target: Fault Parallel, SEE $V_{S30} = 3000$ ft/sec. ....	24
Figure 8: Acceleration, Velocity, and Displacement Time Histories. Seed Motion: 1990 Manjil Earthquake, Abbar Station, L Component. Target: Fault Parallel, SEE $V_{S30} = 3000$ ft/sec. ....	25
Figure 9: Acceleration and Displacement Response Spectra. Seed Motion: 1990 Manjil Earthquake, Abbar Station, Vertical Component. Target: Vertical, SEE $V_{S30} = 3000$ ft/sec. ....	26
Figure 10: Acceleration, Velocity, and Displacement Time Histories. Seed Motion: 1990 Manjil Earthquake, Abbar Station, Vertical Component. Target: Vertical, SEE $V_{S30} = 3000$ ft/sec. ....	27
Figure 11: Acceleration and Displacement Response Spectra. Seed Motion: 1999 Kocaeli Earthquake, Izmit Station, 90 degrees Component. Target: Fault Normal, SEE $V_{S30} = 3000$ ft/sec. ....	28
Figure 12: Acceleration, Velocity, and Displacement Time Histories. Seed Motion: 1999 Kocaeli Earthquake, Izmit Station, 90 degrees Component. Target: Fault Normal, SEE $V_{S30} = 3000$ ft/sec. ....	29
Figure 13: Acceleration and Displacement Response Spectra. Seed Motion: 1999 Kocaeli Earthquake, Izmit Station, 180 degrees Component. Target: Fault Parallel, SEE .	30
Figure 14: Acceleration, Velocity, and Displacement Time Histories. Seed Motion: 1999 Kocaeli Earthquake, Izmit Station, 180 degrees Component. Target: Fault Parallel, SEE $V_{S30} = 3000$ ft/sec. ....	31
Figure 15: Acceleration and Displacement Response Spectra. Seed Motion: 1999 Kocaeli Earthquake, Izmit Station, Vertical Component. Target: Vertical, SEE $V_{S30} = 3000$ ft/sec. ....	32
Figure 16: Acceleration, Velocity, and Displacement Time Histories. Seed Motion: 1999 Kocaeli Earthquake, Izmit Station, Vertical Component. Target: Vertical, SEE $V_{S30} = 3000$ ft/sec. ....	33
Figure 17: Acceleration and Displacement Response Spectra. Seed Motion: 1999 Chi-Chi Earthquake, TCU076 Station, W Component. Target: Fault Normal, SEE $V_{S30} = 3000$ ft/sec. ....	34

**TABLE OF CONTENTS**  
(Continued)

Figure 18: Acceleration, Velocity, and Displacement Time Histories. Seed Motion: 1999 Chi-Chi Earthquake, TCU076 Station, W Component. Target: Fault Normal, SEE  $V_{S30} = 3000$  ft/sec. .... 35

Figure 19: Acceleration and Displacement Response Spectra. Seed Motion: 1999 Chi-Chi Earthquake, TCU076 Station, N Component. Target: Fault Parallel, SEE  $V_{S30} = 3000$  ft/sec. .... 36

Figure 20: Acceleration, Velocity, and Displacement Time Histories. Seed Motion: 1999 Chi-Chi Earthquake, TCU076 Station, N Component. Target: Fault Parallel, SEE  $V_{S30} = 3000$  ft/sec. .... 37

Figure 21: Acceleration and Displacement Response Spectra. Seed Motion: 1999 Chi-Chi Earthquake, TCU076 Station, Vertical Component. Target: Vertical, SEE  $V_{S30} = 3000$  ft/sec. .... 38

Figure 22: Acceleration, Velocity, and Displacement Time Histories. Seed Motion: 1999 Chi-Chi Earthquake, TCU076 Station, Vertical Component. Target: Vertical, SEE  $V_{S30} = 3000$  ft/sec. .... 39

Figure 23: Acceleration and Displacement Response Spectra. Seed Motion: 1990 Manjil Earthquake, Abbar Station, T Component. Target: Fault Normal, SEE  $V_{S30} = 5000$  ft/sec. .... 40

Figure 24: Acceleration, Velocity, and Displacement Time Histories. Seed Motion: 1990 Manjil Earthquake, Abbar Station, T Component. Target: Fault Normal, SEE  $V_{S30} = 5000$  ft/sec. .... 41

Figure 25: Acceleration and Displacement Response Spectra. Seed Motion: 1990 Manjil Earthquake, Abbar Station, L Component. Target: Fault Parallel, SEE  $V_{S30} = 5000$  ft/sec. .... 42

Figure 26: Acceleration, Velocity, and Displacement Time Histories. Seed Motion: 1990 Manjil Earthquake, Abbar Station, L Component. Target: Fault Parallel, SEE  $V_{S30} = 5000$  ft/sec. .... 43

Figure 27: Acceleration and Displacement Response Spectra. Seed Motion: 1990 Manjil Earthquake, Abbar Station, Vertical Component. Target: Vertical, SEE  $V_{S30} = 5000$  ft/sec. .... 44

Figure 28: Acceleration, Velocity, and Displacement Time Histories. Seed Motion: 1990 Manjil Earthquake, Abbar Station, Vertical Component. Target: Vertical, SEE  $V_{S30} = 5000$  ft/sec. .... 45

Figure 29: Acceleration and Displacement Response Spectra. Seed Motion: 1999 Kocaeli Earthquake, Izmit Station, 90 degrees Component. Target: Fault Normal, SEE  $V_{S30} = 5000$  ft/sec. .... 46

Figure 30: Acceleration, Velocity, and Displacement Time Histories. Seed Motion: 1999 Kocaeli Earthquake, Izmit Station, 90 degrees Component. Target: Fault Normal, SEE  $V_{S30} = 5000$  ft/sec. .... 47

Figure 31: Acceleration and Displacement Response Spectra. Seed Motion: 1999 Kocaeli Earthquake, Izmit Station, 180 degrees Component. Target: Fault Parallel, SEE  $V_{S30} = 5000$  ft/sec. .... 48

Figure 32: Acceleration, Velocity, and Displacement Time Histories. Seed Motion: 1999 Kocaeli Earthquake, Izmit Station, 180 degrees Component. Target: Fault Parallel, SEE  $V_{S30} = 5000$  ft/sec. .... 49

**TABLE OF CONTENTS**  
(Continued)

Figure 33: Acceleration and Displacement Response Spectra. Seed Motion: 1999 Kocaeli Earthquake, Izmit Station, Vertical Component. Target: Vertical, SEE $V_{S30} = 5000$ ft/sec. ....	50
Figure 34: Acceleration, Velocity, and Displacement Time Histories. Seed Motion: 1999 Kocaeli Earthquake, Izmit Station, Vertical Component. Target: Vertical, SEE $V_{S30} = 5000$ ft/sec. ....	51
Figure 35: Acceleration and Displacement Response Spectra. Seed Motion: 1999 Chi-Chi Earthquake, TCU076 Station, W Component. Target: Fault Normal, SEE $V_{S30} = 5000$ ft/sec. ....	52
Figure 36: Acceleration, Velocity, and Displacement Time Histories. Seed Motion: 1999 Chi-Chi Earthquake, TCU076 Station, W Component. Target: Fault Normal, SEE $V_{S30} = 5000$ ft/sec. ....	53
Figure 37: Acceleration and Displacement Response Spectra. Seed Motion: 1999 Chi-Chi Earthquake, TCU076 Station, N Component. Target: Fault Parallel, SEE $V_{S30} = 5000$ ft/sec. ....	54
Figure 38: Acceleration, Velocity, and Displacement Time Histories. Seed Motion: 1999 Chi-Chi Earthquake, TCU076 Station, N Component. Target: Fault Parallel, SEE $V_{S30} = 5000$ ft/sec. ....	55
Figure 39: Acceleration and Displacement Response Spectra. Seed Motion: 1999 Chi-Chi Earthquake, TCU076 Station, Vertical Component. Target: Vertical, SEE $V_{S30} = 5000$ ft/sec. ....	56
Figure 40: Acceleration, Velocity, and Displacement Time Histories. Seed Motion: 1999 Chi-Chi Earthquake, TCU076 Station, Vertical Component. Target: Vertical, SEE $V_{S30} = 5000$ ft/sec. ....	57
Figure 41: Acceleration and Displacement Response Spectra. Seed Motion: 1999 Duzce Earthquake, Lamont Station, North Component. Target: Fault Normal, FEE $V_{S30} = 3000$ ft/sec. ....	58
Figure 42: Acceleration, Velocity, and Displacement Time Histories. Seed Motion: 1999 Duzce Earthquake, Lamont Station, <sup>North</sup> Component. Target: Fault Normal, FEE $V_{S30} = 3000$ ft/sec. ....	59
Figure 43: Acceleration and Displacement Response Spectra. Seed Motion: 1999 Duzce Earthquake, Lamont Station, East Component. Target: Fault Parallel, FEE $V_{S30} = 3000$ ft/sec. ....	60
Figure 44: Acceleration, Velocity, and Displacement Time Histories. Seed Motion: 1999 Duzce Earthquake, Lamont Station, East Component. Target: Fault Parallel, FEE $V_{S30} = 3000$ ft/sec. ....	61
Figure 45: Acceleration and Displacement Response Spectra. Seed Motion: 1999 Duzce Earthquake, Lamont Station, Vertical Component. Target: Vertical, FEE $V_{S30} = 3000$ ft/sec. ....	62
Figure 46: Acceleration, Velocity, and Displacement Time Histories. Seed Motion: 1999 Duzce Earthquake, Lamont Station, Vertical Component. Target: Vertical, FEE $V_{S30} = 3000$ ft/sec. ....	63
Figure 47: Acceleration and Displacement Response Spectra. Seed Motion: 1989 Loma Prieta Earthquake, Gilroy Array #6, 0 degrees Component. Target: Fault Normal, FEE $V_{S30} = 3000$ ft/sec. ....	64

**TABLE OF CONTENTS**  
(Continued)

Figure 48: Acceleration, Velocity, and Displacement Time Histories. Seed Motion: 1989 Loma Prieta Earthquake, Gilroy Array #6, 0 degrees Component. Target: Fault Normal, FEE  $V_{S30} = 3000$  ft/sec. .... 65

Figure 49: Acceleration and Displacement Response Spectra. Seed Motion: 1989 Loma Prieta Earthquake, Gilroy Array #6, 90 degrees Component. Target: Fault Parallel, FEE  $V_{S30} = 3000$  ft/sec. .... 66

Figure 50: Acceleration, Velocity, and Displacement Time Histories. Seed Motion: 1989 Loma Prieta Earthquake, Gilroy Array #6, 90 degrees Component. Target: Fault Parallel, FEE  $V_{S30} = 3000$  ft/sec. .... 67

Figure 51: Acceleration and Displacement Response Spectra. Seed Motion: 1989 Loma Prieta Earthquake, Gilroy Array #6, Vertical Component. Target: Vertical, FEE  $V_{S30} = 3000$  ft/sec. .... 68

Figure 52: Acceleration, Velocity, and Displacement Time Histories. Seed Motion: 1989 Loma Prieta Earthquake, Gilroy Array #6, Vertical Component. Target: Vertical, FEE  $V_{S30} = 3000$  ft/sec. .... 69

Figure 53: Acceleration and Displacement Response Spectra. Seed Motion: 1999 Hector Mine Earthquake, 90 degree Component. Target: Fault Normal, FEE  $V_{S30} = 3000$  ft/sec. .... 70

Figure 54: Acceleration, Velocity, and Displacement Time Histories. Seed Motion: 1999 Hector Mine Earthquake, 90 degree Component. Target: Fault Normal, FEE  $V_{S30} = 3000$  ft/sec. .... 71

Figure 55: Acceleration and Displacement Response Spectra. Seed Motion: 1999 Hector Mine Earthquake, 0 degree Component. Target: Fault Parallel, FEE  $V_{S30} = 3000$  ft/sec. .... 72

Figure 56: Acceleration, Velocity, and Displacement Time Histories. Seed Motion: 1999 Hector Mine Earthquake, 0 degree Component. Target: Fault Parallel, FEE  $V_{S30} = 3000$  ft/sec. .... 73

Figure 57: Acceleration and Displacement Response Spectra. Seed Motion: 1999 Hector Mine Earthquake, Vertical Component. Target: Vertical, FEE  $V_{S30} = 3000$  ft/sec. .... 74

Figure 58: Acceleration, Velocity, and Displacement Time Histories. Seed Motion: 1999 Hector Mine Earthquake, Vertical Component. Target: Vertical, FEE  $V_{S30} = 3000$  ft/sec. .... 75

Figure 59: Acceleration and Displacement Response Spectra. Seed Motion: 1999 Duzce Earthquake, Lamont Station, North Component. Target: Fault Normal, FEE  $V_{S30} = 5000$  ft/sec. .... 76

Figure 60: Acceleration, Velocity, and Displacement Time Histories. Seed Motion: 1999 Duzce Earthquake, Lamont Station, North Component. Target: Fault Normal, FEE  $V_{S30} = 5000$  ft/sec. .... 77

Figure 61: Acceleration and Displacement Response Spectra. Seed Motion: 1999 Duzce Earthquake, Lamont Station, East Component. Target: Fault Parallel, FEE  $V_{S30} = 5000$  ft/sec. .... 78

Figure 62: Acceleration, Velocity, and Displacement Time Histories. Seed Motion: 1999 Duzce Earthquake, Lamont Station, East Component. Target: Fault Parallel, FEE  $V_{S30} = 5000$  ft/sec. .... 79

Figure 63: Acceleration and Displacement Response Spectra. Seed Motion: 1999 Duzce Earthquake, Lamont Station, Vertical Component. Target: Vertical, FEE  $V_{S30} = 5000$  ft/sec. .... 80

**TABLE OF CONTENTS**  
(Continued)

Figure 64: Acceleration, Velocity, and Displacement Time Histories. Seed Motion: 1999 Duzce Earthquake, Lamont Station, Vertical Component. Target: Vertical, FEE  $V_{S30} = 5000$  ft/sec. .... 81

Figure 65: Acceleration and Displacement Response Spectra. Seed Motion: 1989 Loma Prieta Earthquake, Gilroy Array #6, 0 degrees Component. Target: Fault Normal, FEE  $V_{S30} = 5000$  ft/sec. .... 82

Figure 66: Acceleration, Velocity, and Displacement Time Histories. Seed Motion: 1989 Loma Prieta Earthquake, Gilroy Array #6, 0 degrees Component. Target: Fault Normal, FEE  $V_{S30} = 5000$  ft/sec. .... 83

Figure 67: Acceleration and Displacement Response Spectra. Seed Motion: 1989 Loma Prieta Earthquake, Gilroy Array #6, 90 degrees Component. Target: Fault Parallel, FEE  $V_{S30} = 5000$  ft/sec. .... 84

Figure 68: Acceleration, Velocity, and Displacement Time Histories. Seed Motion: 1989 Loma Prieta Earthquake, Gilroy Array #6, 90 degrees Component. Target: Fault Parallel, FEE  $V_{S30} = 5000$  ft/sec. .... 85

Figure 69: Acceleration and Displacement Response Spectra. Seed Motion: 1989 Loma Prieta Earthquake, Gilroy Array #6, Vertical Component. Target: Vertical, FEE  $V_{S30} = 5000$  ft/sec. .... 86

Figure 70: Acceleration, Velocity, and Displacement Time Histories. Seed Motion: 1989 Loma Prieta Earthquake, Gilroy Array #6, Vertical Component. Target: Vertical, FEE  $V_{S30} = 5000$  ft/sec. .... 87

Figure 71: Acceleration and Displacement Response Spectra. Seed Motion: 1999 Hector Mine Earthquake, 90 degree Component. Target: Fault Normal, FEE  $V_{S30} = 5000$  ft/sec. .... 88

Figure 72: Acceleration, Velocity, and Displacement Time Histories. Seed Motion: 1999 Hector Mine Earthquake, 90 degree Component. Target: Fault Normal, FEE  $V_{S30} = 5000$  ft/sec. .... 89

Figure 73: Acceleration and Displacement Response Spectra. Seed Motion: 1999 Hector Mine Earthquake, 0 degree Component. Target: Fault Parallel, FEE  $V_{S30} = 5000$  ft/sec. .... 90

Figure 74: Acceleration, Velocity, and Displacement Time Histories. Seed Motion: 1999 Hector Mine Earthquake, 0 degree Component. Target: Fault Parallel, FEE  $V_{S30} = 5000$  ft/sec. .... 91

Figure 75: Acceleration and Displacement Response Spectra. Seed Motion: 1999 Hector Mine Earthquake, Vertical Component. Target: Vertical, FEE  $V_{S30} = 5000$  ft/sec. .... 92

Figure 76: Acceleration, Velocity, and Displacement Time Histories. Seed Motion: 1999 Hector Mine Earthquake, Vertical Component. Target: Vertical, FEE  $V_{S30} = 5000$  ft/sec. .... 93

Figure 77: Attenuation relationship of fling displacement with distance (normalized by the estimated fault displacement) used in the present study. .... 94

Figure 78: Fling period as a function of magnitude (revised Figure 6-9 of Abrahamson, 2001). .... 95

Figure 79: Deaggregation for 1,000 year return period: PGA. .... 96

Figure 80: Deaggregation for 1,000 year return period: T- 1sec. .... 97

Figure 81: Fault parallel time histories and fling time histories, 1990 Manjil Earthquake, SEE scenario,  $V_{S30} = 3000$  ft/sec. .... 98

Figure 82: Fault parallel time histories including fling, 1990 Manjil Earthquake, SEE scenario,  $V_{S30} = 3000$  ft/sec. .... 99

**TABLE OF CONTENTS**  
(Continued)

Figure 83: Comparison of acceleration and displacement response spectra between the original and modified (with fling) time histories, 1990 Manjil Earthquake, SEE scenario, $V_{S30} = 3000$ ft/sec. ....	100
Figure 84: Fault parallel time histories and fling time histories, 1999 Kocaeli Earthquake, SEE scenario, $V_{S30} = 3000$ ft/sec. ....	101
Figure 85: Fault parallel time histories including fling, 1999 Kocaeli Earthquake, SEE scenario, $V_{S30} = 3000$ ft/sec. ....	102
Figure 86: Comparison of acceleration and displacement response spectra between the original and modified (with fling) time histories, 1999 Kocaeli Earthquake, SEE scenario, $V_{S30} = 3000$ ft/sec. ....	103
Figure 87: Fault parallel time histories and fling time histories, 1999 Chi-Chi Earthquake, SEE scenario, $V_{S30} = 3000$ ft/sec. ....	104
Figure 88: Fault parallel time histories including fling, 1999 Chi-Chi Earthquake, SEE scenario, $V_{S30} = 3000$ ft/sec. ....	105
Figure 89: Comparison of acceleration and displacement response spectra between the original and modified (with fling) time histories, 1999 Chi-Chi Earthquake, SEE scenario, $V_{S30} = 3000$ ft/sec. ....	106
Figure 90: Fault parallel time histories and fling time histories, 1990 Manjil Earthquake, SEE scenario, $V_{S30} = 5000$ ft/sec. ....	107
Figure 91: Fault parallel time histories including fling, 1990 Manjil Earthquake, SEE scenario, $V_{S30} = 5000$ ft/sec. ....	108
Figure 92: Comparison of acceleration and displacement response spectra between the original and modified (with fling) time histories, 1990 Manjil Earthquake, SEE scenario, $V_{S30} = 5000$ ft/sec. ....	109
Figure 93: Fault parallel time histories and fling time histories, 1999 Kocaeli Earthquake, SEE scenario, $V_{S30} = 5000$ ft/sec. ....	110
Figure 94: Fault parallel time histories including fling, 1999 Kocaeli Earthquake, SEE scenario, $V_{S30} = 5000$ ft/sec. ....	111
Figure 95: Comparison of acceleration and displacement response spectra between the original and modified (with fling) time histories, 1999 Kocaeli Earthquake, SEE scenario, $V_{S30} = 5000$ ft/sec. ....	112
Figure 96: Fault parallel time histories and fling time histories, 1999 Chi-Chi Earthquake, SEE scenario, $V_{S30} = 5000$ ft/sec. ....	113
Figure 97: Fault parallel time histories including fling, 1999 Chi-Chi Earthquake, SEE scenario, $V_{S30} = 5000$ ft/sec. ....	114
Figure 98: Comparison of acceleration and displacement response spectra between the original and modified (with fling) time histories, 1999 Chi-Chi Earthquake, SEE scenario, $V_{S30} = 5000$ ft/sec. ....	115

**APPENDIX**

Appendix A Ground Motions for the Doyle Drive Replacement Project By Norman A. Abrahamson, Inc.

## **PART 1: SEISMIC HAZARD ASSESSMENT AND GROUND MOTION DEVELOPMENT**

Doyle Drive Replacement Project  
San Francisco, California

### **1.0 INTRODUCTION**

AMEC Geomatrix, Inc. (AMEC) prepared this ground motion study for the Doyle Drive Replacement Project, located in San Francisco, California. This report summarizes the development of the rock design response spectra, spectrum-compatible time histories, site response analyses and strain-compatible soil model parameters required for the seismic evaluation of the project site. This study was conducted in accordance with Subconsultant Agreement No. 131558/17 authorized by the Arup PB Joint Venture under the prime agreement No. 06/07-29.

The seismic evaluations were conducted for three structures along the project alignment, including the Main Post Tunnels, the Battery Tunnels, and the Lincoln Retaining Wall No. 8. The results of the seismic evaluations also may be appropriate for use for other structures along the project alignment as described in this report.

### **1.1 SCOPE OF WORK**

The scope of work for this study includes the following tasks:

1. Conduct site-specific probabilistic and deterministic seismic hazard analyses;
2. Develop rock design ground motion corresponding to the Safety Evaluation Earthquake (SEE) and the Functional Evaluation Earthquake (FEE), including modification for near field effects;
3. Select seed time histories appropriate for the SEE and FEE;
4. Develop three sets of three-component spectrally matched time histories each for the SEE and FEE;
5. Evaluate effects of permanent ground deformation on SEE response spectra, and adjust fault-parallel SEE time histories for this permanent deformation (fault fling effects);
6. Conduct site response analyses to provide free-field interface rock motions and develop average strain-compatible dynamic soil properties for use in dynamic soil-structure interaction analyses;
7. Incorporate fling effects in soil response motions; and
8. Prepare report documenting approach, methodology, and results of evaluations.

The work was performed by AMEC-Geomatrix, Inc. in association with Norman A. Abrahamson, Inc. (AMEC subconsultant). The site-specific probabilistic and deterministic seismic hazard assessment was performed by Dr. Norm Abrahamson working in conjunction with AMEC Geomatrix. The results of the assessment by Dr. Abrahamson are presented in Appendix A. The spectral matching for the time histories and the modification of the time histories and response spectra for fault fling effects were performed by AMEC Geomatrix. Dr. Abrahamson recommended the seed time histories (see Appendix A) used in the development of the spectrum-compatible rock motions and also reviewed the spectrum-compatible time histories including the incorporation of the fling effects. This report presents Part 1: Seismic Hazard Assessment and Ground Motion Development and documents Items 1 to 5 of the study. The site response analyses and modification of the soil response motions for fault fling effects (Tasks 6 and 7 above) are presented in separate reports (Part 2: Site Response Analysis; Part 3: Fling Effects on Soil Motions).

## **1.2 PROJECT DESCRIPTION**

Doyle Drive, or Route 101, serves as the south access to the Golden Gate Bridge from the Marina District of San Francisco. Winding 1.5 miles along the northern edge of San Francisco, the roadway is the primary highway and transit linkage through San Francisco, between counties to the south (San Mateo and Santa Clara) and to the north (Marin and Sonoma). The project area extends from the Golden Gate Bridge Toll Plaza southeast to Broderick Street. The existing Doyle Drive is considered structurally and seismically unsafe and is scheduled to be replaced. The Presidio Parkway was unanimously identified as the Preferred Alternative for the Doyle Drive replacement from the project Environmental Impact Report/Statement (EIR/EIS) Process. The Presidio Parkway is a world-class design to replace the existing roadway that, when constructed, will improve the seismic, structural and traffic safety of Doyle Drive.

The Doyle Drive replacement project includes several structures that are being redesigned at present. Specific structures identified by Arup PB JV and Caltrans that may need information from this study for design purposes are as follows:

- Main Post Tunnels: approximately 1,000 ft long;
- Battery Tunnels: approximately 850 ft long;
- Retaining Wall No. 8 (non-standard): approximately 1,200 ft long;
- Highway 1 (Ruckman/Storey): approximately 450 ft long;
- High Viaduct: approximately 1,300 ft long;

- Tennessee Hollow: approximately 400 ft long;
- Girard NB Ramp: approximately 400 ft long; and
- Gorgas Ramp: approximately 250 ft long.

This ground motion study was performed using a single site location near the middle of the project alignment and based on representative shear wave velocities for the subsurface rock conditions identified along the extent of the project. The shear wave velocities, represented as  $V_{S30}$  (the average shear wave velocity in the upper 30 meters [ $\sim 100$  feet]), identified by the project team as appropriate to use for rock outcrop site conditions are equal to 3,000 feet per second (ft/sec) and 5,000 ft/sec. The response spectra (either for 3,000 or 5,000 ft/sec) to be used for design of a specific structure should be selected based on the site conditions for that structure. In addition, depending on the nature of the soil and rock conditions at the specific location of the structures noted above, it may be necessary to further modify the response spectra or to conduct site response analysis to represent the ground motion input for the structure.

### **1.3 REPORT ORGANIZATION**

The site specific ground motion hazard analysis and selection of design response spectra are described in Section 2. The selection of seed time histories is described in Section 3 and the development of spectrally matched time histories is described in Section 4. The modification of the time histories/response spectra for fault fling effects is described in Section 5. References are presented in Section 6.

### **1.4 LIMITATIONS**

In the performance of our professional services, AMEC Geomatrix, its employees, and its agents comply with the standards of care and skill ordinarily exercised by members of our profession practicing in the same or similar localities. No warranty, either express or implied, is made or intended in connection with the work performed by us, or by the proposal for consulting or other services, or by the furnishing of oral or written reports or findings. We are responsible for the conclusions contained in this report, which are based on data and information related only to the specific project and locations discussed herein. In the event others make conclusions or our recommendations based on these conclusions, such conclusions and recommendations are not our responsibility unless we have been given an opportunity to review and concur with such conclusions or recommendations in writing.

## 2.0 SITE-SPECIFIC SEISMIC HAZARD ASSESSMENT

Both a probabilistic seismic hazard analysis (PSHA) and a deterministic seismic hazard analysis (DSHA) were performed to characterize earthquake ground shaking that may occur at the project sites during future seismic events in the region. The PSHA and DSHA were conducted by Dr. Abrahamson using his seismic hazard codes (software programs). The PSHA was conducted to estimate the probability of exceedance of peak ground acceleration (PGA) and response spectral accelerations ( $S_a$ ) at the site during selected exposure times. The DSHA was conducted to estimate the largest ground motion response that would result from a maximum earthquake on any active fault source near the project sites. The response spectra were then modified to include near-field effects, including rupture directivity and the directional nature of the shaking intensity of ground motion (i.e. the fault-normal (FN) and fault-parallel (FP) effects).

The site-specific seismic hazard analysis was performed to develop the design response spectra that represent two earthquake scenarios; Safety Evaluation Earthquake (SEE) and Functional Evaluation Earthquake (FEE) based on the Caltrans criteria. The SEE is defined as the larger of either the median (50th percentile) ground motion from the maximum credible earthquake (DSHA) or the ground motion with a 1000-year return period (PSHA). The FEE is defined as the ground motion with a 50 percent probability of exceedance in 50 years, or alternatively, the ground motion with a return period of 108 years (PSHA).

### 2.1 APPROACH FOR PROBABILISTIC GROUND MOTION ANALYSIS

The probabilistic seismic hazard analysis, commonly termed PSHA, is based on an assessment of the recurrence of earthquakes on potential seismic sources in the greater San Francisco Bay region and on ground motion attenuation relationships appropriate for the types of seismic sources in the region and the subsurface conditions interpreted for the project site. Results of the hazard analysis are expressed as relationships between amplitudes of peak ground acceleration and spectral acceleration, and the annual frequencies or return periods (return period being the reciprocal of annual frequency) for exceeding those ground motion amplitudes.

The PSHA analysis procedure requires the specification of probability functions to describe the uncertainty in both the time and location of future earthquakes and the uncertainty in the ground motion level that will be produced at the project site. The basic elements of the analysis are:

- identification of potential (active) seismic sources that could significantly contribute to seismic hazard at the project site;

- specification of an earthquake recurrence relationship for each seismic source, defining the frequency of occurrence of various magnitude earthquakes up to the maximum magnitude possible on the source;
- specification of attenuation relationships defining ground motion levels as a function of earthquake magnitude and distance from an earthquake rupture; and
- calculation of the probability of exceedance of peak ground acceleration and spectral accelerations (i.e., seismic hazard) using inputs from the elements above, and development of equal-hazard (i.e., equal-probability-of-exceedance) response spectra from the results.

The probabilistic seismic hazard analysis conducted for this study is based on the seismic source model and earthquake probabilities developed by the U.S. Geological Survey Working Group on California Earthquake Probabilities (WGCEP, 2003; referred to as WG03). The recently completed California-wide assessment of earthquake probabilities (WGCEP, 2008) includes an update to the results of the WG03 study, but this update does not identify any significant new information regarding major faults in the San Francisco Bay Area, and does not include the more comprehensive assessment of real-time probability models incorporated in the WG03 study. Therefore, as described in Appendix A, this study uses the more comprehensive model developed by the WG03 as a basis for the PSHA. The major fault sources that could cause large earthquakes and strong ground shaking at the project sites include the San Gregorio, San Andreas, and Hayward faults as shown in Figure 2-1 of Appendix A.

## **2.2 ATTENUATION RELATIONSHIPS**

A ground motion attenuation model relates the amplitudes of peak acceleration and response spectral acceleration to earthquake magnitude and source-to-site distance. Past studies of strong-motion data indicate that the ground motions from various types of earthquake sources considered in this analysis exhibit different characteristics in terms of the scaling of ground motion amplitudes with magnitude, source-to-site distance, and period of vibration. In addition, different attenuation models are required for different types of seismic sources.

For each seismic source, alternative ground motion attenuation relationships were utilized. The uncertainty in the predicted value of a ground motion parameter for each attenuation relationship was modeled by assigning a statistical distribution around the median value in accordance with values given by the authors of the respective attenuation relationships used in this study.

The ground motion attenuation relationships selected for use in this analysis are those developed for Pacific Earthquake Engineering Research Center (PEER) Next Generation

Attenuation (NGA) project. The ground motion models provide estimates of spectral accelerations in the period range of 0.01 seconds to 10 seconds (spectral frequencies of 0.1 to 100 Hz), representing the randomly oriented average horizontal component of ground motions. Four of the models provide ground motion estimates as a function of the average shear wave velocity of the top 30 meters of the site,  $V_{S30}$ . The selection and weighting of the attenuation relationships is described in detail in Appendix A. Two cases relating to shear wave velocities ( $V_{S30}$ ) of 3,000 ft/sec and 5,000 ft/sec were used to compute rock motions so as to represent different rock conditions along the corridor.

### 2.3 RESULTS OF PROBABILISTIC SEISMIC HAZARDS ANALYSIS

The basic results of the PSHA are presented in terms of annual frequency of exceedance versus spectral acceleration (commonly referred to as hazard curves). The PSHA results were computed for a single site location (122.462W, 37.801N) and two  $V_{S30}$  values, viz. 3000 feet/sec and 5000 feet/sec, and are shown in Appendix A. As described in Appendix A, the San Andreas fault is the dominant contributor to the hazard for return periods greater than 200 years and the Hayward fault is the dominant contributor to hazard for return periods less than 200 years.

Having obtained the annual frequency of exceedance of a certain level of horizontal response spectral acceleration, the probability of exceeding that level within any time period of interest is then obtained assuming a Poisson distribution, as follows:

$$p_e = 1 - \exp(-\mu t) \quad (2-1)$$

in which " $p_e$ " is the probability of exceedance, " $\mu$ " is the annual frequency of events that exceed that level of ground motion, and " $t$ " is the specified time period of interest.

For this study, we provide five-percent damped horizontal equal hazard response spectra corresponding to return periods of 108 and 1000 years. Deaggregation of the seismic hazard shows the contribution of earthquakes in different magnitude and distance ranges to the spectral acceleration, for the selected return periods of 108 and 1000 years. As shown in Appendix A, the dominant contribution to the ground motion hazard results from large magnitude (M6+) earthquakes occurring at distances of 5 to 20 km from the project site for the 1000 year return period, and occurring at distances of 5 to 50 km from the project site for the 108 year return period. These probabilistic equal hazard response spectra are modified for near-field fault rupture effects (directivity and fault normal/parallel effects) using the methodology of Somerville et al. (1997) and modified by Abrahamson (2000) as described in Appendix A.

## 2.4 DETERMINISTIC RESPONSE SPECTRA

Median deterministic response spectra are developed for maximum earthquakes occurring on various sources that contributed significantly to the total hazard for the PSHA, as well as for sources located near the project site. We considered maximum earthquake scenarios for the San Andreas, San Gregorio, and the Hayward-Rodgers Creek fault zones, which represent the largest contributions to the ground motion hazard in the PSHA (Appendix A). The deterministic spectra were developed using the same weighted attenuation relationships used for the probabilistic analysis.

Based on comparison of median deterministic results for a  $M_W$  8 earthquake on the San Andreas fault, a  $M_W$  7.3 earthquake on the Hayward-Rodgers Creek fault, and a  $M_W$  7.4 earthquake on the San Gregorio fault, and based on the closest distance of the project site to these faults, the strongest ground motions at the site result from the  $M_W$  8.0 earthquake occurring on the San Andreas fault. Therefore, the deterministic spectra are based on the maximum expected earthquake for the San Andreas fault ( $M_W$  8.0 at a distance of 9.1 km) (Table 4.1 of Appendix A). The deterministic response spectra are modified for near-field fault rupture effects (fault normal/parallel effects) as described in Appendix A.

## 2.5 SEE AND FEE RESPONSE SPECTRA

The SEE is defined as the larger of either the median (50th percentile) ground motion from the maximum credible earthquake (DSHA) or the ground motion with a 1000-year return period (PSHA). The comparison of these spectra shown in Appendix A indicates that 1000-year uniform hazard spectra (UHS) exceed the deterministic spectra at all periods. The deaggregation shows that the earthquake magnitude corresponding to the SEE varies as follows:  $M_W$  7.4 at short periods (less than 0.5 second),  $M_W$  7.5 for intermediate periods (between 0.75 seconds and 3 seconds), and  $M_W$  7.6 at long periods (greater than 4 seconds).

The FEE is defined as the ground motion with a return period of 108 years (PSHA). The deaggregation shows that the earthquake magnitude corresponding to the FEE varies from  $M_W$  6.9 at short periods (less than 0.2 second) to  $M_W$  7.1 at long periods (greater than 1 second).

Vertical response spectra were developed for the SEE and FEE by applying a vertical to horizontal spectra ratio to the horizontal spectra. The ratios were estimated for the ground motions corresponding to the dominant magnitude and distance contribution to the SEE and FEE.

Figure 1 and Figure 2 show the computed acceleration response spectra (5% damping), respectively, for the SEE and the FEE. Figure 3 and Figure 4 show the corresponding

displacement response spectra (5% damping), respectively, for the SEE and the FEE. The horizontal components (fault-normal and fault-parallel) and the vertical component response spectra for the SEE scenario, for the two  $V_{S30}$  cases, are listed in Table 1. Spectra for the FEE scenario are listed in Table 2. The results shown in Tables 1 and 2 are appropriate for use at all locations considered in this study.

**Table 1: Site-specific SEE Response Spectra (5% damping in g's) for Fault-normal (FN), Fault-parallel (FP), and Vertical (Z) Components for the Doyle Drive Replacement Project**

Period	SEE Spectra ( $V_{S30} = 3000$ ft/sec)			SEE Spectra ( $V_{S30} = 5000$ ft/sec)		
	FN	FP	Z	FN	FP	Z
0.01	0.462	0.462	0.403	0.421	0.421	0.367
0.02	0.473	0.473	0.412	0.435	0.435	0.379
0.03	0.512	0.512	0.509	0.476	0.476	0.473
0.05	0.614	0.614	0.712	0.577	0.577	0.669
0.075	0.778	0.778	0.904	0.732	0.732	0.849
0.1	0.931	0.931	0.945	0.875	0.875	0.888
0.12	1.000	1.000	0.900	0.935	0.935	0.842
0.15	1.090	1.090	0.839	1.014	1.014	0.780
0.17	1.100	1.100	0.765	1.018	1.018	0.708
0.2	1.110	1.110	0.683	1.021	1.021	0.628
0.24	1.069	1.069	0.599	0.983	0.983	0.551
0.3	0.989	0.989	0.504	0.910	0.910	0.463
0.4	0.858	0.858	0.411	0.790	0.790	0.378
0.5	0.739	0.739	0.346	0.680	0.680	0.318
0.75	0.554	0.542	0.266	0.510	0.498	0.245
1	0.449	0.428	0.217	0.413	0.393	0.200
1.5	0.328	0.295	0.160	0.301	0.272	0.147
2	0.253	0.210	0.124	0.232	0.192	0.114
3	0.175	0.126	0.087	0.158	0.113	0.078
4	0.137	0.088	0.067	0.121	0.078	0.059
5	0.109	0.067	0.054	0.096	0.059	0.047
6	0.084	0.053	0.044	0.074	0.047	0.039
7.5	0.055	0.040	0.035	0.048	0.035	0.031
10	0.028	0.024	0.024	0.024	0.021	0.021

**Table 2: Site-specific FEE Response Spectra (5% damping in g's) for Fault-normal (FN), Fault-parallel (FP), and Vertical (Z) Components for the Doyle Drive Replacement Project.**

Period	FEE Spectra ( $V_{S30} = 3000$ ft/sec)			FEE Spectra ( $V_{S30} = 5000$ ft/sec)		
	FN	FP	Z	FN	FP	Z
0.01	0.172	0.172	0.127	0.156	0.156	0.115
0.02	0.175	0.175	0.129	0.161	0.161	0.119
0.03	0.187	0.187	0.151	0.173	0.173	0.140
0.05	0.222	0.222	0.198	0.207	0.207	0.184
0.075	0.285	0.285	0.254	0.265	0.265	0.236
0.1	0.336	0.336	0.270	0.312	0.312	0.251
0.12	0.364	0.364	0.269	0.335	0.335	0.248
0.15	0.394	0.394	0.256	0.359	0.359	0.233
0.17	0.398	0.398	0.235	0.360	0.360	0.212
0.2	0.401	0.401	0.216	0.361	0.361	0.194
0.24	0.380	0.380	0.190	0.342	0.342	0.171
0.3	0.346	0.346	0.160	0.311	0.311	0.144
0.4	0.298	0.298	0.130	0.268	0.268	0.117
0.5	0.246	0.246	0.108	0.222	0.222	0.097
0.75	0.173	0.172	0.079	0.156	0.154	0.071
1	0.136	0.133	0.065	0.122	0.120	0.058
1.5	0.090	0.088	0.044	0.081	0.079	0.040
2	0.063	0.060	0.033	0.057	0.054	0.030
3	0.038	0.034	0.022	0.034	0.031	0.020
4	0.026	0.023	0.017	0.023	0.020	0.015
5	0.019	0.017	0.013	0.017	0.015	0.011
6	0.015	0.013	0.010	0.013	0.011	0.009
7.5	0.009	0.009	0.008	0.008	0.008	0.007
10	0.005	0.005	0.005	0.005	0.005	0.004

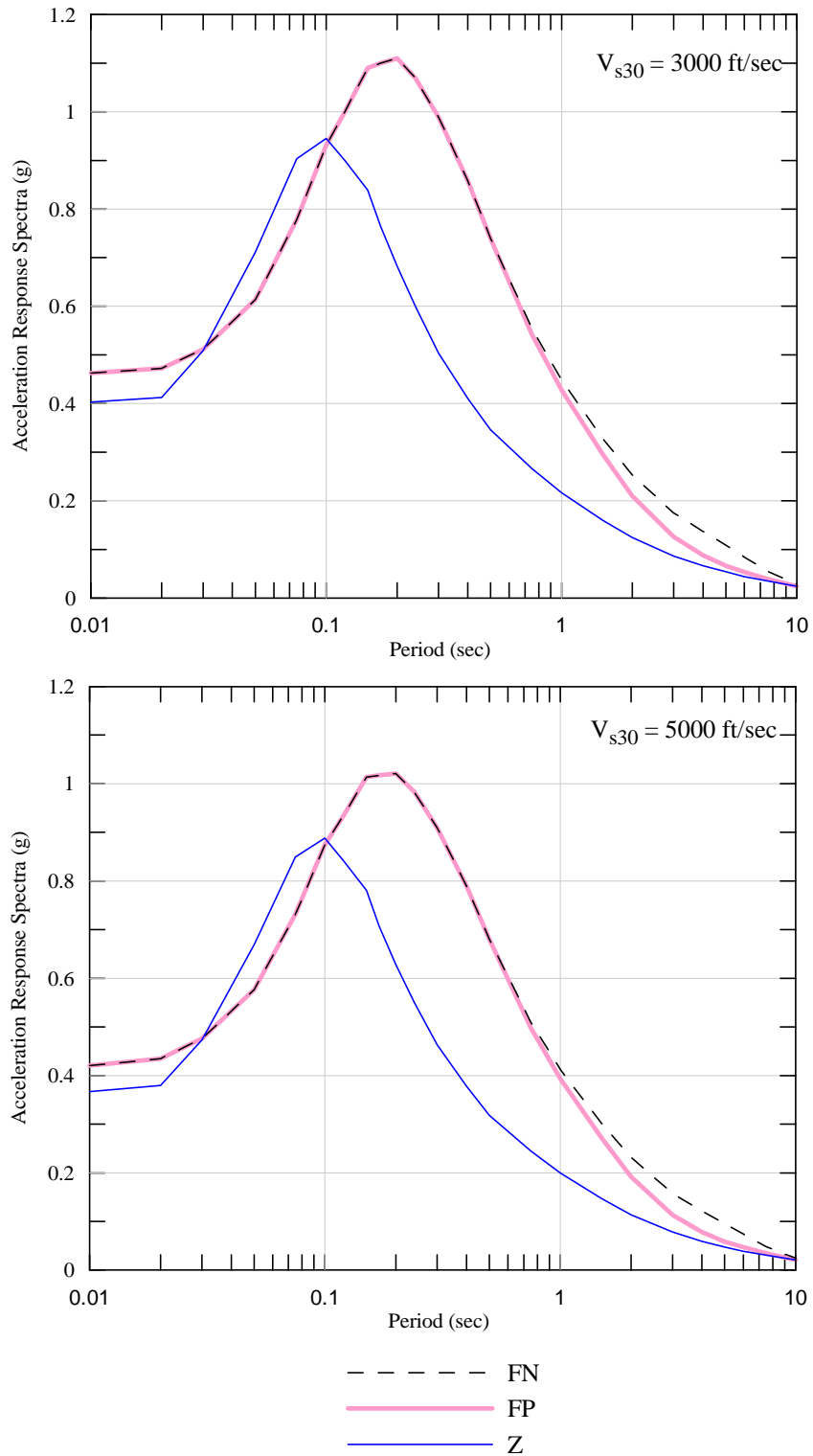


**Figure 1: Acceleration Response Spectra (5% Damping in g's) for SEE Scenario**

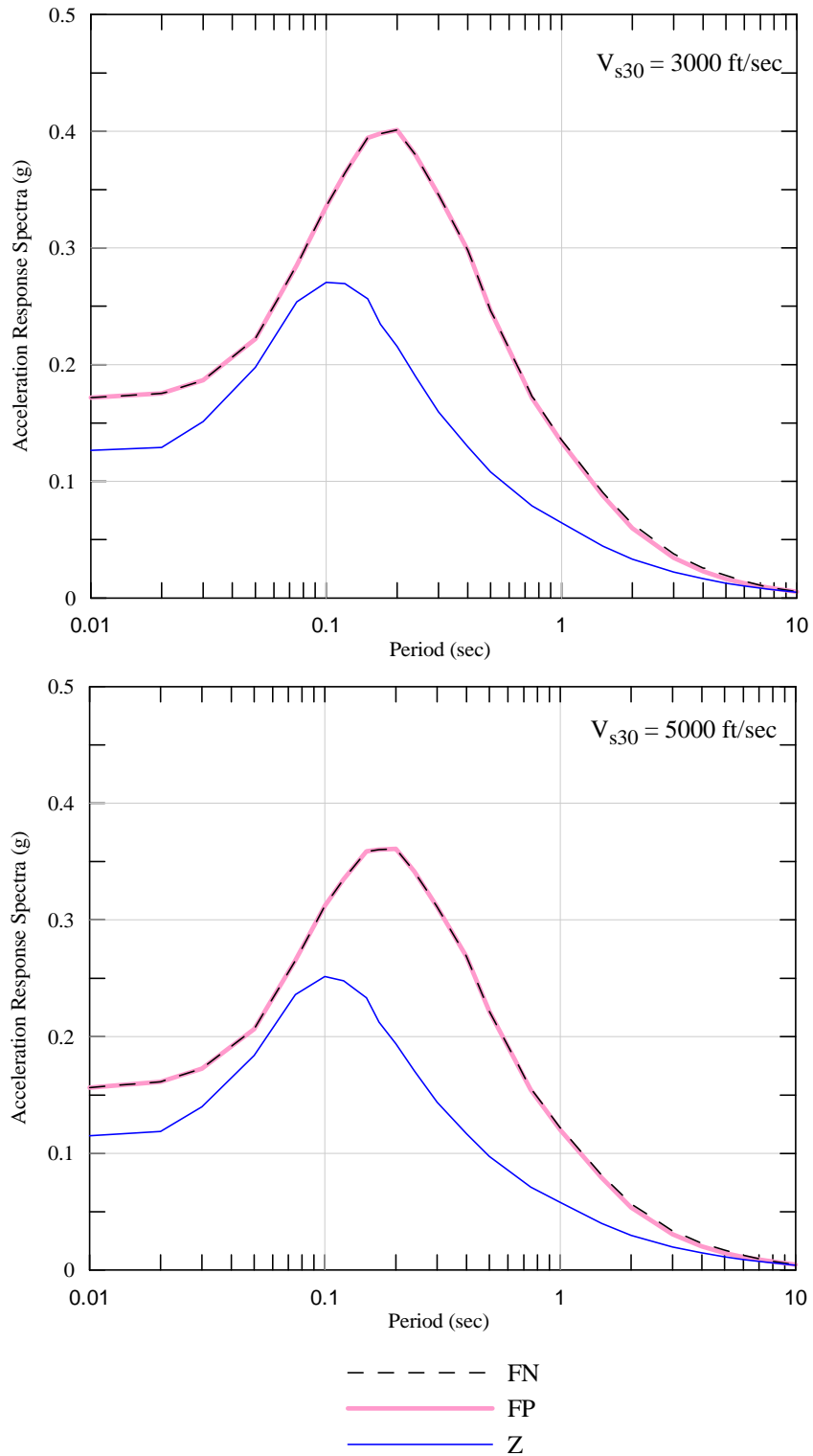


**Figure 2: Acceleration Response Spectra (5% Damping in g's) for FEE Scenario**

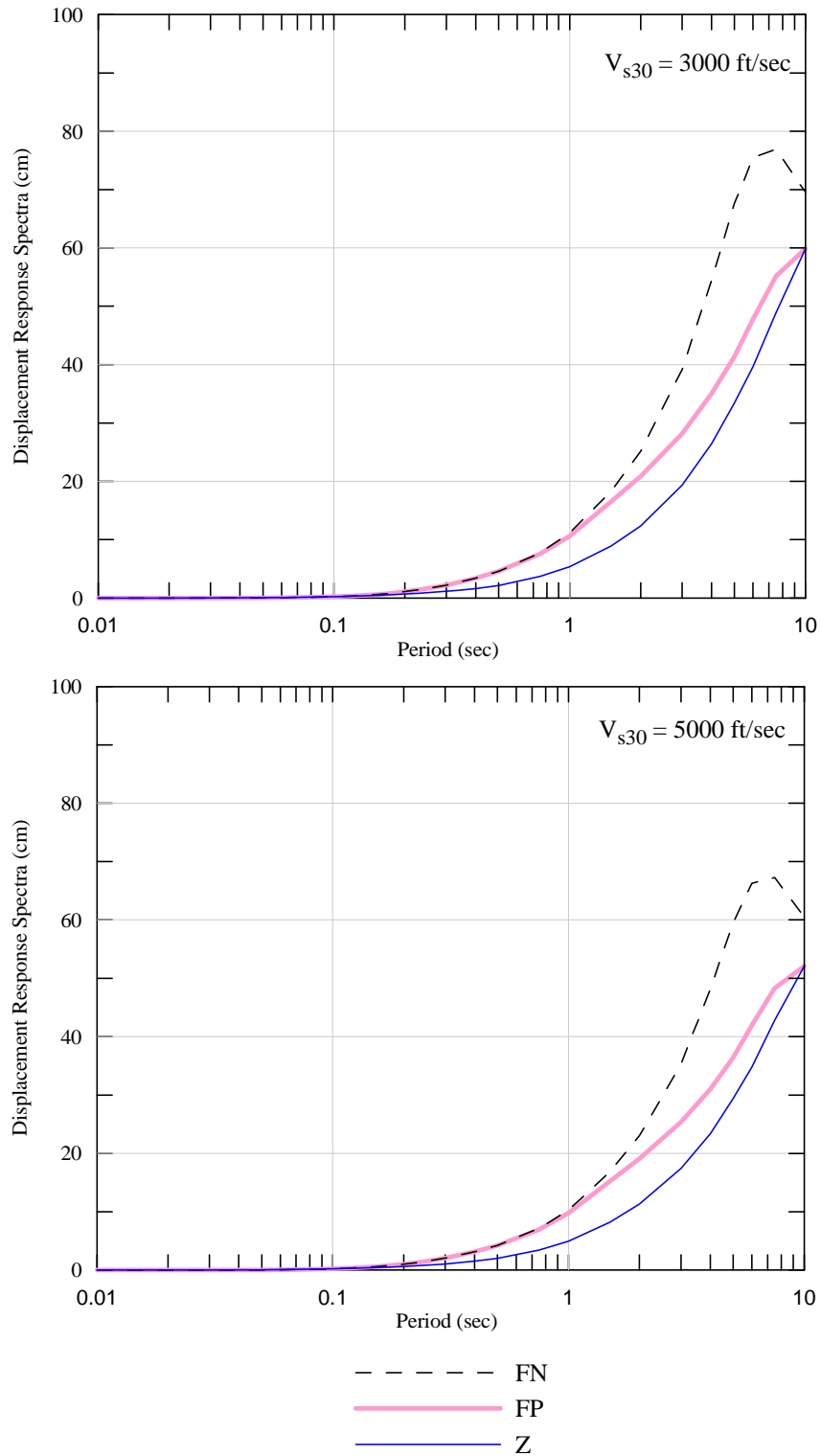


**Figure 3: Displacement Response Spectra (5% Damping in cm's) for SEE Scenario**

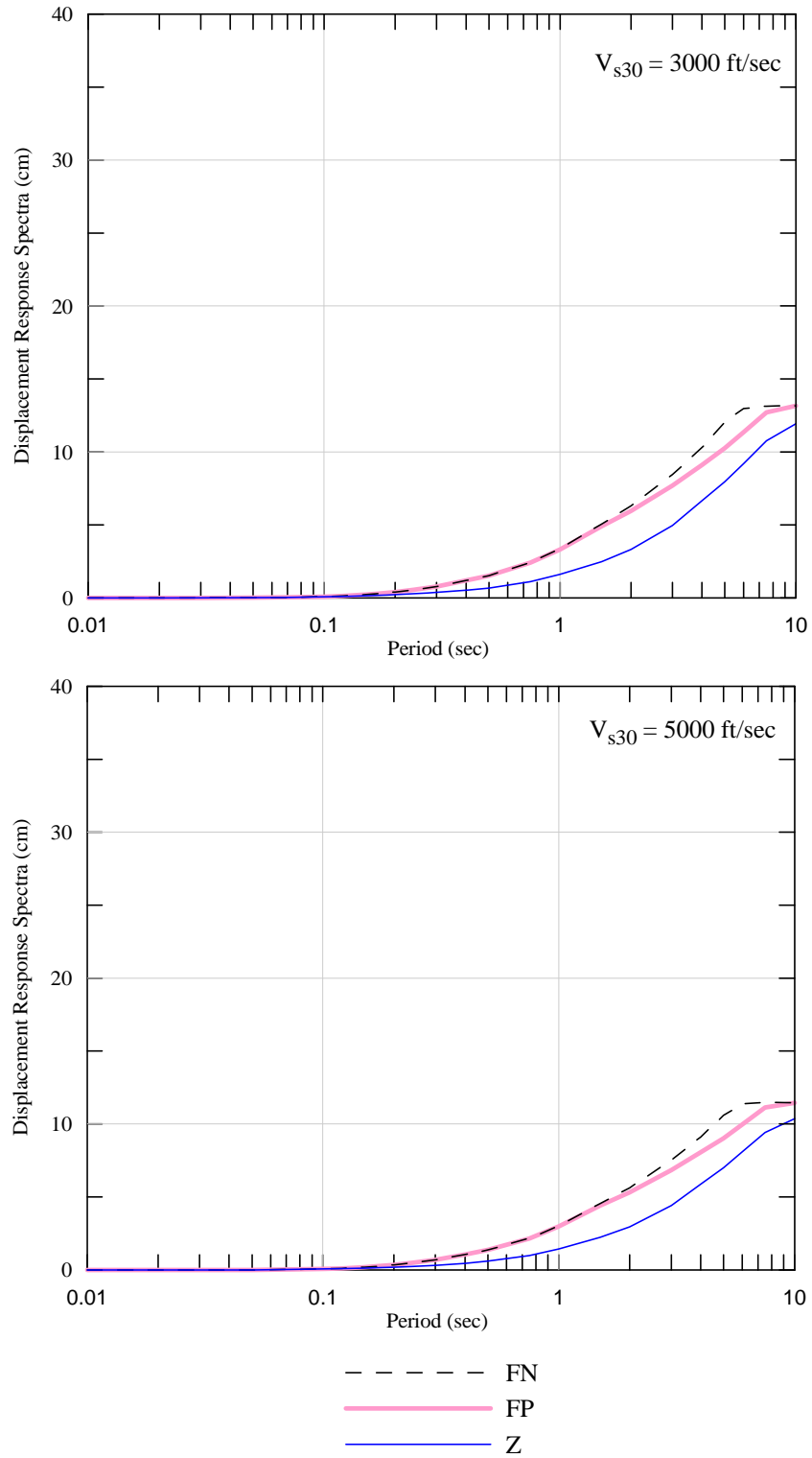


**Figure 4: Displacement Response Spectra (5% Damping in cm's) for FEE Scenario**

### 3.0 SELECTION OF SEED TIME HISTORIES

The seed time histories needed for developing the spectrum-compatible motions were selected based on the seismological properties of the dominant earthquakes contributing to the spectral shape of the horizontal components of the SEE and FEE response spectra. The selected records as recommended by Dr. Abrahamson (Appendix A) are presented in Table 3. These time histories were modified to be spectrum-compatible with the SEE and FEE response spectra for the  $V_{S30}$  of 3000 and 5000 ft/sec. Subsequent sections present the time histories that were matched to the SEE and FEE response spectra, and thus, a total of 36 spectrum-compatible time histories were developed. Modifications to the fault-parallel (FP) component for the SEE event to account for the near-fault fling effects are presented in Section 5.0.

**Table 3: Seed Time Histories for Spectral Matching**

Scenario	Earthquake	Station	Magnitude	Distance (km)	$V_{S30}$ (m/s)	Comp FN	Comp FP	Low Freq <sup>1</sup> (Hz)
SEE	1990 Manjil, Iran	Abbar	7.37	12.6	724	T	L	0.130
	1999 Kocaeli, Turkey	Izmit	7.51	7.2	811	090	180	0.125
	1999 Chi-Chi, Taiwan	TCU 076	7.62	2.8	615	E	N	0.063
FEE	1989 Loma Prieta	Gilroy #6	6.93	18.3	663	N	E	0.250
	1999 Duzce, Turkey	Lamont 1061	7.14	11.5	481	000	090	0.088
	1999 Hector Mine	Hector	7.13	11.7	685	090	000	0.025

Note:

1. Lowest usable frequency from NGA flat file.

## **4.0 DEVELOPMENT OF SPECTRUM-COMPATIBLE TIME HISTORIES OF ROCK MOTION**

Section 4 presents the development of the spectrum-compatible rock time histories for the Safety Evaluation Earthquake (SEE) and the Functionality Evaluation Earthquake (FEE).

### **4.1 SPECTRUM MATCHING PROCESS**

Spectrum-compatible time histories were developed using the method of Lilhanand and Tseng (1988) and later modified by Abrahamson (1992). The initial seed time histories described in the previous section were modified to be “tightly matched” with the selected response spectra. The modifications were made in the time domain using the program RSPMATCH (Abrahamson, 1993). This procedure only adjusts the time history locally, in an iterative manner, for spectral value of each period and damping. The adjustment is performed by adding/subtracting a small perturbation to the initial time history using a finite-duration wavelet and thus preserves the non-stationary characteristics of the initial time history. After the final iteration, each time history is baseline corrected to remove the numerical drift obtained during the matching process.

### **4.2 ANALYSIS OF CHARACTERISTICS OF SPECTRUM-COMPATIBLE TIME HISTORY**

To quantify the effects of the spectrum matching procedure, several characteristics of the scaled (original time histories scaled to their corresponding target peak ground acceleration) and spectrum-compatible time histories were compared. Figure 5 to Figure 40 present comparisons between response spectra (5% damped) of the scaled and spectrum-compatible time histories, and the target response spectra for the SEE criteria; and Figure 41 to Figure 76 present comparisons for the FEE criteria. These figures also present the comparison of acceleration, velocity, displacement time histories, and normalized Arias Intensity between scaled and spectrum-compatible time histories.

The PGA, PGV, PGD, and duration of the spectrally-matched time histories are summarized in Table 4 and. It can be seen that most of the computed PGV fall within the range recommended by Dr. Abrahamson (Appendix A) in Table 6.

**Table 4: Summary of ground motion parameters of spectrum-compatible time histories, SEE and FEE criteria at  $V_{S30} = 3000$  ft/sec**

Earthquake	Station	Criteria	Component	PGA (g)	PGV (cm/s)	PGD (cm)	Duration <sup>1</sup> (sec)
Manjil	Abbar	SEE	FN	0.46	44.7	28.6	30.6
			FP	0.46	39.4	25.5	29.0
			UP	0.41	36.1	19.6	29.2
Kocaeli	Izmit		FN	0.46	51.8	30.8	14.8
			FP	0.46	44.6	31.1	18.1
			UP	0.40	28.7	26.2	19.3
Chi-Chi	TCU076		FN	0.46	61.9	31.2	30.6
			FP	0.46	46.6	38.4	28.9
			UP	0.40	24.4	18.8	30.0
Duzce	Lamont	FEE	FN	0.17	12.2	6.2	17.2
			FP	0.18	17.4	6.5	16.2
			UP	0.13	8.6	4.5	20.1
Loma Prieta	Gilroy #6		FN	0.17	20.0	11.5	14.7
			FP	0.17	10.9	5.2	14.0
			UP	0.12	9.9	9.5	16.8
Hector Mine	Hector		FN	0.18	15.0	8.3	11.7
			FP	0.17	11.9	5.1	12.3
			UP	0.13	7.0	4.4	15.7

Note:

1. Significant duration defined as time between 5 to 95% of total energy.

**Table 5: Summary of ground motion parameters of spectrum-compatible time histories, SEE and FEE criteria at  $V_{S30} = 5000$  ft/sec**

0	Station	Criteria	Component	PGA (g)	PGV (cm/s)	PGD (cm)	Duration <sup>1</sup> (sec)
Manjil	Abbar	SEE	FN	0.42	39.3	24.4	30.3
			FP	0.42	40.8	18.0	28.8
			UP	0.40	27.5	15.3	28.8
Kocaeli	Izmit		FN	0.42	53.5	28.6	14.9
			FP	0.42	37.1	33.0	17.5
			UP	0.37	24.5	16.9	19.9
Chi-Chi	TCU076		FN	0.42	56.2	26.7	30.6
			FP	0.42	42.4	33.7	28.8
			UP	0.36	21.7	17.4	29.9
Duzce	Lamont	FN	0.16	11.2	3.8	16.8	
		FP	0.16	16.7	5.3	16.2	
		UP	0.12	7.0	3.7	20.1	
Loma Prieta	Gilroy #6	FN	0.16	11.8	6.8	14.7	
		FP	0.15	9.6	3.6	13.7	
		UP	0.11	6.4	6.7	16.5	
Hector Mine	Hector	FN	0.15	14.4	8.2	11.6	
		FP	0.16	10.0	5.4	12.6	
		UP	0.12	6.5	4.6	15.4	

**Table 6: Recommended range of PGV (cm/sec) at  $V_{S30} = 3000$  and  $5000$  ft/sec (Abrahamson, 2008, Appendix A)**

Criteria	$V_{S30}$ (ft/sec)	FN	FP	Z
SEE	3000	62 (42-93)	59 (40-89)	30 (20-45)
	5000	57 (39-86)	55 (37-82)	28 (19-41)
FEE	3000	15 (10-23)	15 (10-23)	7.3 (4.9-10.9)
	5000	14 (9-21)	14 (9-20)	6.6 (4.4-9.8)

## 5.0 MODIFICATION OF FAULT PARALLEL COMPONENTS OF THE SEE FOR FLING EFFECTS

Section 5 documents the modification of the spectrum-compatible fault-parallel acceleration time histories to incorporate the near-fault fling effects. The near-fault fling effects are only applied to the SEE ground motions. Dr. Abrahamson (personal communication, 2009) indicated that the fling effects are insignificant for the FEE ground motion because the mean rupture distance for the FEE is larger than 20 km (Appendix A). Therefore, no modifications to account for fling effects were made to the FEE time histories.

Following the procedure developed by Abrahamson (2001), the fling time history is added to each of the fault-parallel spectrum-compatible SEE time histories presented in Section 4.

### 5.1 GROUND MOTION DUE TO PERMANENT TECTONIC DEFORMATION

The movement of ground associated with the permanent offset of the ground (fling) often causes large long-period pulses, especially for a site located close to a fault. This fling-step is polarized onto the component parallel to the slip direction (FP component).

Abrahamson (2001) derived the equation of average slip on fault  $D_{fault}$  and the resulting equation is as follows:

$$\ln(D_{fault}) = 1.15M - 2.83 \quad (5-1)$$

where  $D_{fault}$  (cm) is the average displacement on the fault plane and  $M$  is the earthquake magnitude. Abrahamson (2001) assumed the attenuation of the amplitude of the fling to be a function of distance from the fault following the  $\cot^{-1}$  model. The tectonic displacement at a given site is as follows:

$$D_{site} = 0.5D_{fault} \cot^{-1}(\alpha R) / (\pi / 2) \quad (5-2)$$

where  $D_{site}$  (cm) is the tectonic displacement,  $R$  (km) is the rupture distance, and  $\alpha$  is a constant parameter determined to be 0.22 (Abrahamson, 2001). The 0.5 factor implies the assumption of splitting the tectonic deformation equally to the two sides of the fault.

Since

$$\cot^{-1}(x) = \pi / 2 - \tan^{-1}(x) \quad (5-3)$$

Equation (5-2) results in:

$$D_{site} = D_{fault} (\pi / 2 - \tan^{-1}(\alpha R)) / \pi \quad (5-4)$$

Figure 77 presents the attenuation relationship of the normalized site displacement with respect to fault displacement as suggested by equation (5-4).

The functional form of the fling acceleration is assumed to be a single cycle of sine-wave with the amplitude and duration estimated empirically. The fling period ( $T_{fling}$ ) is assumed to be a function of magnitude of the earthquake as determined from the following relation (Abrahamson, 2001):

$$\ln(T_{fling}) = -6.96 + 1.15M \quad (5-5)$$

Figure 78 presents the model prediction of fling period compared with three data points from earthquake records (Abrahamson, 2001). The amplitude of the fling can be estimated using displacement at the site and the fling period (Abrahamson, 2001) as follows:

$$A(g) = \frac{D_{site} 2\pi}{981T_{fling}^2} \quad (5-6)$$

The fling is conservatively assumed to arrive at the time of the beginning of the large velocity pulse,  $t_1$ , causing constructive interference between fling and the transient displacement of the spectrum compatible ground motion. The acceleration response spectrum of the time history that includes the effects of fling should envelop that of the original time history.

## 5.2 DEVELOPMENT OF FAULT-PARALLEL ACCELERATION TIME HISTORIES

### 5.2.1 Input Parameters for SEE

For Doyle Drive Replacement Project, the parameters to determine fling acceleration time history are magnitude and rupture distance of 7.6 and 13 km, respectively. These parameters were taken from deaggregation of 1,000 year return period at PGA and  $T = 1$  sec, as shown in Figure 79 and Figure 80 of the main text and Figure 4-7 of Appendix A.

### 5.2.2 Method

Following Abrahamson (2002), the procedures to develop a time history that include fling effects are:

- Determine fling parameters including fling period ( $T_{\text{fling}}$ ) and amplitude ( $A$ ) from equations 5-1 and (5-4) to (5-6), as described in previous sections.
- Determine fling arrival time  $t_1$  and polarity such that the fling velocity will constructively interfere with the velocity from the transient time history.
- Compute fling acceleration time history by assuming a single cycle of sine-wave form.
- Compute the total fault-parallel ground motion by adding fling time history to spectrum-compatible acceleration time history.
- Compute the spectrum of the total fault-parallel ground motion; this should envelop that of the original time history.

### 5.2.3 Results for SEE

Three earthquakes including 1990 Manjil Earthquake, 1999 Kocaeli Earthquake, and 1999 Chi-Chi Earthquake, were adjusted to be compatible with SEE target response spectra as presented in Section 4. Horizontal time histories, fault parallel component, were modified to include fling time history.

Figure 81 to Figure 89 and Figure 90 to Figure 98 present the original time histories, fling time histories, modified time histories, and acceleration and displacement response spectra for  $V_{S30}$  of 3000 and 5000 ft/sec, respectively. It can be seen that the arrival time of the fling was chosen to constructively interfere with the original time histories. Response spectra of the modified time histories envelop those of original time histories.

## 6.0 REFERENCES

- Abrahamson, N.A., 1992, Non-Stationary Spectral Matching: Presented at 87<sup>th</sup> Annual Meeting of the Seismological Society of America; also Seismological Research Letters, Vol. 63, No.1.
- Abrahamson, N.A., 1993, Non-Stationary Spectral Matching Program RSPMATCH: User Manual.
- Abrahamson, N.A., 2000, Effects of rupture directivity on probabilistic seismic hazard analysis: Proceedings of the 6th International Conference on Seismic Zonation, Palm Springs, California, 6 p.
- Abrahamson, N.A., 2001, Development of Fling Model for Diablo Canyon ISFSI: Pacific Gas and Electric Company, Geosciences Department, Calc. No. GEO.DCPP.01.12.
- Abrahamson, N.A., 2002, Development of 5 sets of Faults Parallel Acceleration Time Histories That Include the Effects of Fling for the DCPD ISFSI: Pacific Gas and Electric Company, Geosciences Department, Calc. No. GEO.DCPP.01.14.
- Abrahamson, N.A., 2009, Ground Motions for the Doyle Drive Replacement Project by Norman A. Abrahamson, inc.: Consulting report prepared by Norman A. Abrahamson, Inc., Piedmont, CA
- Lilhanand, K., Tseng, W.S., 1988, Development and Application of Realistic Earthquake Time Histories Compatible with Multiple Damping Response Spectra: Proceedings of the 9<sup>th</sup> World Conference on Earthquake Engineering, Tokyo, Japan, Vol. II, pp. 819-824.
- Somerville, P.G., Smith, N.F., Graves, R.W., and Abrahamson, N.A., 1997, Modification of empirical strong motion attenuation relations to include the amplitude and duration effects of rupture directivity: Seismological Research Letters, v.68, no. 1, pp.199-222, January/February.
- Working Group on California Earthquake Probabilities (WGCEP), 2003, Earthquake probabilities in the San Francisco Bay Region, 2002 to 2031: U.S. Geological Survey Open File Report 03-214 [<http://pubs.usgs.gov/of/2003/of03-214/>].
- WGCEP, 2008, The Uniform California Earthquake Rupture Forecast, Version 2 (UCERF 2): U.S. Geological Survey Open-File Report 2007-1437 and California Geological Survey Special Report 203 [<http://pubs.usgs.gov/of/2007/1437/>].

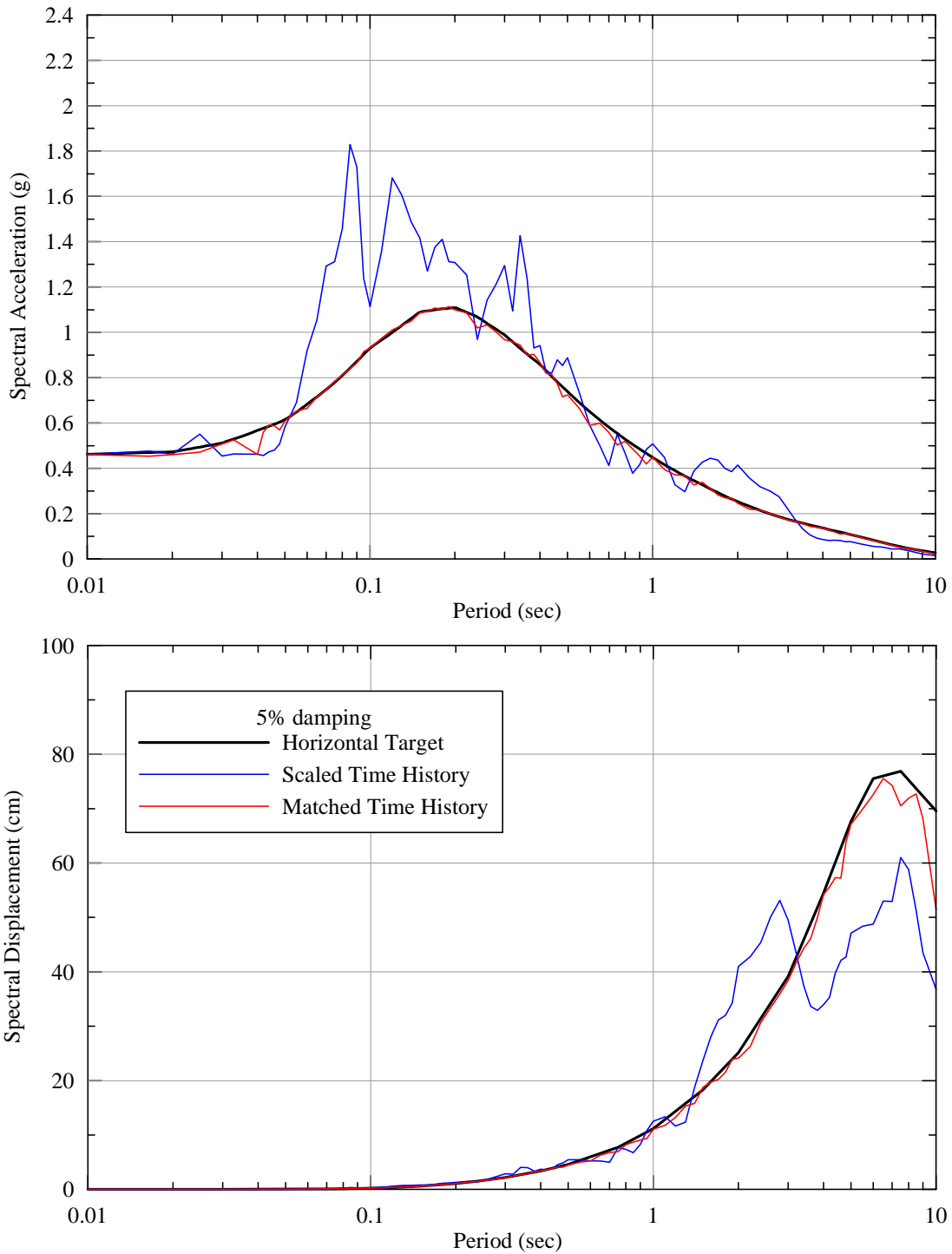


**Figure 5: Acceleration and Displacement Response Spectra. Seed Motion: 1990 Manjil Earthquake, Abbar Station, T Component. Target: Fault Normal, SEE  $V_{S30} = 3000$  ft/sec.**

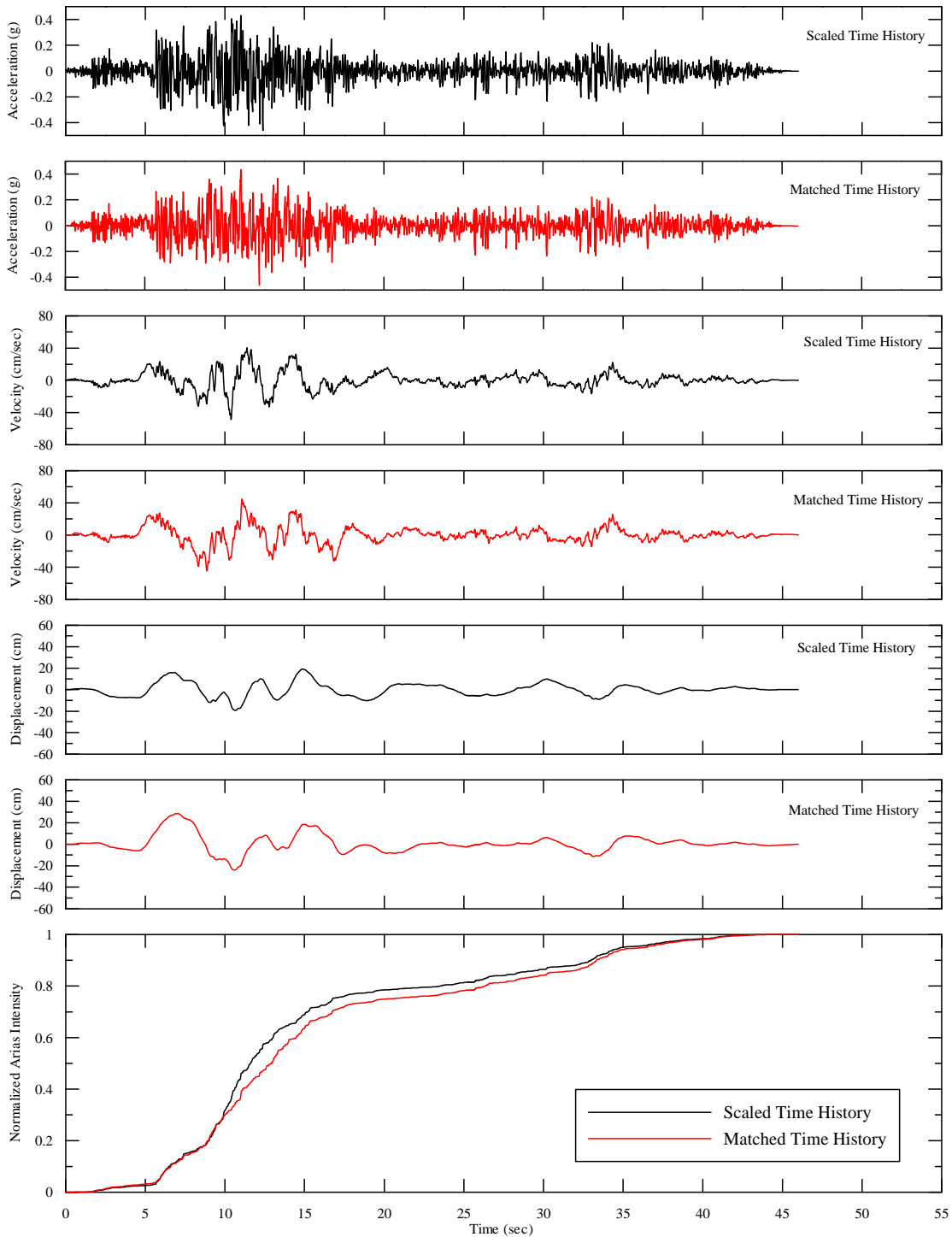


**Figure 6: Acceleration, Velocity, and Displacement Time Histories. Seed Motion: 1990 Manjil Earthquake, Abbar Station, T Component. Target: Fault Normal, SEE  $V_{S30} = 3000$  ft/sec.**

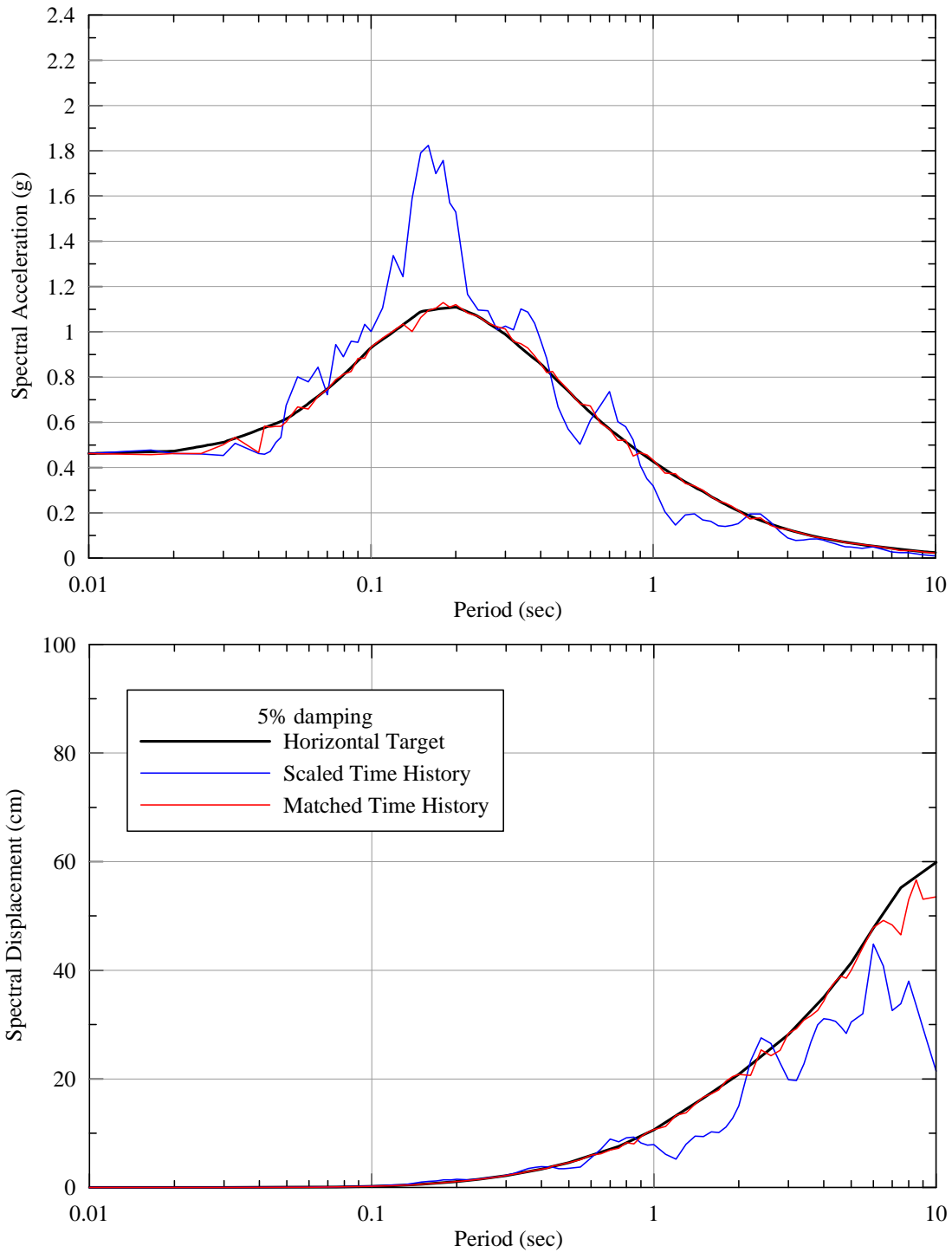


**Figure 7: Acceleration and Displacement Response Spectra. Seed Motion: 1990 Manjil Earthquake, Abbar Station, L Component. Target: Fault Parallel, SEE  $V_{S30} = 3000$  ft/sec.**

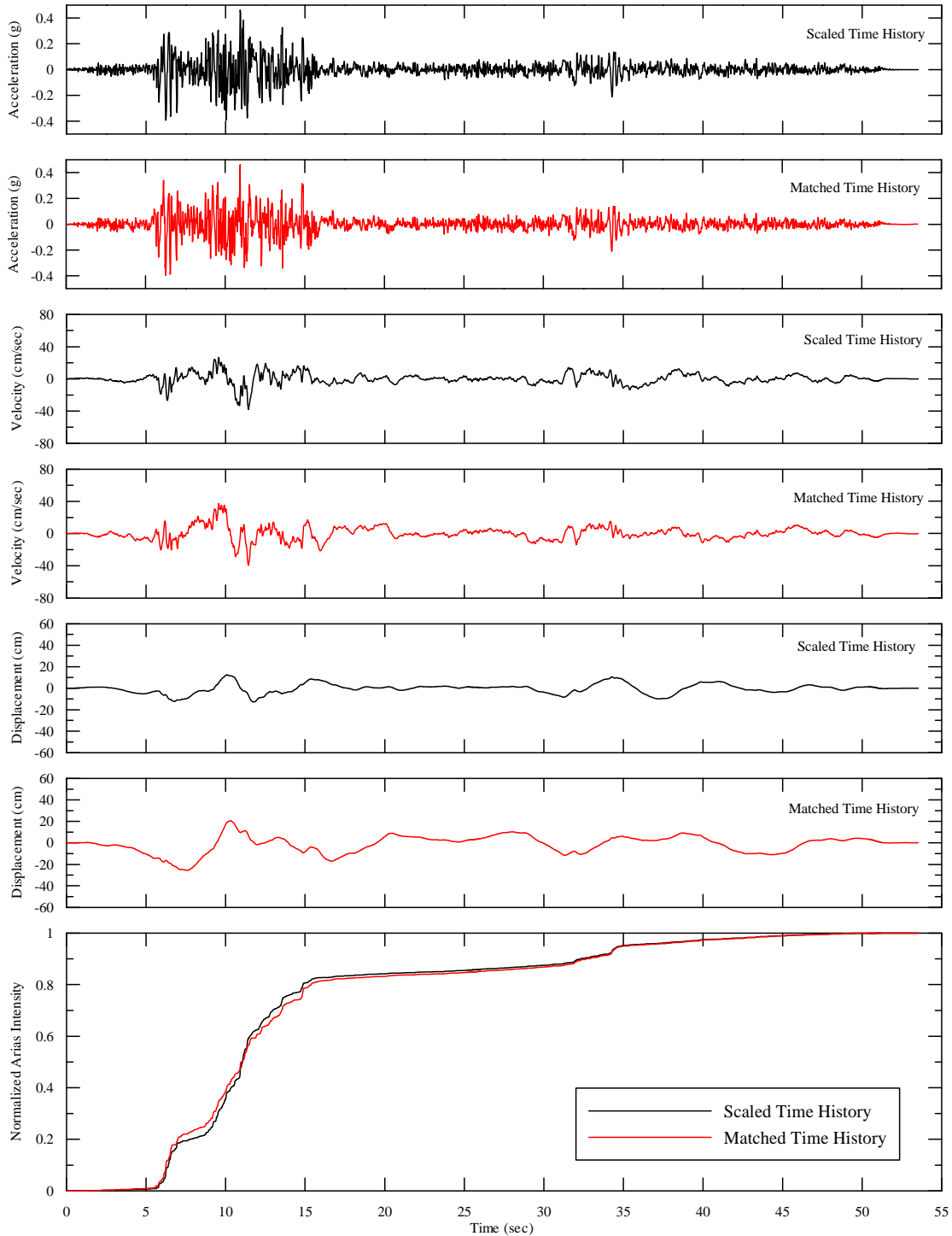


**Figure 8: Acceleration, Velocity, and Displacement Time Histories. Seed Motion: 1990 Manjil Earthquake, Abbar Station, L Component. Target: Fault Parallel, SEE  $V_{S30} = 3000$  ft/sec.**

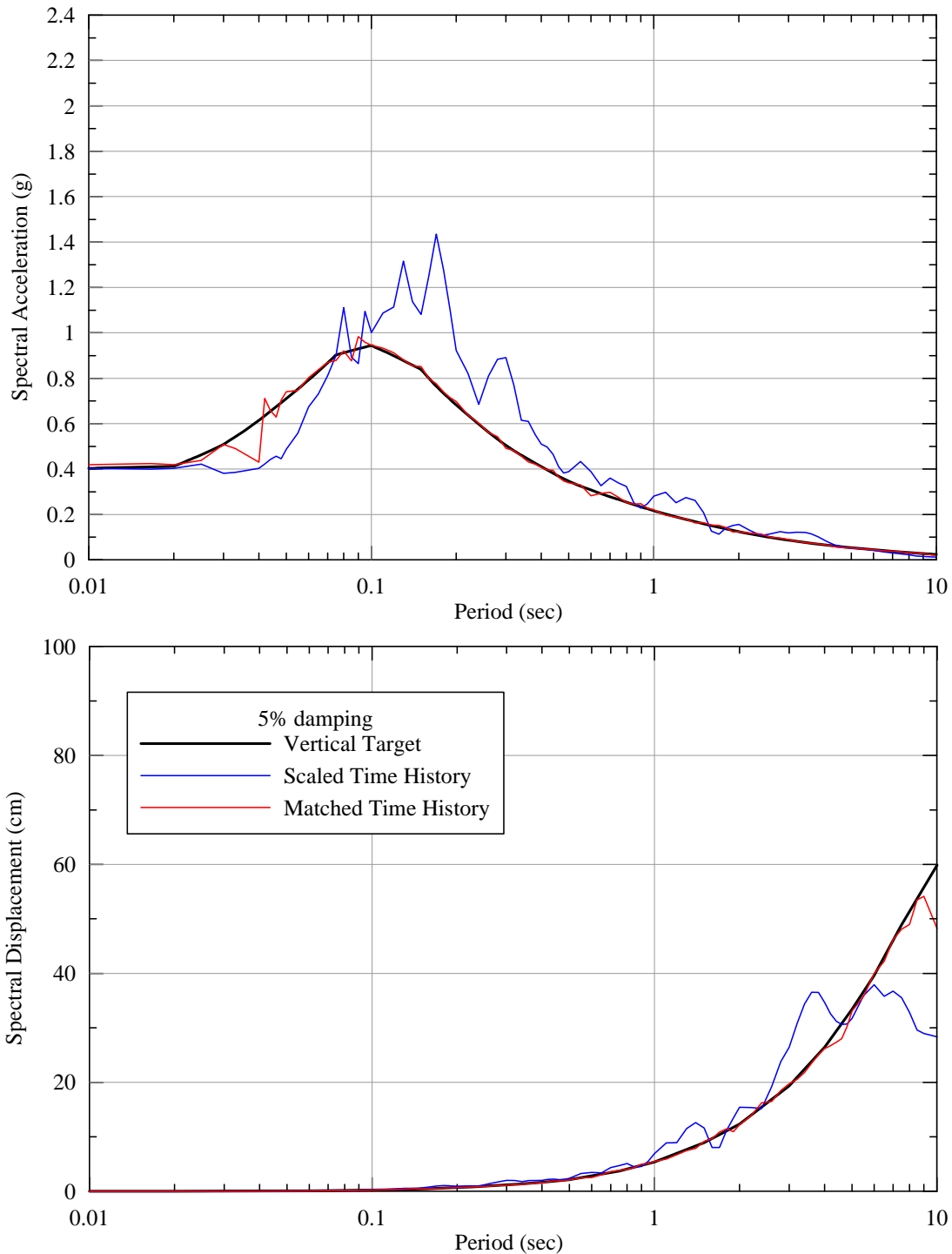


**Figure 9: Acceleration and Displacement Response Spectra. Seed Motion: 1990 Manjil Earthquake, Abbar Station, Vertical Component. Target: Vertical, SEE  $V_{S30} = 3000$  ft/sec.**

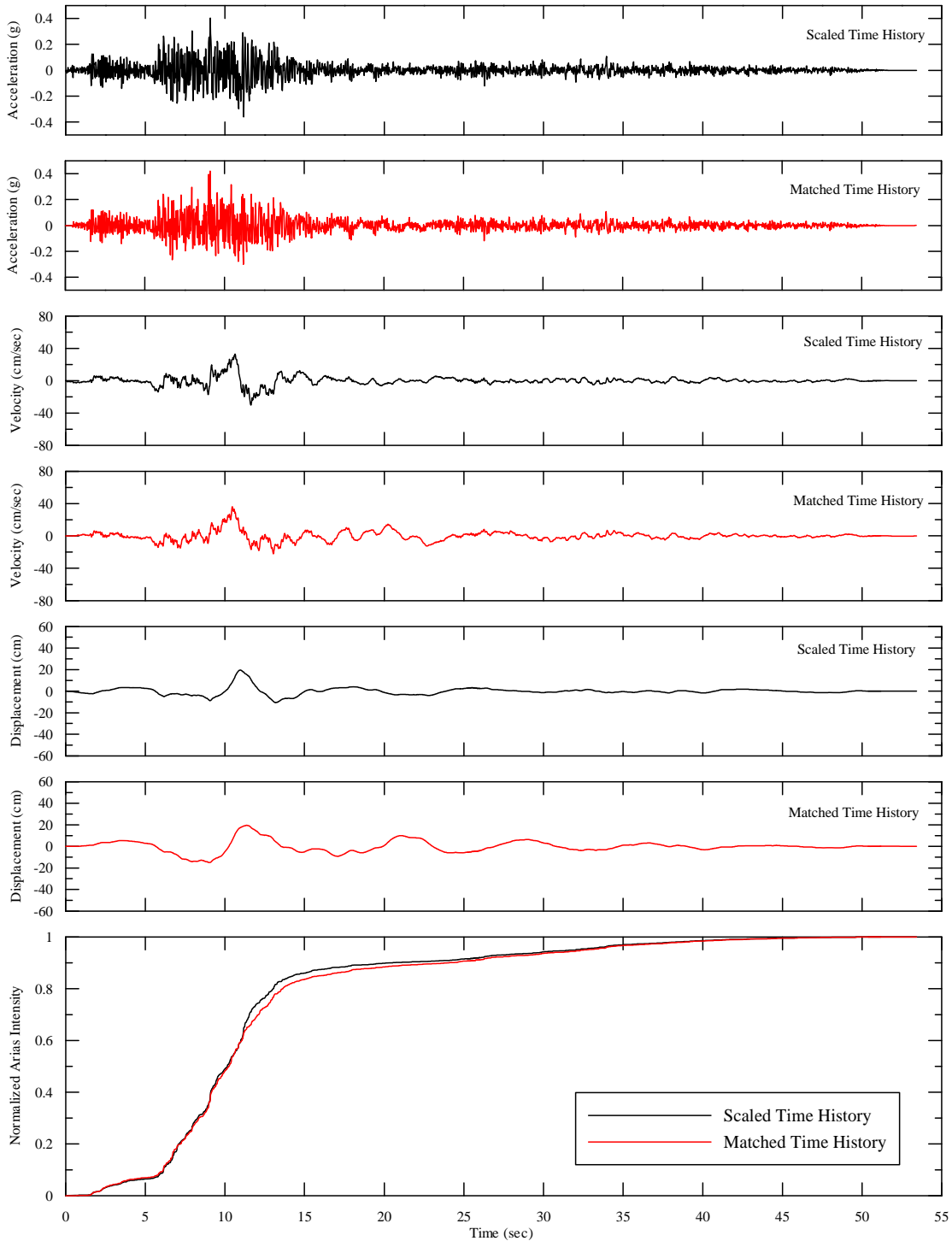


**Figure 10: Acceleration, Velocity, and Displacement Time Histories. Seed Motion: 1990 Manjil Earthquake, Abbar Station, Vertical Component. Target: Vertical, SEE  $V_{S30} = 3000$  ft/sec.**

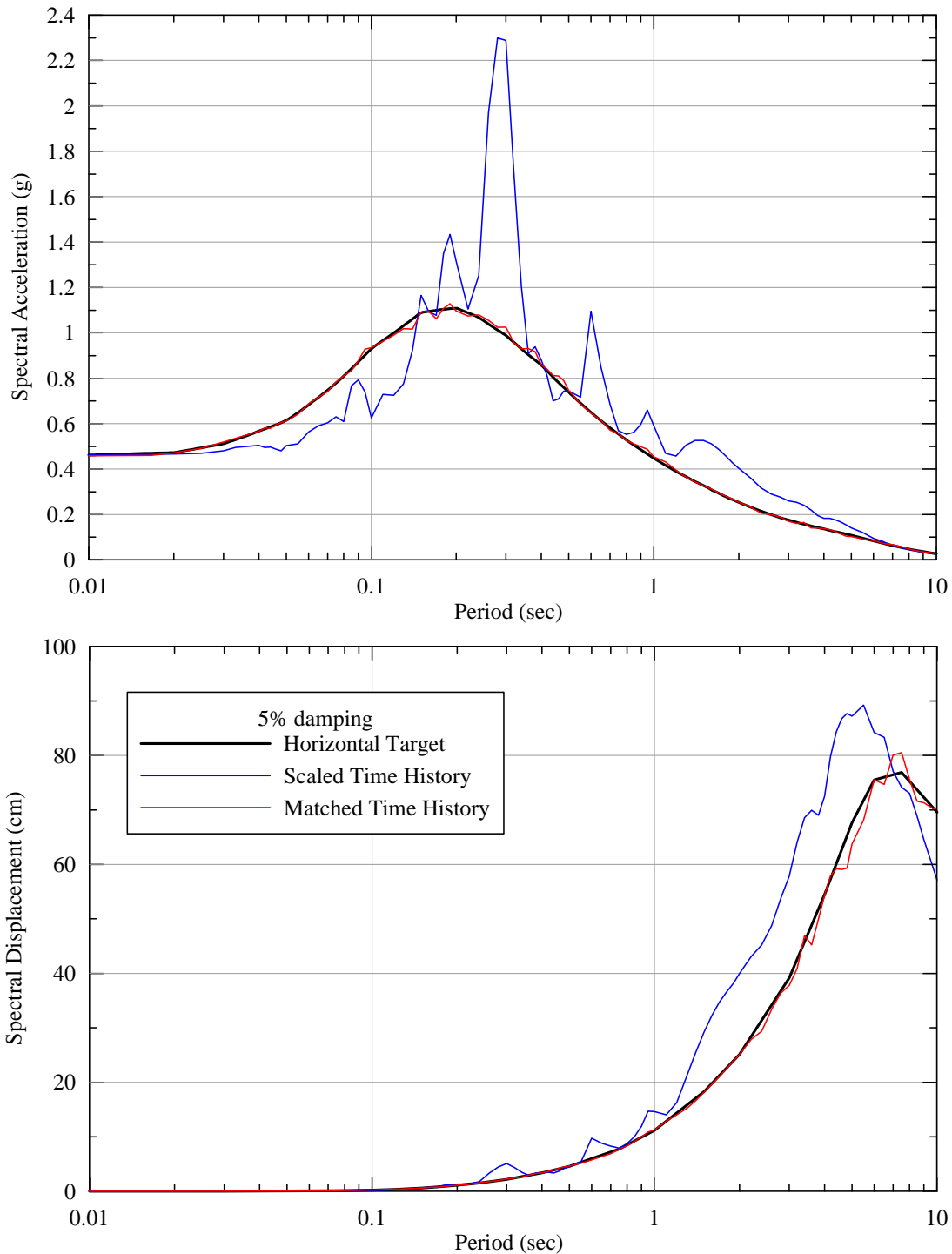


**Figure 11: Acceleration and Displacement Response Spectra. Seed Motion: 1999 Kocaeli Earthquake, Izmit Station, 90 degrees Component. Target: Fault Normal, SEE  $V_{S30} = 3000$  ft/sec.**

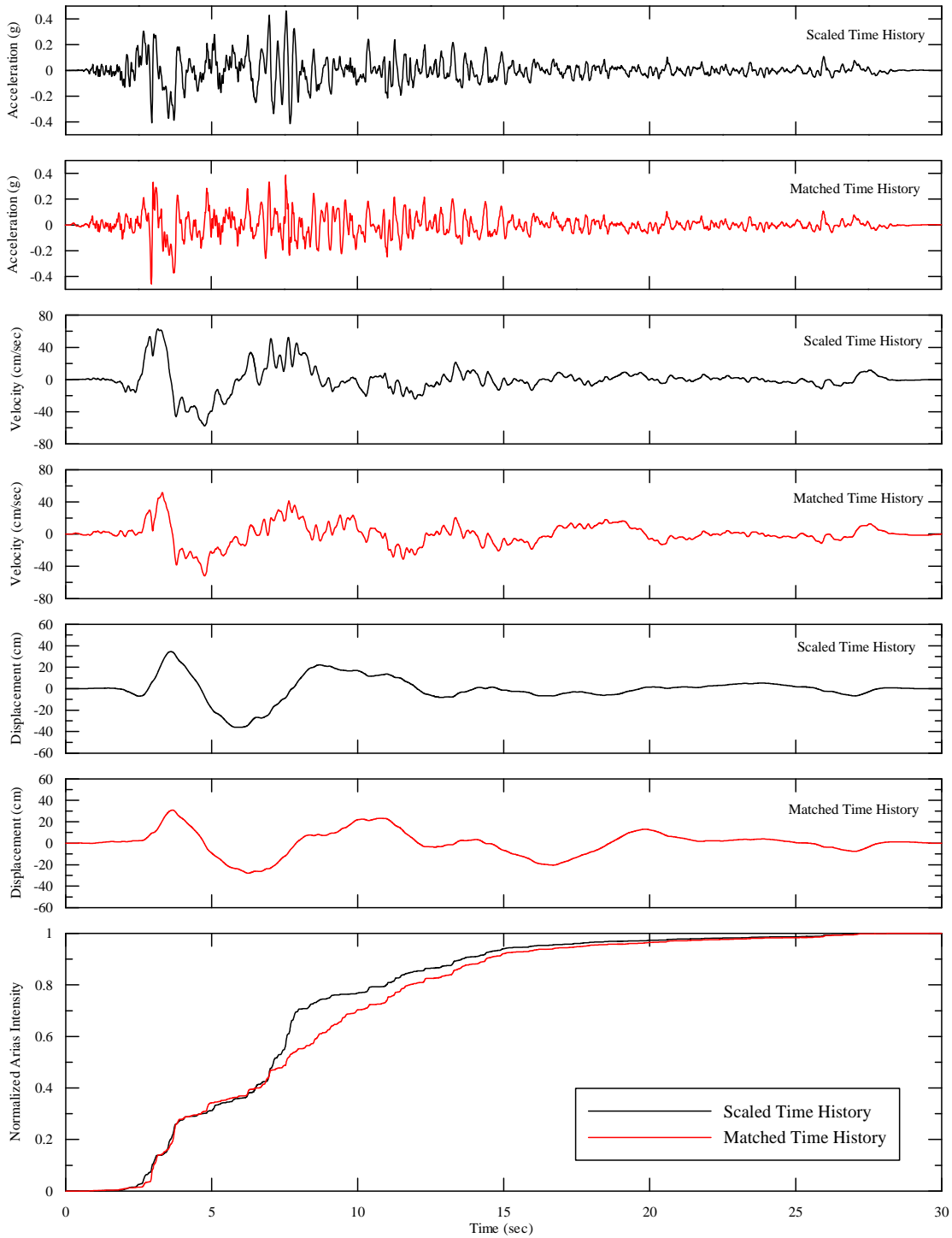


**Figure 12: Acceleration, Velocity, and Displacement Time Histories. Seed Motion: 1999 Kocaeli Earthquake, Izmit Station, 90 degrees Component. Target: Fault Normal, SEE  $V_{S30} = 3000$  ft/sec.**

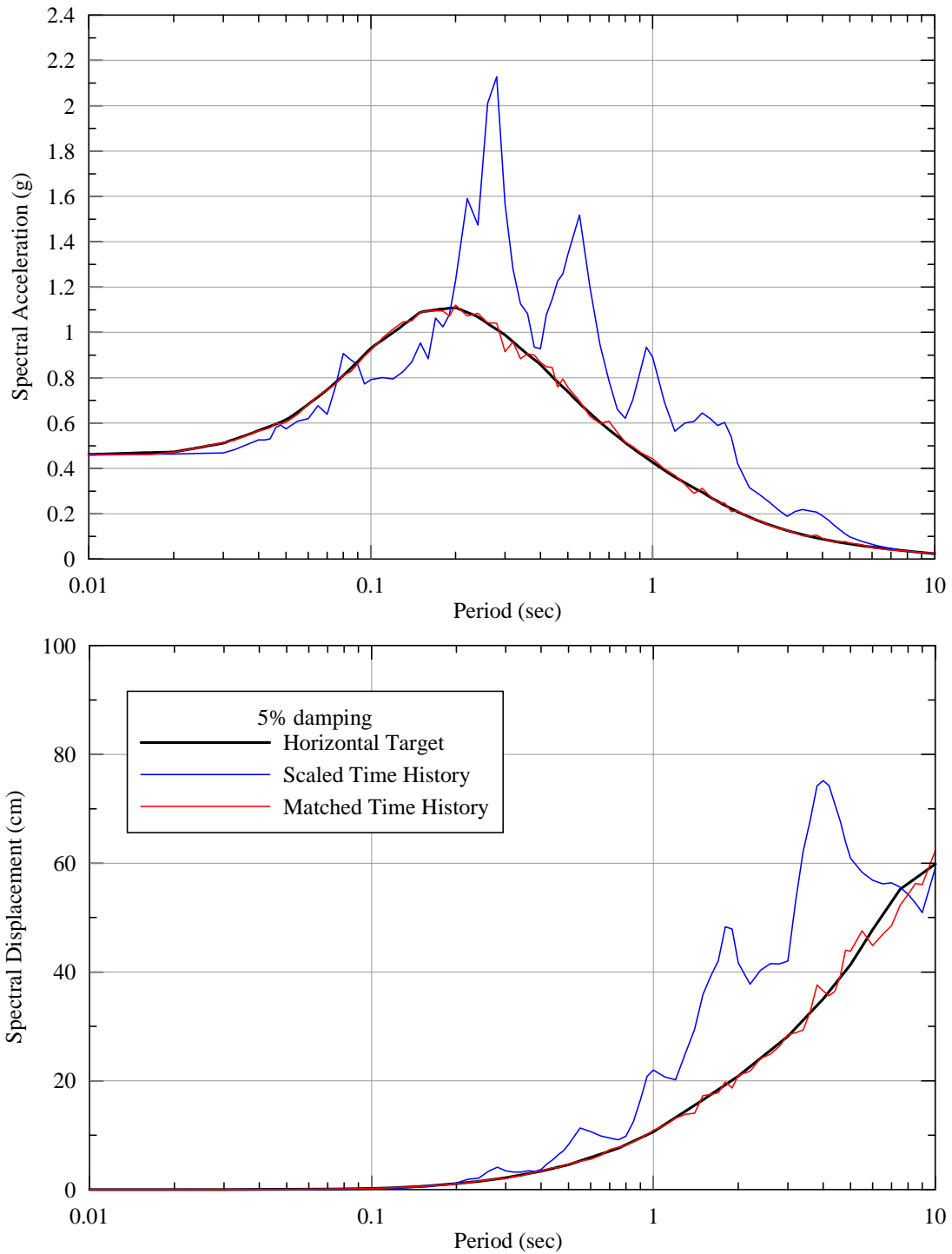


**Figure 13: Acceleration and Displacement Response Spectra. Seed Motion: 1999 Kocaeli Earthquake, Izmit Station, 180 degrees Component. Target: Fault Parallel, SEE**

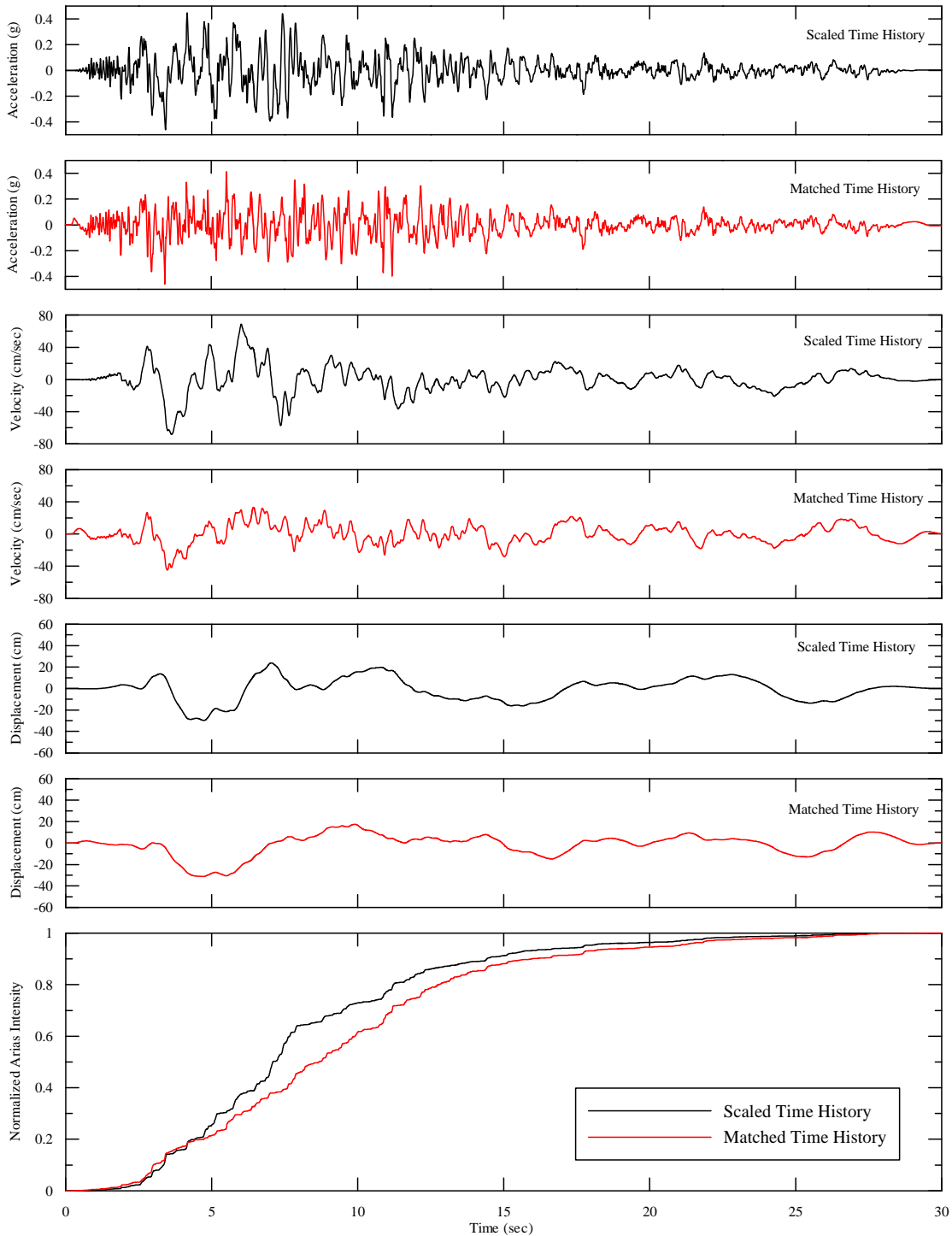


**Figure 14: Acceleration, Velocity, and Displacement Time Histories. Seed Motion: 1999 Kocaeli Earthquake, Izmit Station, 180 degrees Component. Target: Fault Parallel, SEE  $V_{S30} = 3000$  ft/sec.**

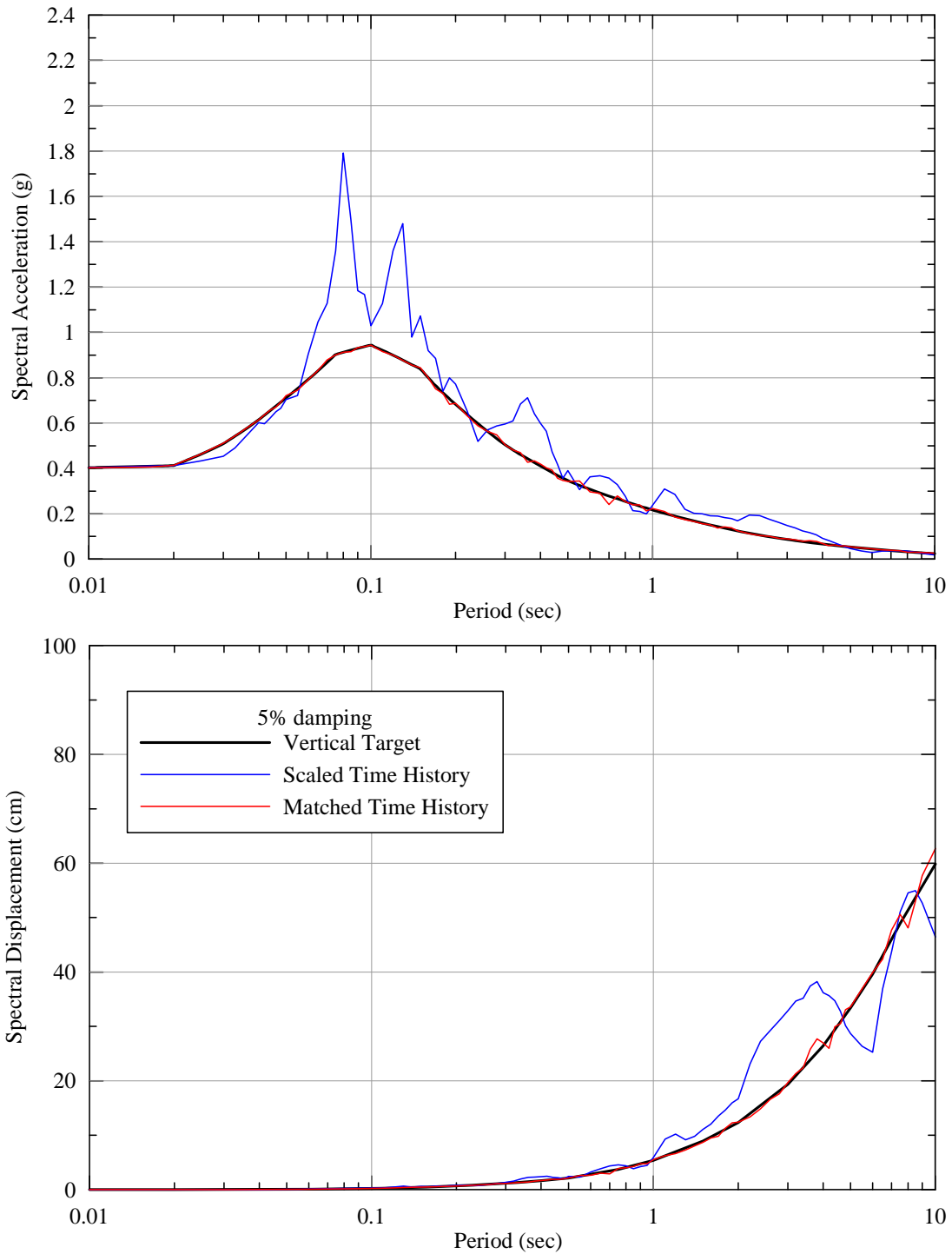


**Figure 15: Acceleration and Displacement Response Spectra. Seed Motion: 1999 Kocaeli Earthquake, Izmit Station, Vertical Component. Target: Vertical, SEE  $V_{S30} = 3000$  ft/sec.**

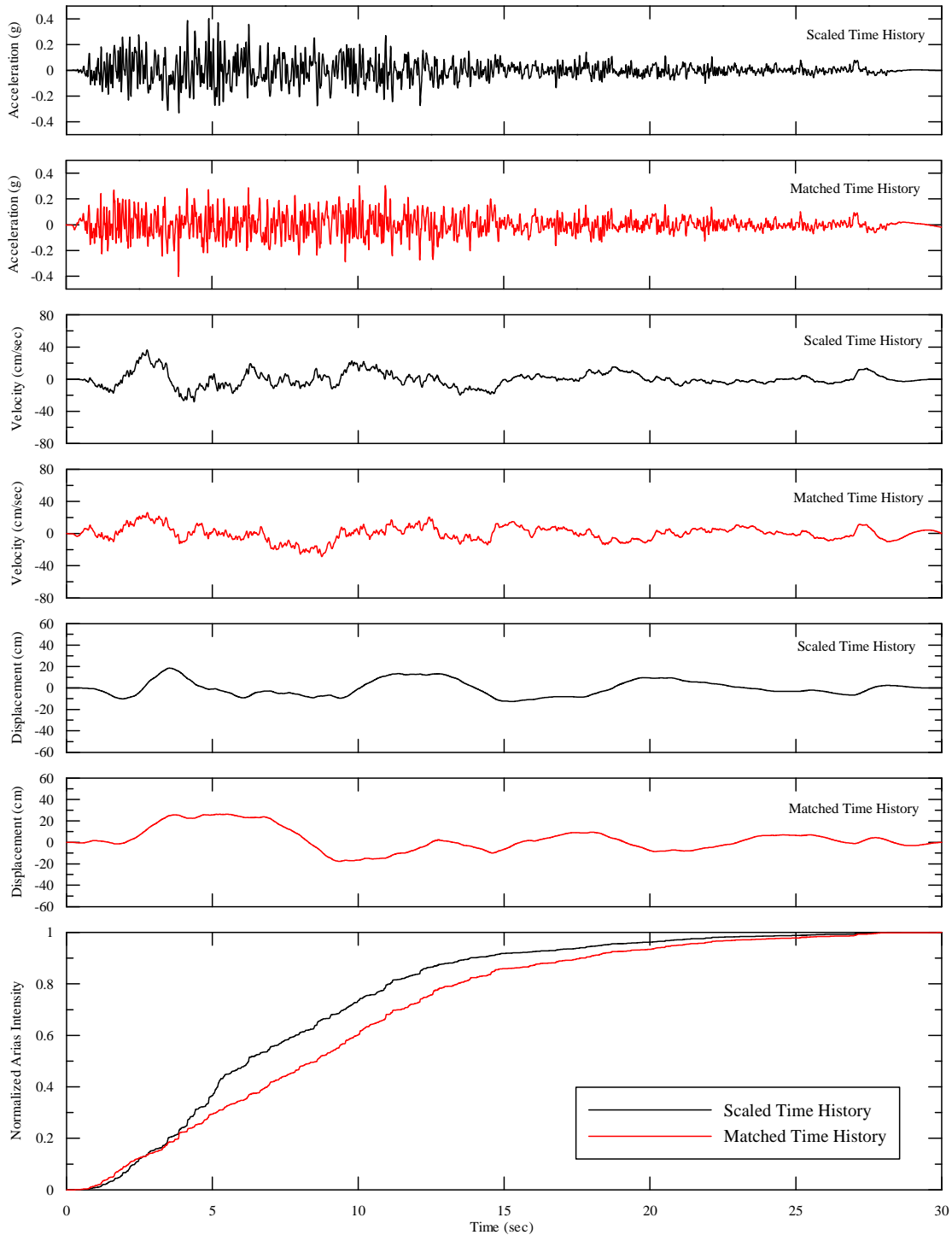


**Figure 16: Acceleration, Velocity, and Displacement Time Histories. Seed Motion: 1999 Kocaeli Earthquake, Izmit Station, Vertical Component. Target: Vertical, SEE  $V_{S30} = 3000$  ft/sec.**

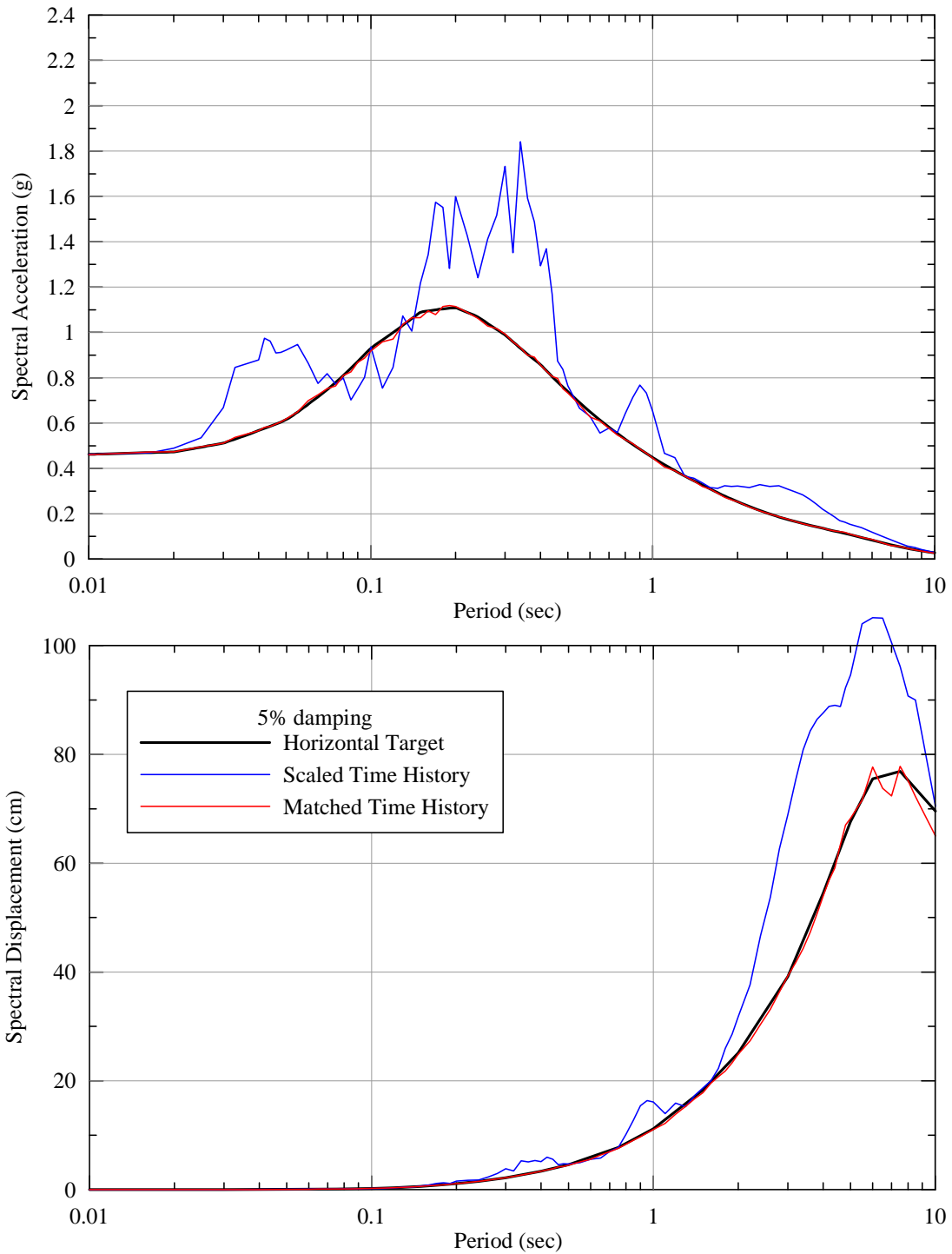


**Figure 17: Acceleration and Displacement Response Spectra. Seed Motion: 1999 Chi-Chi Earthquake, TCU076 Station, W Component. Target: Fault Normal, SEE  $V_{S30} = 3000$  ft/sec.**

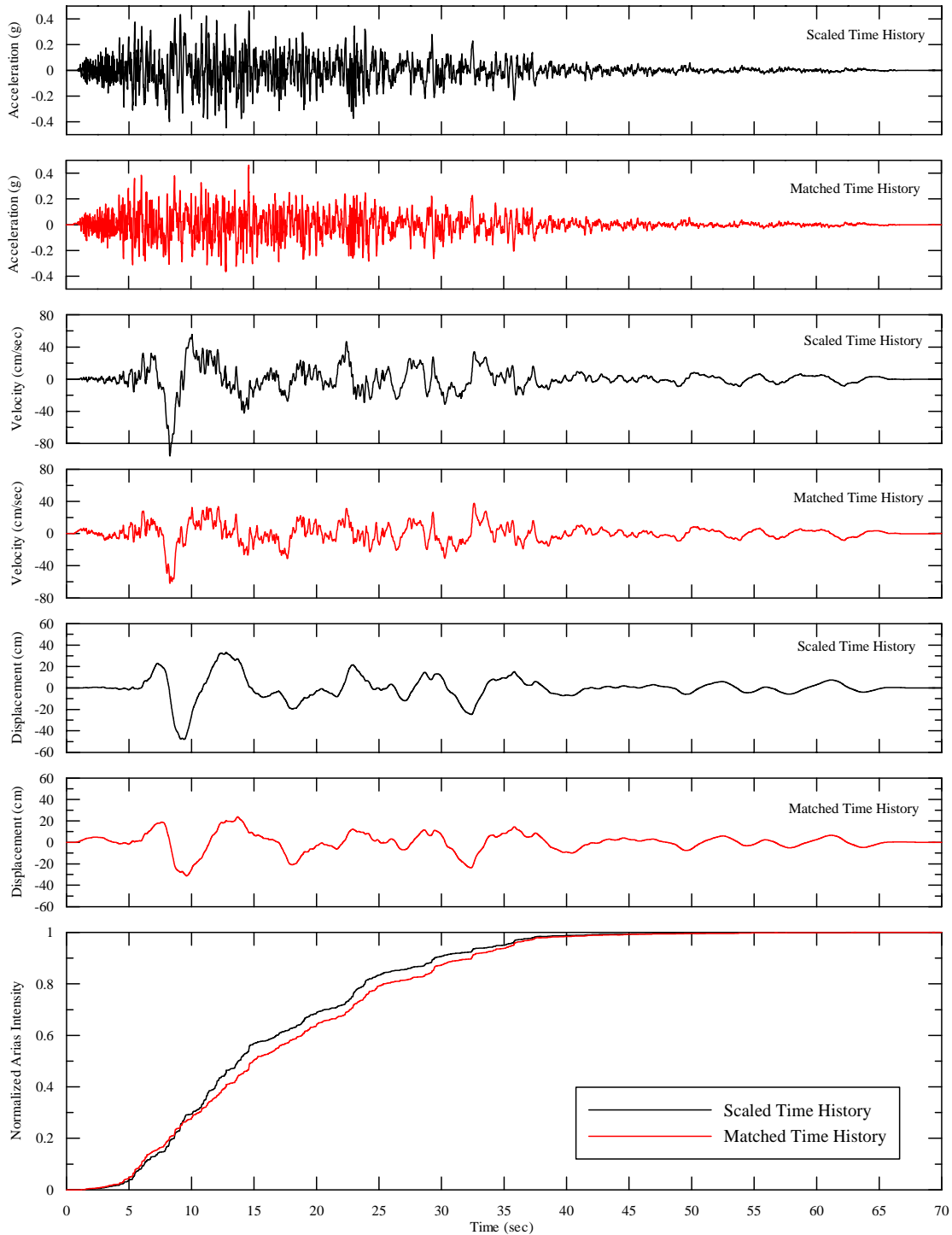


**Figure 18: Acceleration, Velocity, and Displacement Time Histories. Seed Motion: 1999 Chi-Chi Earthquake, TCU076 Station, W Component. Target: Fault Normal, SEE  $V_{S30} = 3000$  ft/sec.**

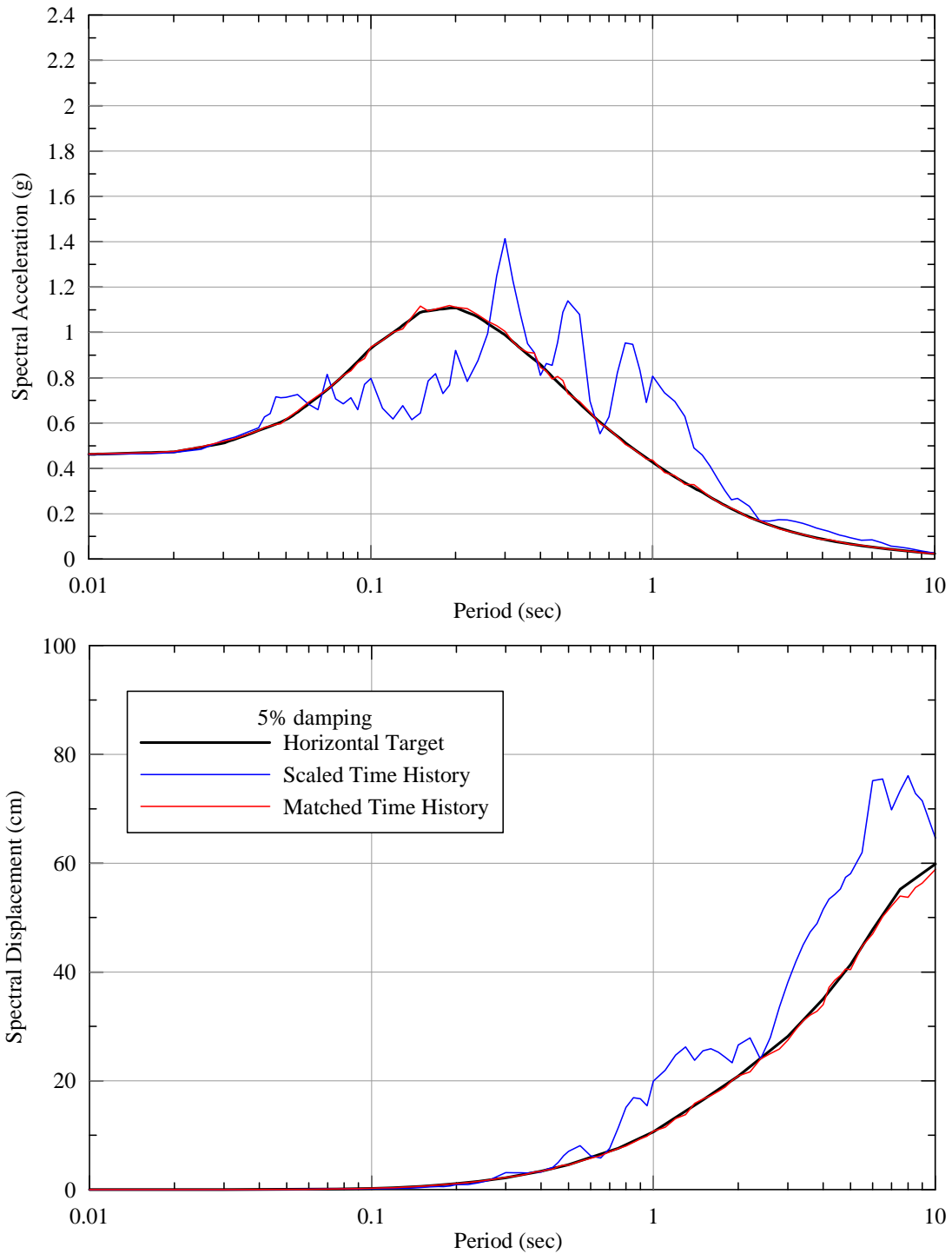


**Figure 19: Acceleration and Displacement Response Spectra. Seed Motion: 1999 Chi-Chi Earthquake, TCU076 Station, N Component. Target: Fault Parallel, SEE  $V_{S30} = 3000$  ft/sec.**

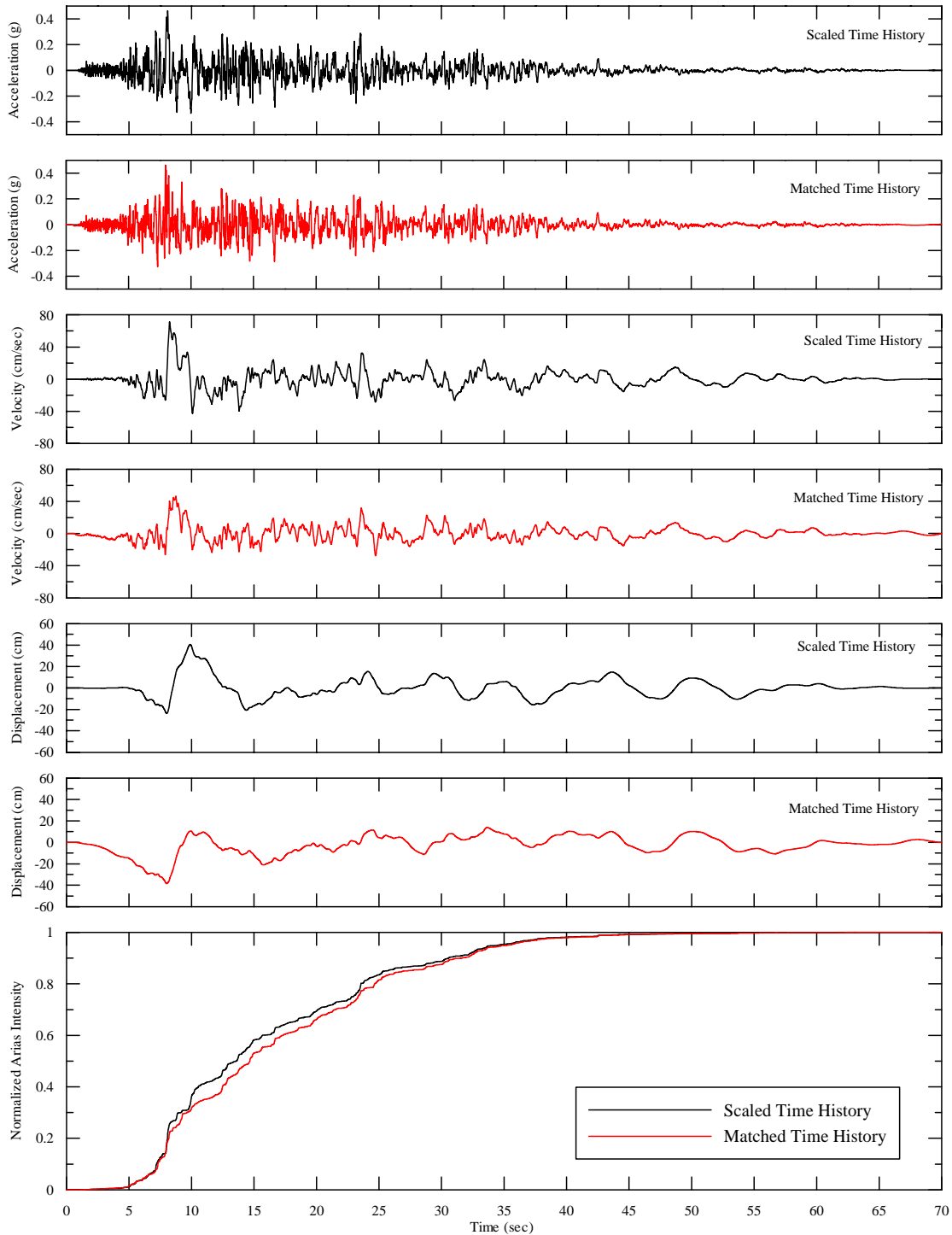


**Figure 20: Acceleration, Velocity, and Displacement Time Histories. Seed Motion: 1999 Chi-Chi Earthquake, TCU076 Station, N Component. Target: Fault Parallel, SEE  $V_{S30} = 3000$  ft/sec.**

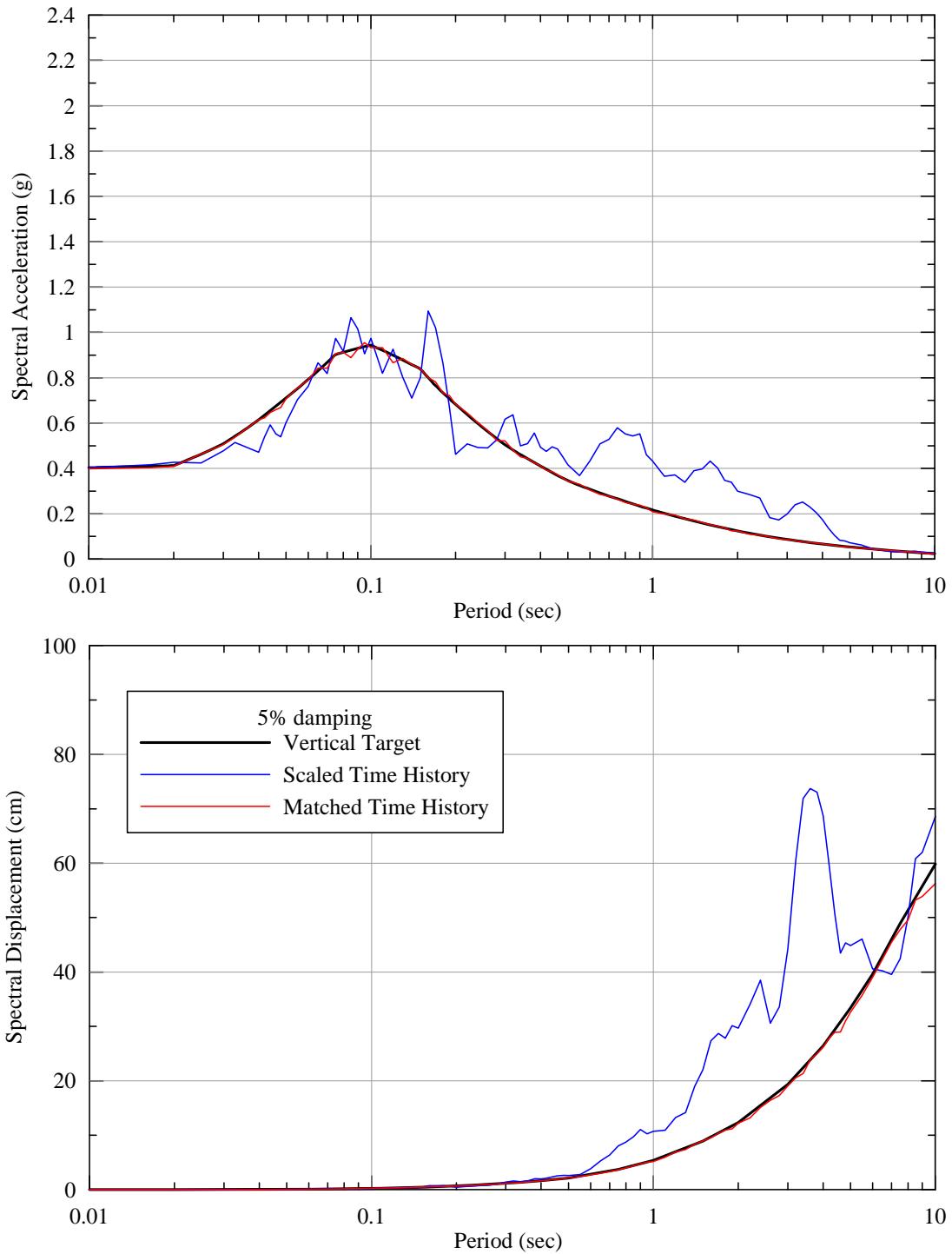


**Figure 21: Acceleration and Displacement Response Spectra. Seed Motion: 1999 Chi-Chi Earthquake, TCU076 Station, Vertical Component. Target: Vertical, SEE  $V_{S30} = 3000$  ft/sec.**

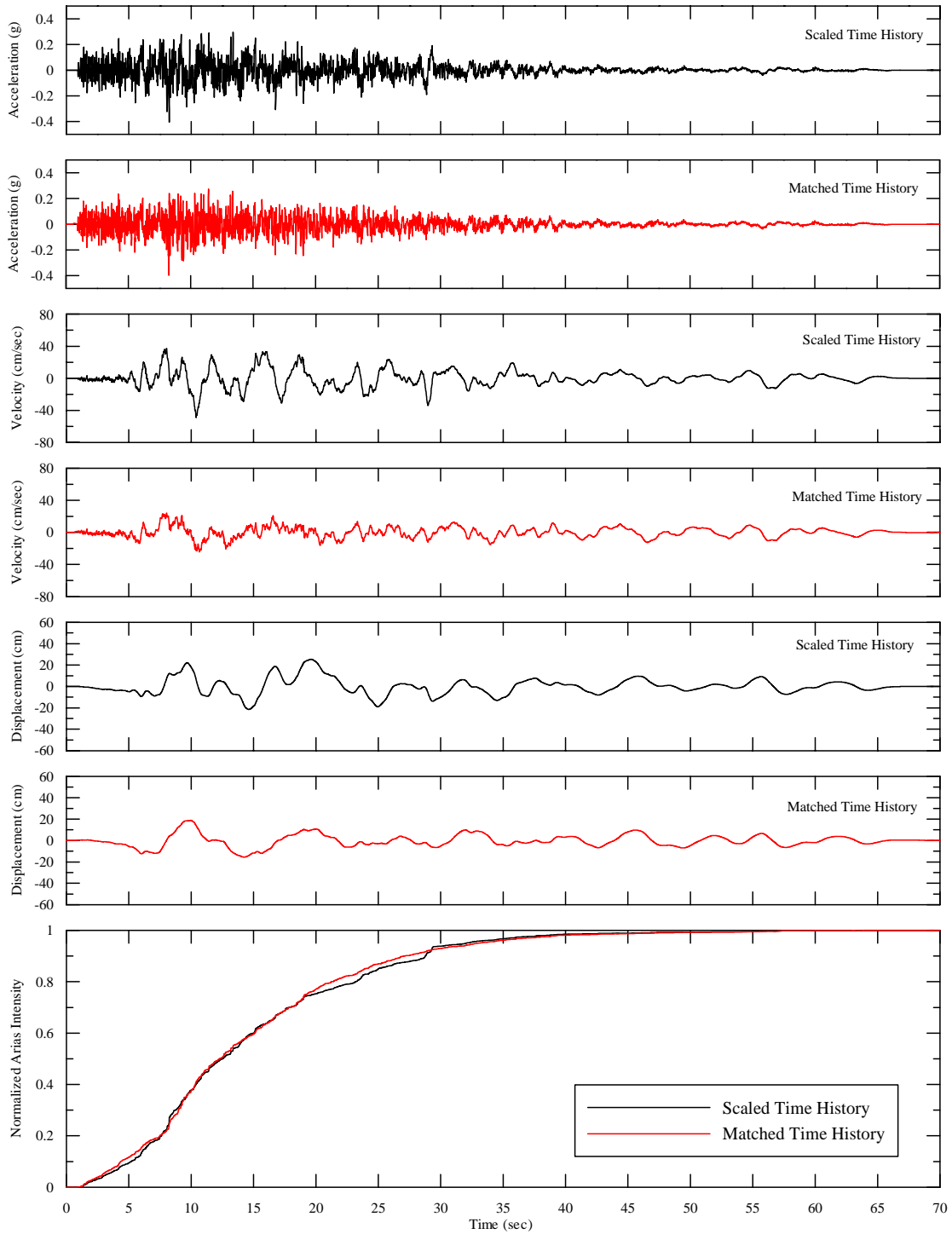


**Figure 22: Acceleration, Velocity, and Displacement Time Histories. Seed Motion: 1999 Chi-Chi Earthquake, TCU076 Station, Vertical Component. Target: Vertical, SEE  $V_{S30} = 3000$  ft/sec.**

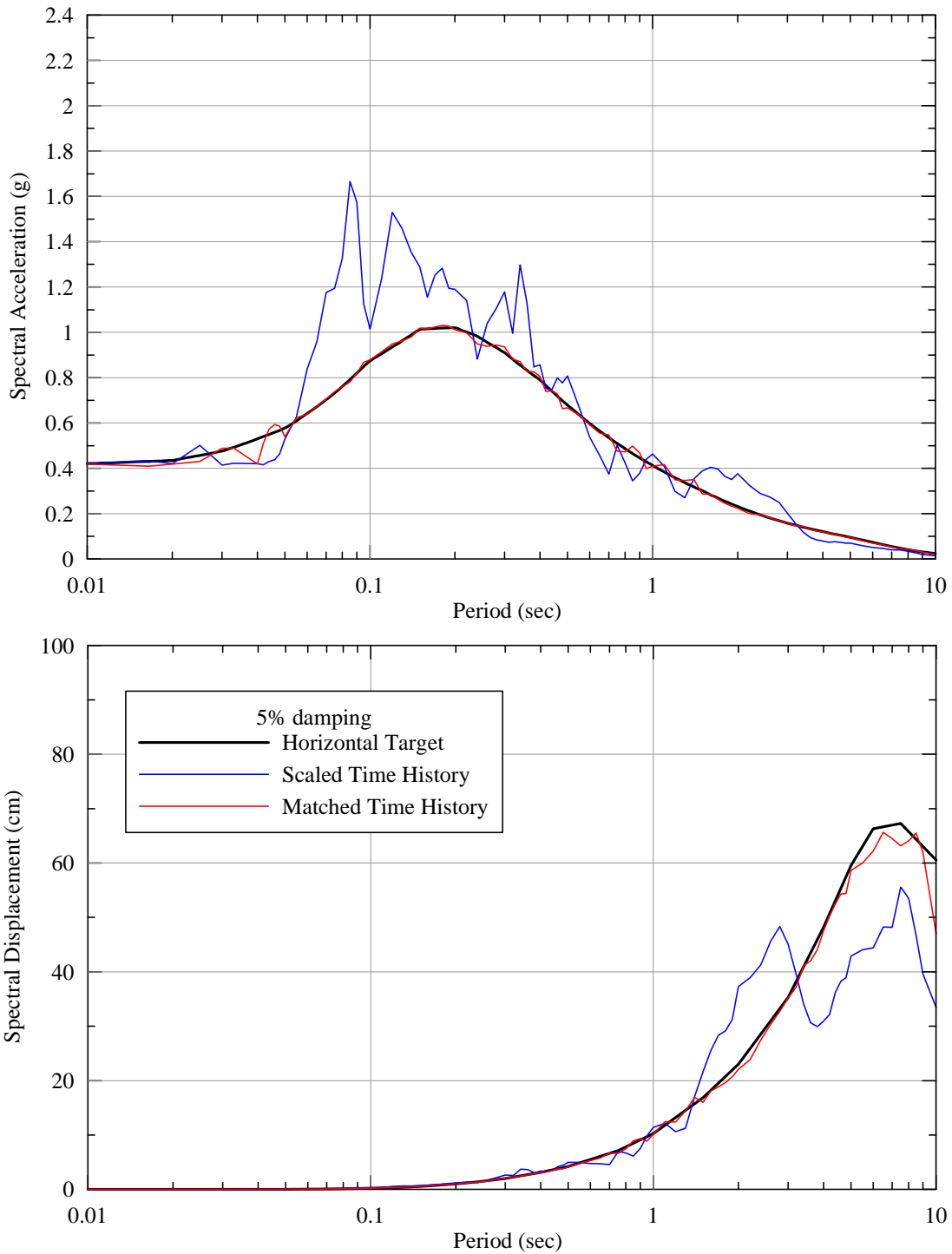


**Figure 23: Acceleration and Displacement Response Spectra. Seed Motion: 1990 Manjil Earthquake, Abbar Station, T Component. Target: Fault Normal, SEE  $V_{S30} = 5000$  ft/sec.**

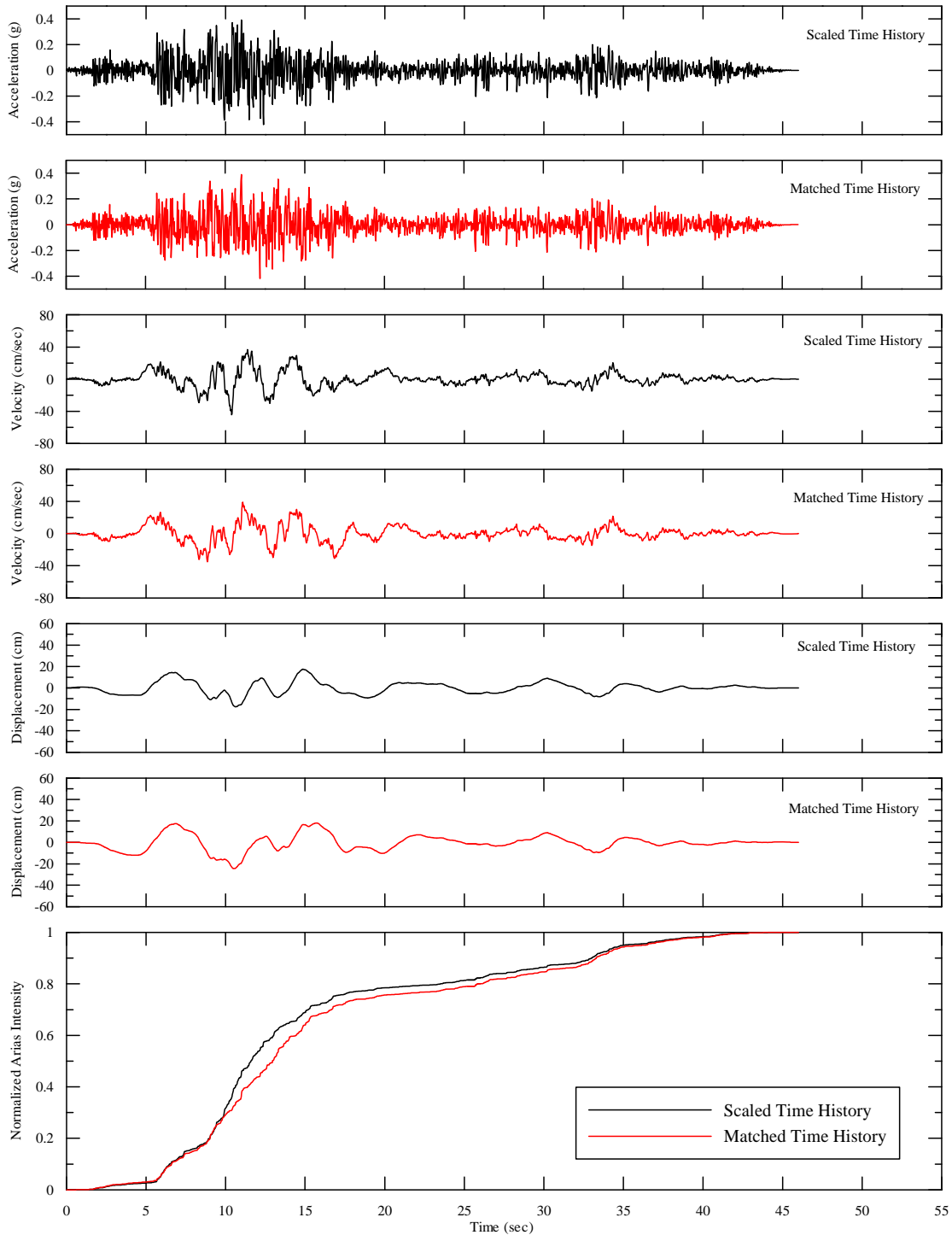


**Figure 24: Acceleration, Velocity, and Displacement Time Histories. Seed Motion: 1990 Manjil Earthquake, Abbar Station, T Component. Target: Fault Normal, SEE  $V_{S30} = 5000$  ft/sec.**

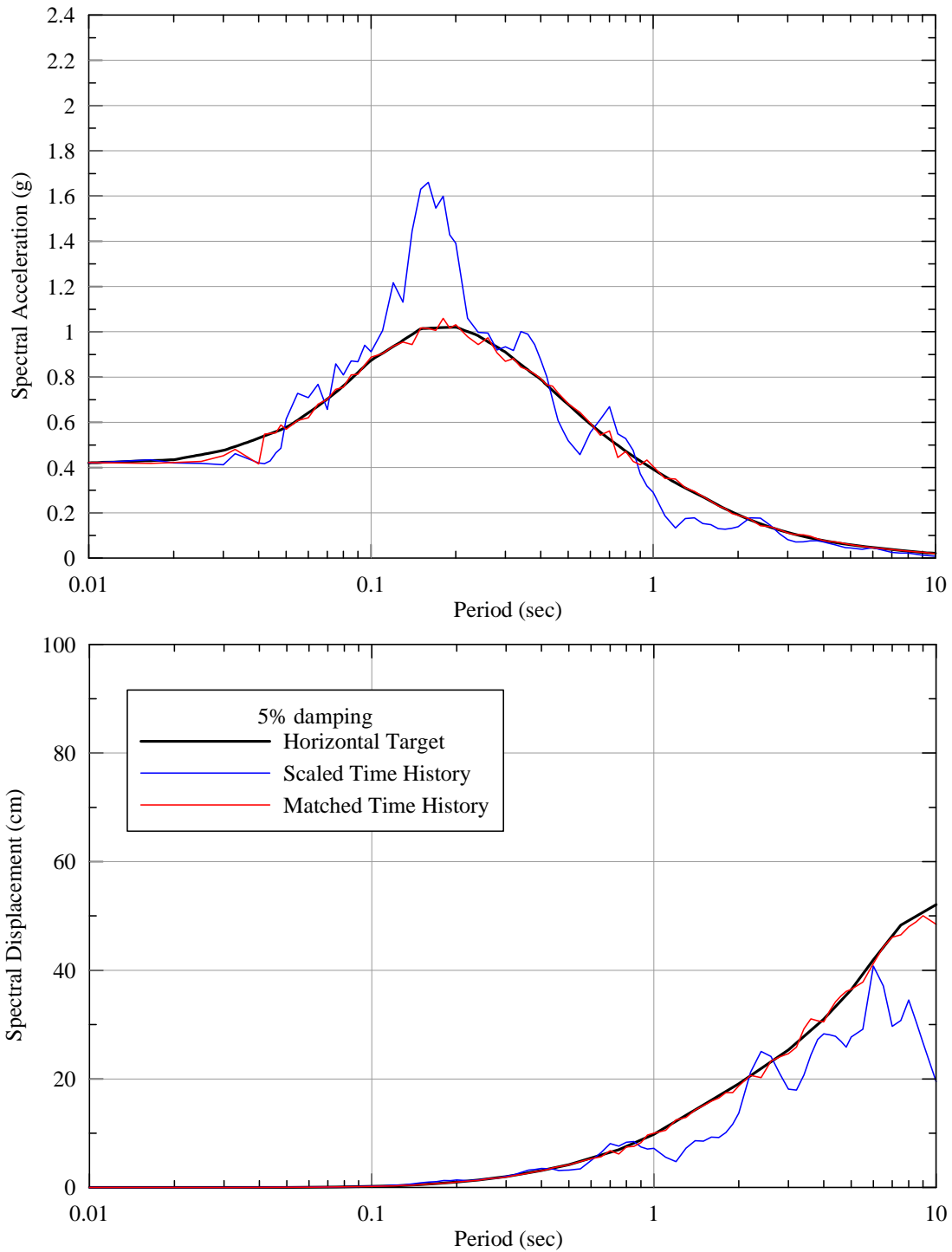


**Figure 25: Acceleration and Displacement Response Spectra. Seed Motion: 1990 Manjil Earthquake, Abbar Station, L Component. Target: Fault Parallel, SEE  $V_{S30} = 5000$  ft/sec.**

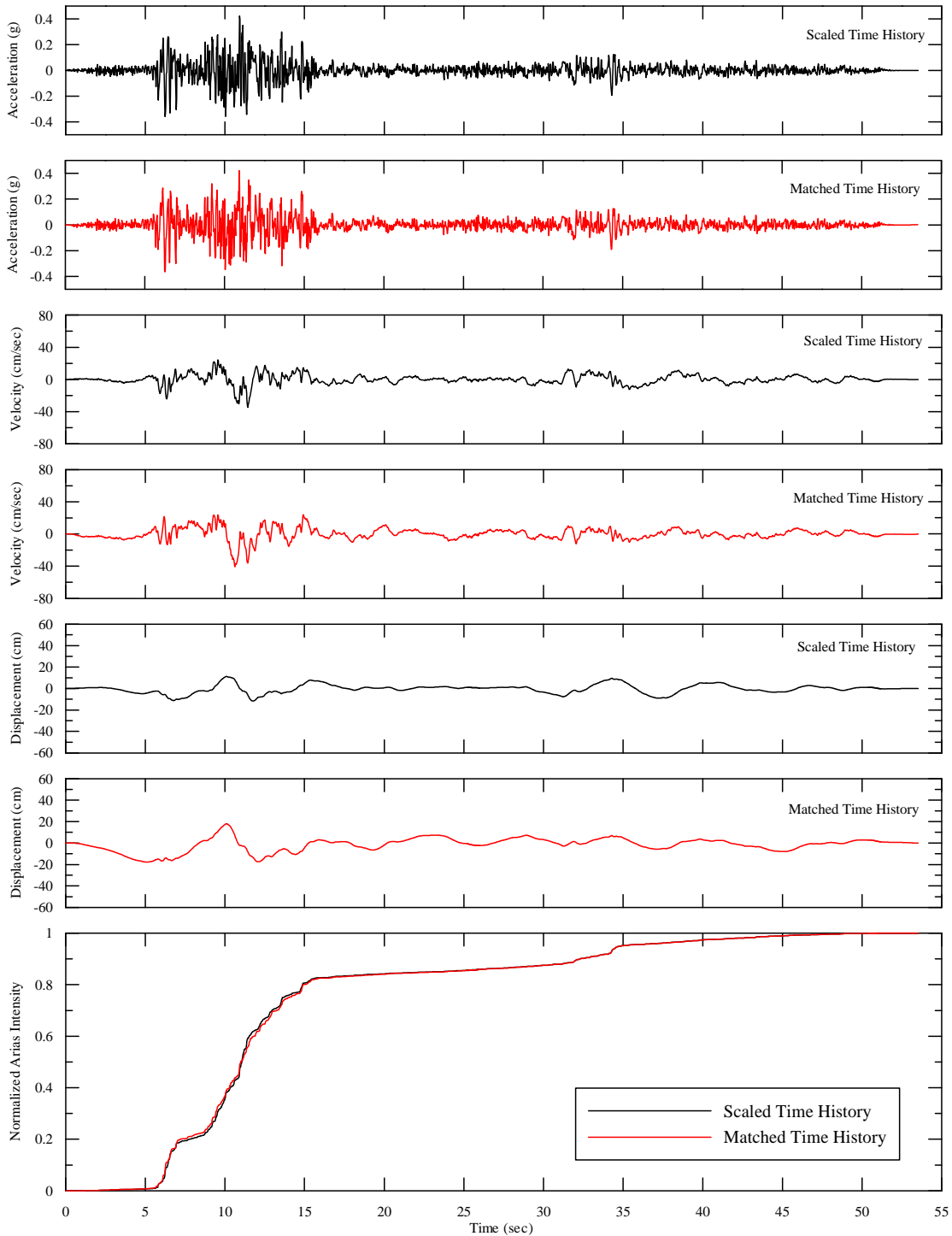


**Figure 26: Acceleration, Velocity, and Displacement Time Histories. Seed Motion: 1990 Manjil Earthquake, Abbar Station, L Component. Target: Fault Parallel, SEE  $V_{S30} = 5000$  ft/sec.**

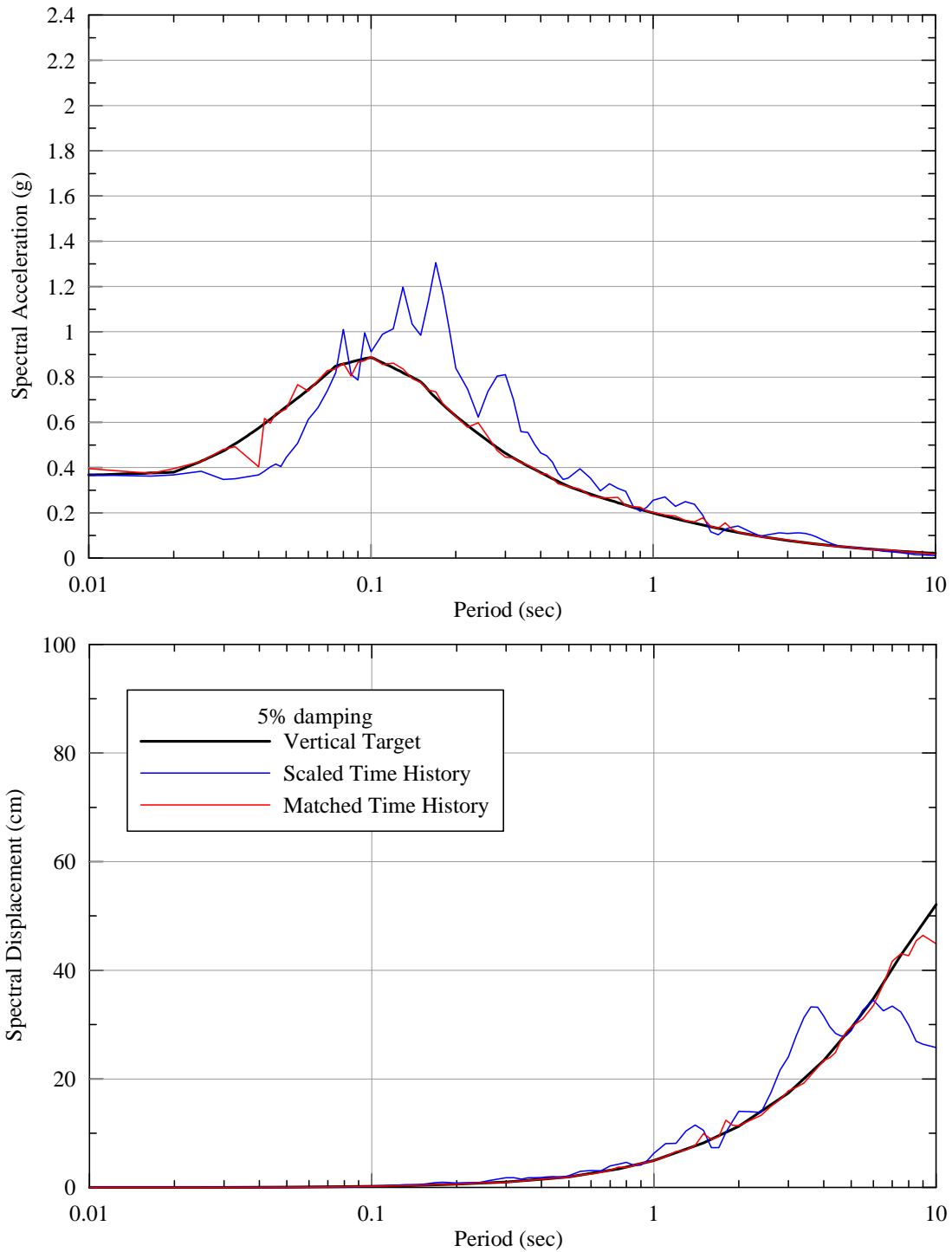


**Figure 27: Acceleration and Displacement Response Spectra. Seed Motion: 1990 Manjil Earthquake, Abbar Station, Vertical Component. Target: Vertical, SEE  $V_{S30} = 5000$  ft/sec.**

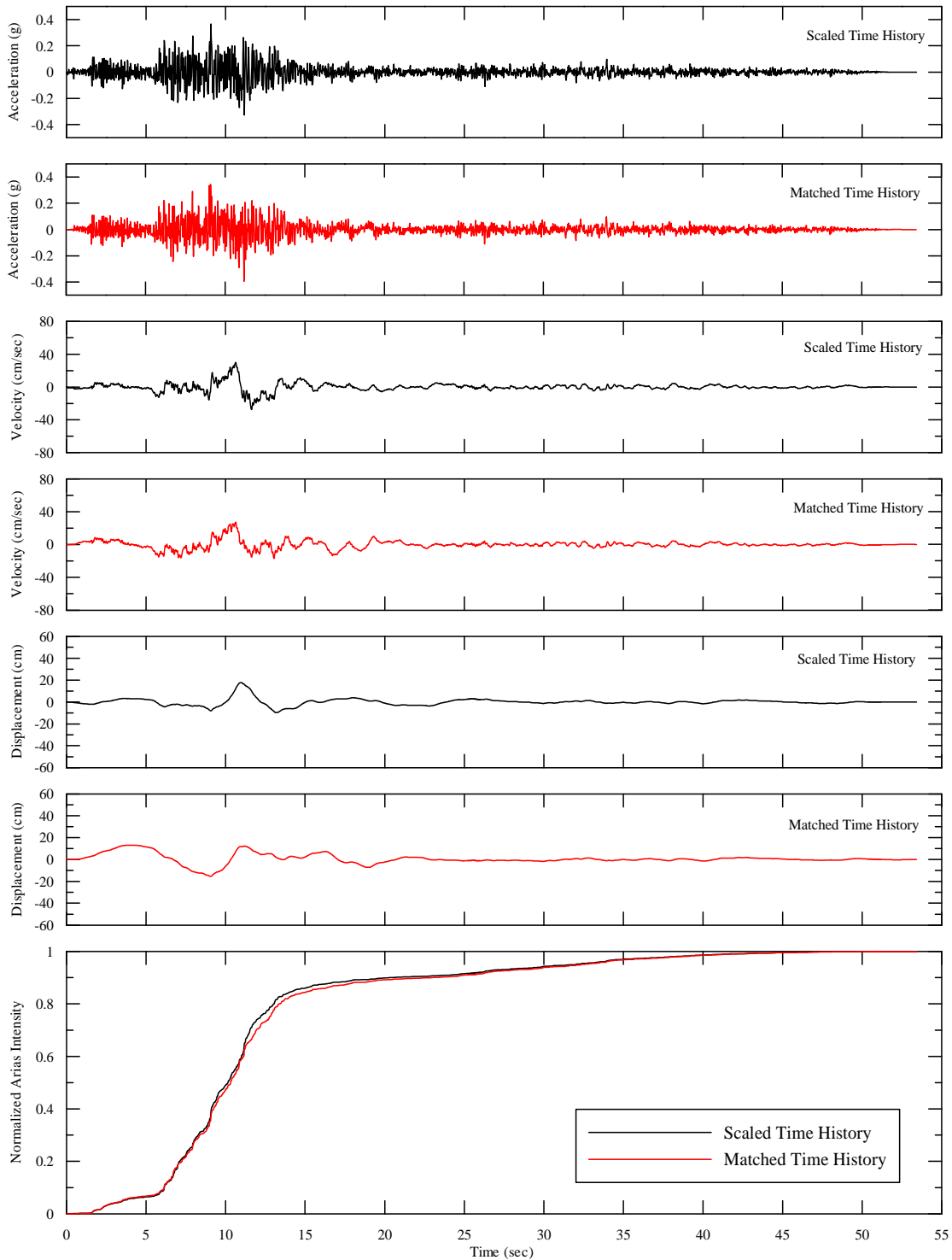


**Figure 28: Acceleration, Velocity, and Displacement Time Histories. Seed Motion: 1990 Manjil Earthquake, Abbar Station, Vertical Component. Target: Vertical, SEE  $V_{S30} = 5000$  ft/sec.**

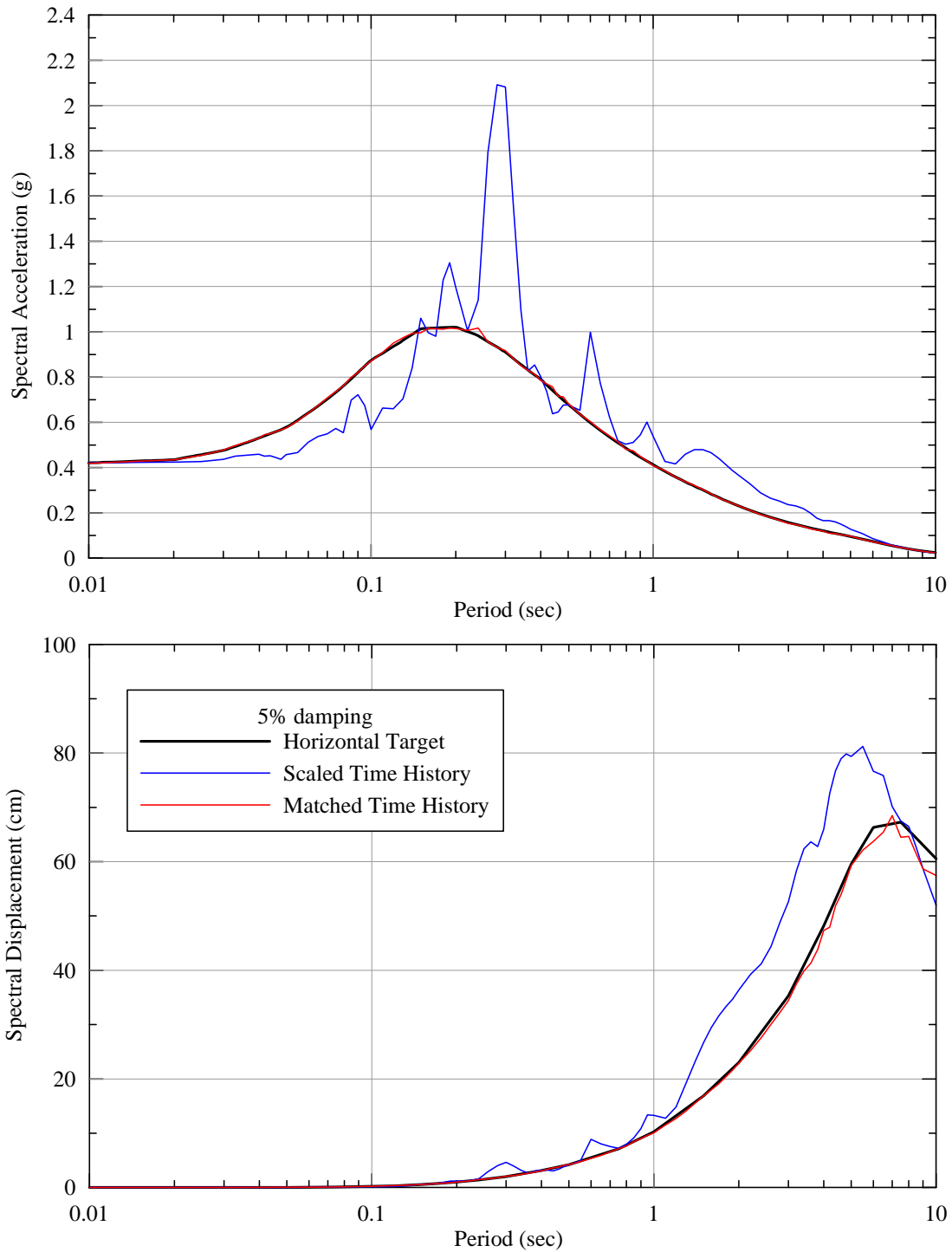


**Figure 29: Acceleration and Displacement Response Spectra. Seed Motion: 1999 Kocaeli Earthquake, Izmit Station, 90 degrees Component. Target: Fault Normal, SEE  $V_{S30} = 5000$  ft/sec.**

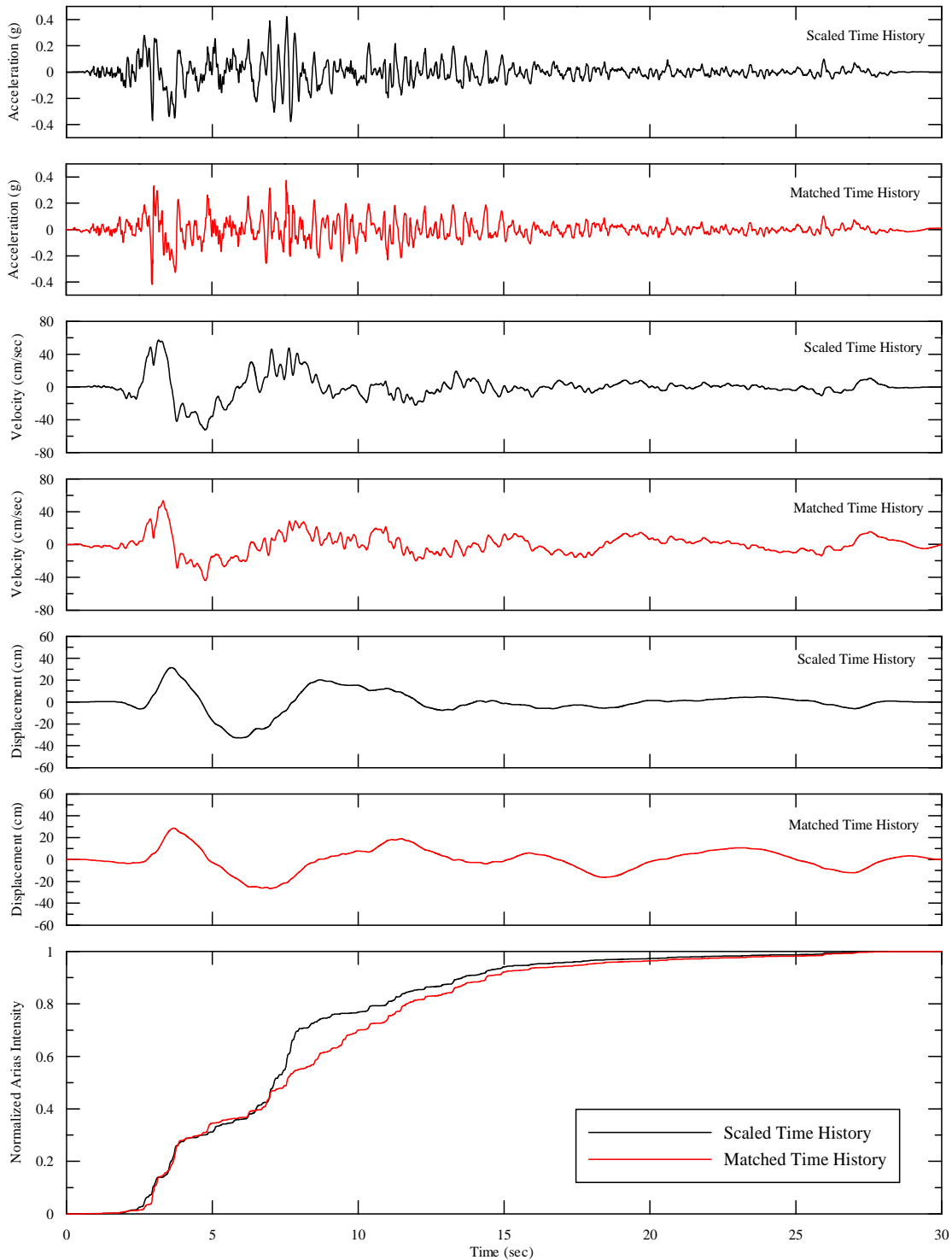


**Figure 30: Acceleration, Velocity, and Displacement Time Histories. Seed Motion: 1999 Kocaeli Earthquake, Izmit Station, 90 degrees Component. Target: Fault Normal, SEE  $V_{S30} = 5000$  ft/sec.**

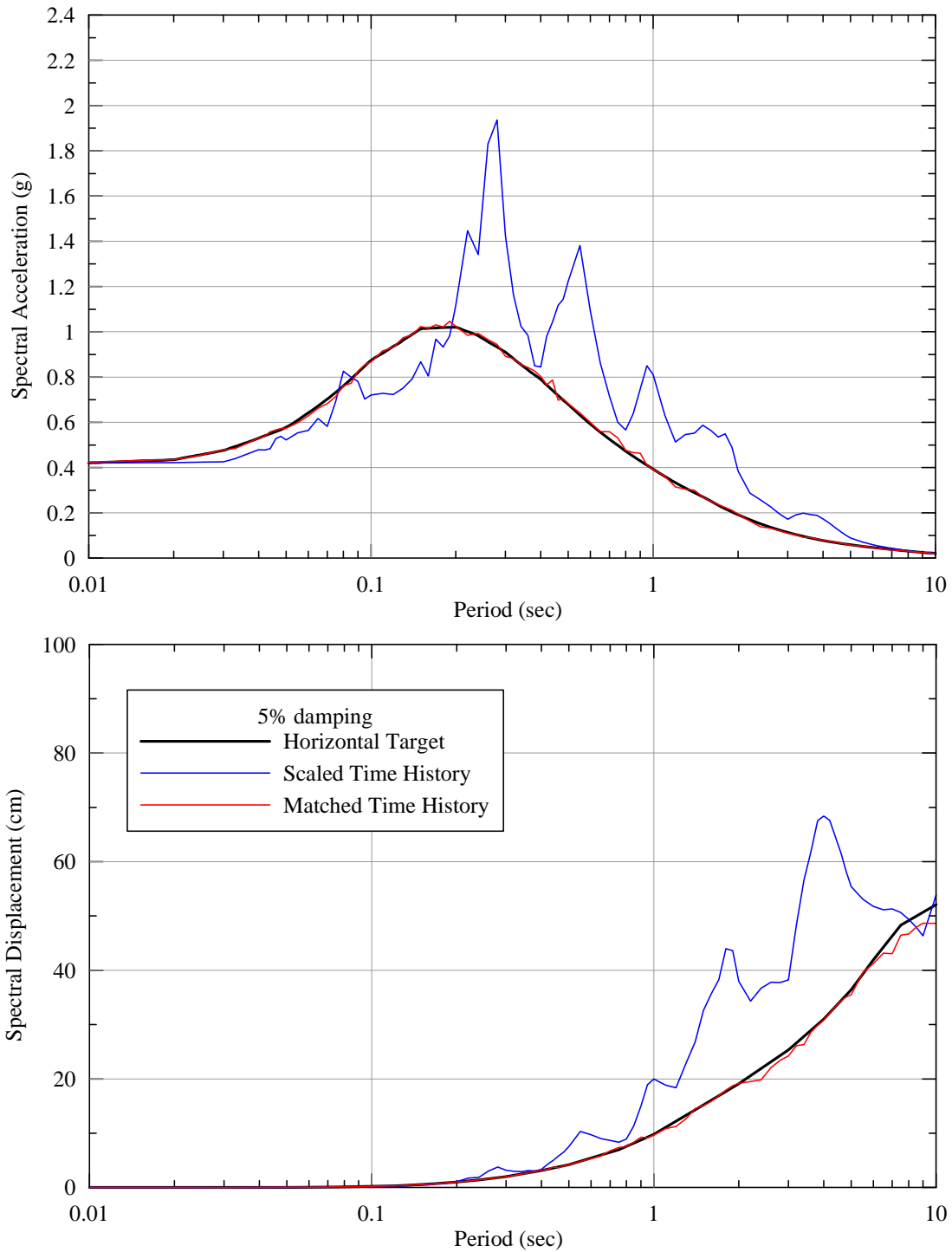


**Figure 31: Acceleration and Displacement Response Spectra. Seed Motion: 1999 Kocaeli Earthquake, Izmit Station, 180 degrees Component. Target: Fault Parallel, SEE  $V_{S30} = 5000$  ft/sec.**

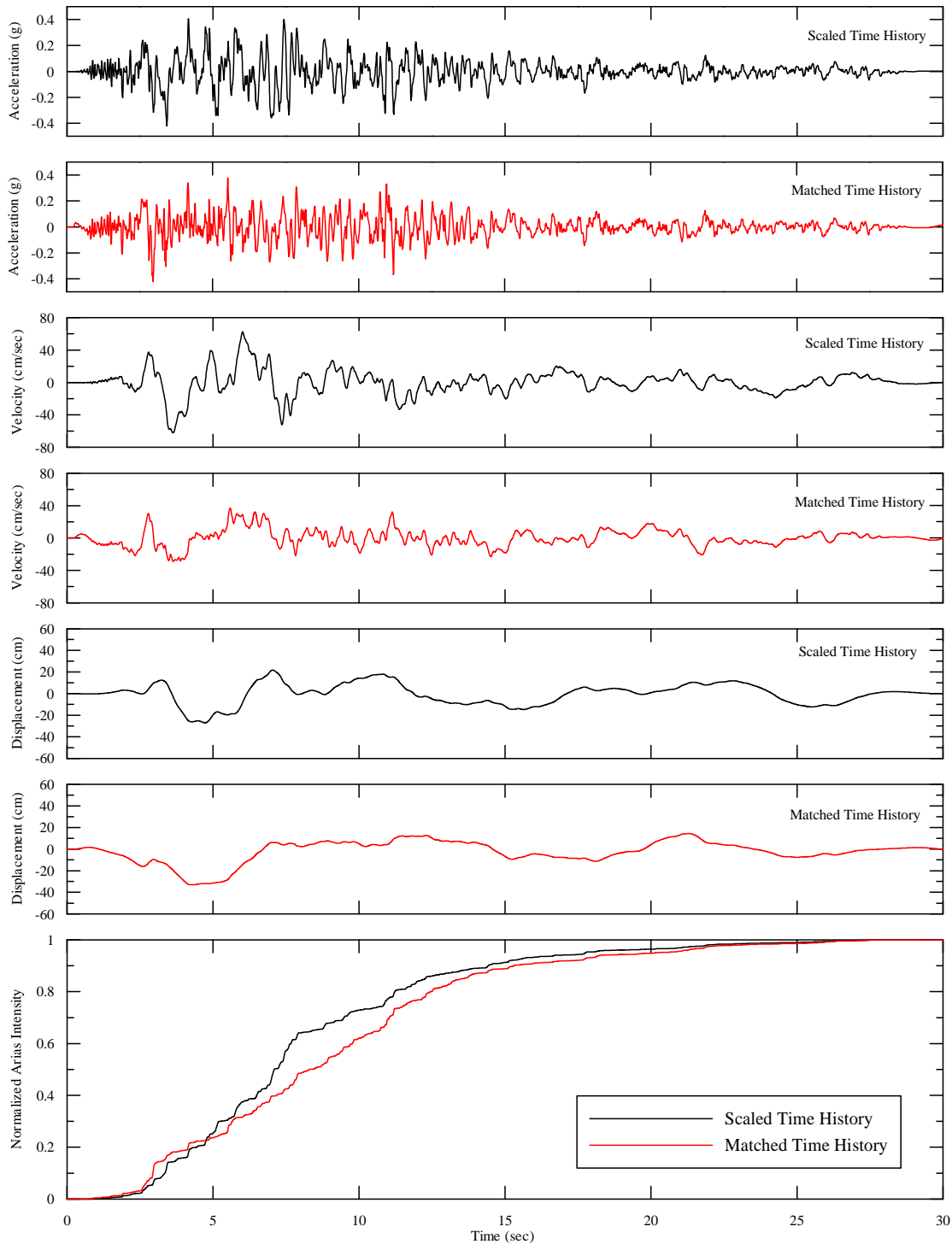


**Figure 32: Acceleration, Velocity, and Displacement Time Histories. Seed Motion: 1999 Kocaeli Earthquake, Izmit Station, 180 degrees Component. Target: Fault Parallel, SEE  $V_{S30} = 5000$  ft/sec.**

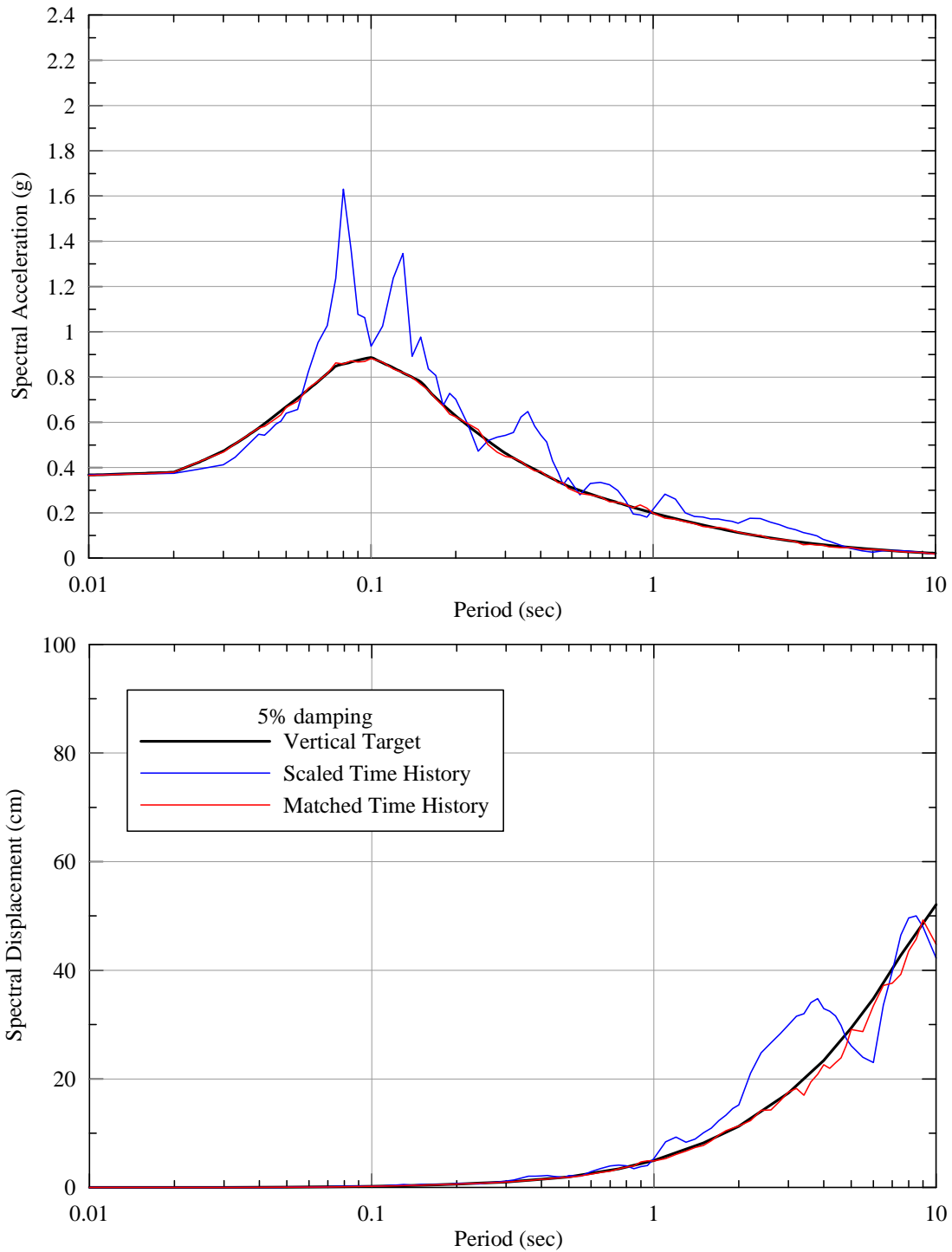


**Figure 33: Acceleration and Displacement Response Spectra. Seed Motion: 1999 Kocaeli Earthquake, Izmit Station, Vertical Component. Target: Vertical, SEE  $V_{S30} = 5000$  ft/sec.**

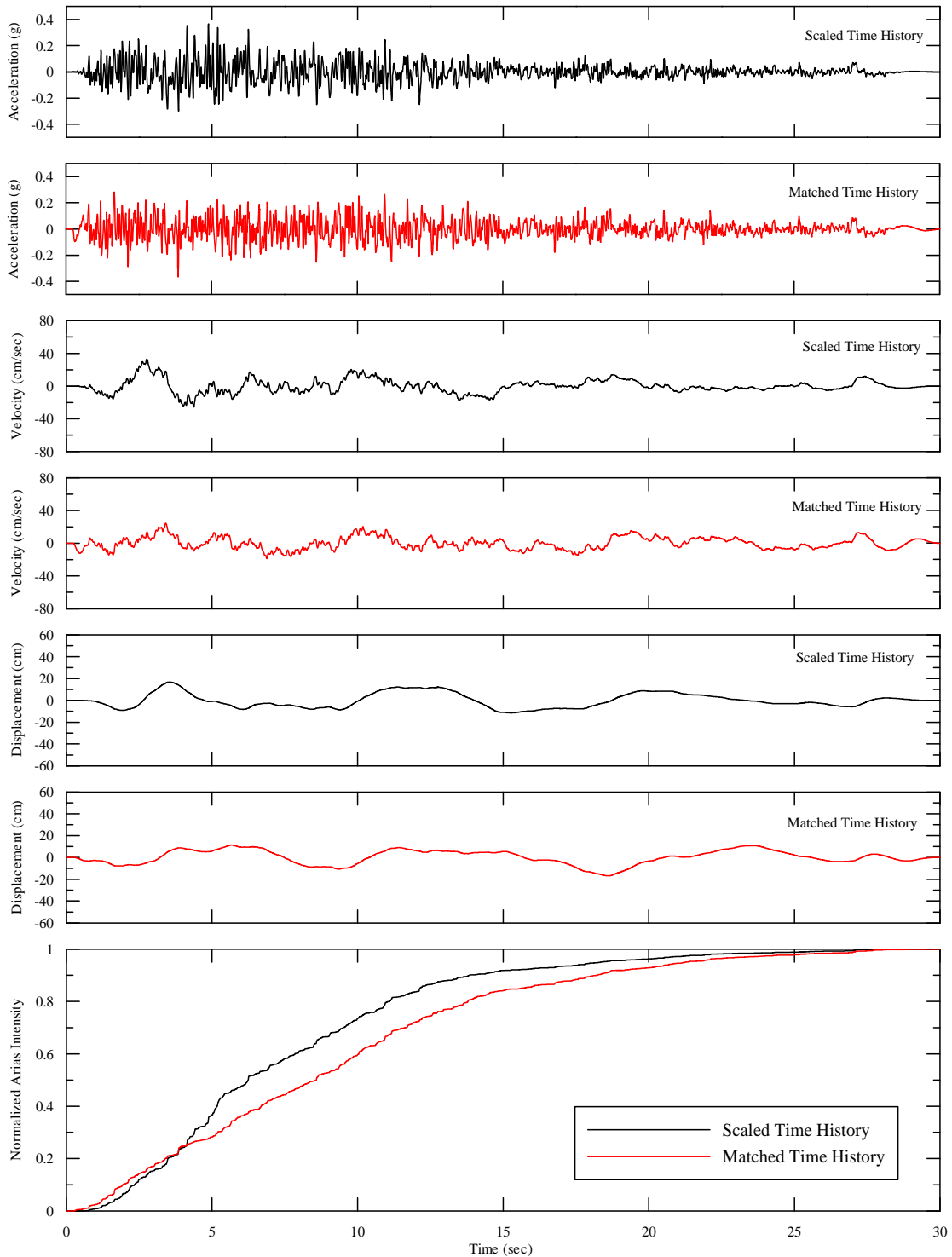


**Figure 34: Acceleration, Velocity, and Displacement Time Histories. Seed Motion: 1999 Kocaeli Earthquake, Izmit Station, Vertical Component. Target: Vertical, SEE  $V_{S30} = 5000$  ft/sec.**

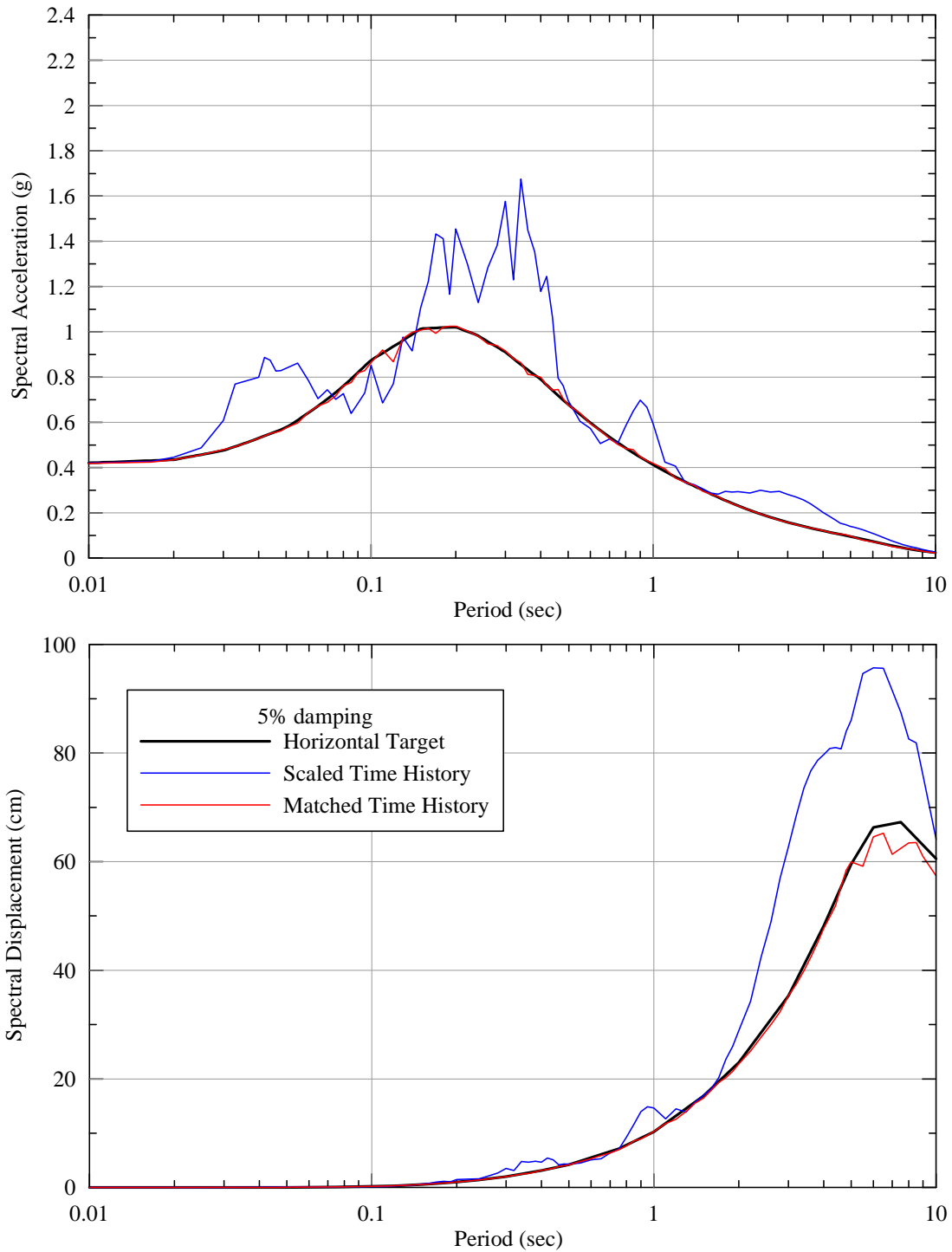


**Figure 35: Acceleration and Displacement Response Spectra. Seed Motion: 1999 Chi-Chi Earthquake, TCU076 Station, W Component. Target: Fault Normal, SEE  $V_{S30} = 5000$  ft/sec.**

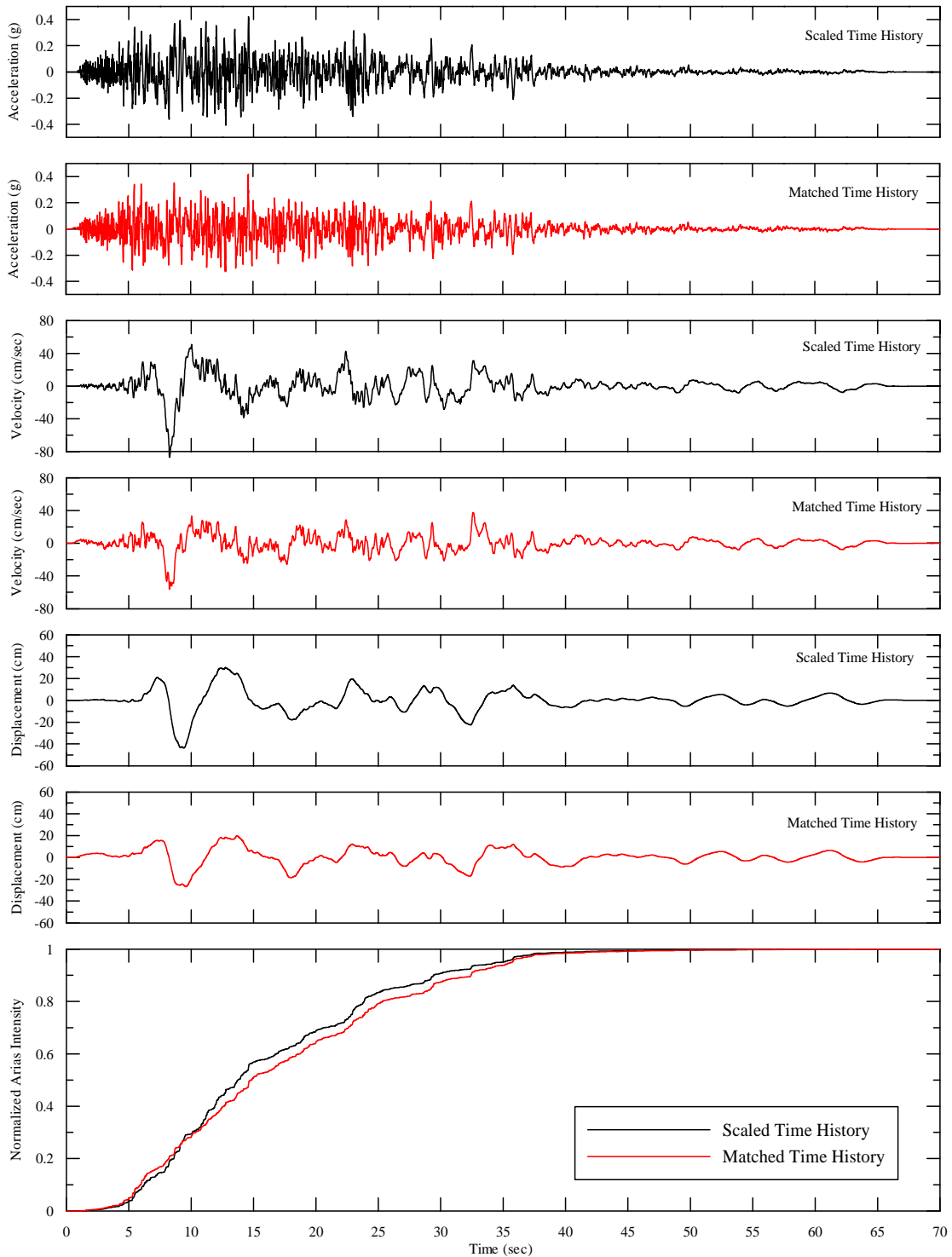


**Figure 36: Acceleration, Velocity, and Displacement Time Histories. Seed Motion: 1999 Chi-Chi Earthquake, TCU076 Station, W Component. Target: Fault Normal, SEE  $V_{S30} = 5000$  ft/sec.**

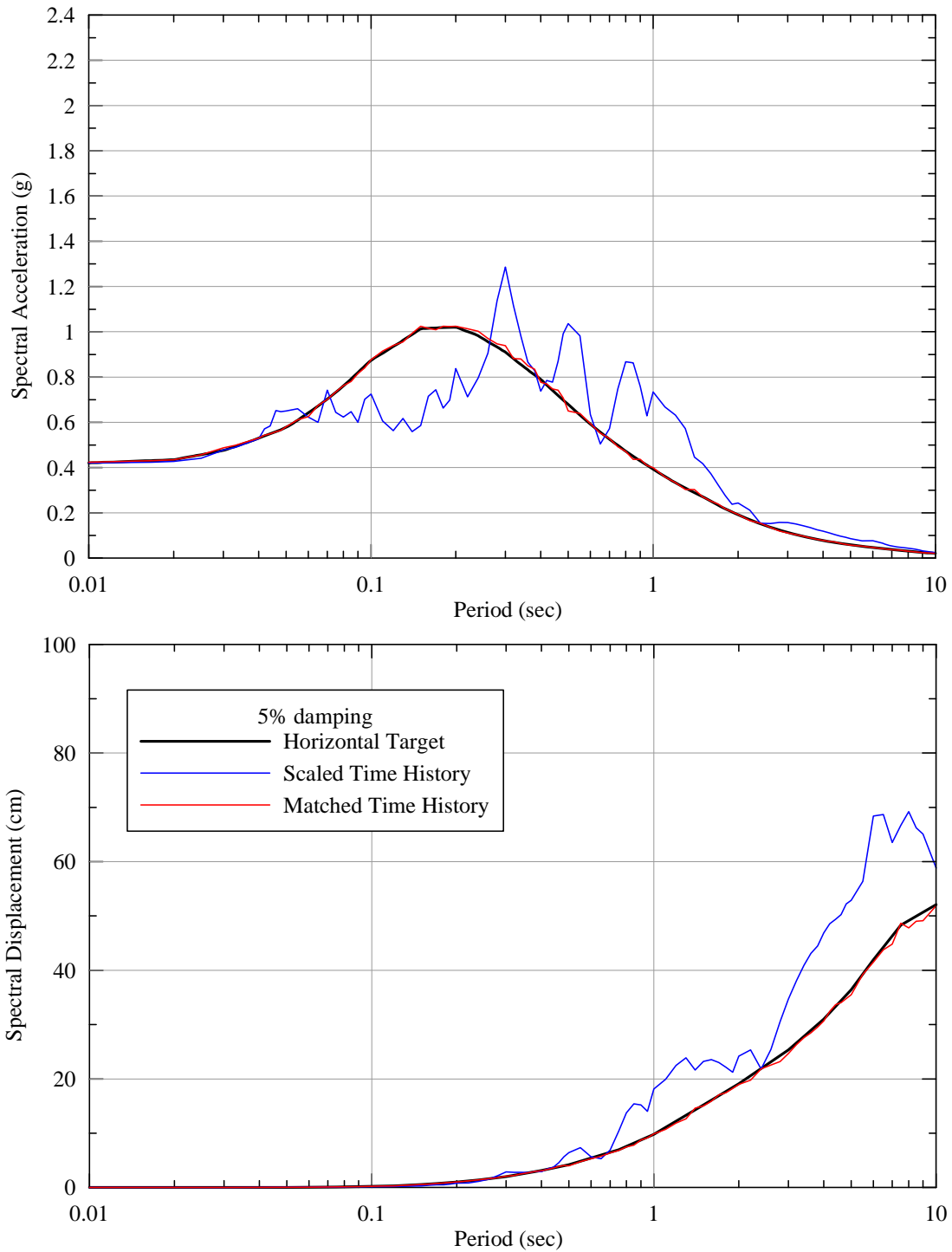


**Figure 37: Acceleration and Displacement Response Spectra. Seed Motion: 1999 Chi-Chi Earthquake, TCU076 Station, N Component. Target: Fault Parallel, SEE  $V_{S30} = 5000$  ft/sec.**

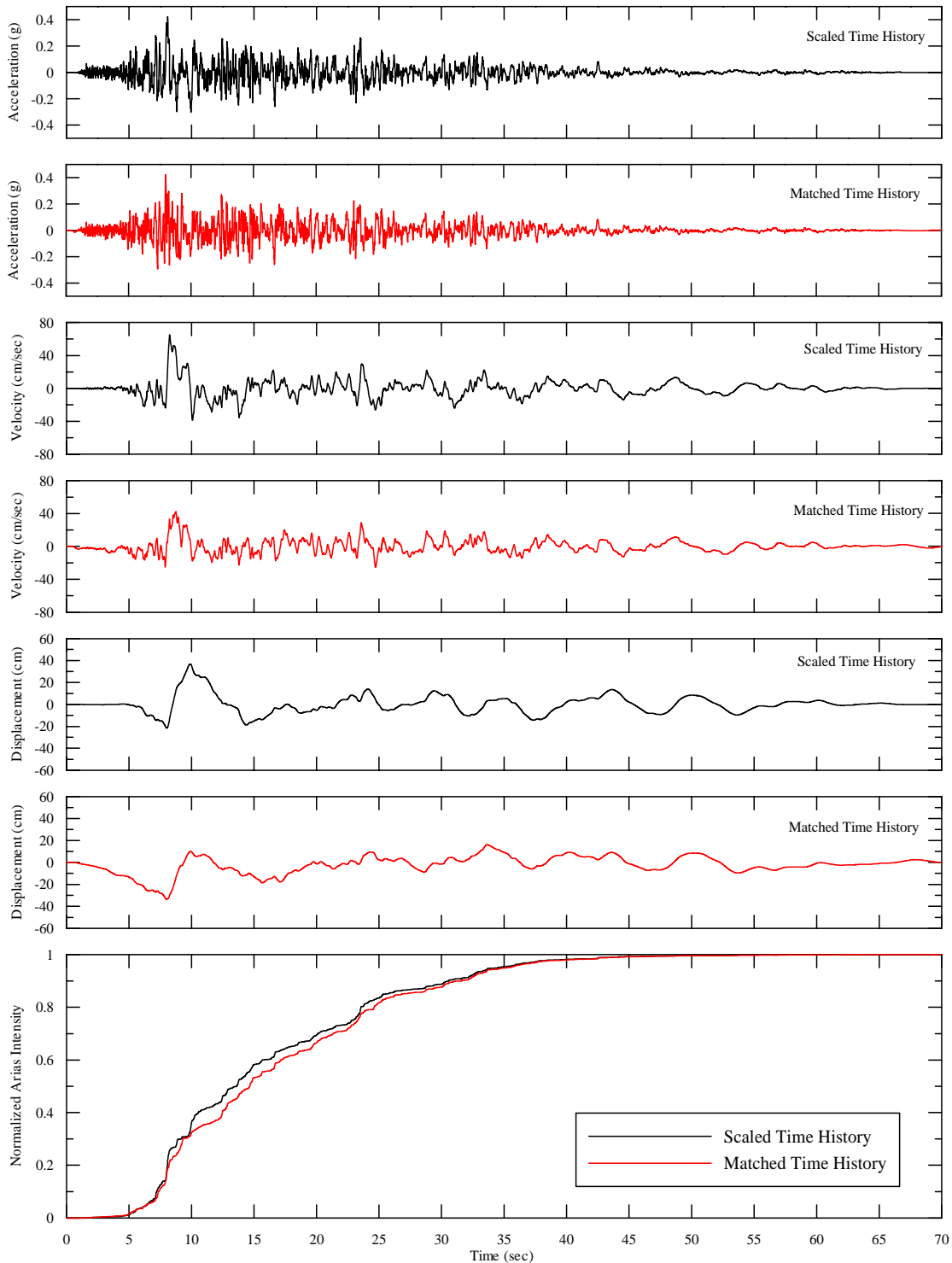


**Figure 38: Acceleration, Velocity, and Displacement Time Histories. Seed Motion: 1999 Chi-Chi Earthquake, TCU076 Station, N Component. Target: Fault Parallel, SEE  $V_{S30} = 5000$  ft/sec.**

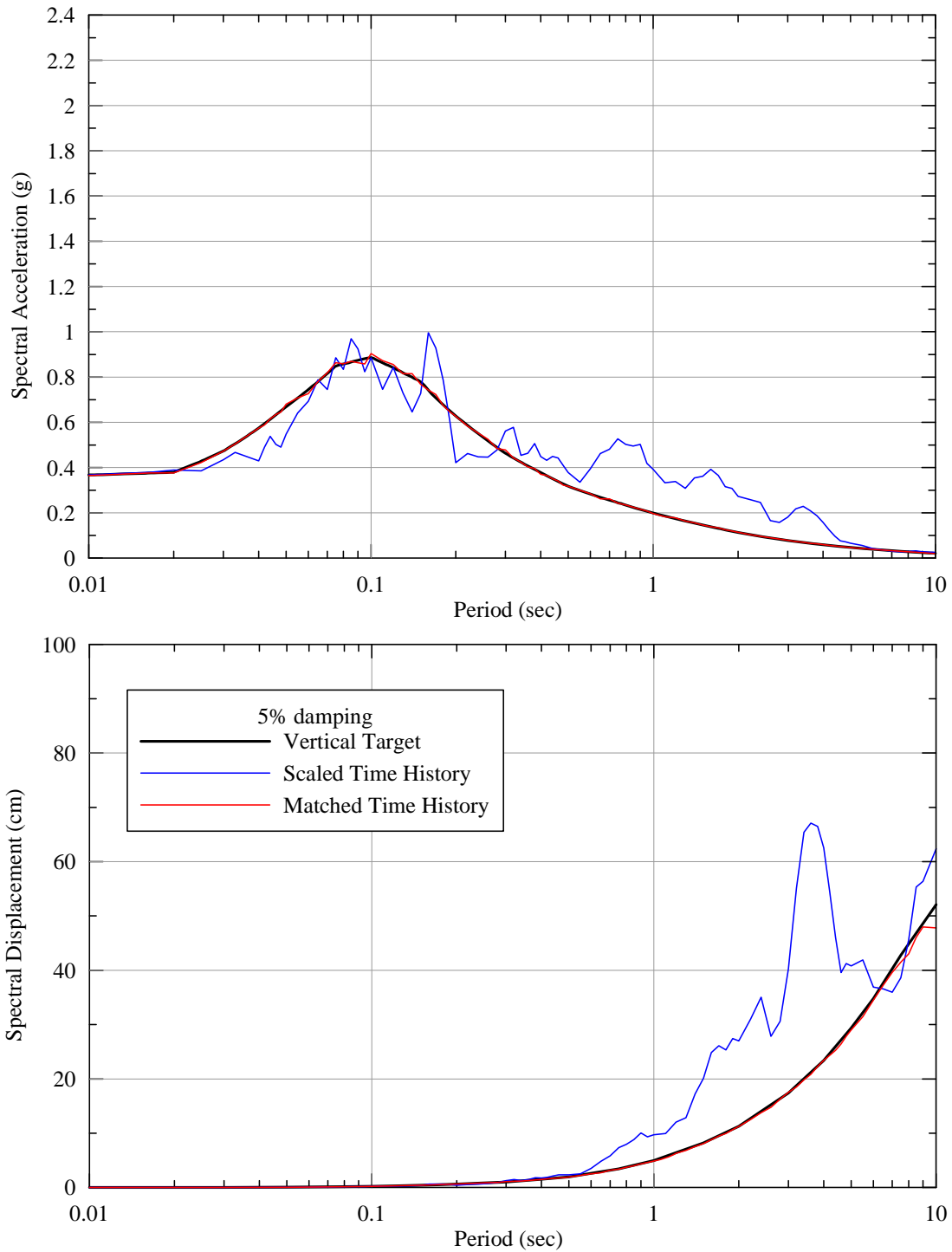


**Figure 39: Acceleration and Displacement Response Spectra. Seed Motion: 1999 Chi-Chi Earthquake, TCU076 Station, Vertical Component. Target: Vertical, SEE  $V_{S30} = 5000$  ft/sec.**

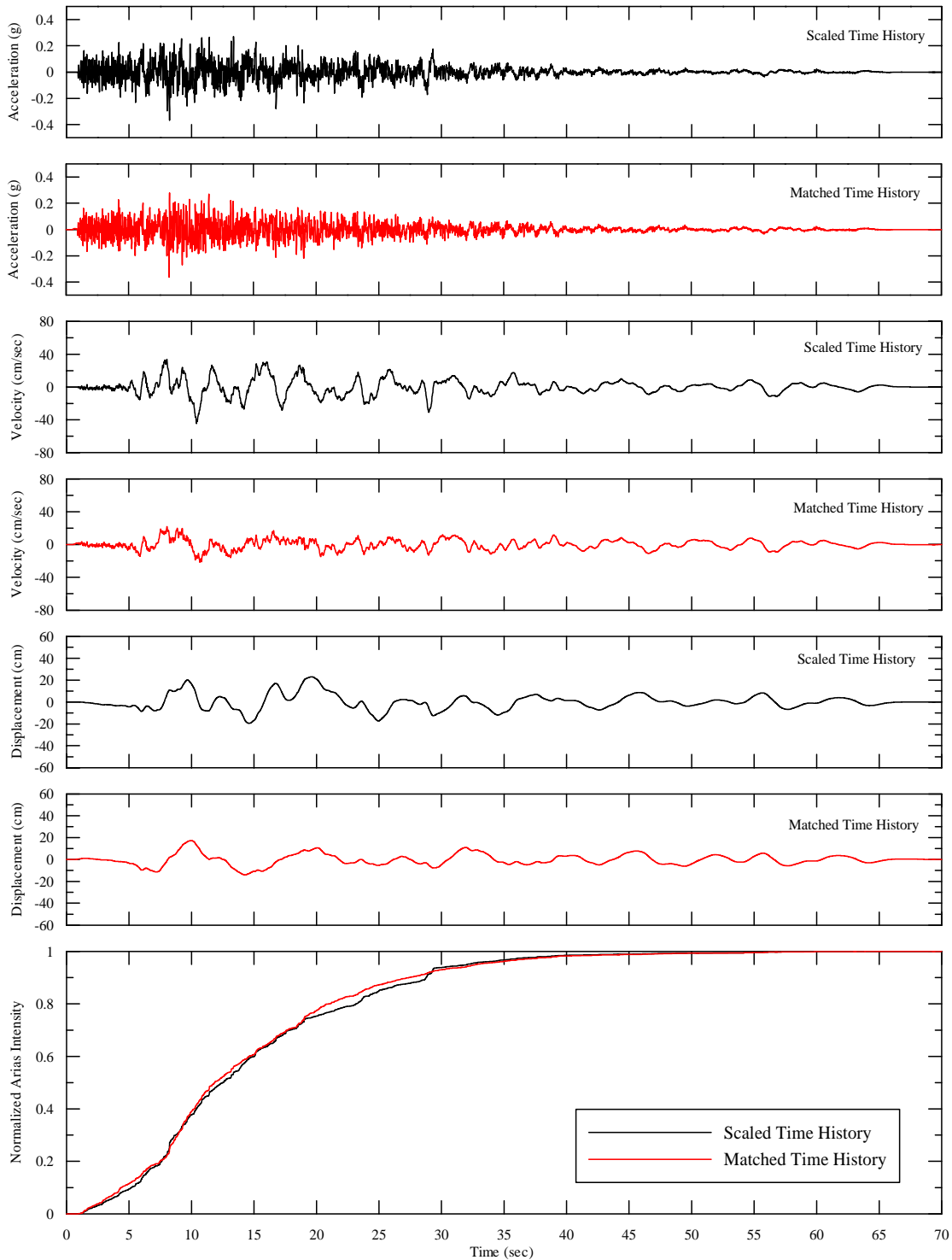


**Figure 40: Acceleration, Velocity, and Displacement Time Histories. Seed Motion: 1999 Chi-Chi Earthquake, TCU076 Station, Vertical Component. Target: Vertical, SEE  $V_{S30} = 5000$  ft/sec.**

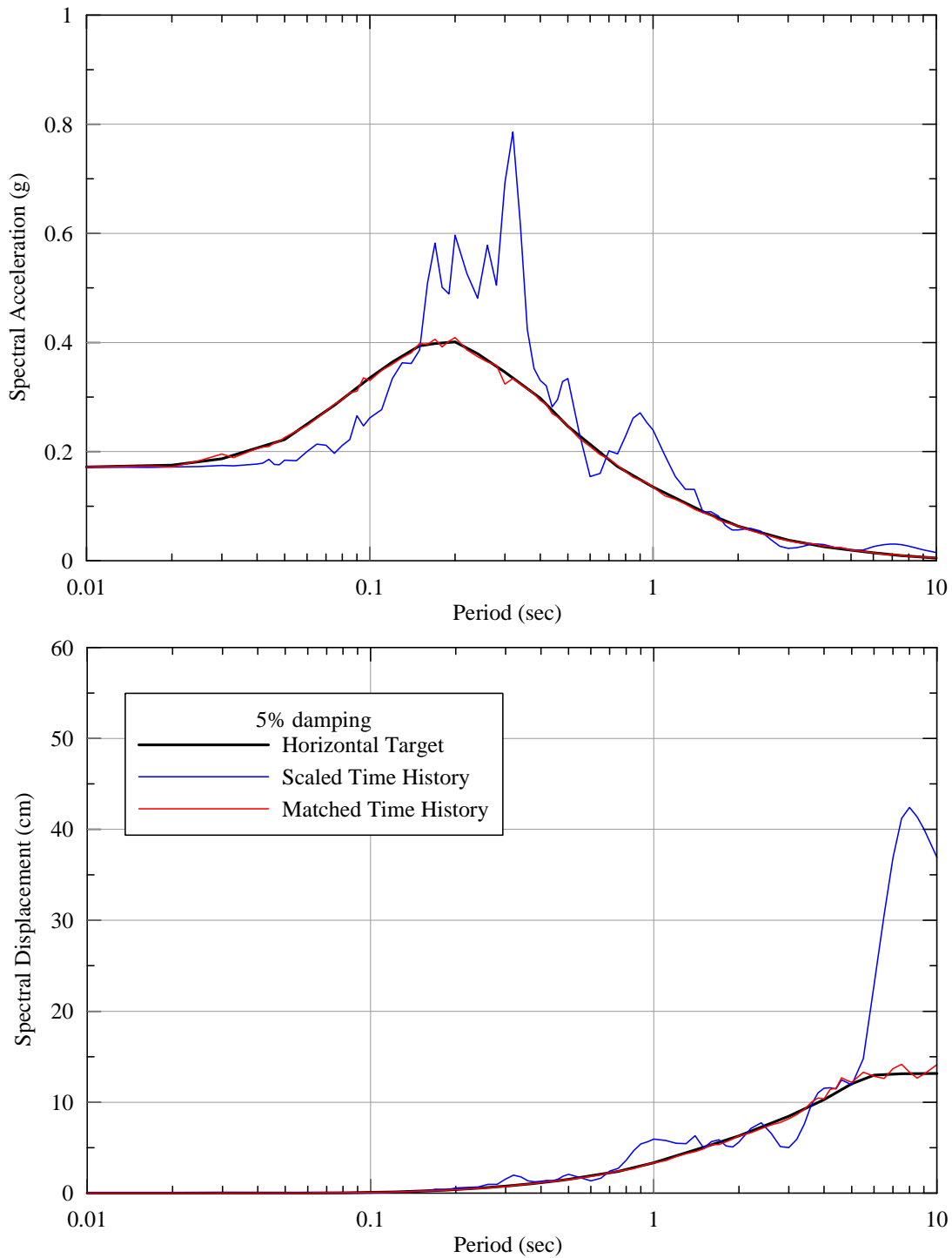


**Figure 41: Acceleration and Displacement Response Spectra. Seed Motion: 1999 Duzce Earthquake, Lamont Station, North Component. Target: Fault Normal, FEE  $V_{S30} = 3000$  ft/sec.**

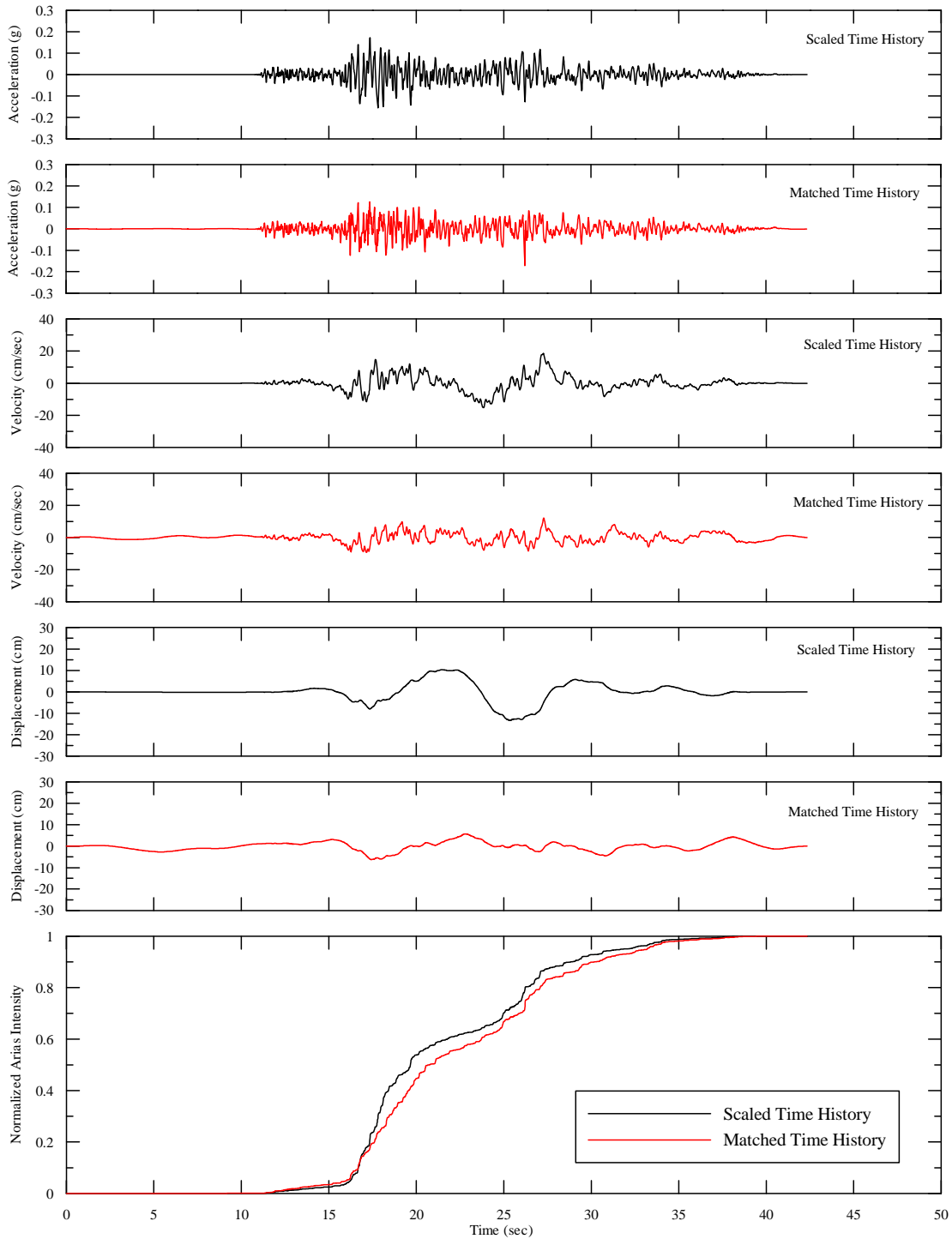


**Figure 42: Acceleration, Velocity, and Displacement Time Histories. Seed Motion: 1999 Duzce Earthquake, Lamont Station, North Component. Target: Fault Normal, FEE  $V_{S30} = 3000$  ft/sec.**

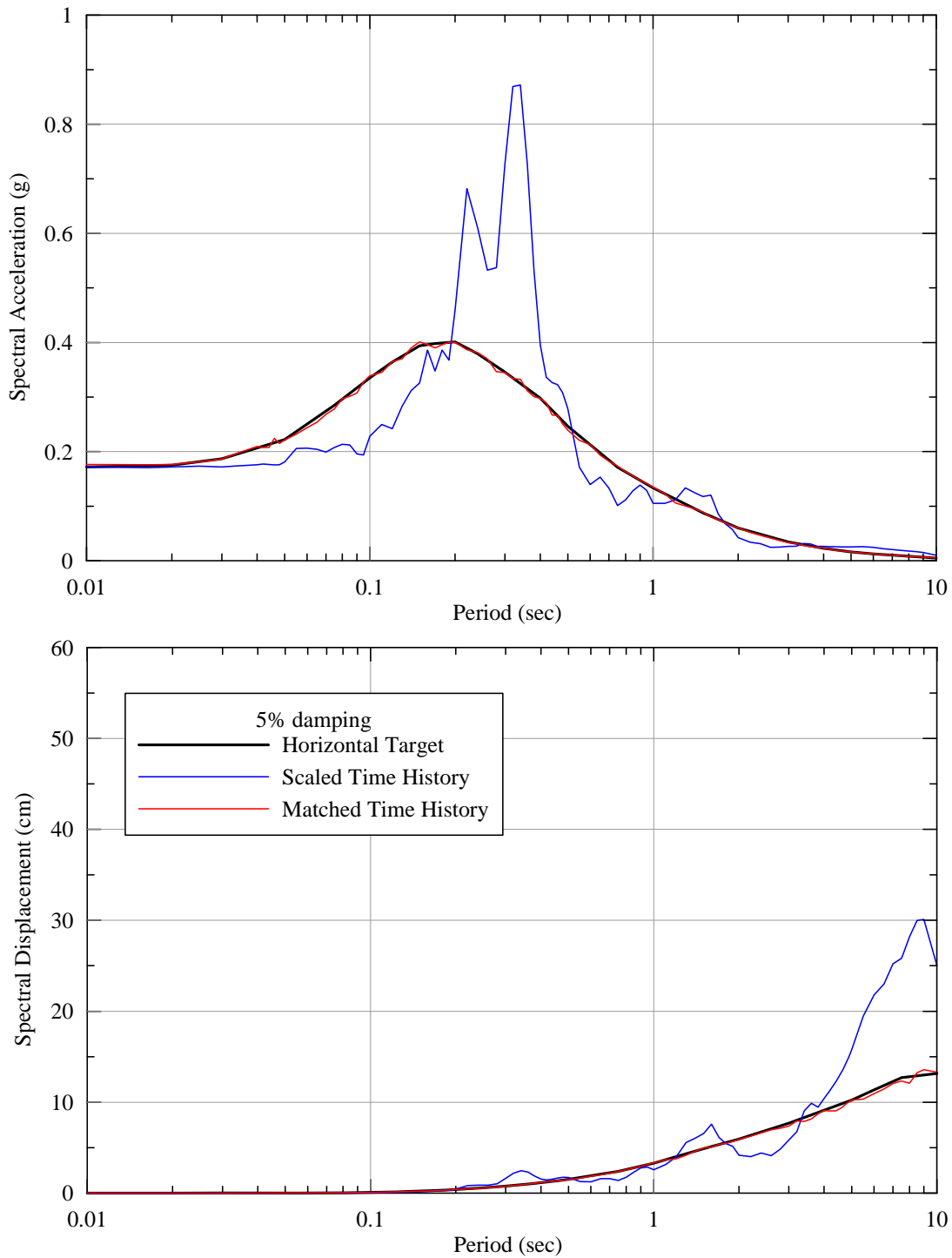


**Figure 43: Acceleration and Displacement Response Spectra. Seed Motion: 1999 Duzce Earthquake, Lamont Station, East Component. Target: Fault Parallel, FEE  $V_{S30} = 3000$  ft/sec.**

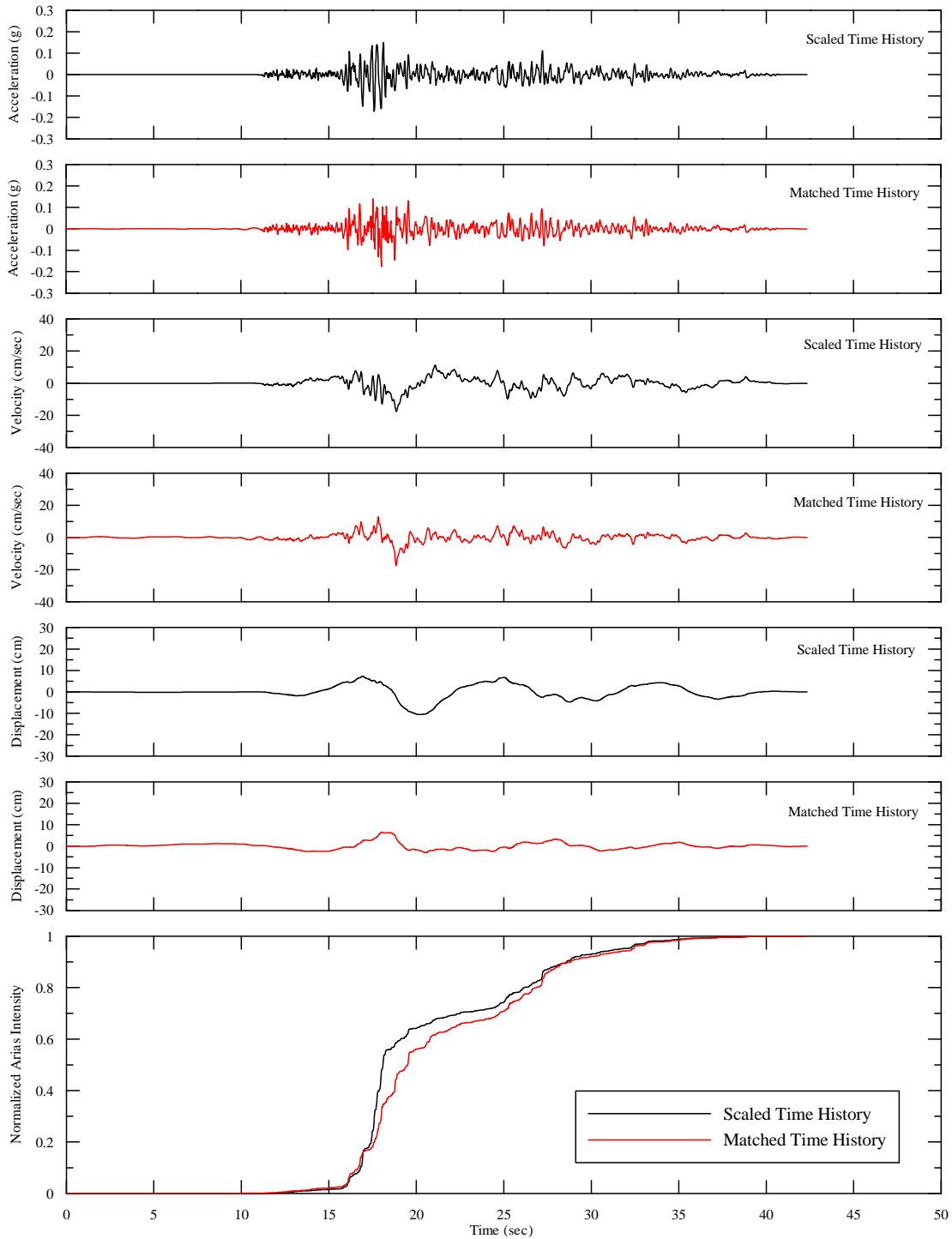


**Figure 44: Acceleration, Velocity, and Displacement Time Histories. Seed Motion: 1999 Duzce Earthquake, Lamont Station, East Component. Target: Fault Parallel, FEE  $V_{S30} = 3000$  ft/sec.**

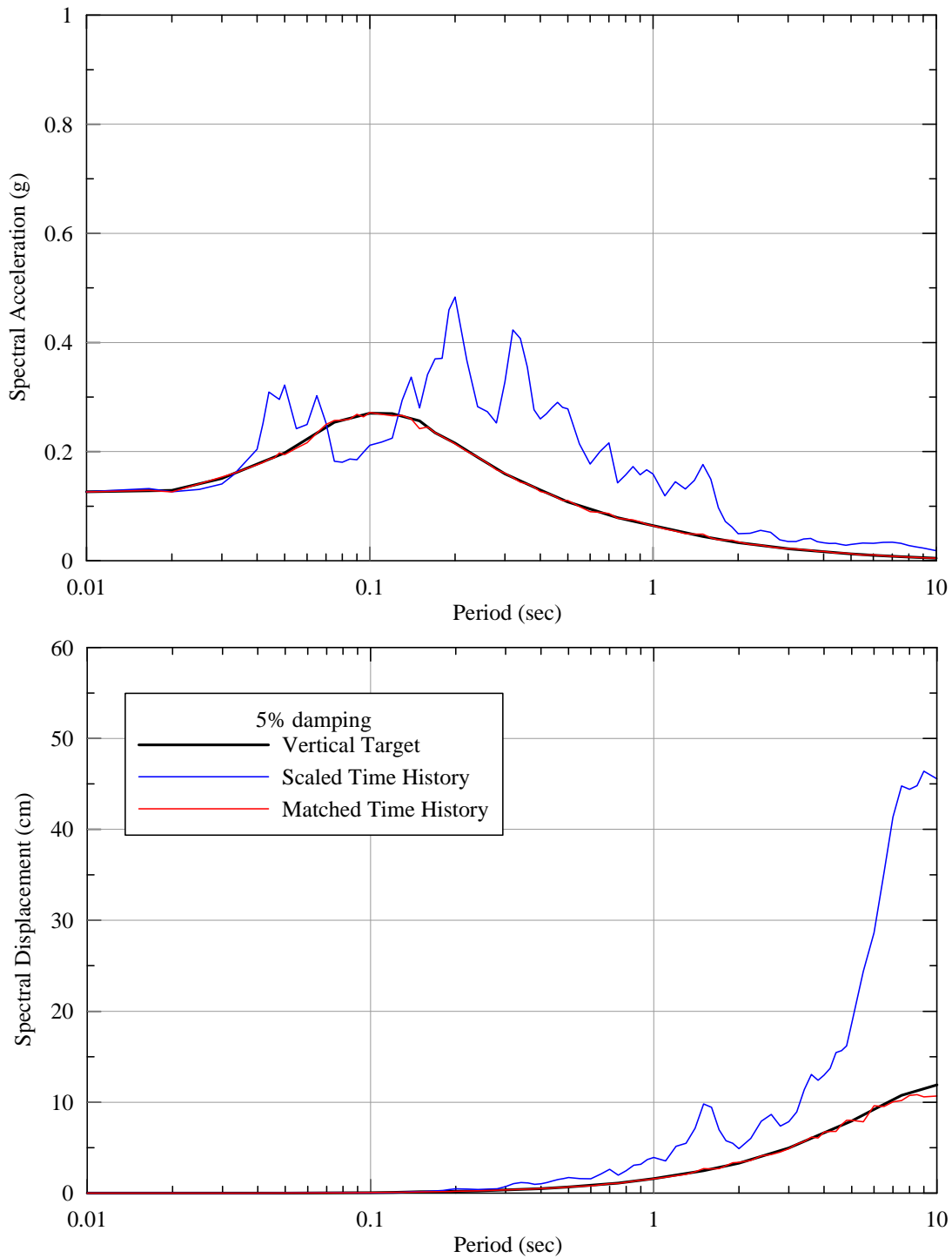


**Figure 45: Acceleration and Displacement Response Spectra. Seed Motion: 1999 Duzce Earthquake, Lamont Station, Vertical Component. Target: Vertical, FEE  $V_{S30} = 3000$  ft/sec.**

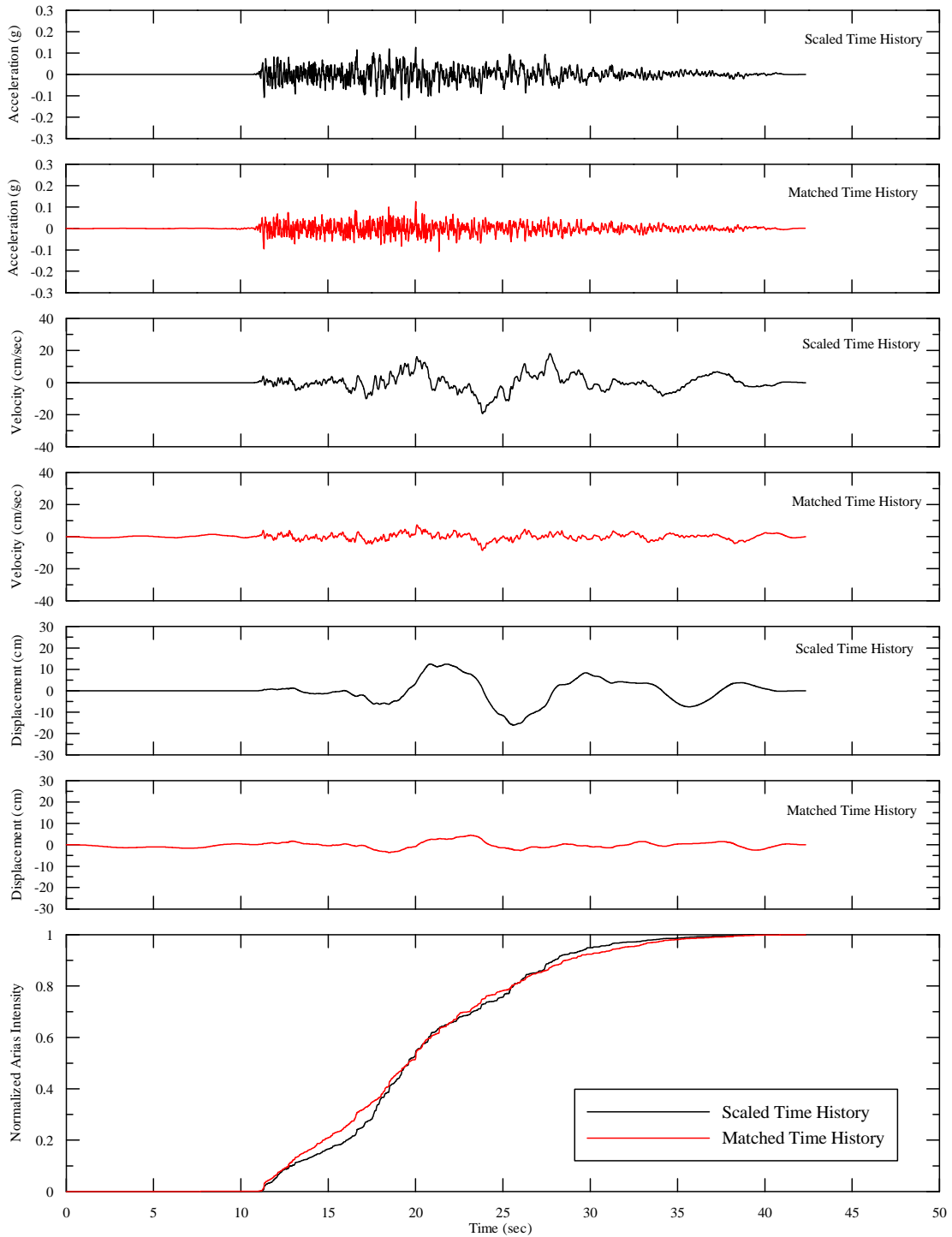


**Figure 46: Acceleration, Velocity, and Displacement Time Histories. Seed Motion: 1999 Duzce Earthquake, Lamont Station, Vertical Component. Target: Vertical, FEE  $V_{S30} = 3000$  ft/sec.**

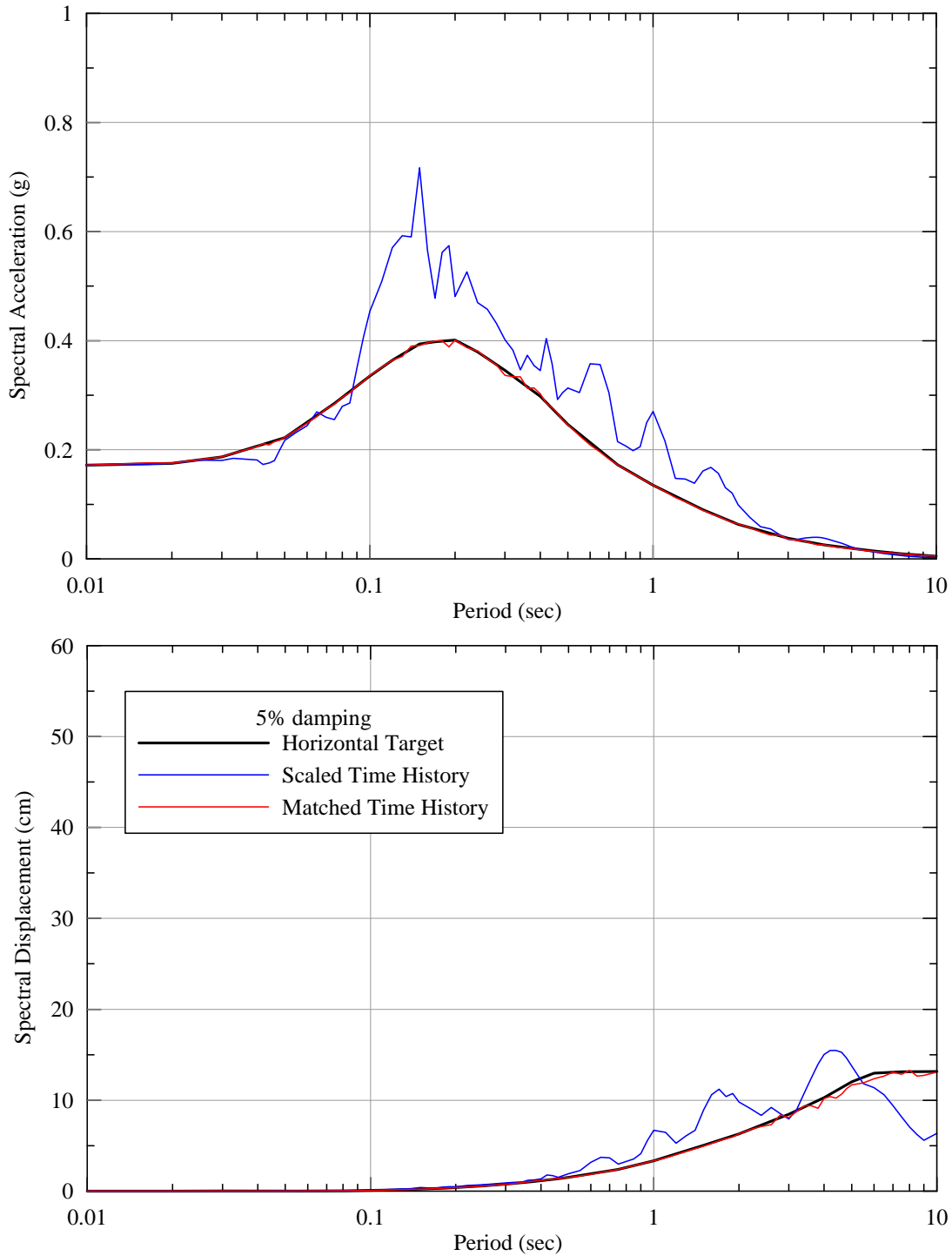


**Figure 47: Acceleration and Displacement Response Spectra. Seed Motion: 1989 Loma Prieta Earthquake, Gilroy Array #6, 0 degrees Component. Target: Fault Normal, FEE  $V_{S30} = 3000$  ft/sec.**

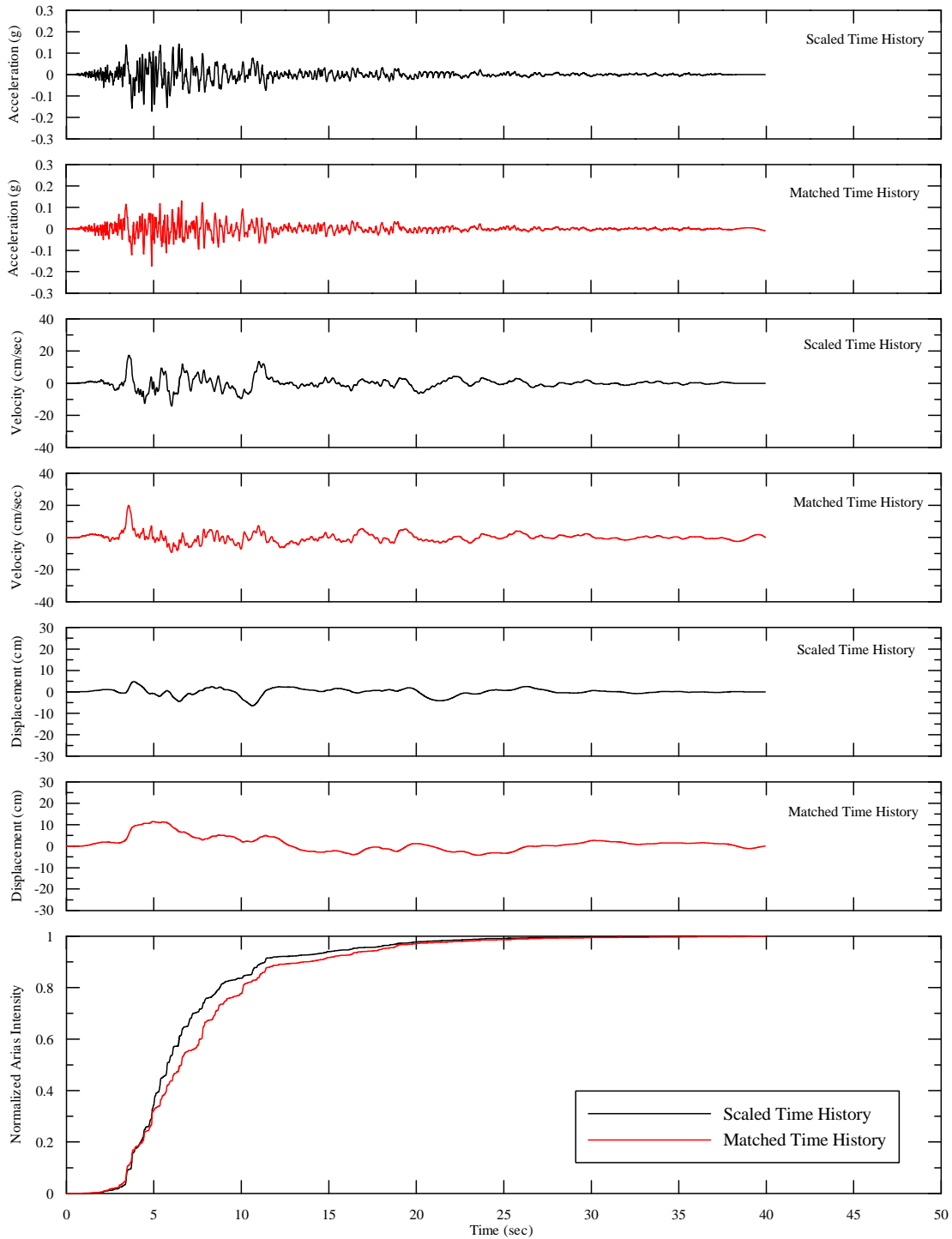


**Figure 48: Acceleration, Velocity, and Displacement Time Histories. Seed Motion: 1989 Loma Prieta Earthquake, Gilroy Array #6, 0 degrees Component. Target: Fault Normal, FEE  $V_{S30} = 3000$  ft/sec.**

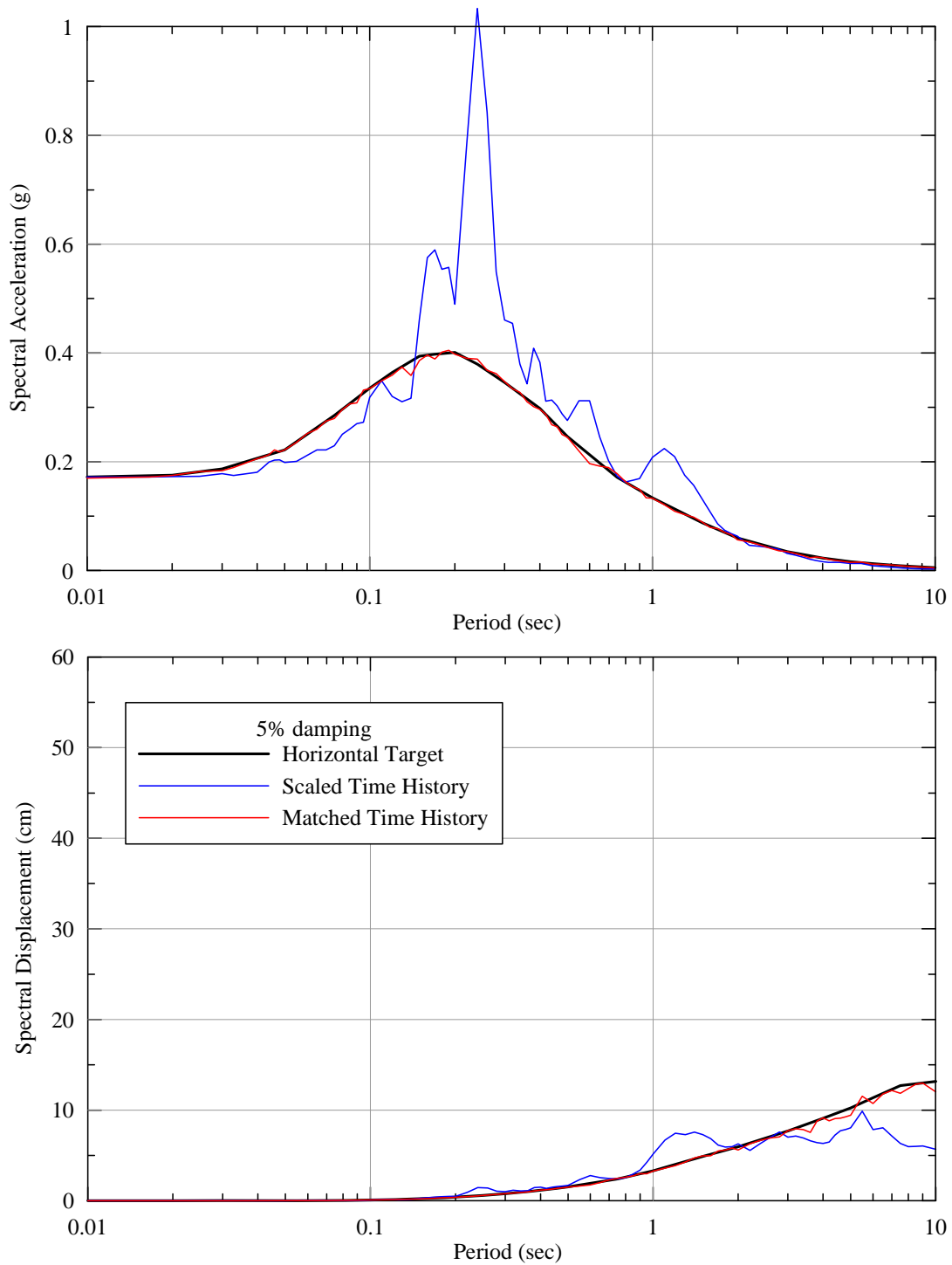


**Figure 49: Acceleration and Displacement Response Spectra. Seed Motion: 1989 Loma Prieta Earthquake, Gilroy Array #6, 90 degrees Component. Target: Fault Parallel, FEE  $V_{S30} = 3000$  ft/sec.**

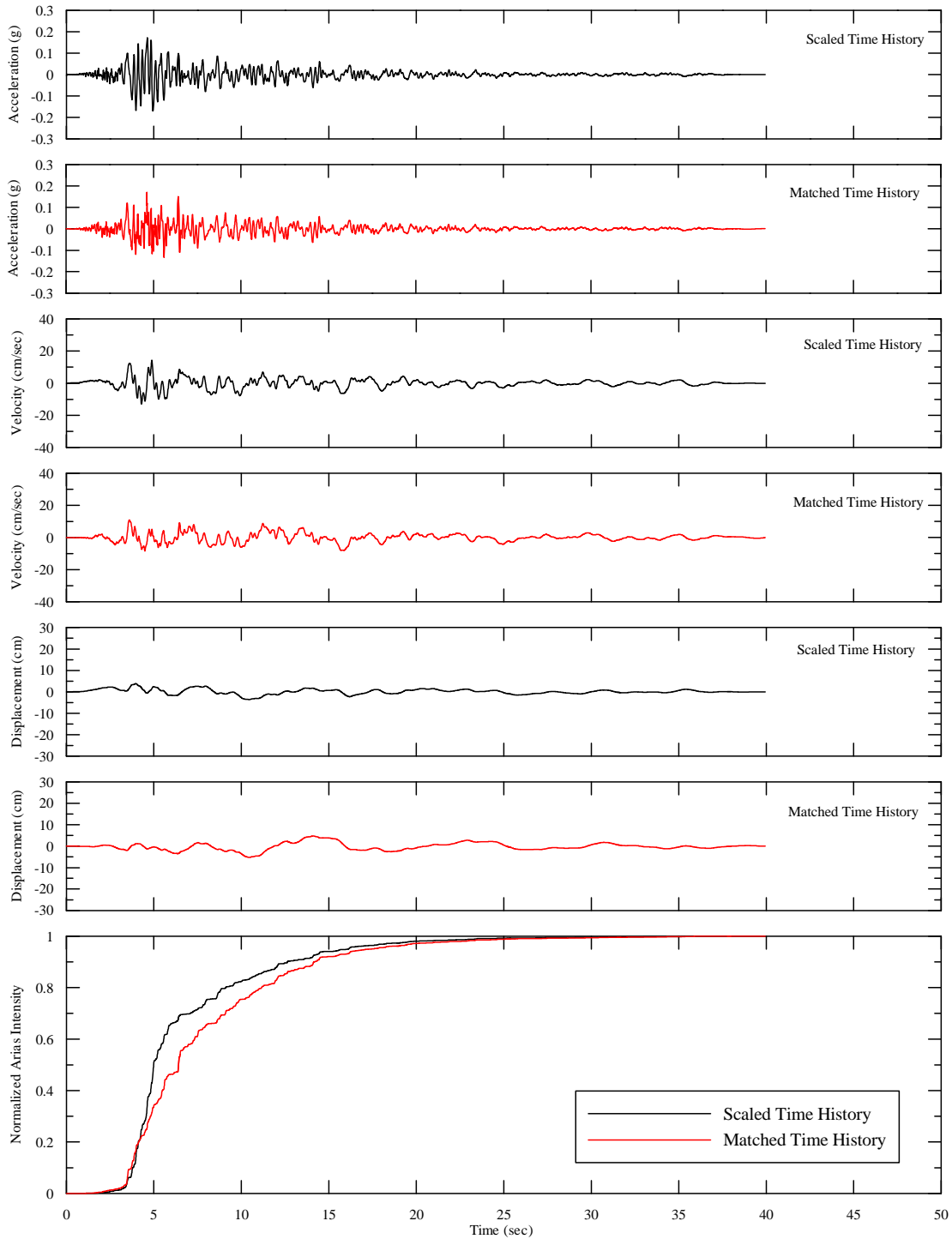


**Figure 50: Acceleration, Velocity, and Displacement Time Histories. Seed Motion: 1989 Loma Prieta Earthquake, Gilroy Array #6, 90 degrees Component. Target: Fault Parallel, FEE  $V_{S30} = 3000$  ft/sec.**

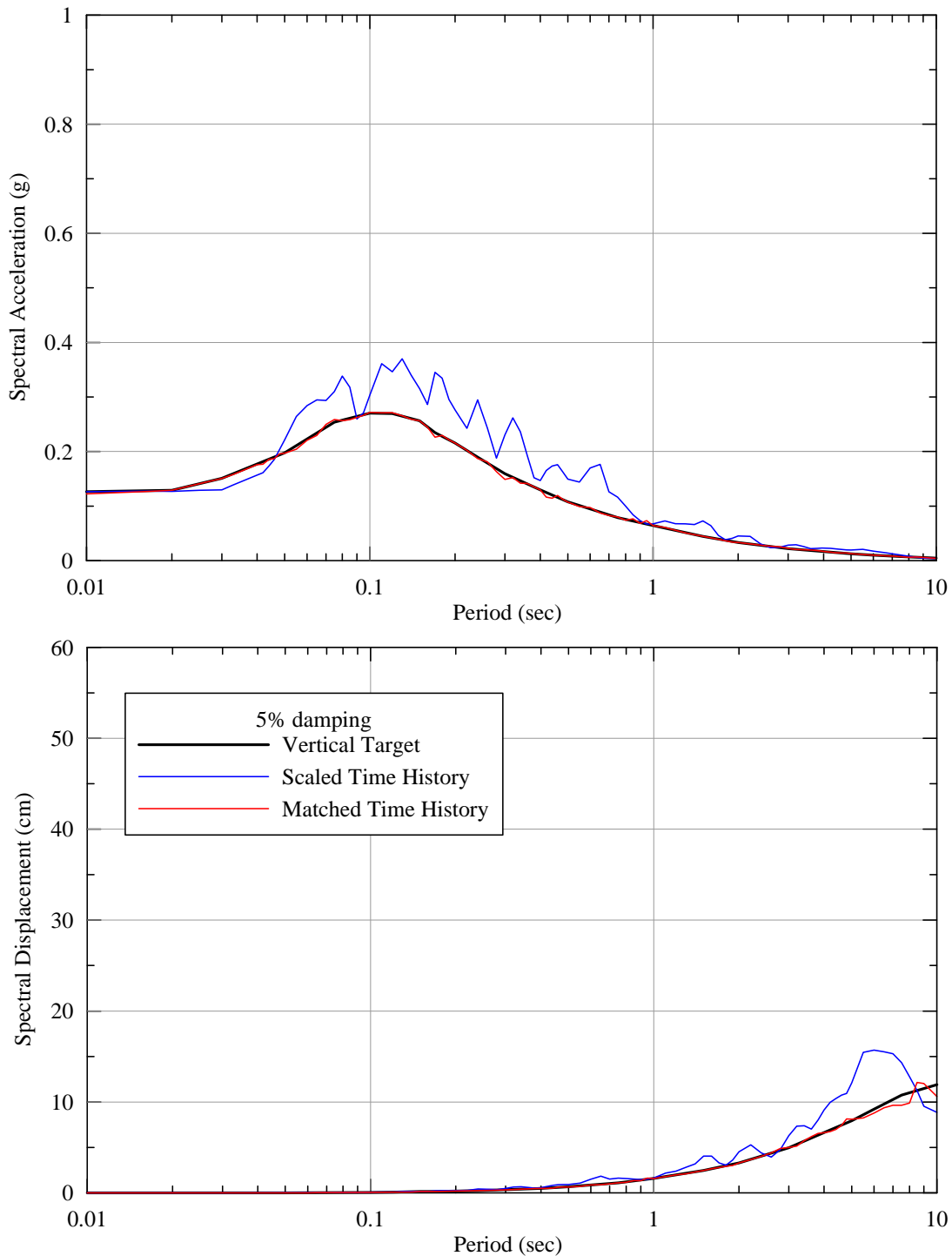


**Figure 51: Acceleration and Displacement Response Spectra. Seed Motion: 1989 Loma Prieta Earthquake, Gilroy Array #6, Vertical Component. Target: Vertical, FEE  $V_{S30} = 3000$  ft/sec.**

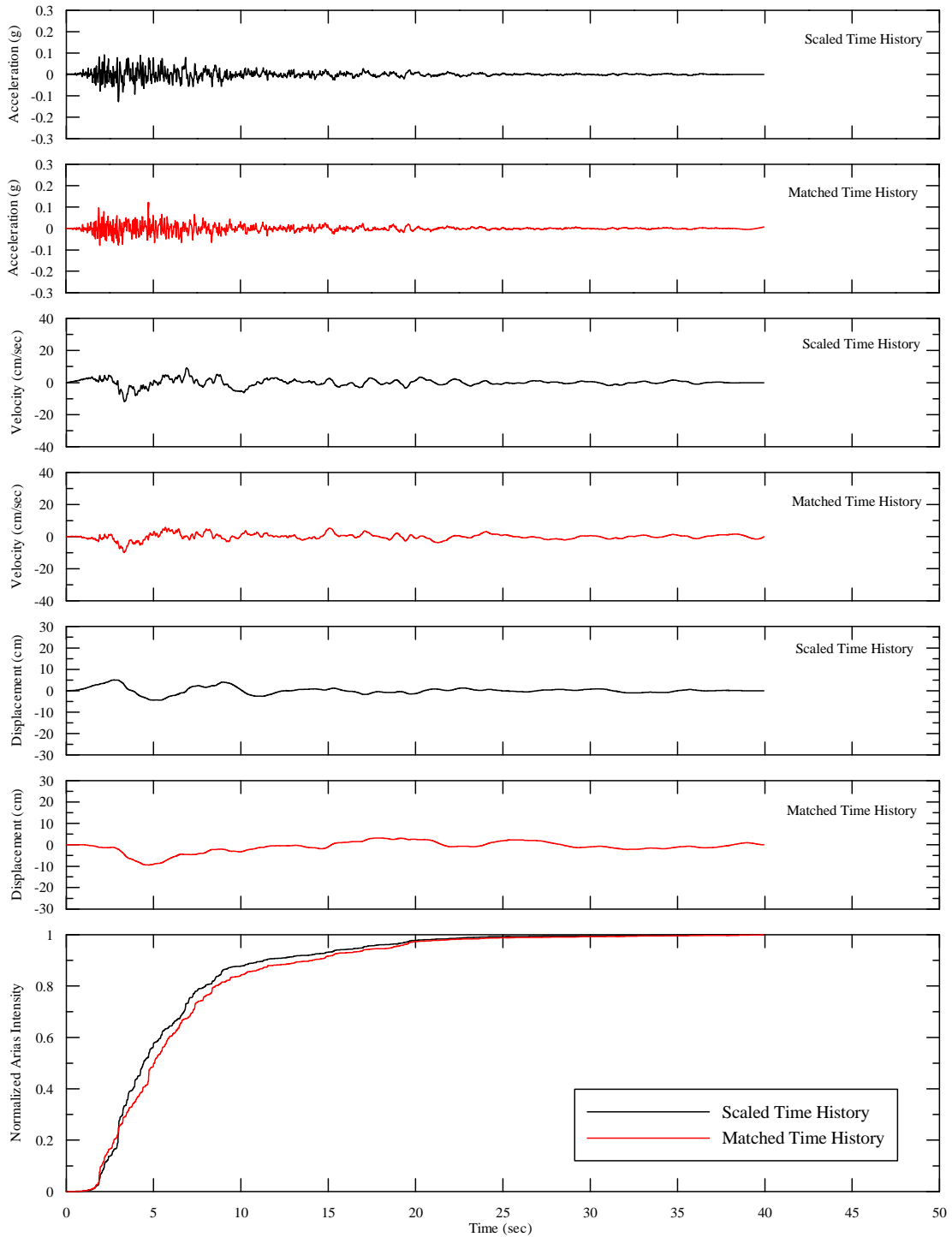


**Figure 52: Acceleration, Velocity, and Displacement Time Histories. Seed Motion: 1989 Loma Prieta Earthquake, Gilroy Array #6, Vertical Component. Target: Vertical, FEE  $V_{S30} = 3000$  ft/sec.**

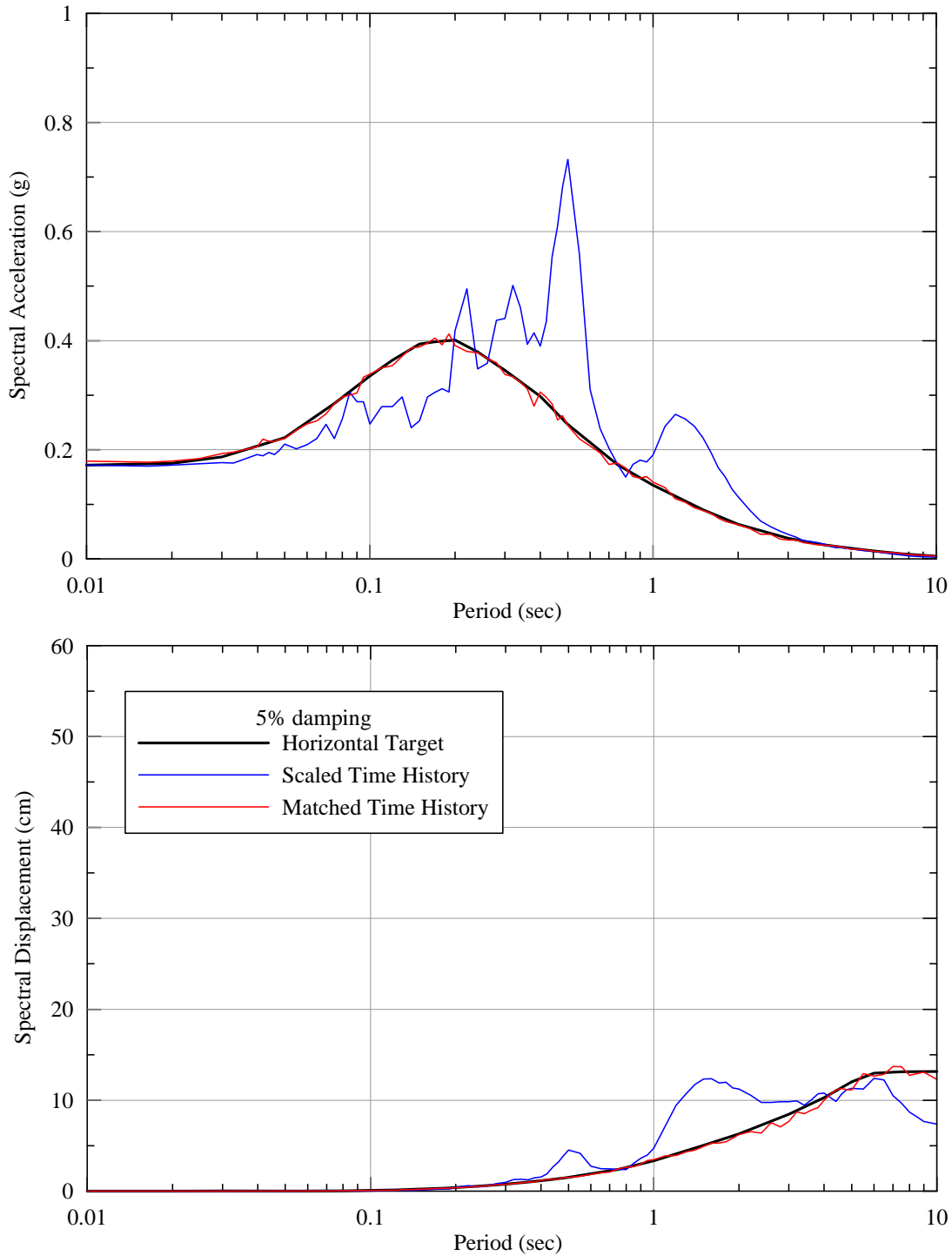


**Figure 53: Acceleration and Displacement Response Spectra. Seed Motion: 1999 Hector Mine Earthquake, 90 degree Component. Target: Fault Normal, FEE  $V_{S30} = 3000$  ft/sec.**

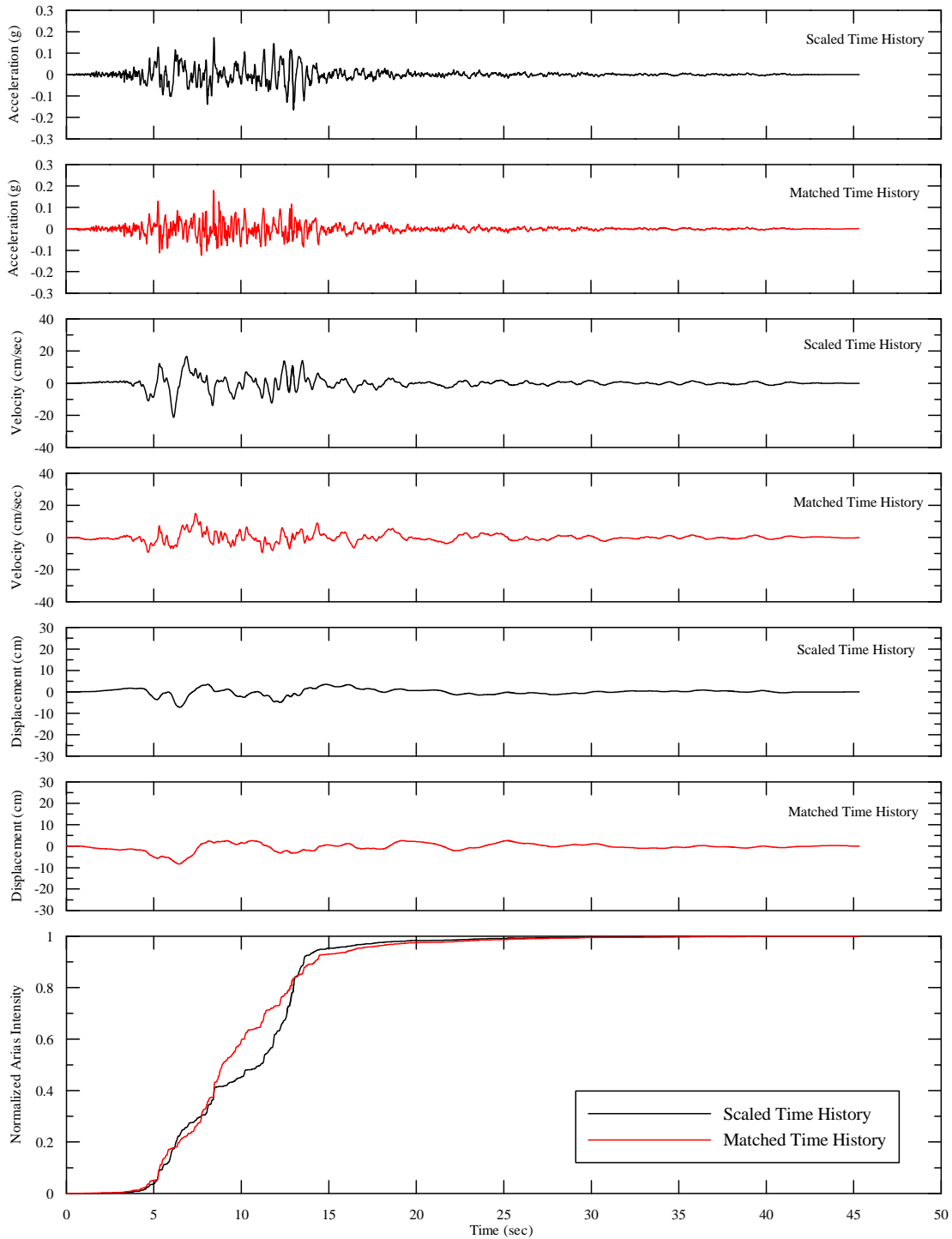


**Figure 54: Acceleration, Velocity, and Displacement Time Histories. Seed Motion: 1999 Hector Mine Earthquake, 90 degree Component. Target: Fault Normal, FEE  $V_{S30} = 3000$  ft/sec.**

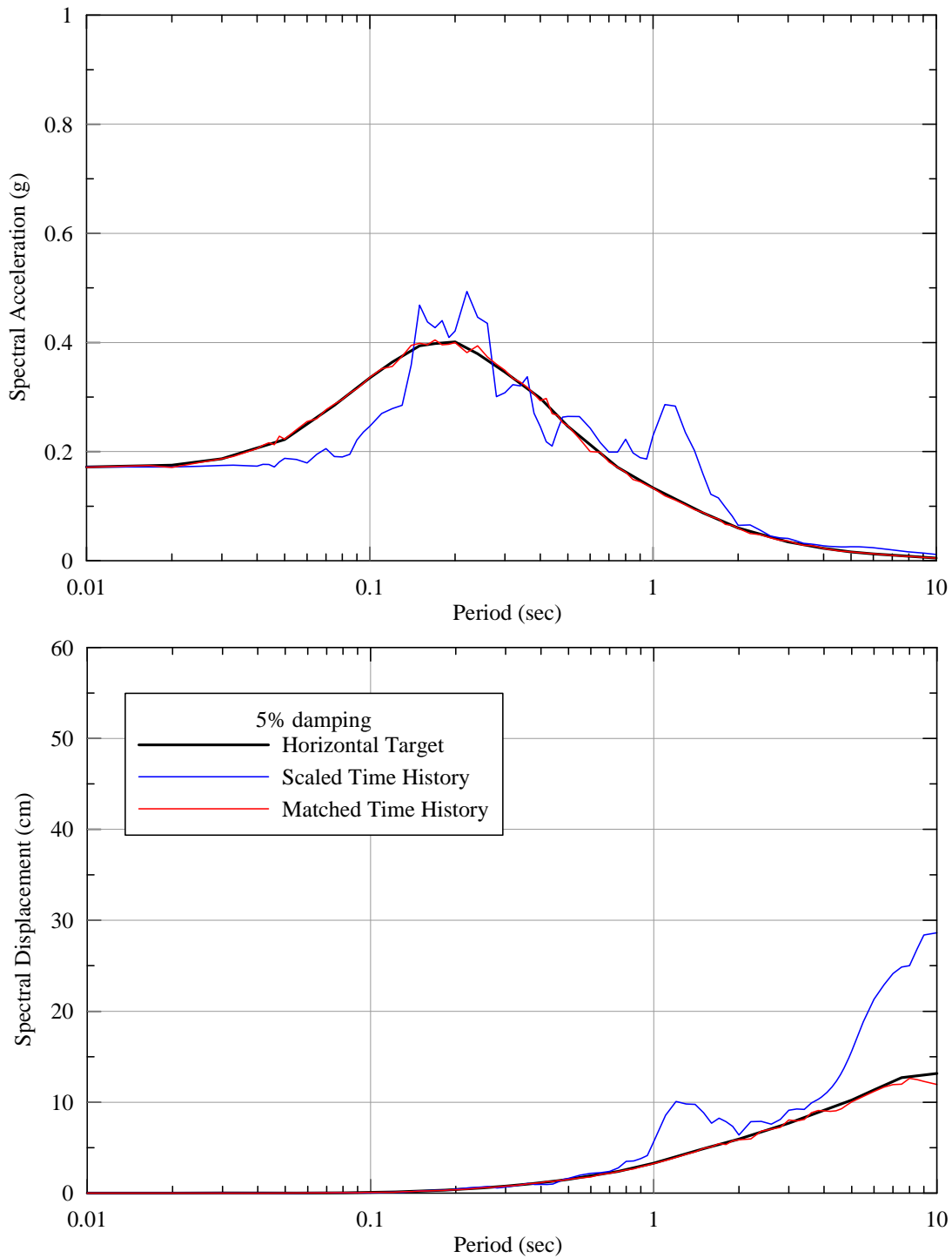


**Figure 55: Acceleration and Displacement Response Spectra. Seed Motion: 1999 Hector Mine Earthquake, 0 degree Component. Target: Fault Parallel, FEE  $V_{S30} = 3000$  ft/sec.**

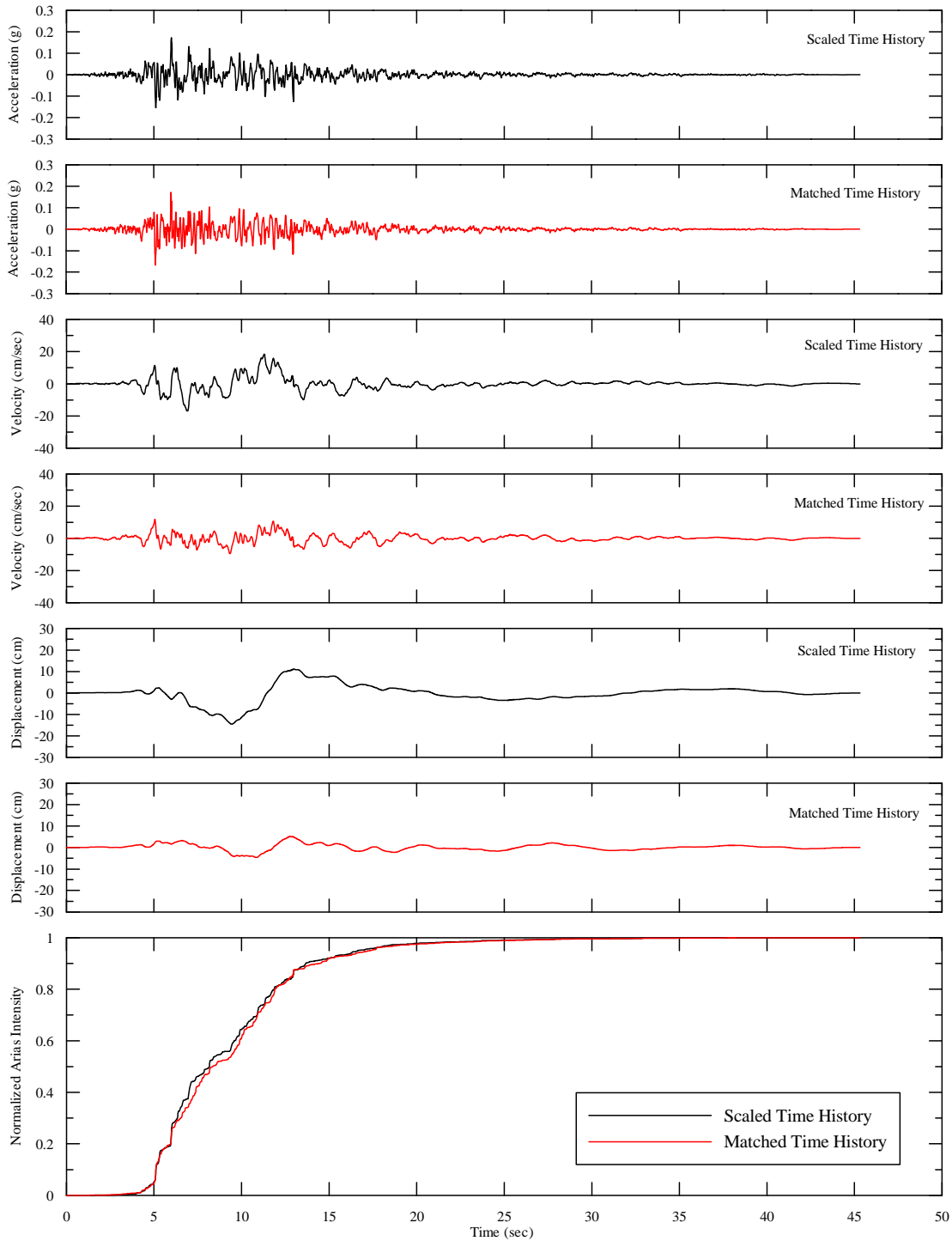


**Figure 56: Acceleration, Velocity, and Displacement Time Histories. Seed Motion: 1999 Hector Mine Earthquake, 0 degree Component. Target: Fault Parallel, FEE  $V_{s30} = 3000$  ft/sec.**

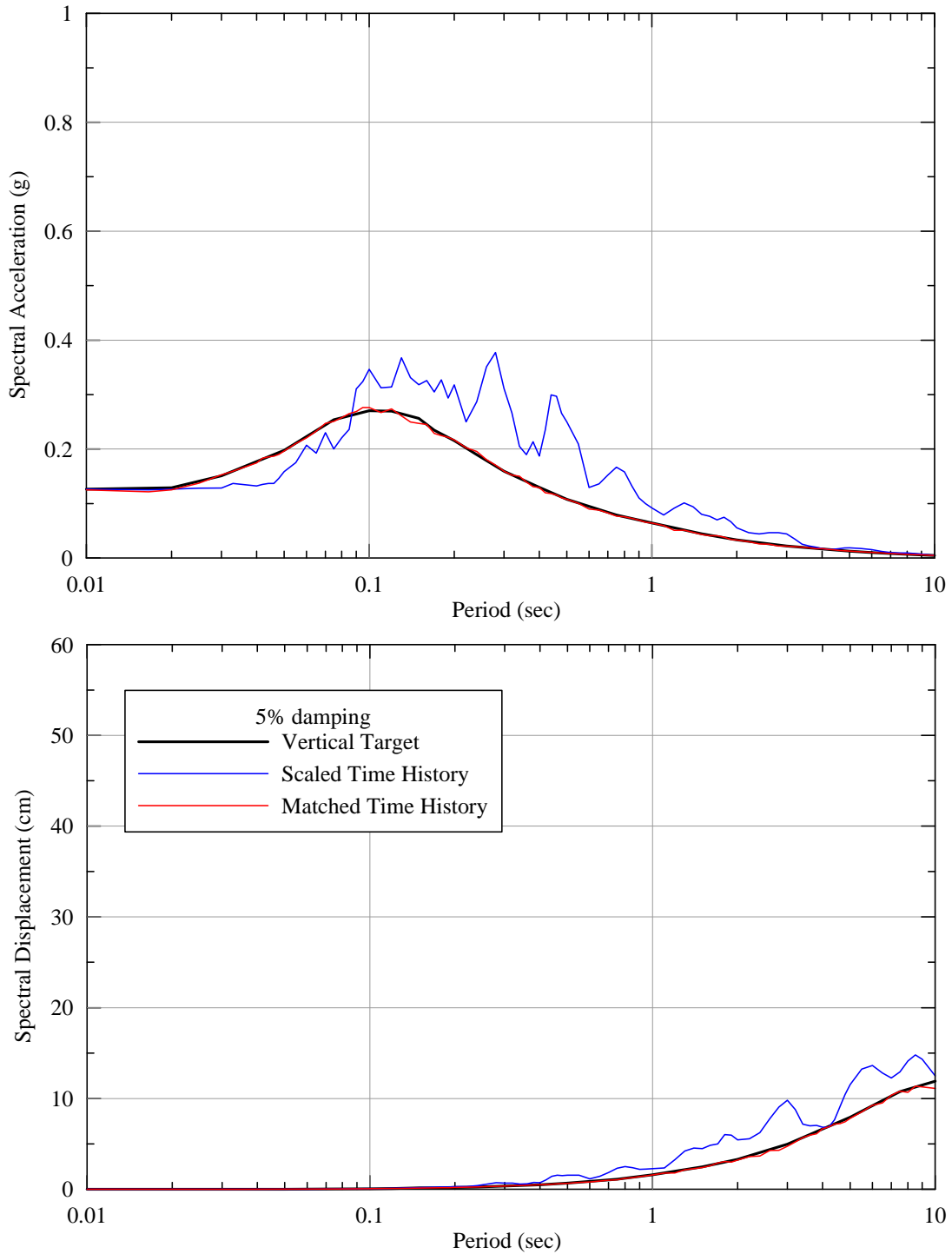


**Figure 57: Acceleration and Displacement Response Spectra. Seed Motion: 1999 Hector Mine Earthquake, Vertical Component. Target: Vertical, FEE  $V_{S30} = 3000$  ft/sec.**

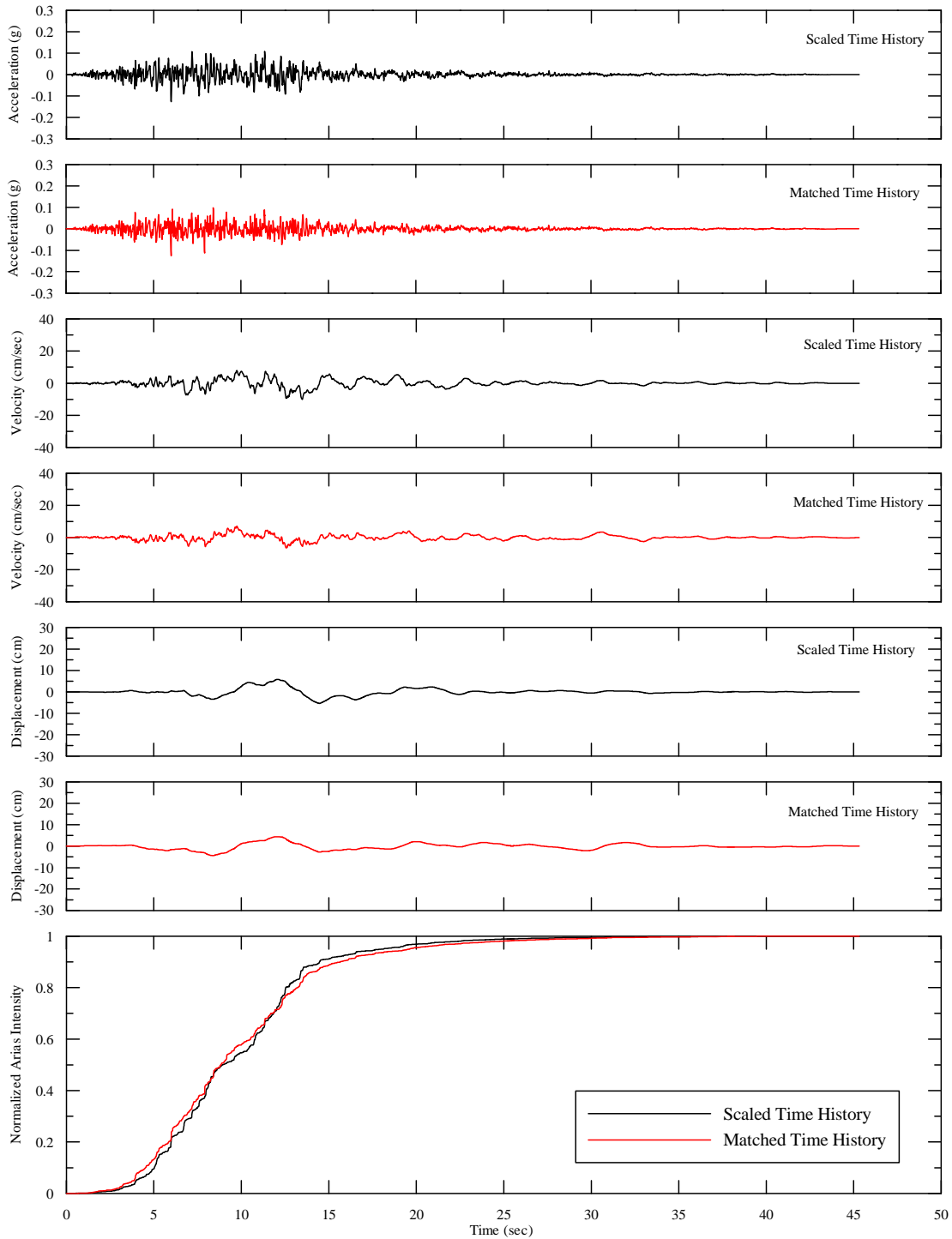


**Figure 58: Acceleration, Velocity, and Displacement Time Histories. Seed Motion: 1999 Hector Mine Earthquake, Vertical Component. Target: Vertical, FEE  $V_{S30} = 3000$  ft/sec.**

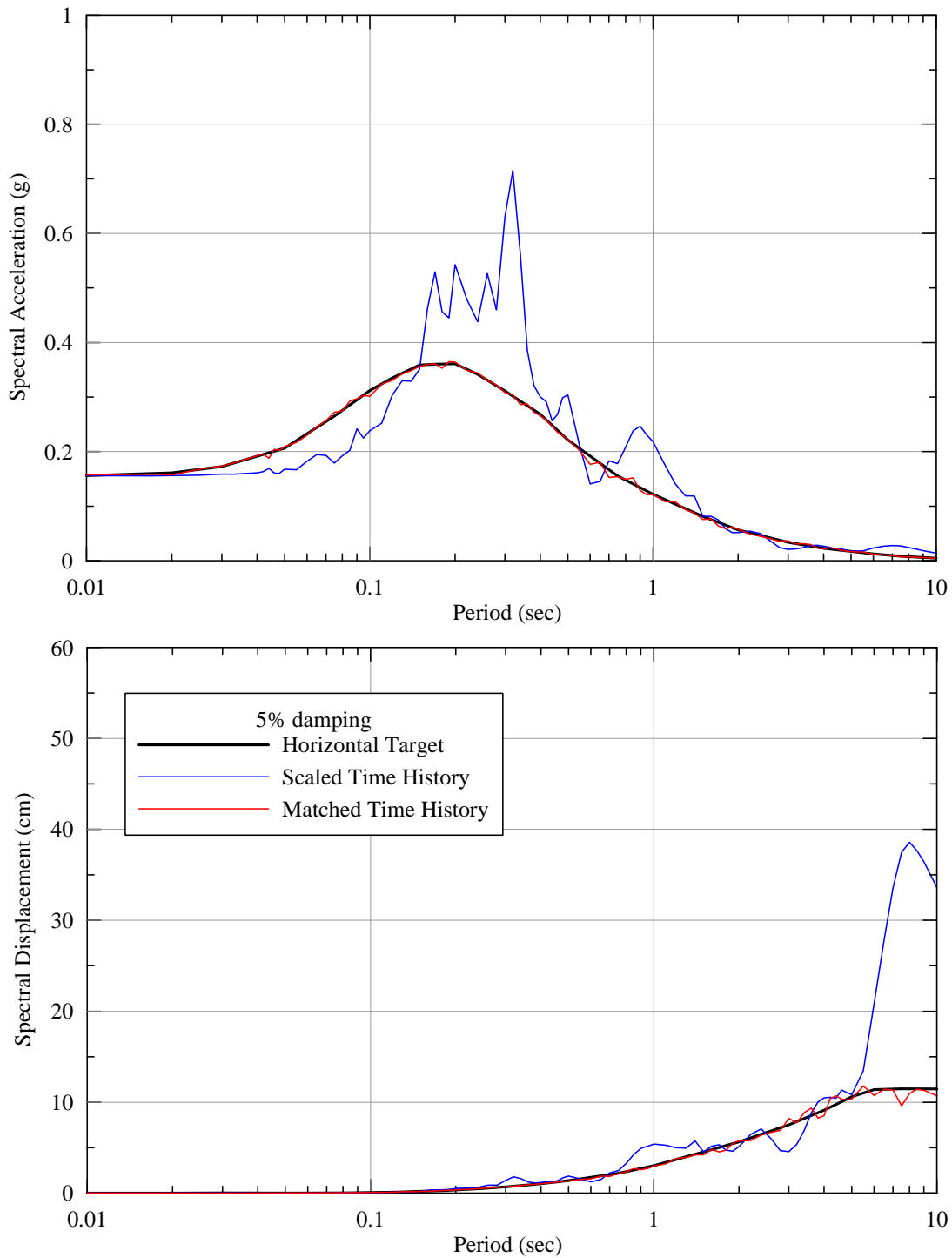


**Figure 59: Acceleration and Displacement Response Spectra. Seed Motion: 1999 Duzce Earthquake, Lamont Station, North Component. Target: Fault Normal, FEE  $V_{S30} = 5000$  ft/sec.**

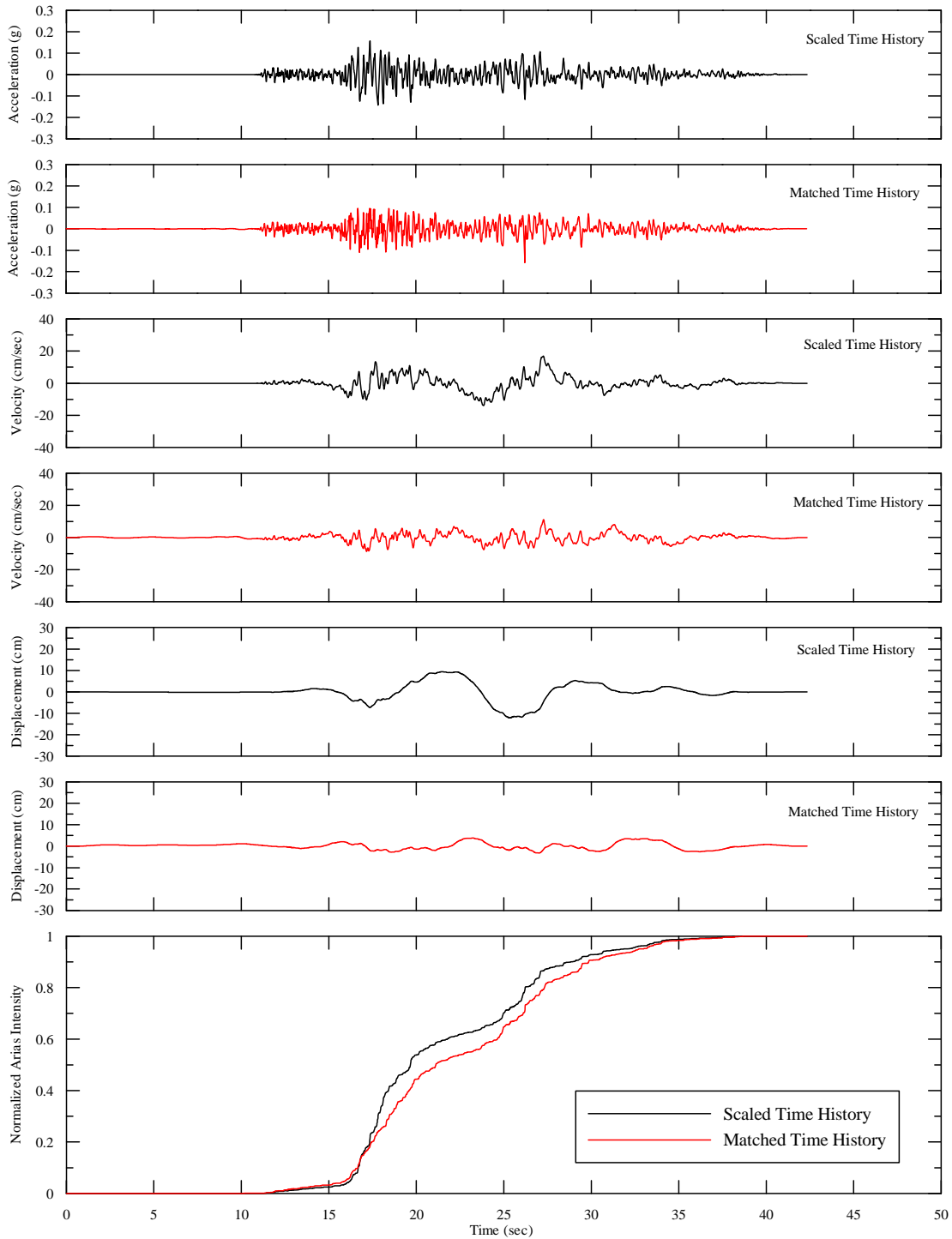


**Figure 60: Acceleration, Velocity, and Displacement Time Histories. Seed Motion: 1999 Duzce Earthquake, Lamont Station, North Component. Target: Fault Normal, FEE  $V_{S30} = 5000$  ft/sec.**

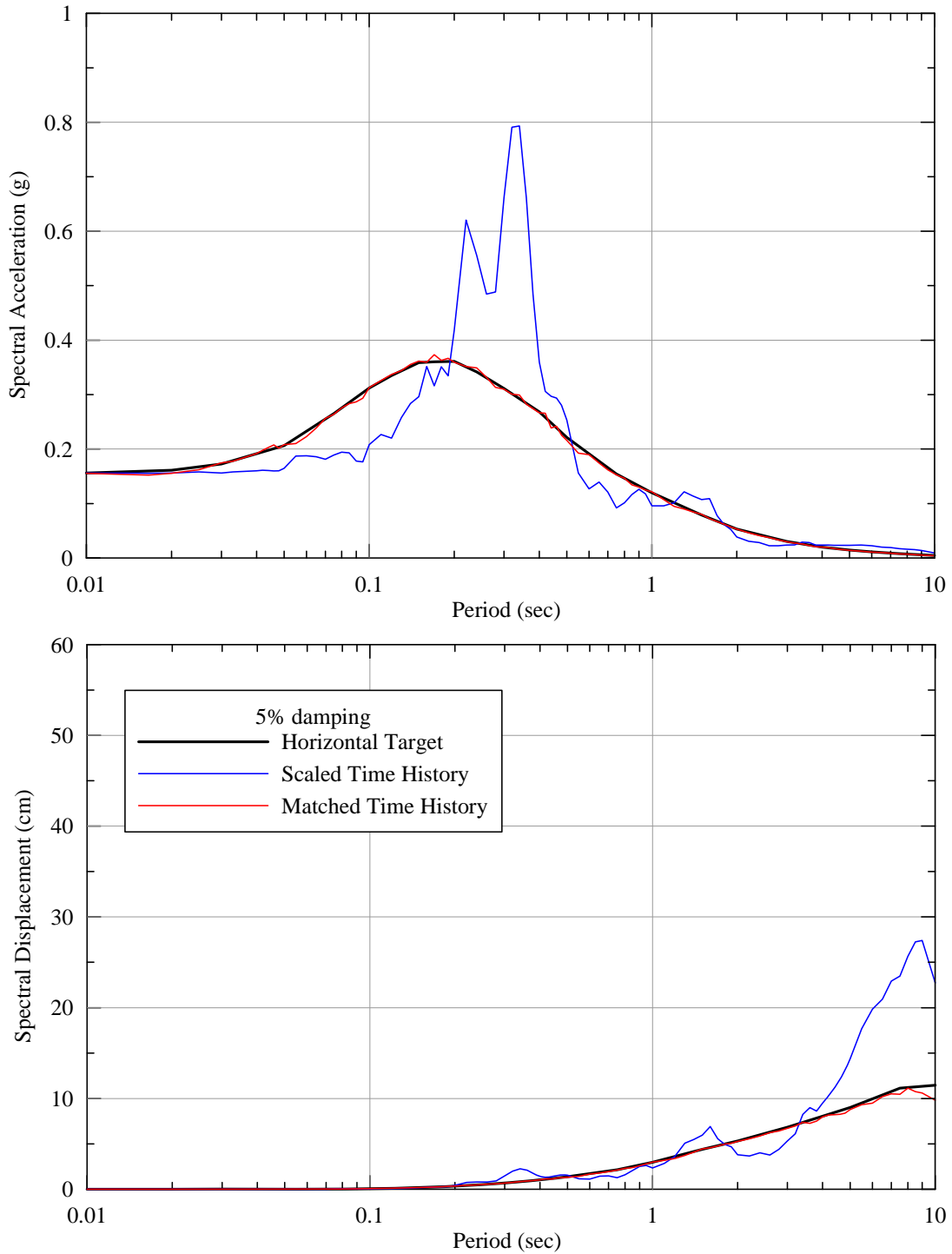


**Figure 61: Acceleration and Displacement Response Spectra. Seed Motion: 1999 Duzce Earthquake, Lamont Station, East Component. Target: Fault Parallel, FEE  $V_{S30} = 5000$  ft/sec.**

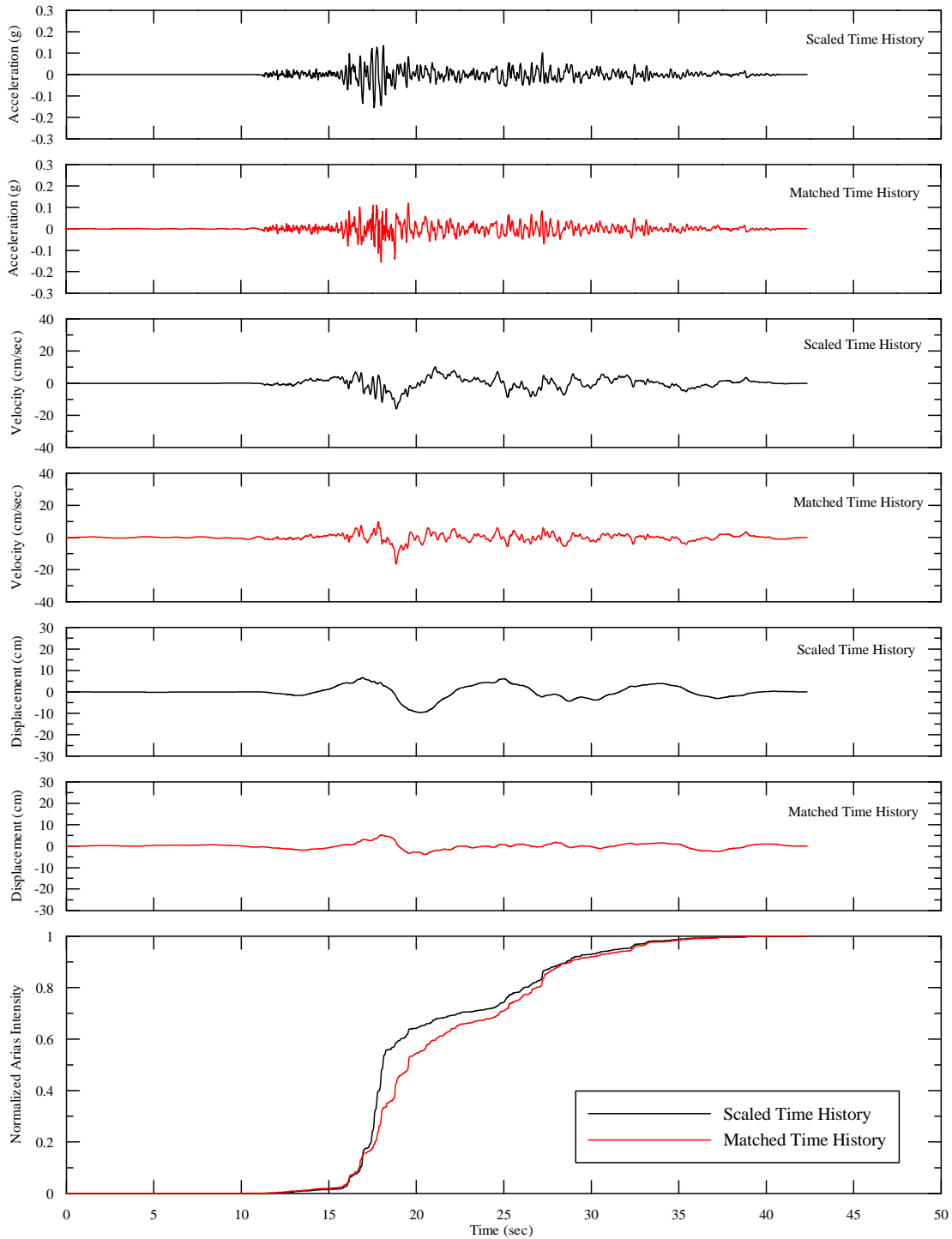


**Figure 62: Acceleration, Velocity, and Displacement Time Histories. Seed Motion: 1999 Duzce Earthquake, Lamont Station, East Component. Target: Fault Parallel, FEE  $V_{S30} = 5000$  ft/sec.**

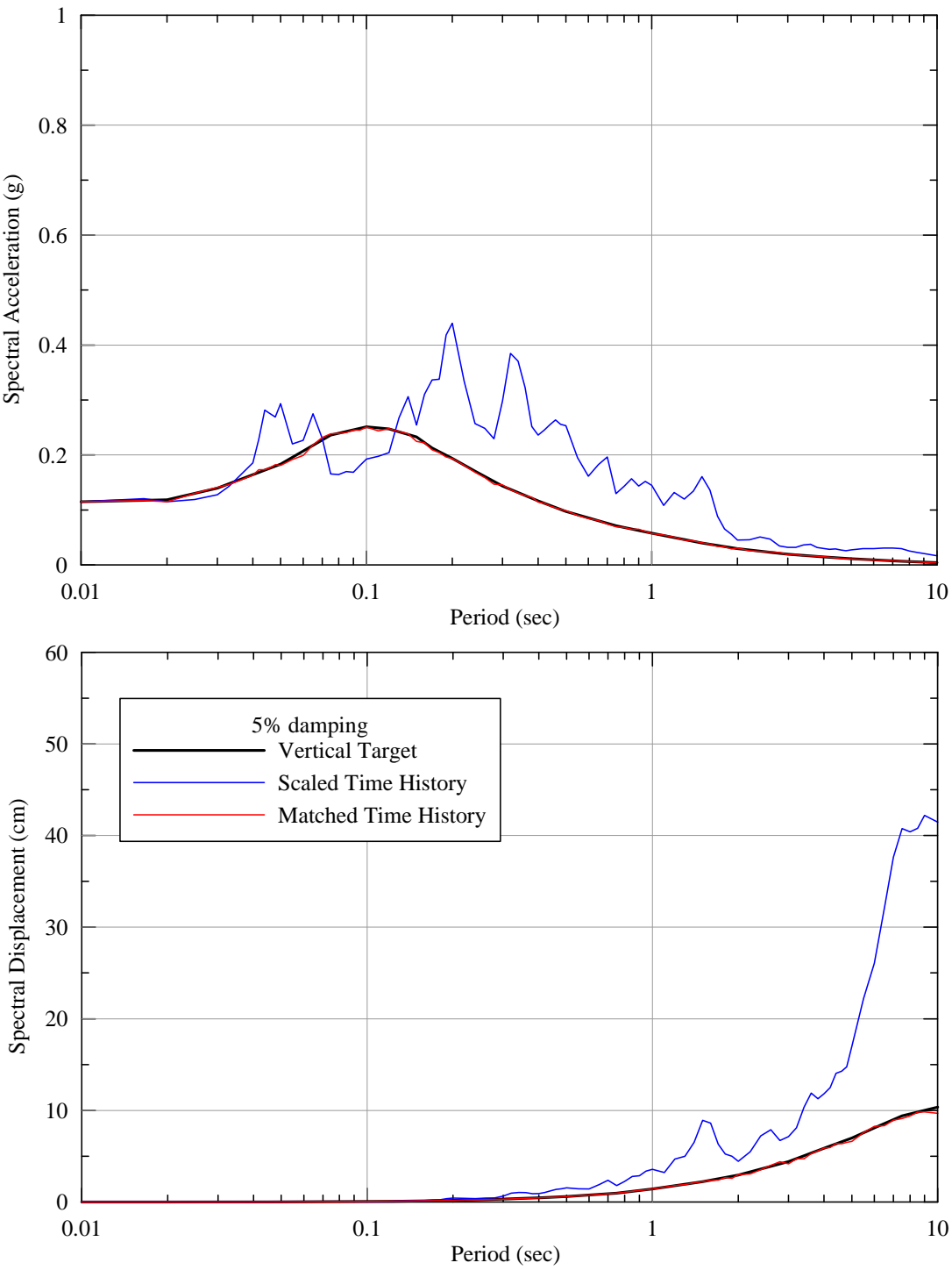


**Figure 63: Acceleration and Displacement Response Spectra. Seed Motion: 1999 Duzce Earthquake, Lamont Station, Vertical Component. Target: Vertical, FEE  $V_{S30} = 5000$  ft/sec.**

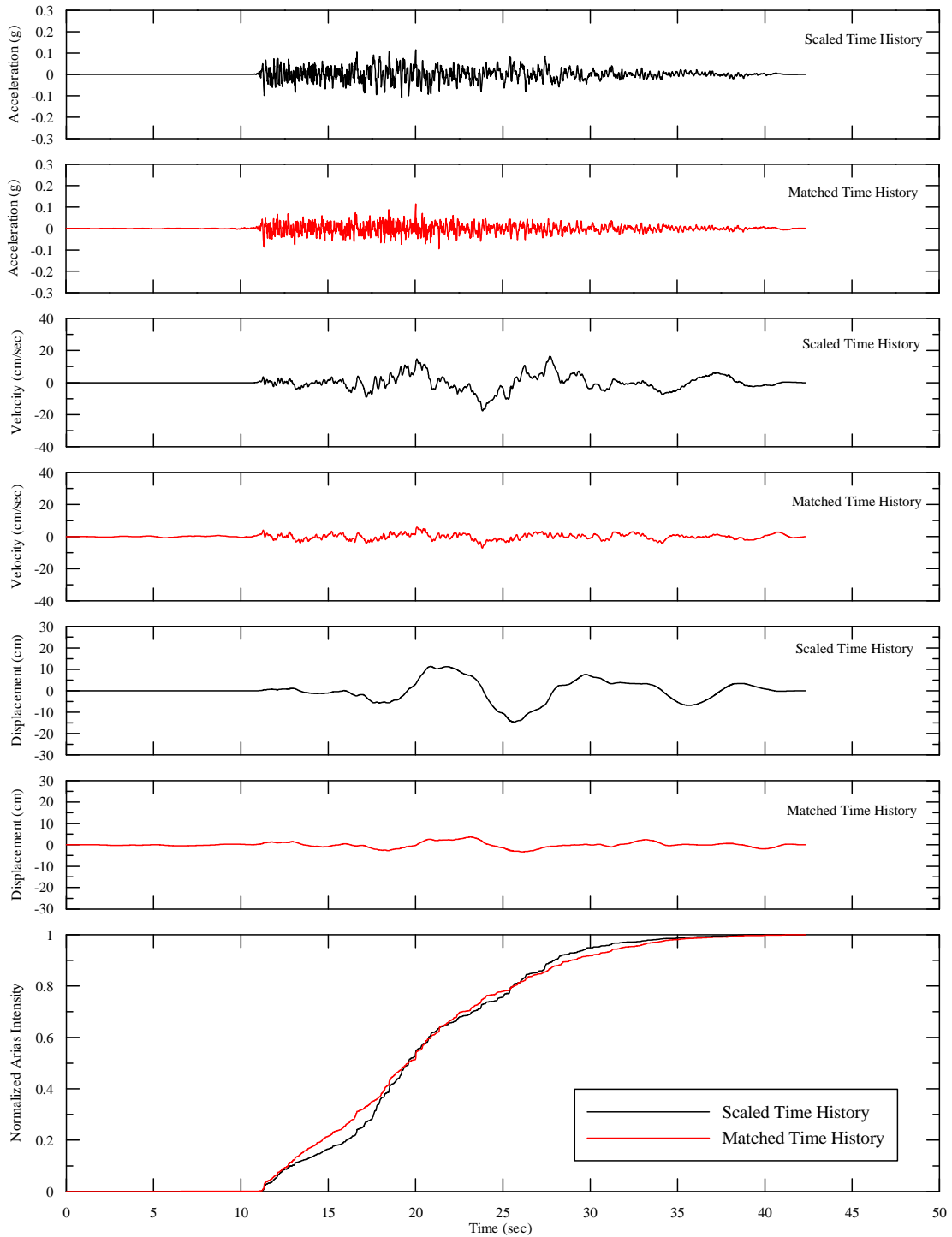


**Figure 64: Acceleration, Velocity, and Displacement Time Histories. Seed Motion: 1999 Duzce Earthquake, Lamont Station, Vertical Component. Target: Vertical, FEE  $V_{S30} = 5000$  ft/sec.**

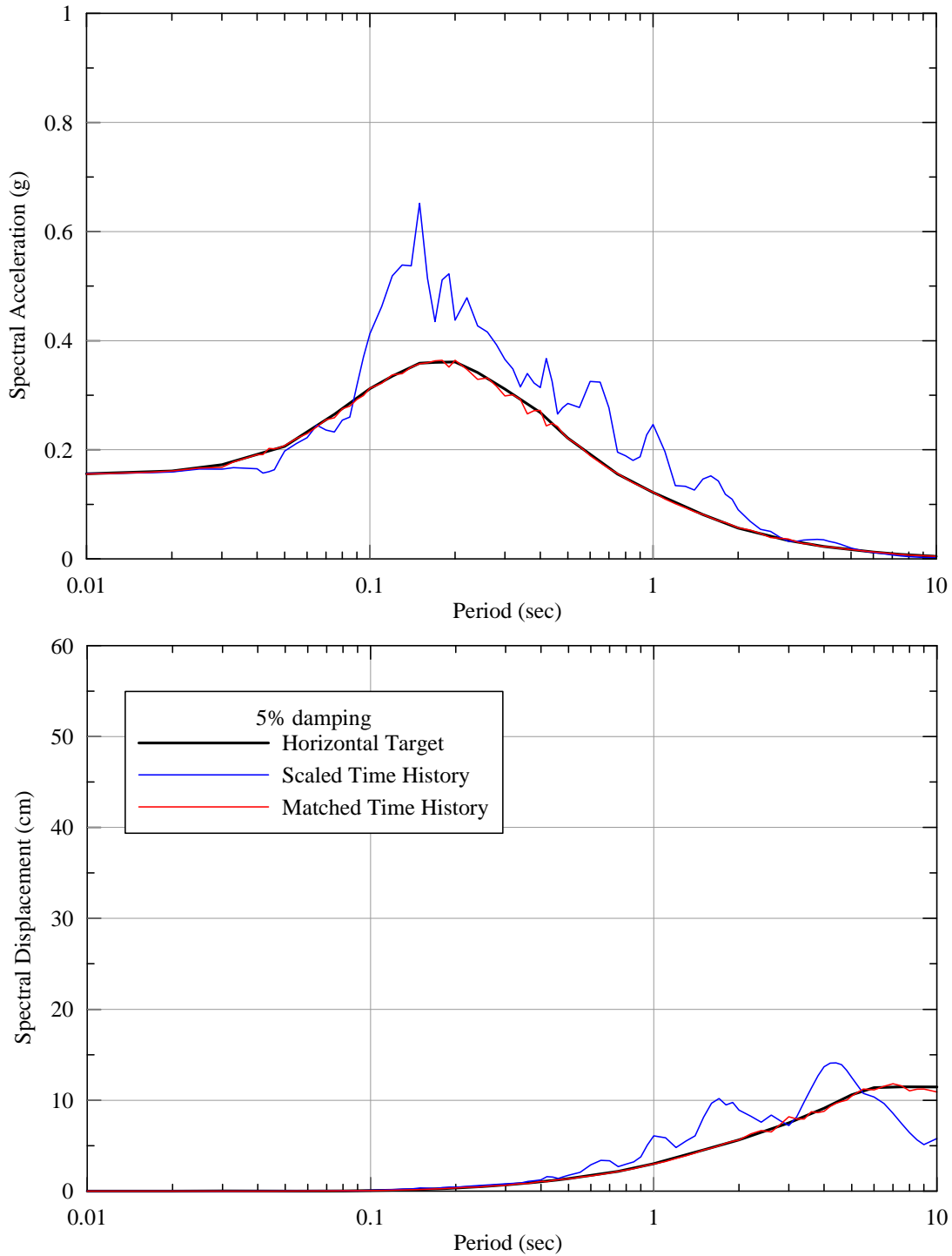


**Figure 65: Acceleration and Displacement Response Spectra. Seed Motion: 1989 Loma Prieta Earthquake, Gilroy Array #6, 0 degrees Component. Target: Fault Normal, FEE  $V_{S30} = 5000$  ft/sec.**

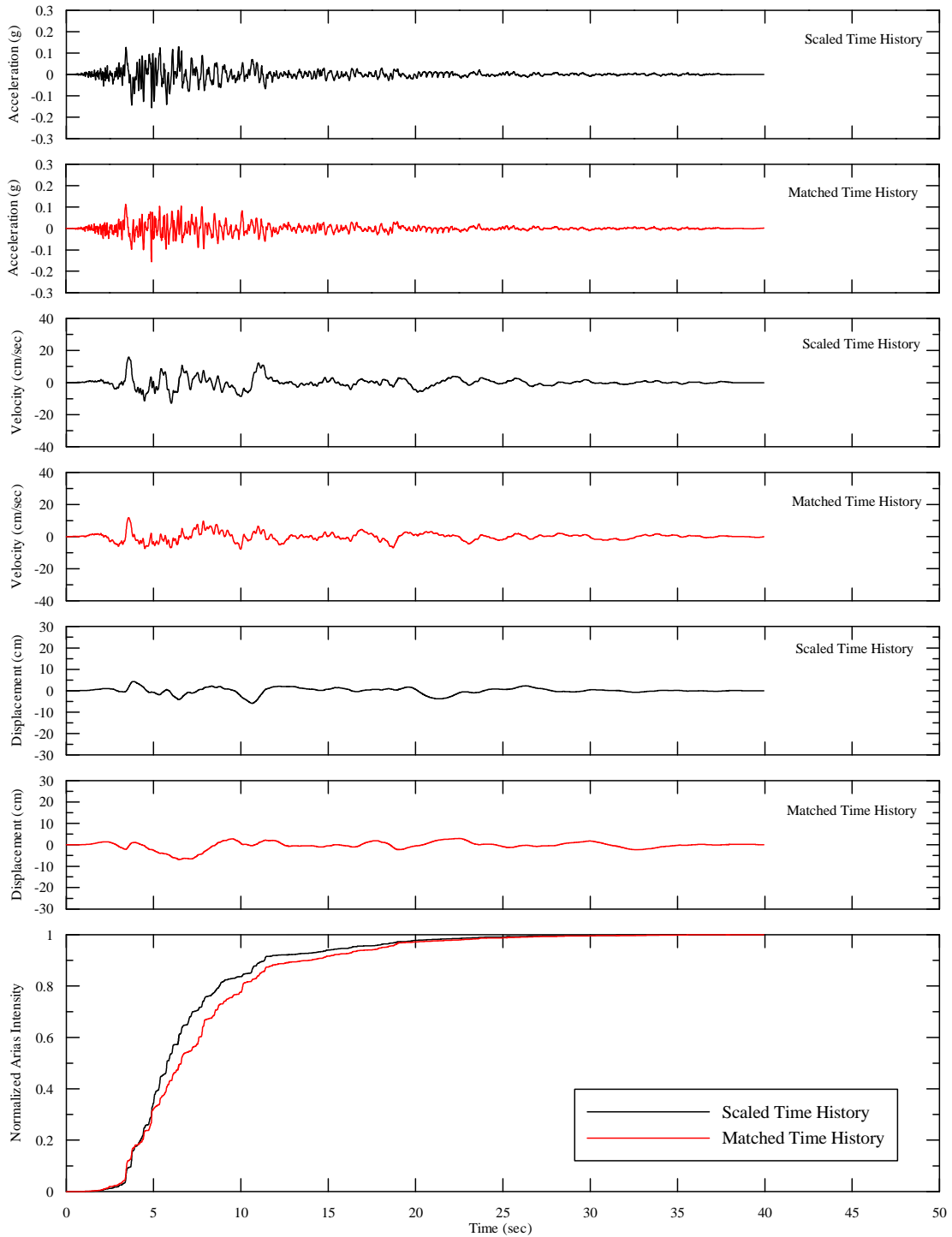


**Figure 66: Acceleration, Velocity, and Displacement Time Histories. Seed Motion: 1989 Loma Prieta Earthquake, Gilroy Array #6, 0 degrees Component. Target: Fault Normal, FEE  $V_{S30} = 5000$  ft/sec.**

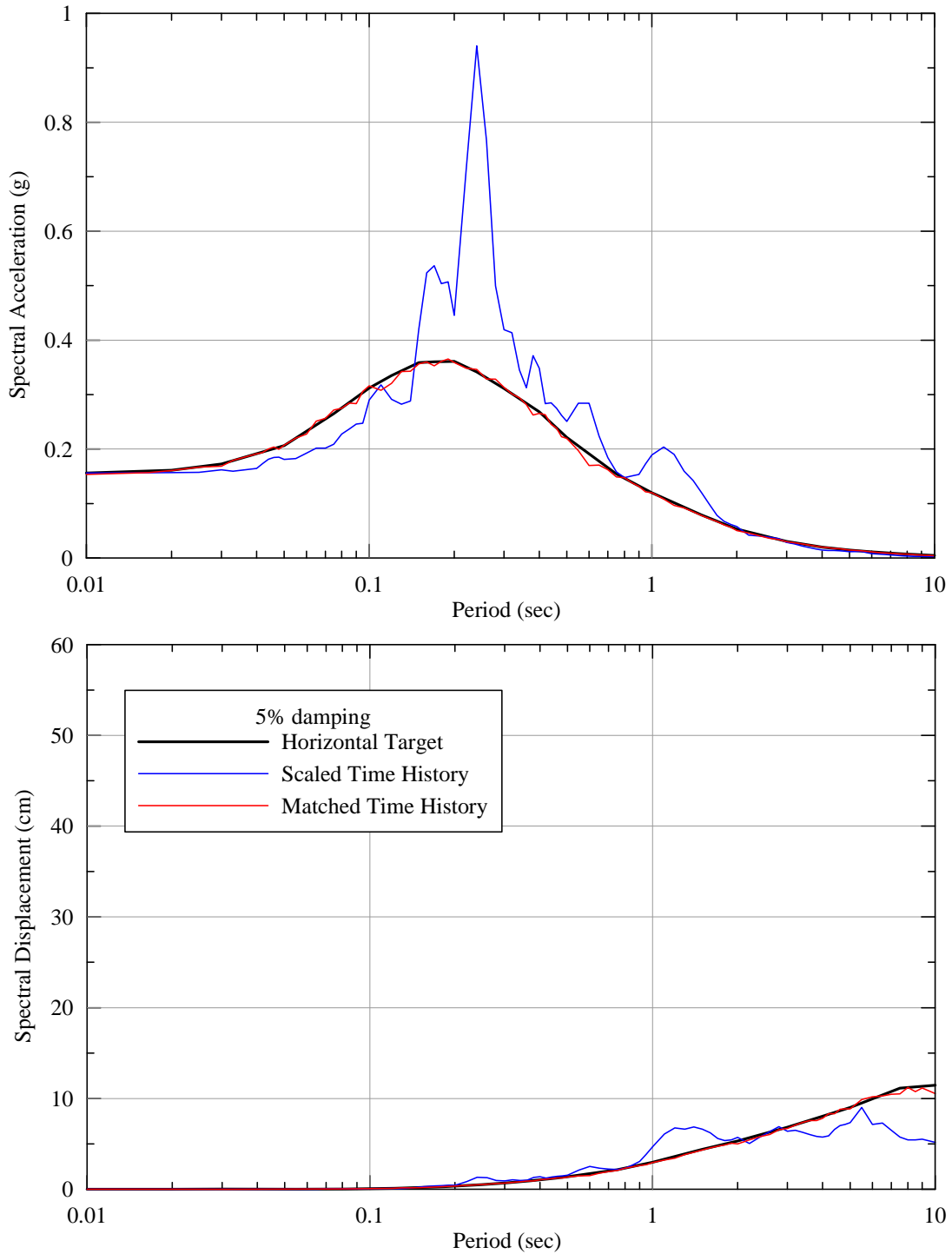


**Figure 67: Acceleration and Displacement Response Spectra. Seed Motion: 1989 Loma Prieta Earthquake, Gilroy Array #6, 90 degrees Component. Target: Fault Parallel, FEE  $V_{S30} = 5000$  ft/sec.**

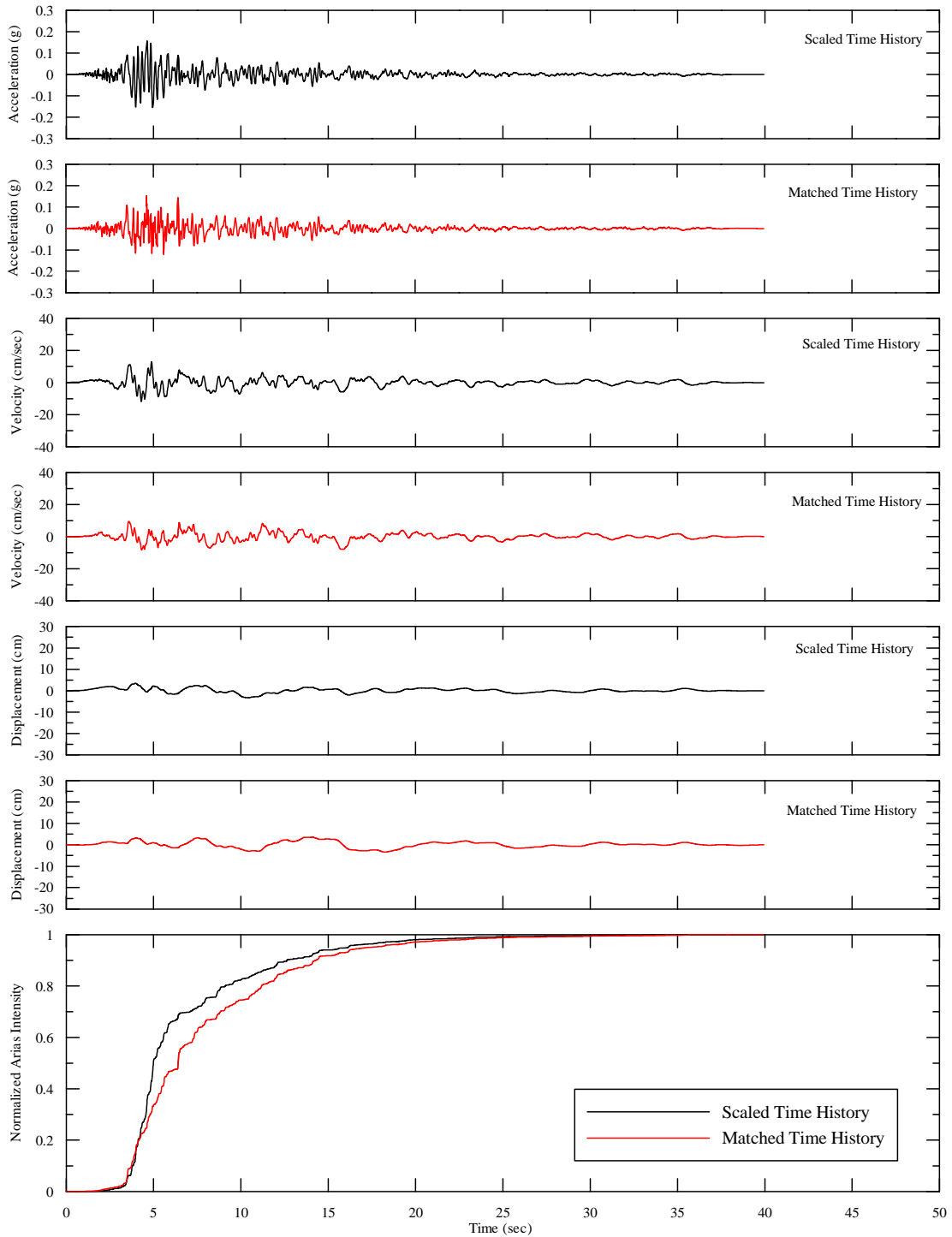


**Figure 68: Acceleration, Velocity, and Displacement Time Histories. Seed Motion: 1989 Loma Prieta Earthquake, Gilroy Array #6, 90 degrees Component. Target: Fault Parallel, FEE  $V_{S30} = 5000$  ft/sec.**

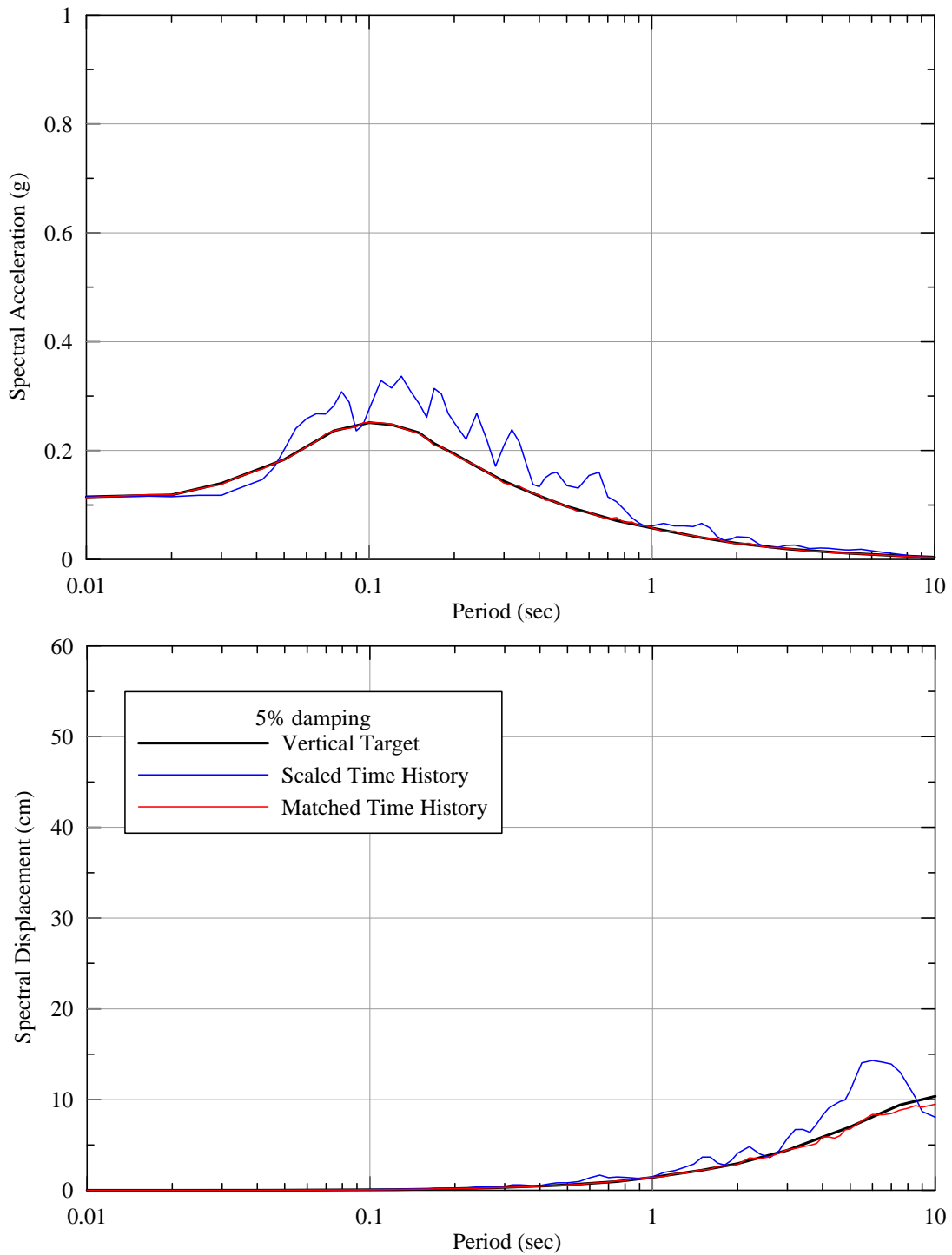


**Figure 69: Acceleration and Displacement Response Spectra. Seed Motion: 1989 Loma Prieta Earthquake, Gilroy Array #6, Vertical Component. Target: Vertical, FEE  $V_{S30} = 5000$  ft/sec.**

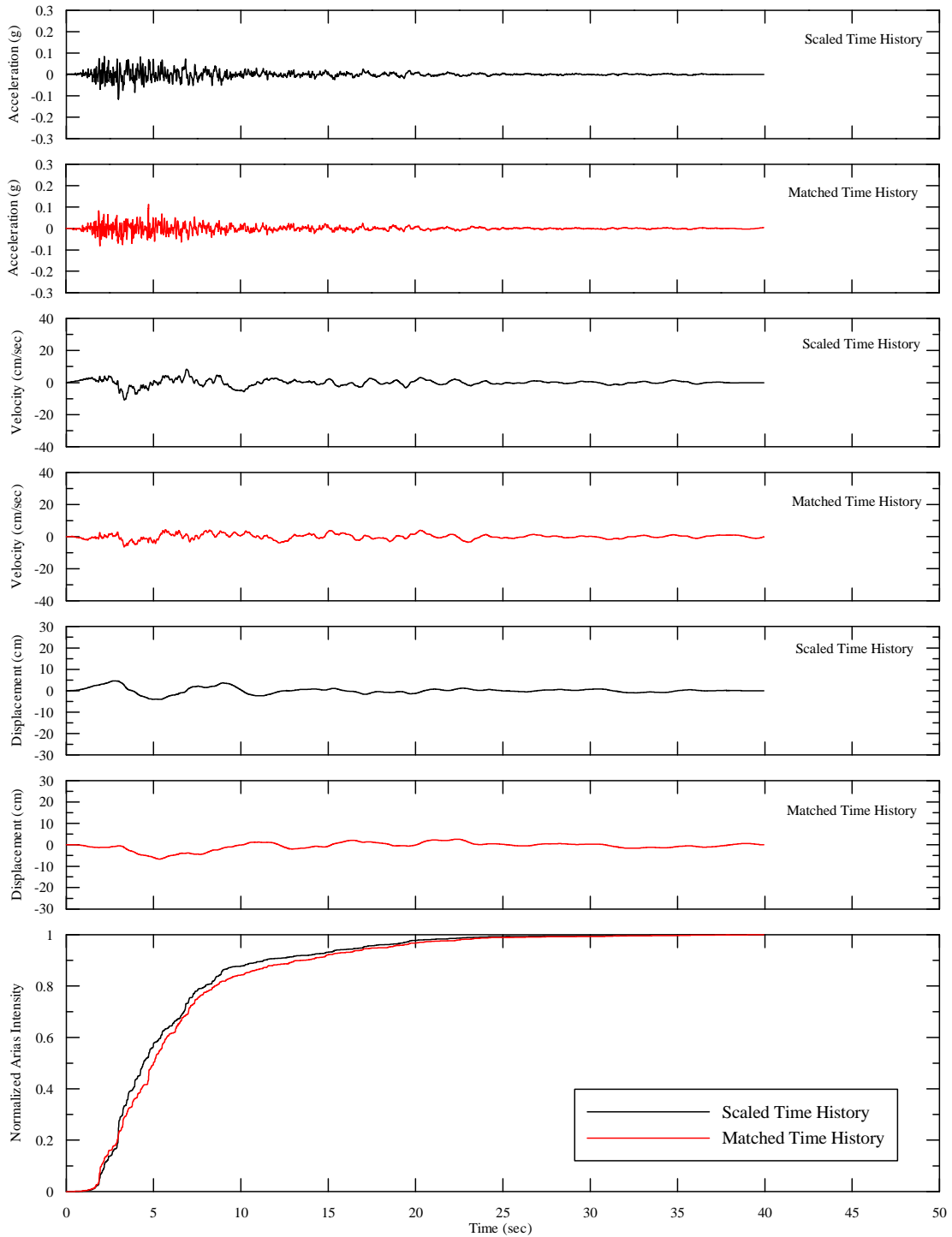


**Figure 70: Acceleration, Velocity, and Displacement Time Histories. Seed Motion: 1989 Loma Prieta Earthquake, Gilroy Array #6, Vertical Component. Target: Vertical, FEE  $V_{S30} = 5000$  ft/sec.**

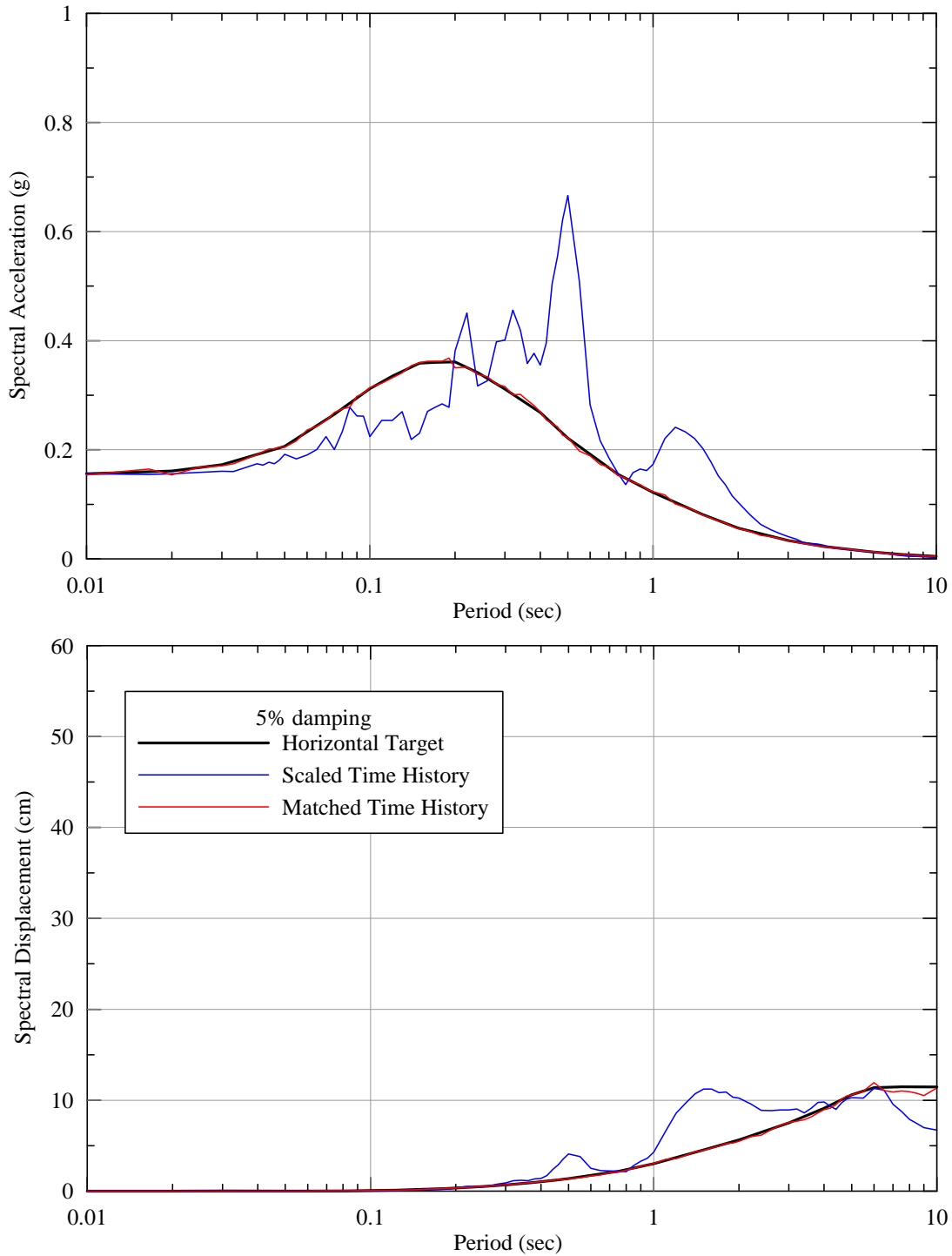


**Figure 71: Acceleration and Displacement Response Spectra. Seed Motion: 1999 Hector Mine Earthquake, 90 degree Component. Target: Fault Normal, FEE  $V_{S30} = 5000$  ft/sec.**

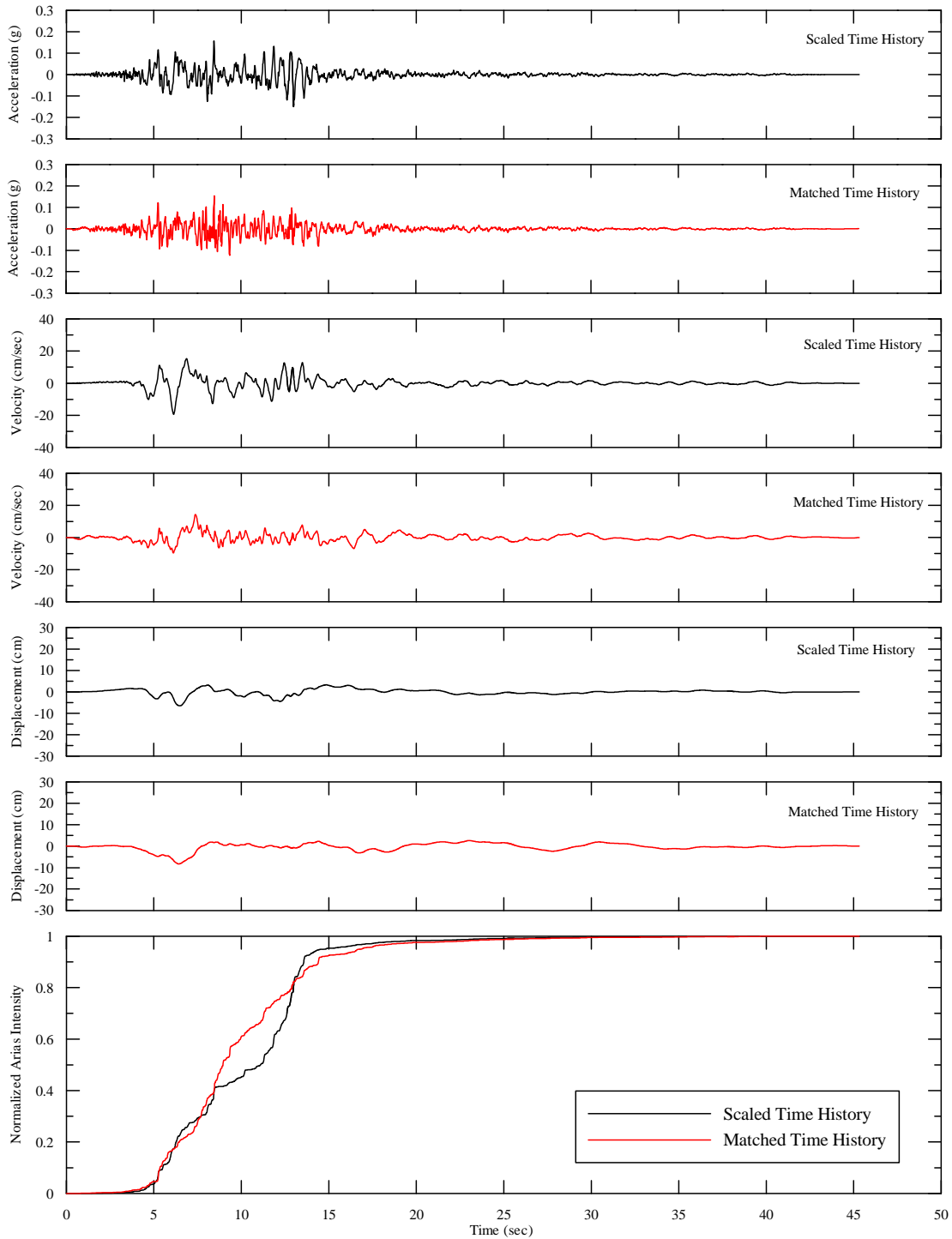


**Figure 72: Acceleration, Velocity, and Displacement Time Histories. Seed Motion: 1999 Hector Mine Earthquake, 90 degree Component. Target: Fault Normal, FEE  $V_{s30} = 5000$  ft/sec.**

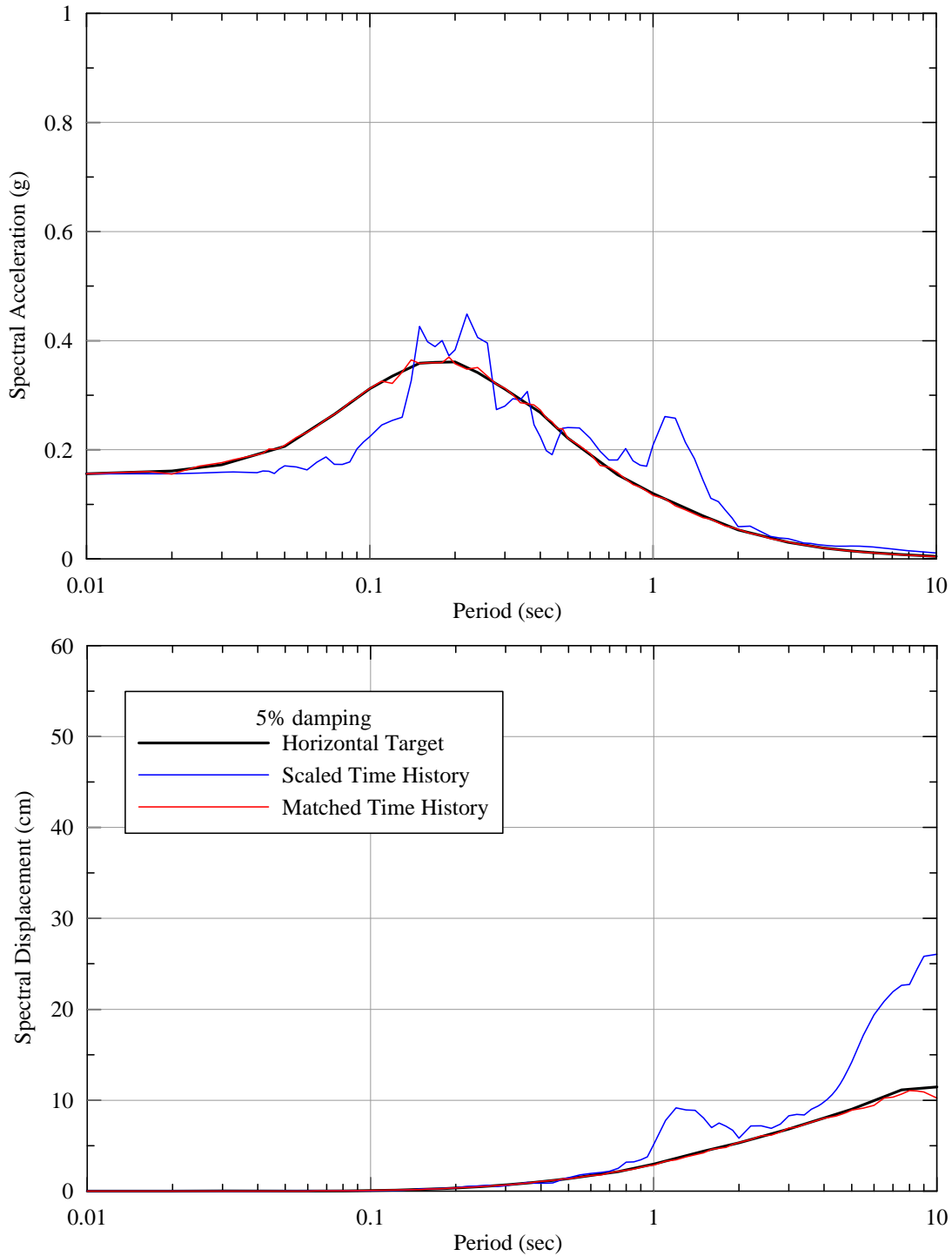


**Figure 73: Acceleration and Displacement Response Spectra. Seed Motion: 1999 Hector Mine Earthquake, 0 degree Component. Target: Fault Parallel, FEE  $V_{S30} = 5000$  ft/sec.**

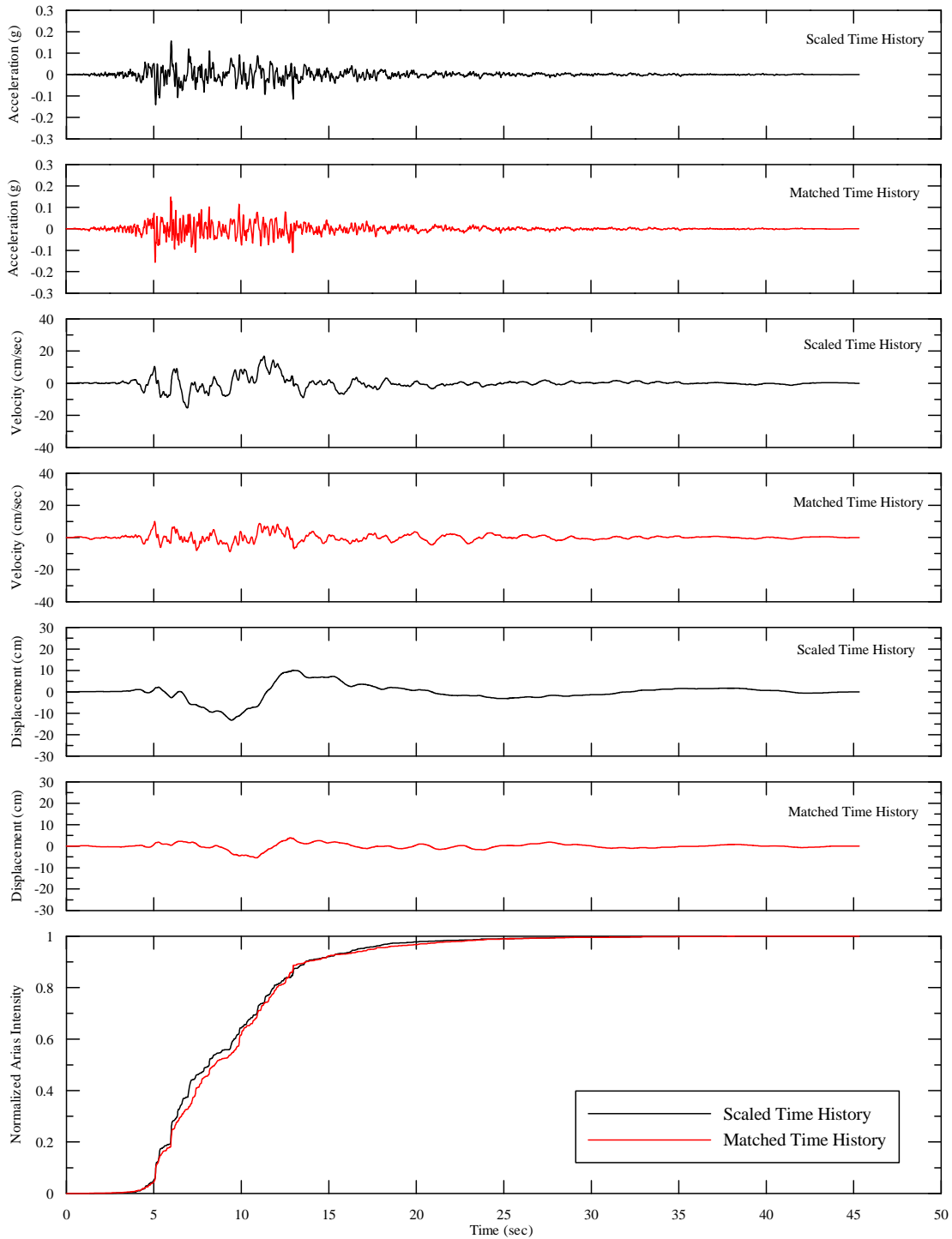


**Figure 74: Acceleration, Velocity, and Displacement Time Histories. Seed Motion: 1999 Hector Mine Earthquake, 0 degree Component. Target: Fault Parallel, FEE  $V_{s30} = 5000$  ft/sec.**

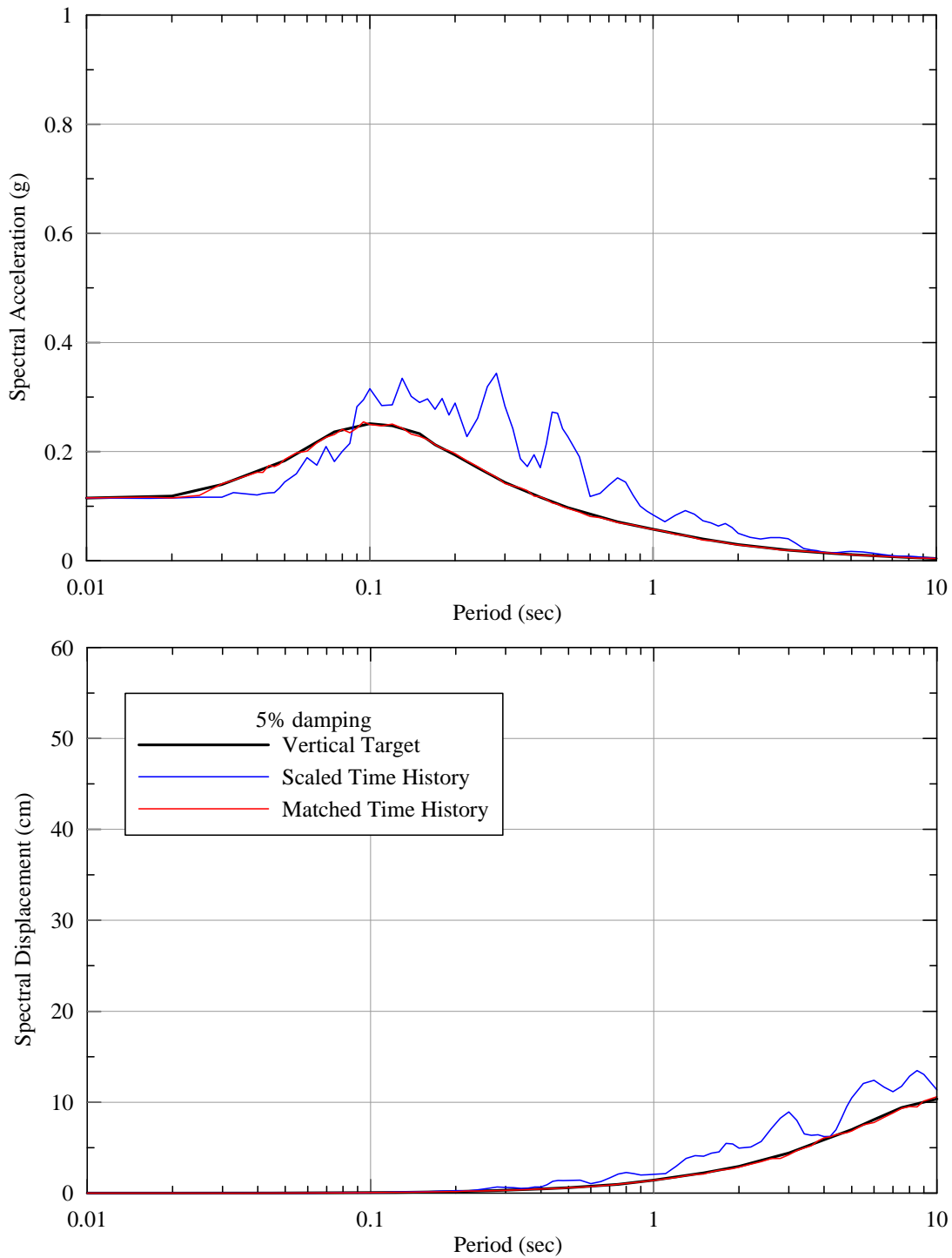


**Figure 75: Acceleration and Displacement Response Spectra. Seed Motion: 1999 Hector Mine Earthquake, Vertical Component. Target: Vertical, FEE  $V_{S30} = 5000$  ft/sec.**

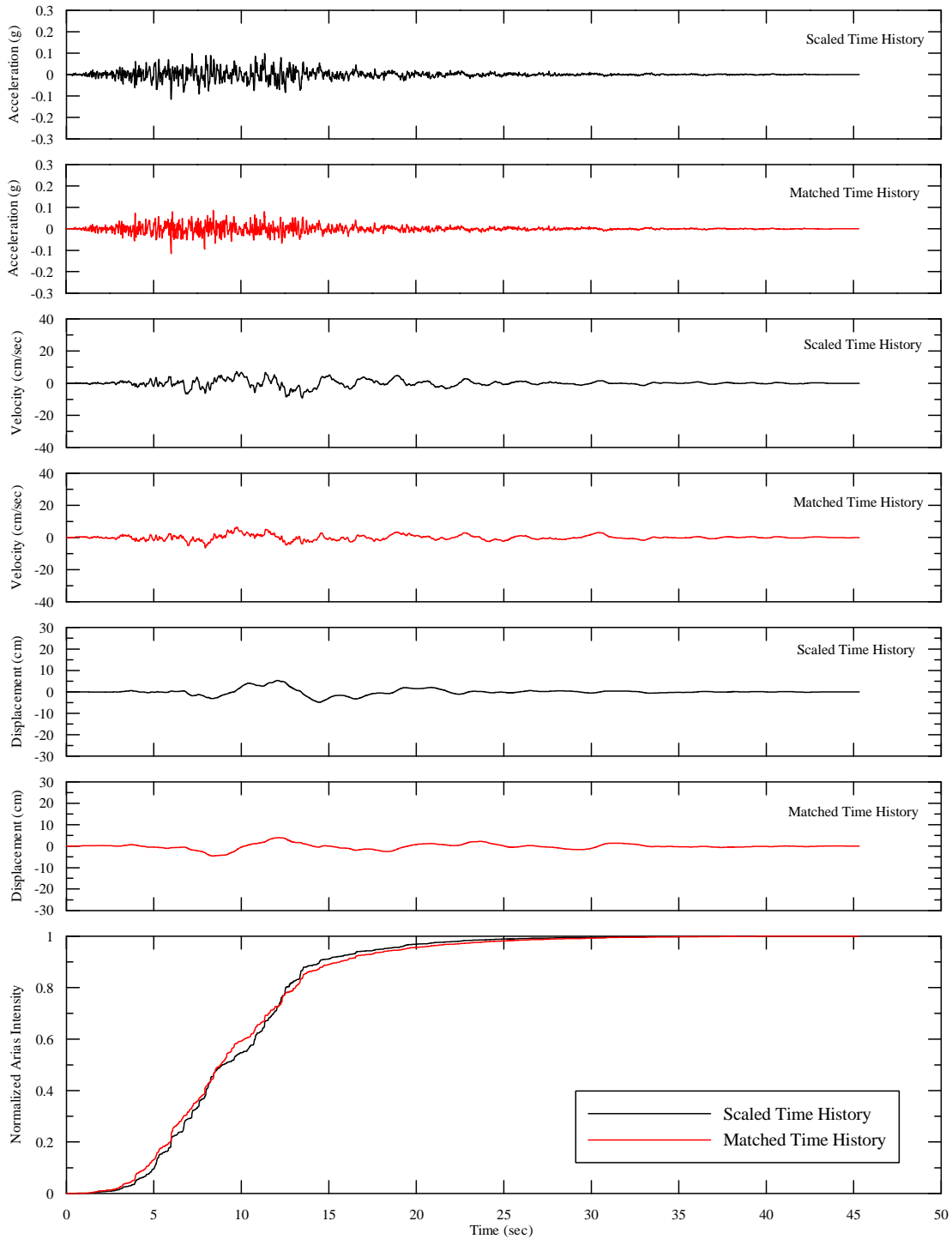


**Figure 76: Acceleration, Velocity, and Displacement Time Histories. Seed Motion: 1999 Hector Mine Earthquake, Vertical Component. Target: Vertical, FEE  $V_{S30} = 5000$  ft/sec.**

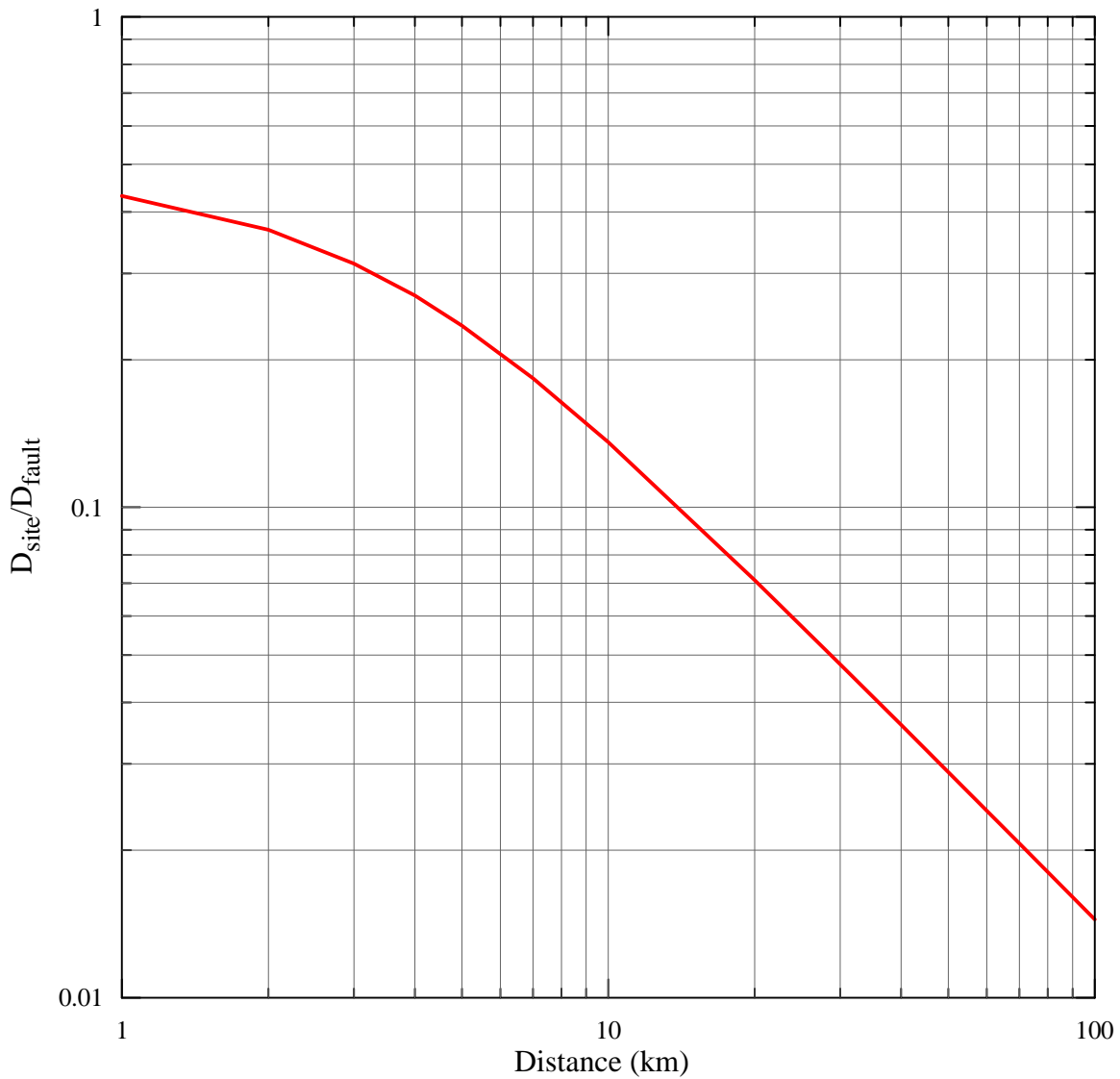


**Figure 77: Attenuation relationship of fling displacement with distance (normalized by the estimated fault displacement) used in the present study.**

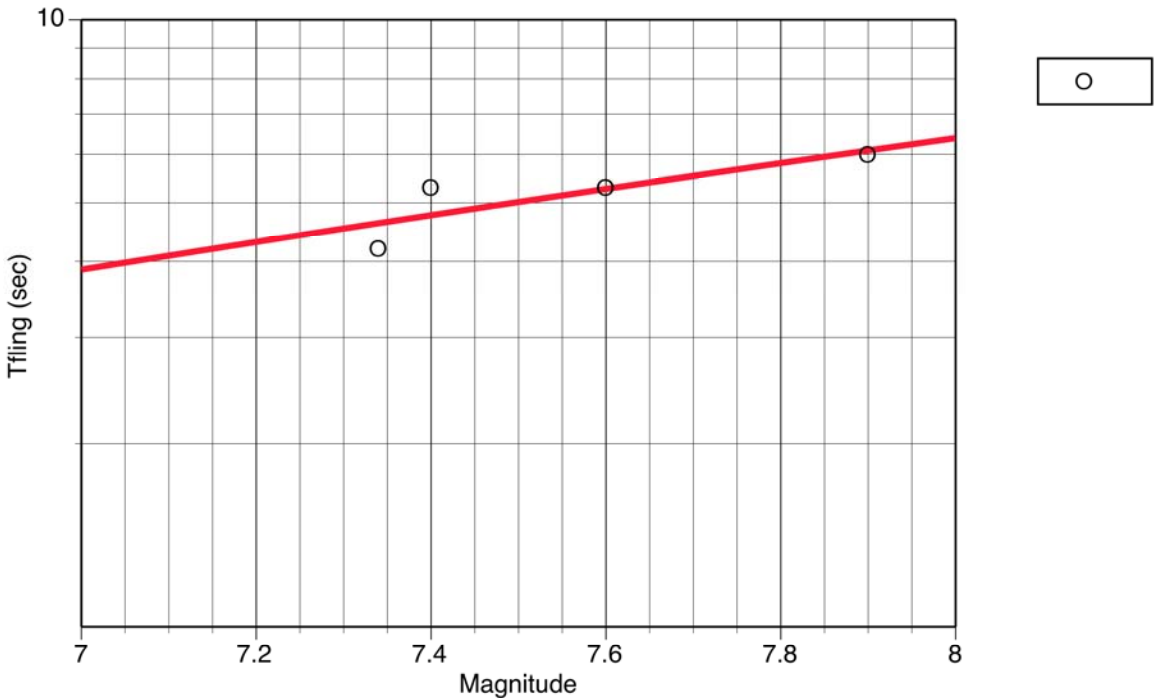


Figure 78: Fling period as a function of magnitude (revised Figure 6-9 of Abrahamson, 2001).

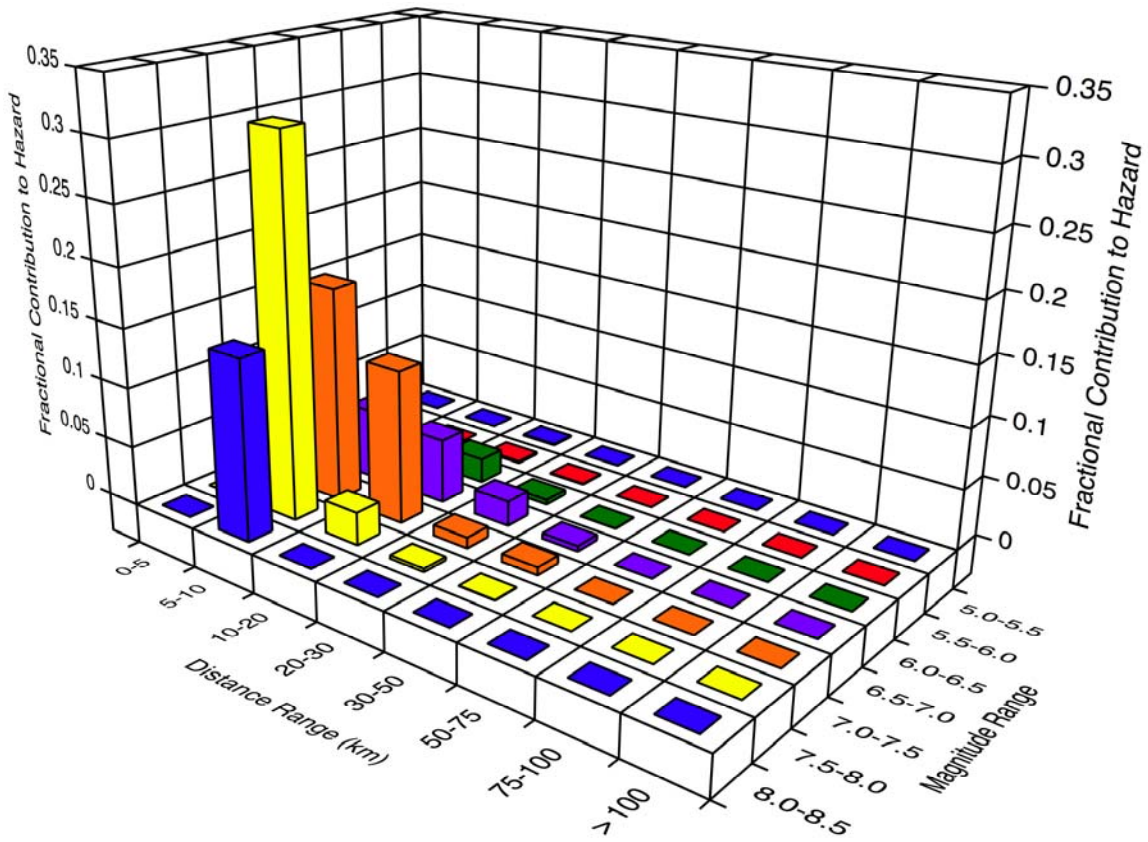


Figure 79: Deaggregation for 1,000 year return period: PGA.

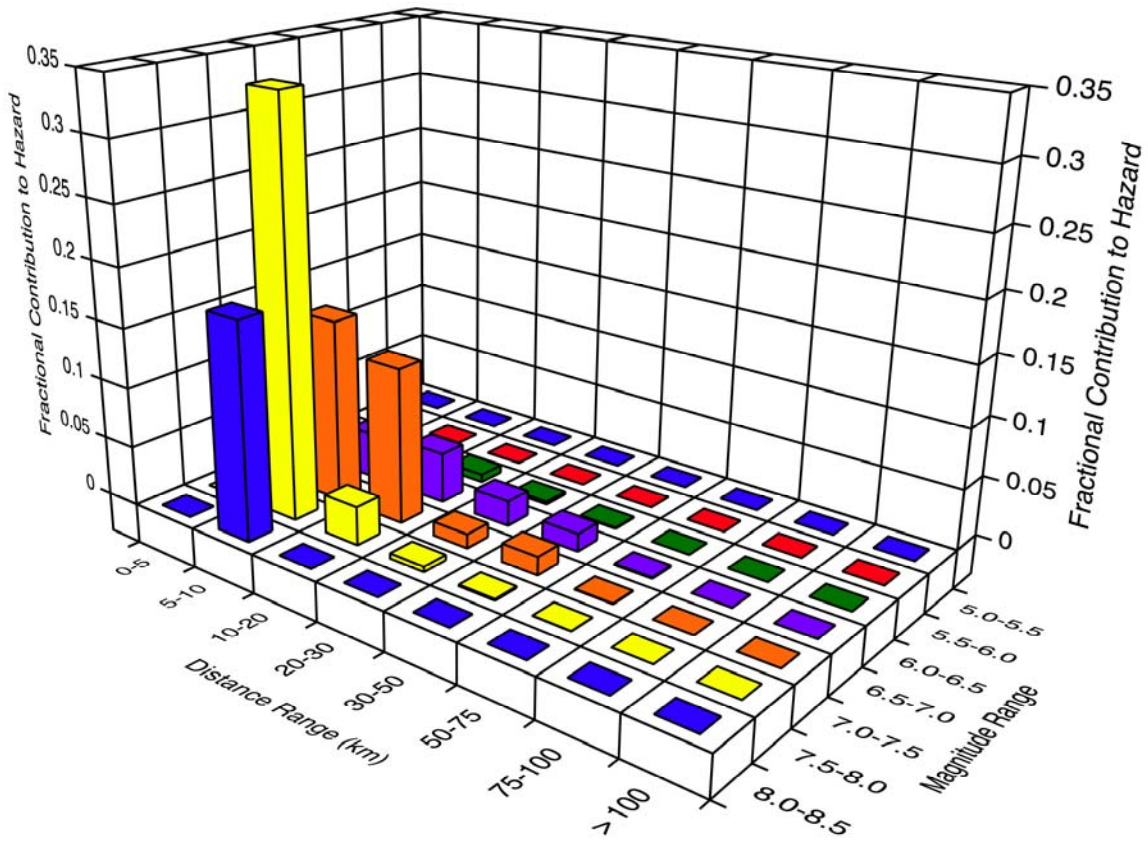
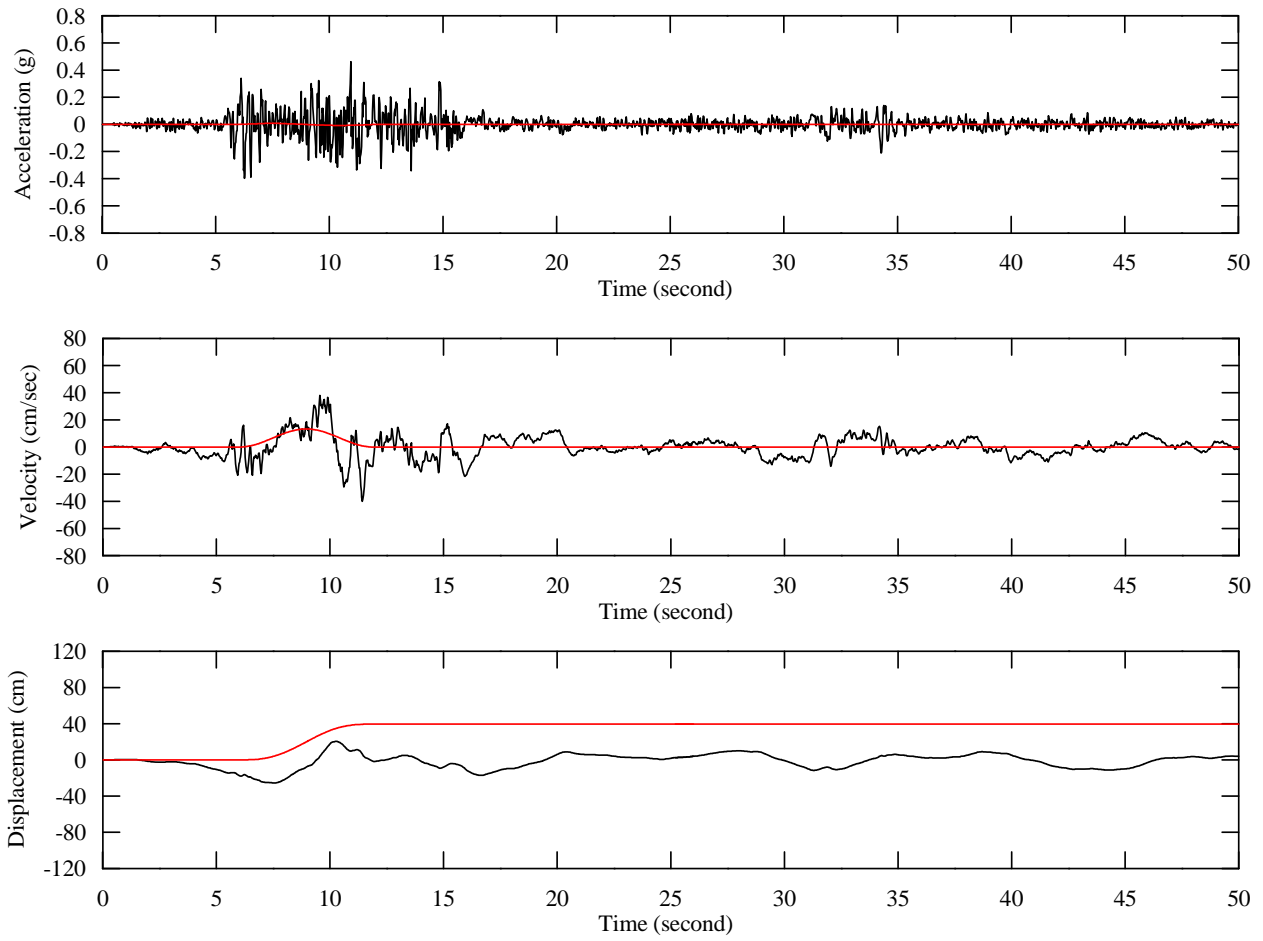
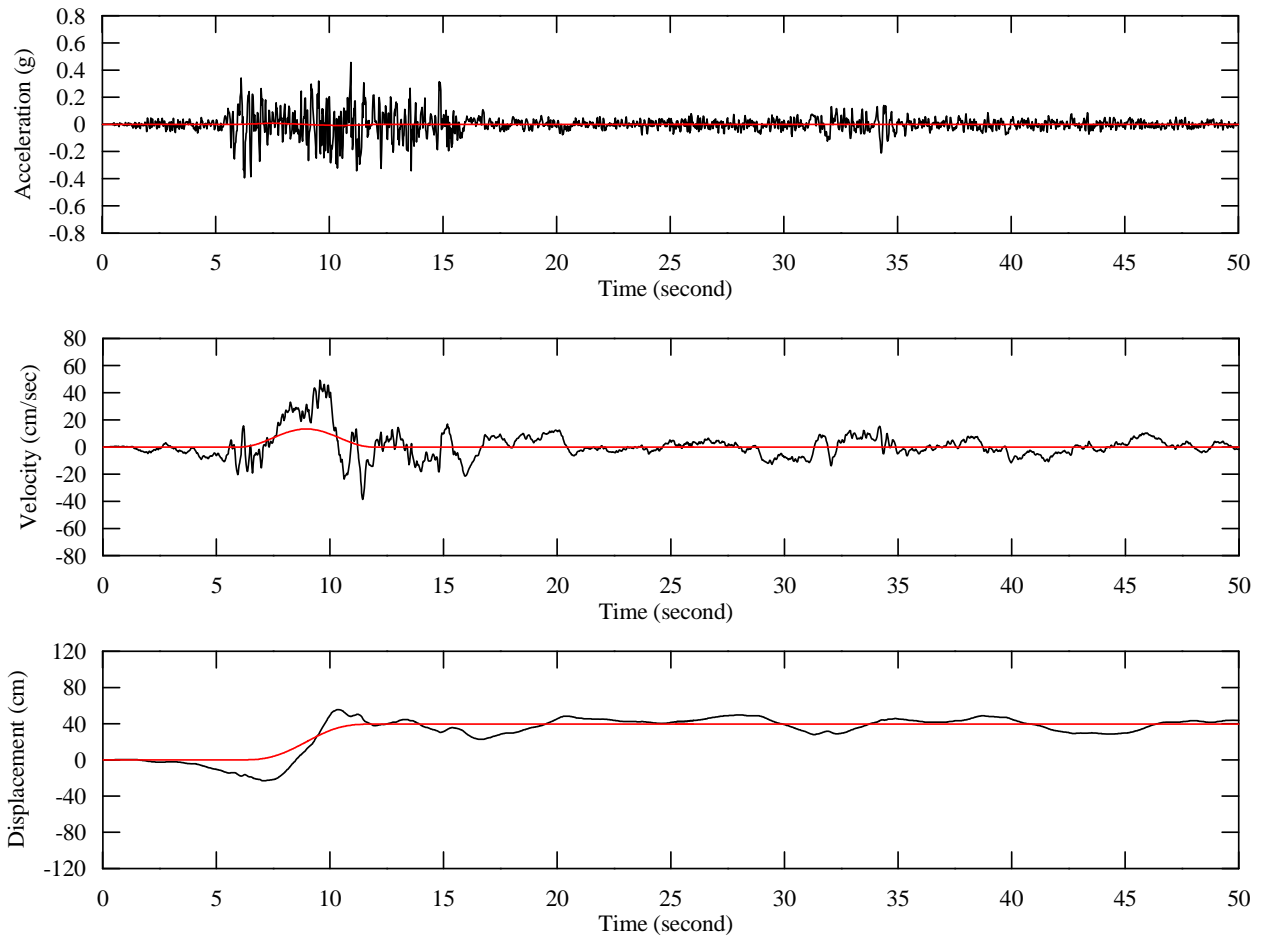


Figure 80: Deaggregation for 1,000 year return period: T- 1sec.



**Figure 81: Fault parallel time histories and fling time histories, 1990 Manjil Earthquake, SEE scenario,  $V_{S30} = 3000$  ft/sec.**



**Figure 82: Fault parallel time histories including fling, 1990 Manjil Earthquake, SEE scenario,  $V_{s30} = 3000$  ft/sec.**

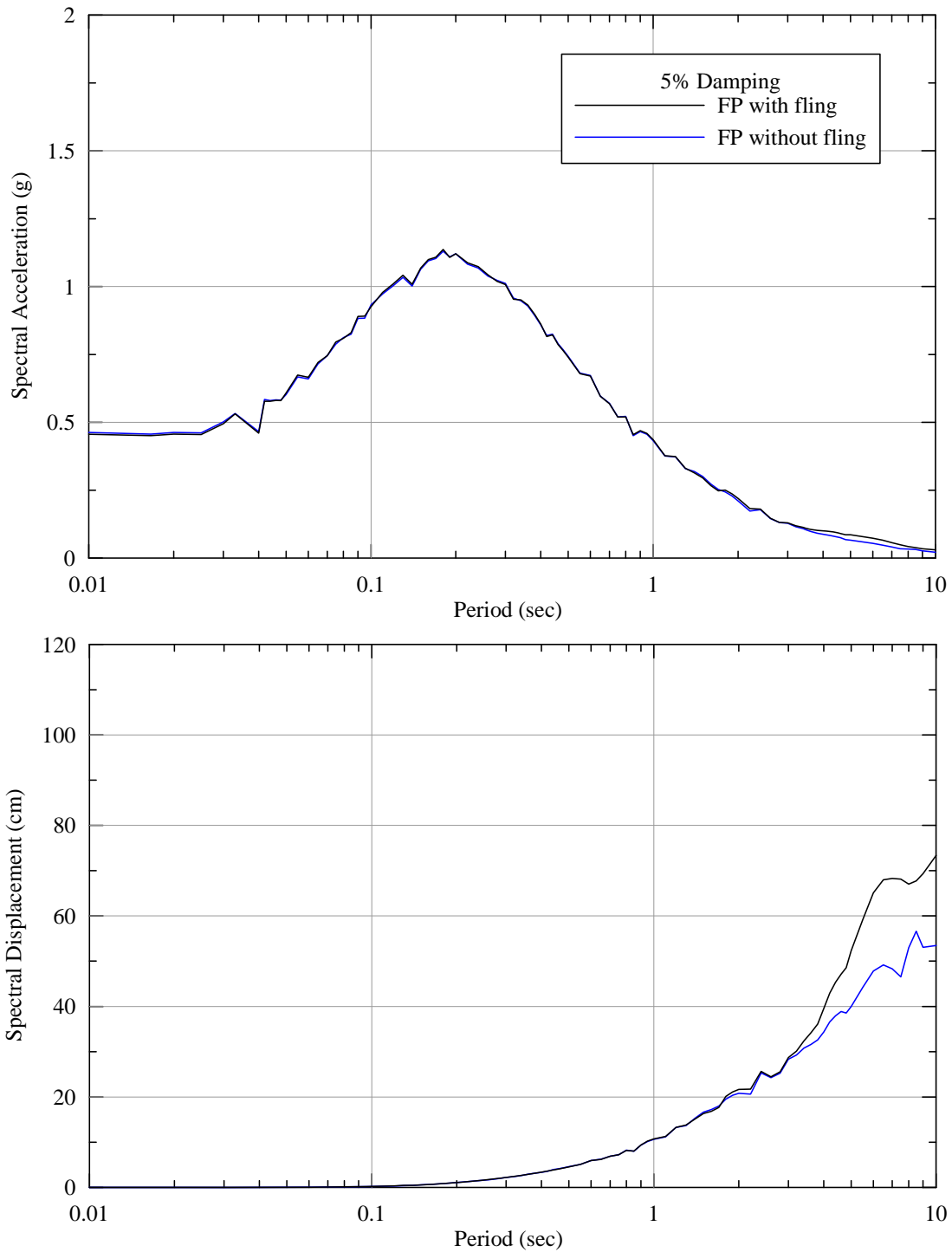


**Figure 83: Comparison of acceleration and displacement response spectra between the original and modified (with fling) time histories, 1990 Manjil Earthquake, SEE scenario,  $V_{S30} = 3000$  ft/sec.**

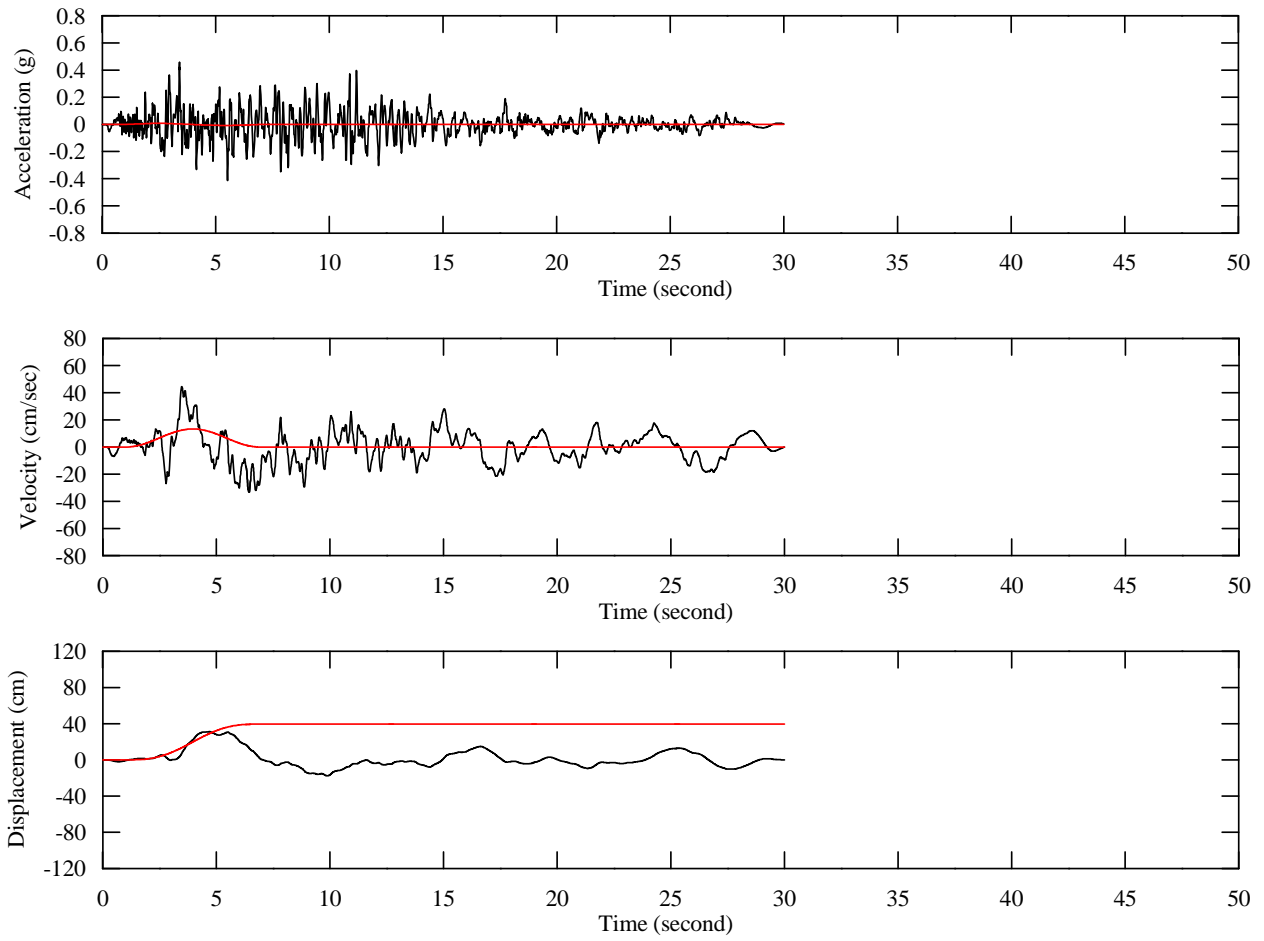


**Figure 84: Fault parallel time histories and fling time histories, 1999 Kocaeli Earthquake, SEE scenario,  $V_{S30} = 3000$  ft/sec.**

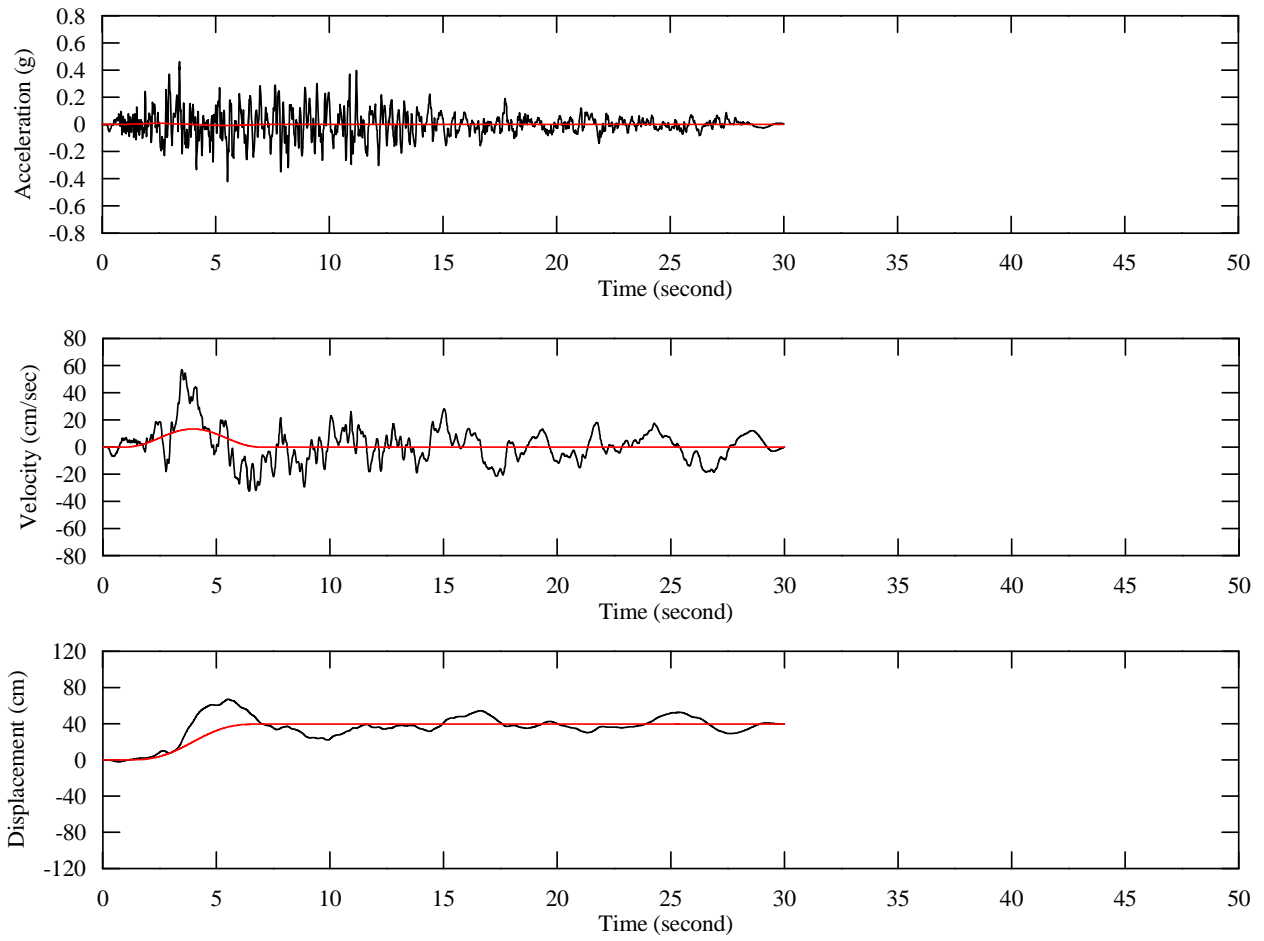


**Figure 85: Fault parallel time histories including fling, 1999 Kocaeli Earthquake, SEE scenario,  $V_{S30} = 3000$  ft/sec.**

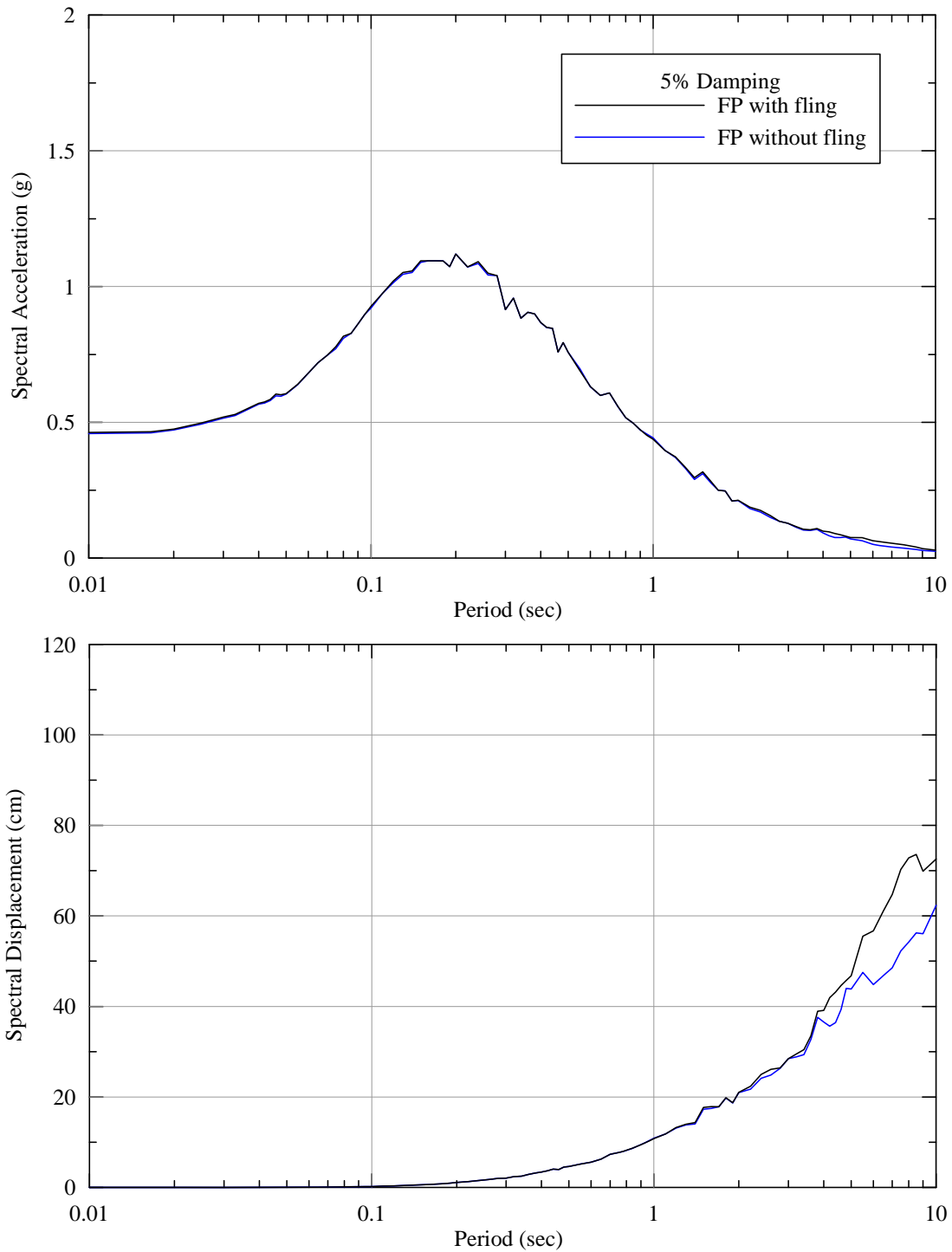


**Figure 86: Comparison of acceleration and displacement response spectra between the original and modified (with fling) time histories, 1999 Kocaeli Earthquake, SEE scenario,  $V_{S30} = 3000$  ft/sec.**

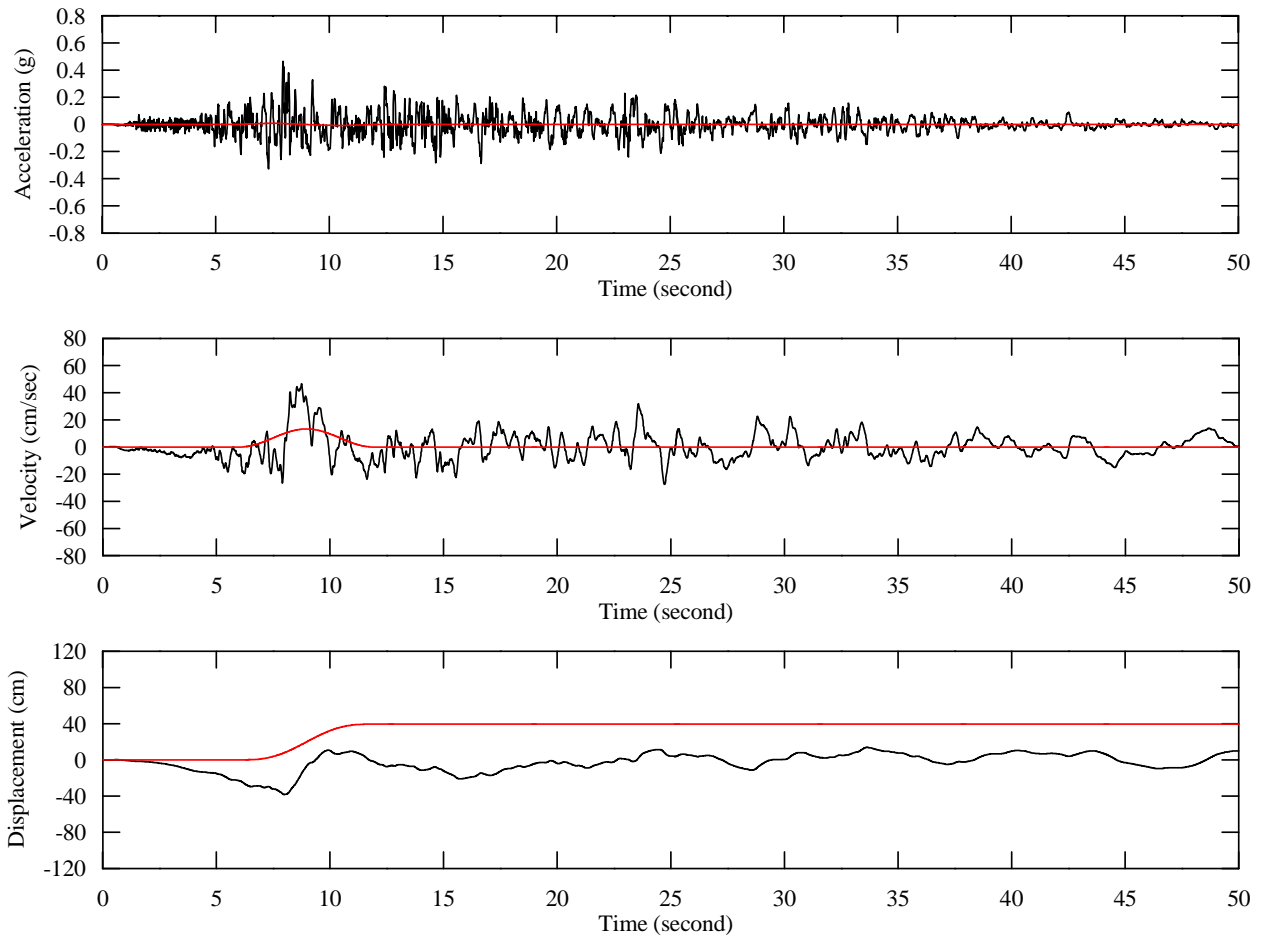


**Figure 87: Fault parallel time histories and fling time histories, 1999 Chi-Chi Earthquake, SEE scenario,  $V_{S30} = 3000$  ft/sec.**

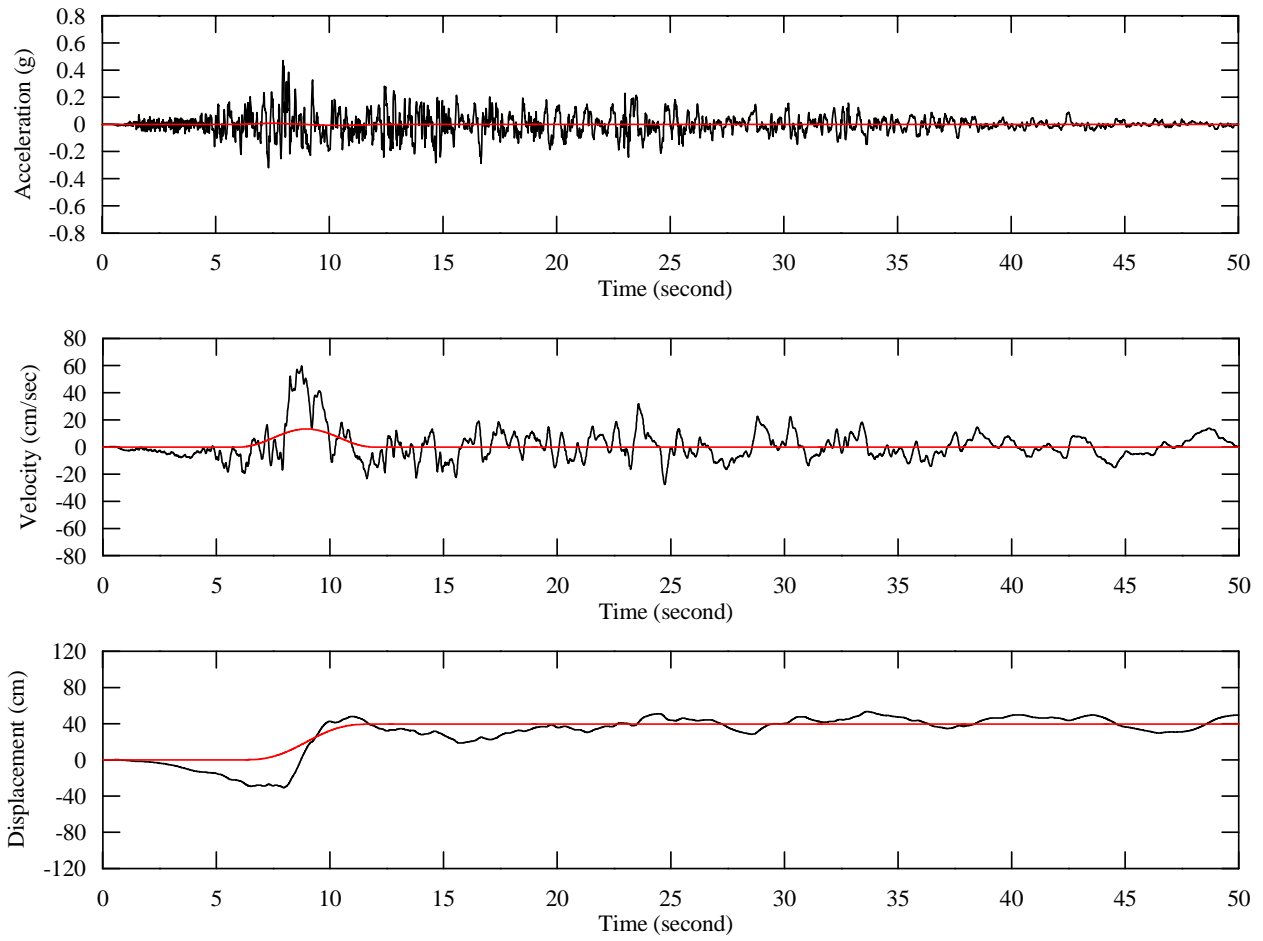


**Figure 88: Fault parallel time histories including fling, 1999 Chi-Chi Earthquake, SEE scenario,  $V_{S30} = 3000$  ft/sec.**

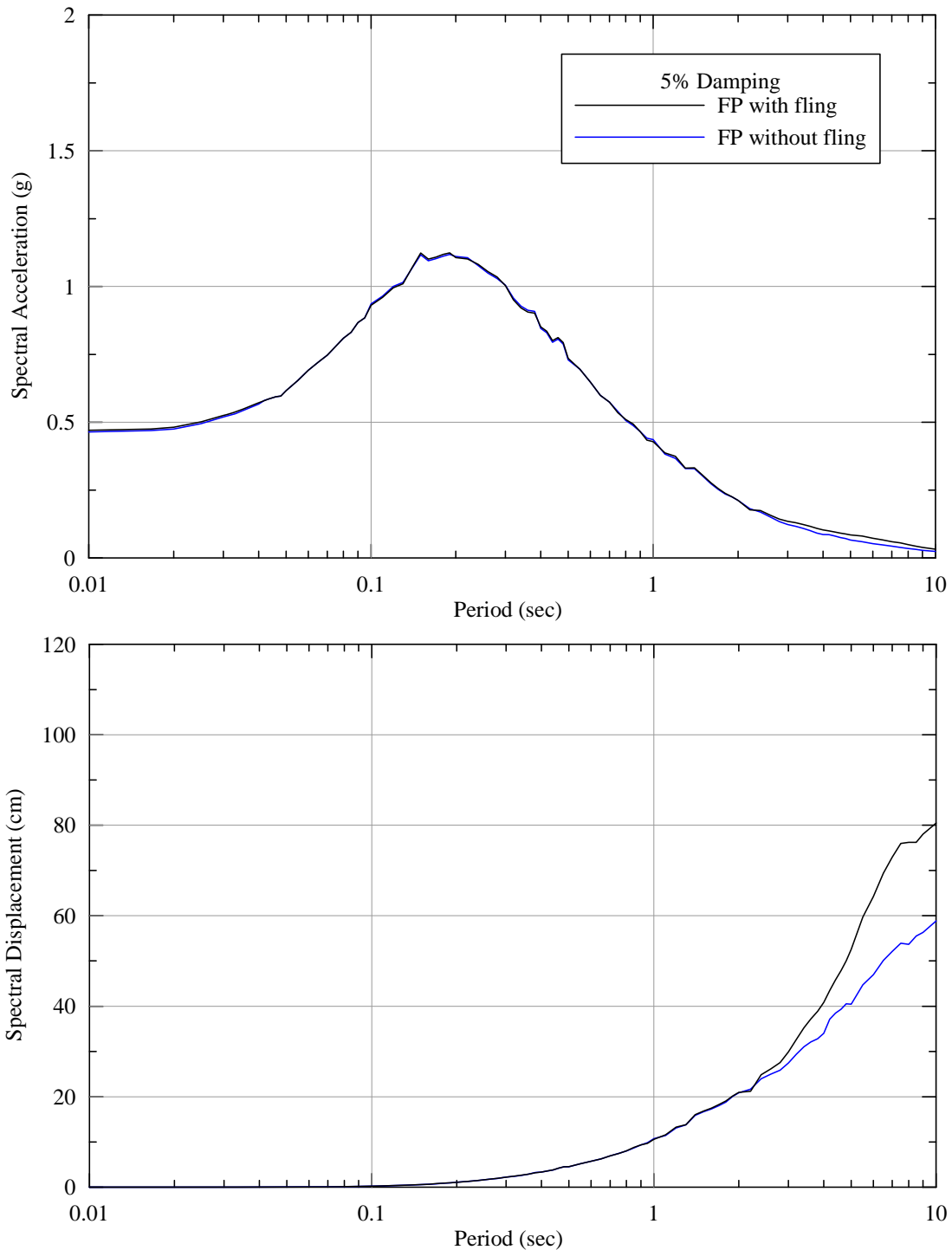


**Figure 89: Comparison of acceleration and displacement response spectra between the original and modified (with fling) time histories, 1999 Chi-Chi Earthquake, SEE scenario,  $V_{S30} = 3000$  ft/sec.**

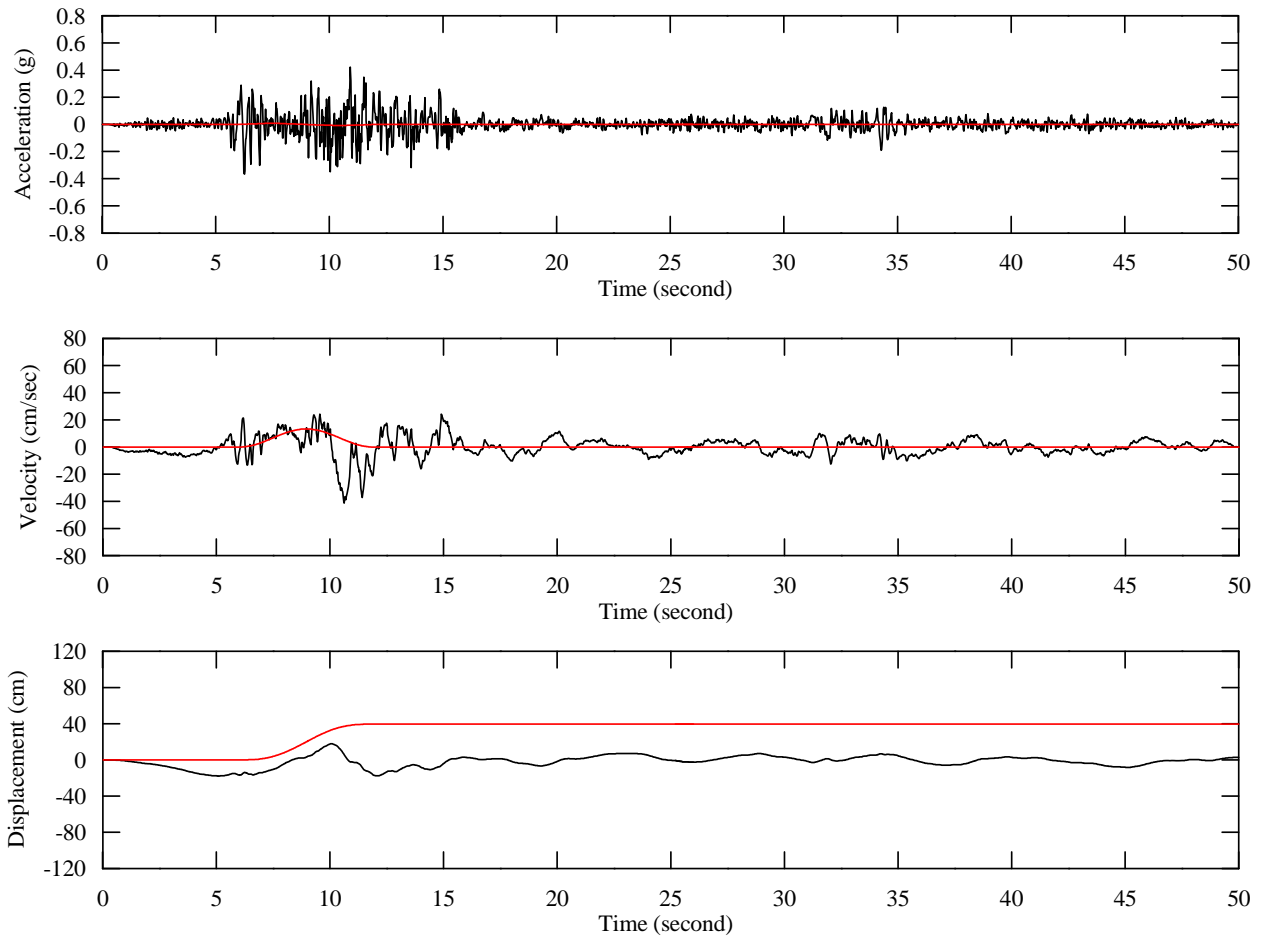


**Figure 90: Fault parallel time histories and fling time histories, 1990 Manjil Earthquake, SEE scenario,  $V_{S30} = 5000$  ft/sec.**

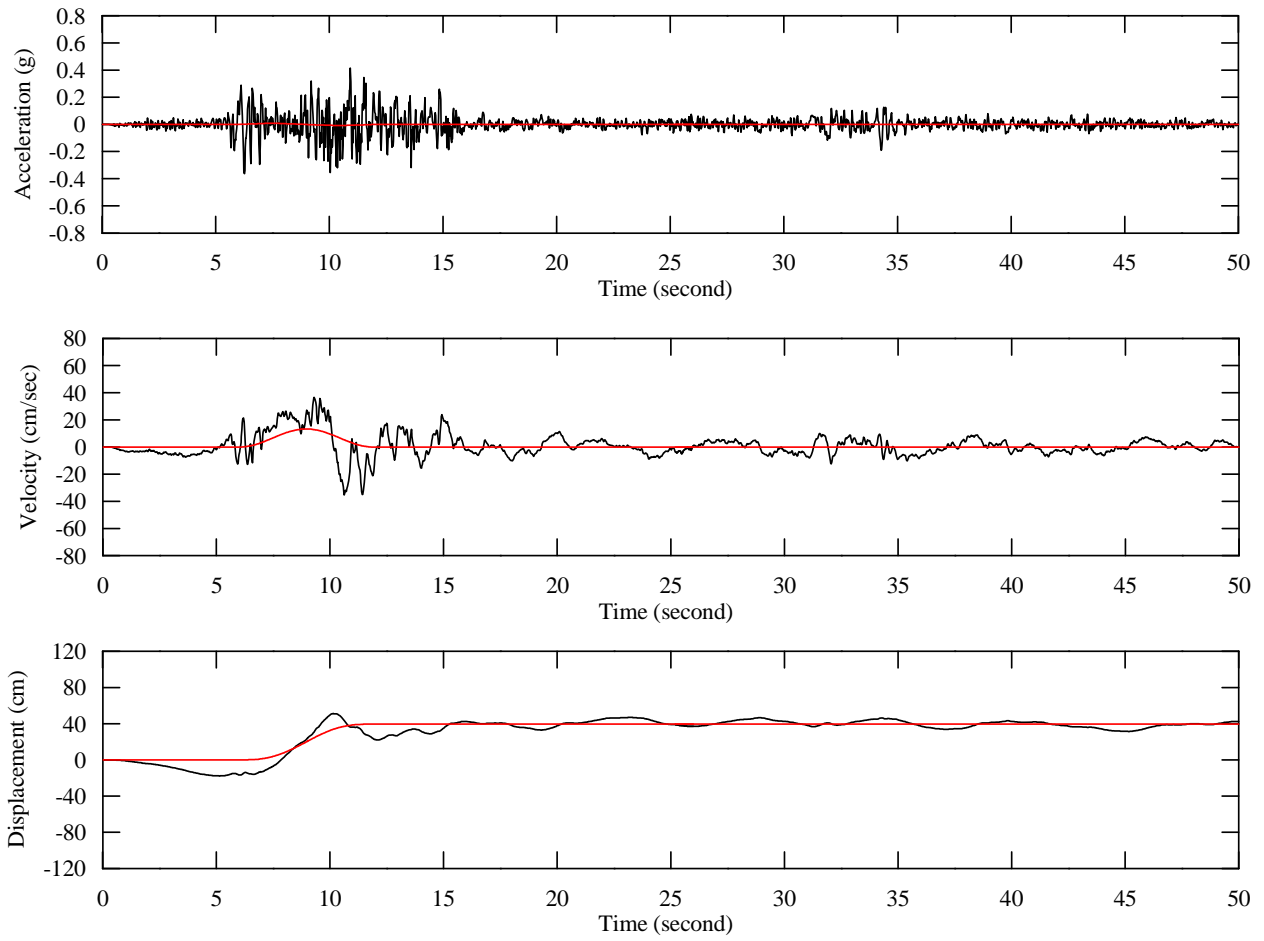


**Figure 91: Fault parallel time histories including fling, 1990 Manjil Earthquake, SEE scenario,  $V_{S30} = 5000$  ft/sec.**

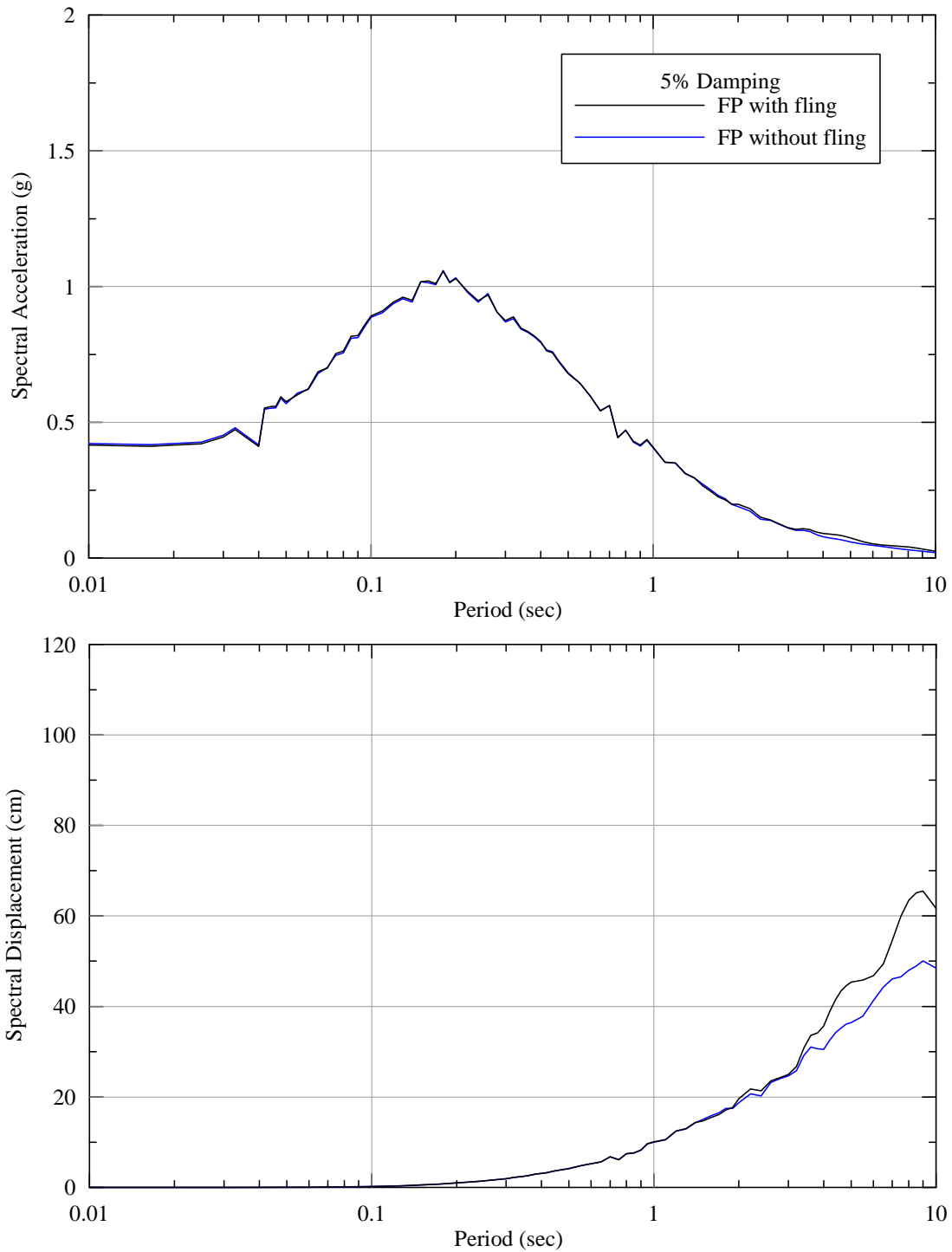


**Figure 92: Comparison of acceleration and displacement response spectra between the original and modified (with fling) time histories, 1990 Manjil Earthquake, SEE scenario,  $V_{S30} = 5000$  ft/sec.**

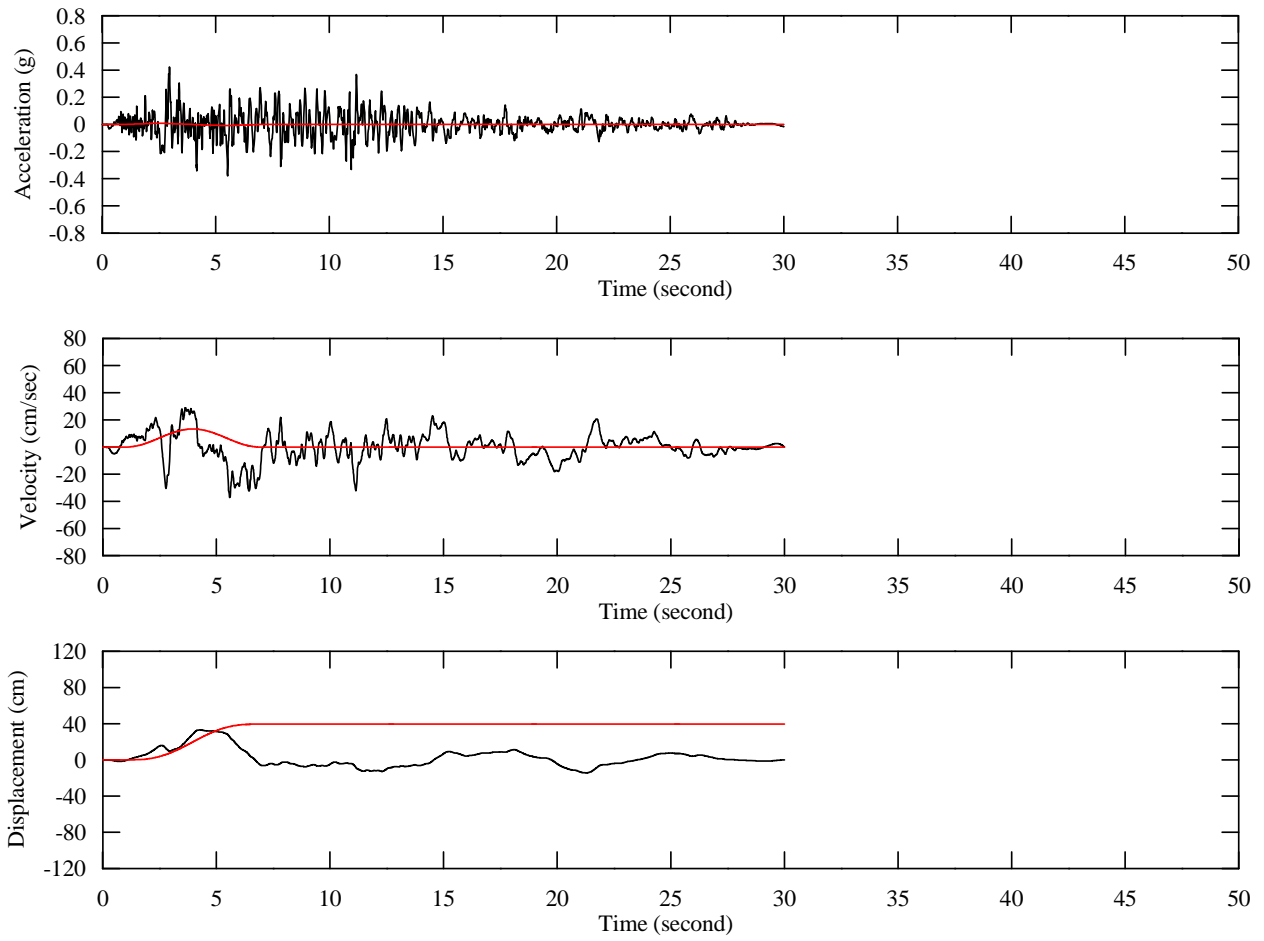


**Figure 93: Fault parallel time histories and fling time histories, 1999 Kocaeli Earthquake, SEE scenario,  $V_{S30} = 5000$  ft/sec.**

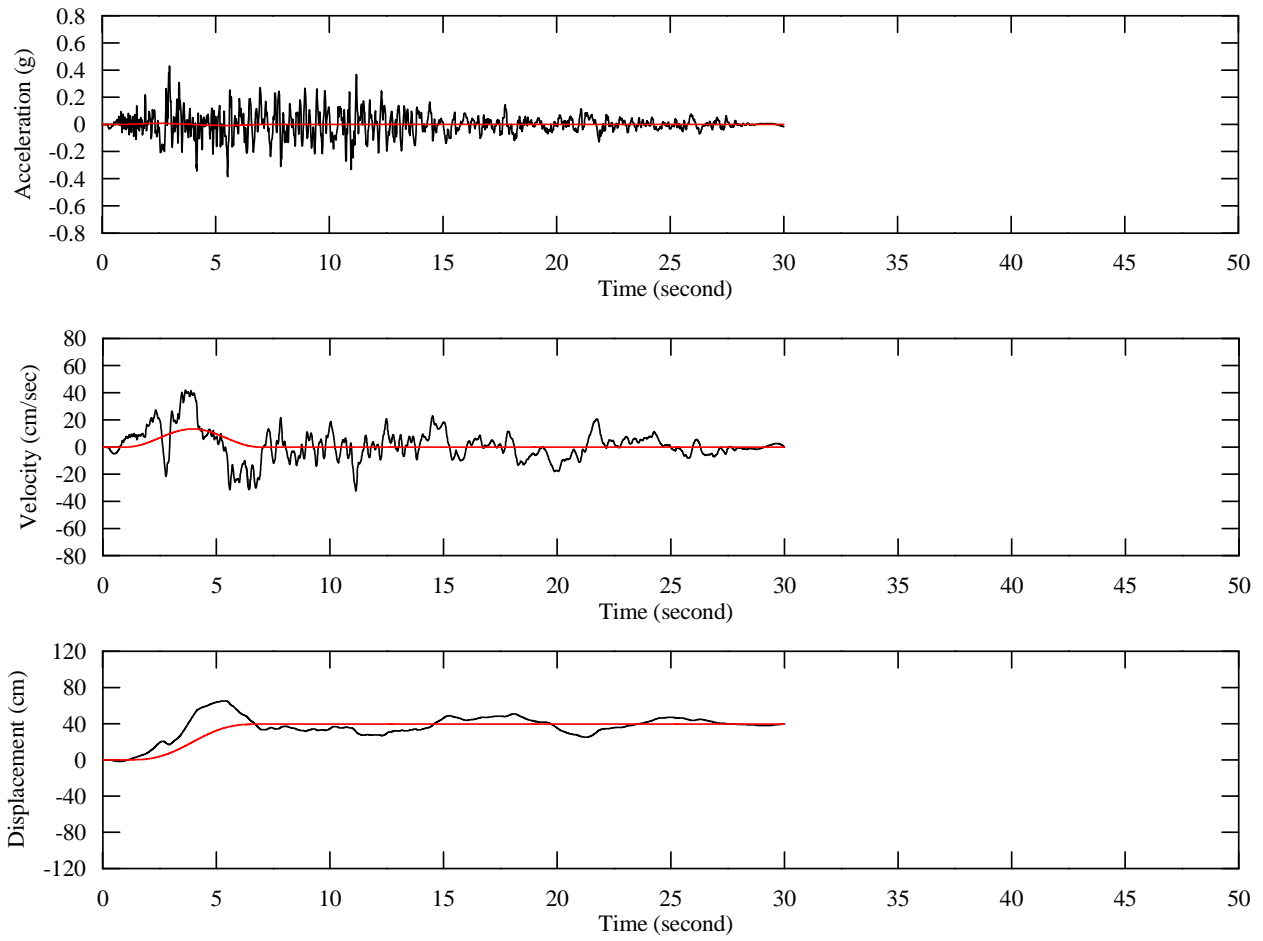


**Figure 94: Fault parallel time histories including fling, 1999 Kocaeli Earthquake, SEE scenario,  $V_{S30} = 5000$  ft/sec.**

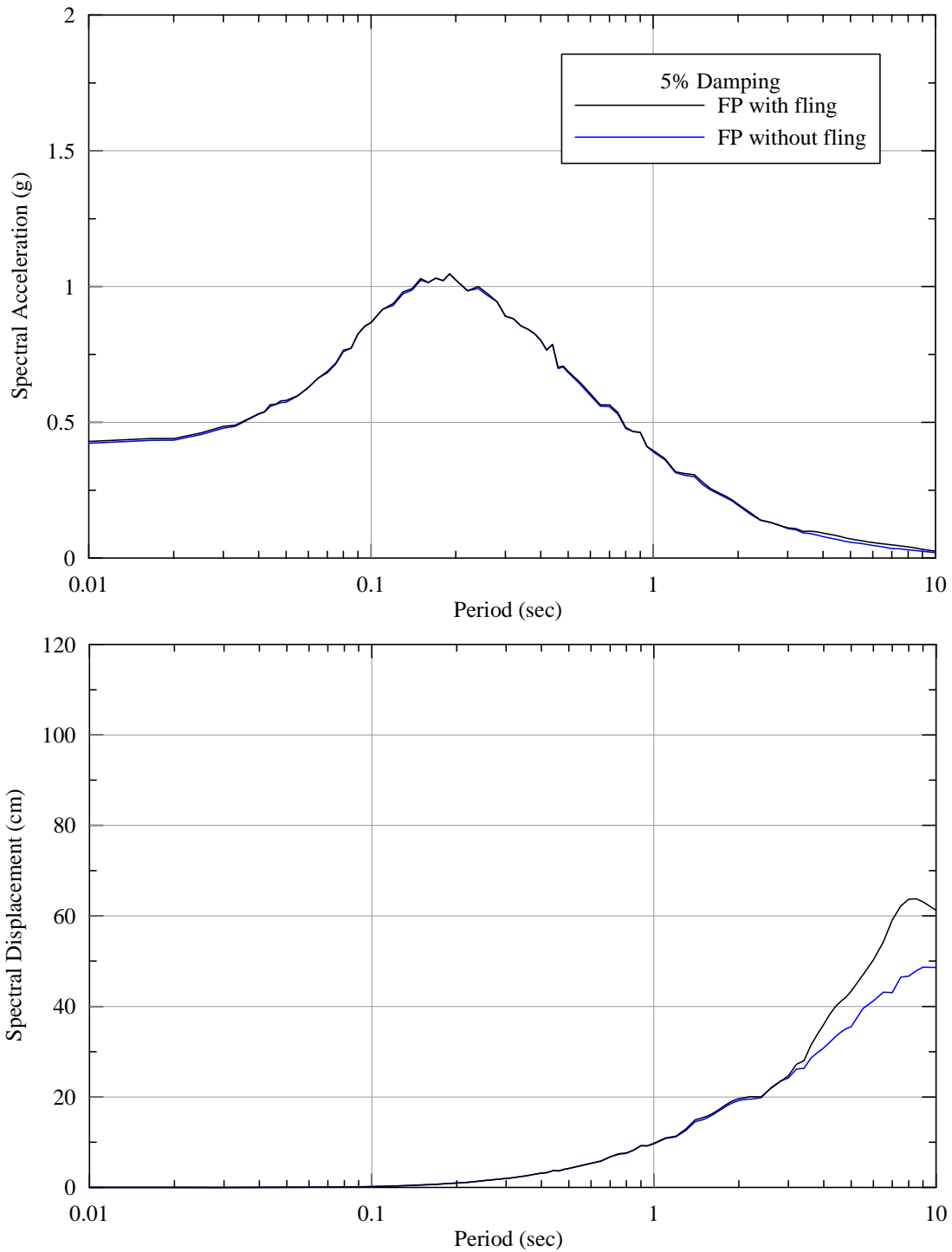


**Figure 95: Comparison of acceleration and displacement response spectra between the original and modified (with fling) time histories, 1999 Kocaeli Earthquake, SEE scenario,  $V_{S30} = 5000$  ft/sec.**

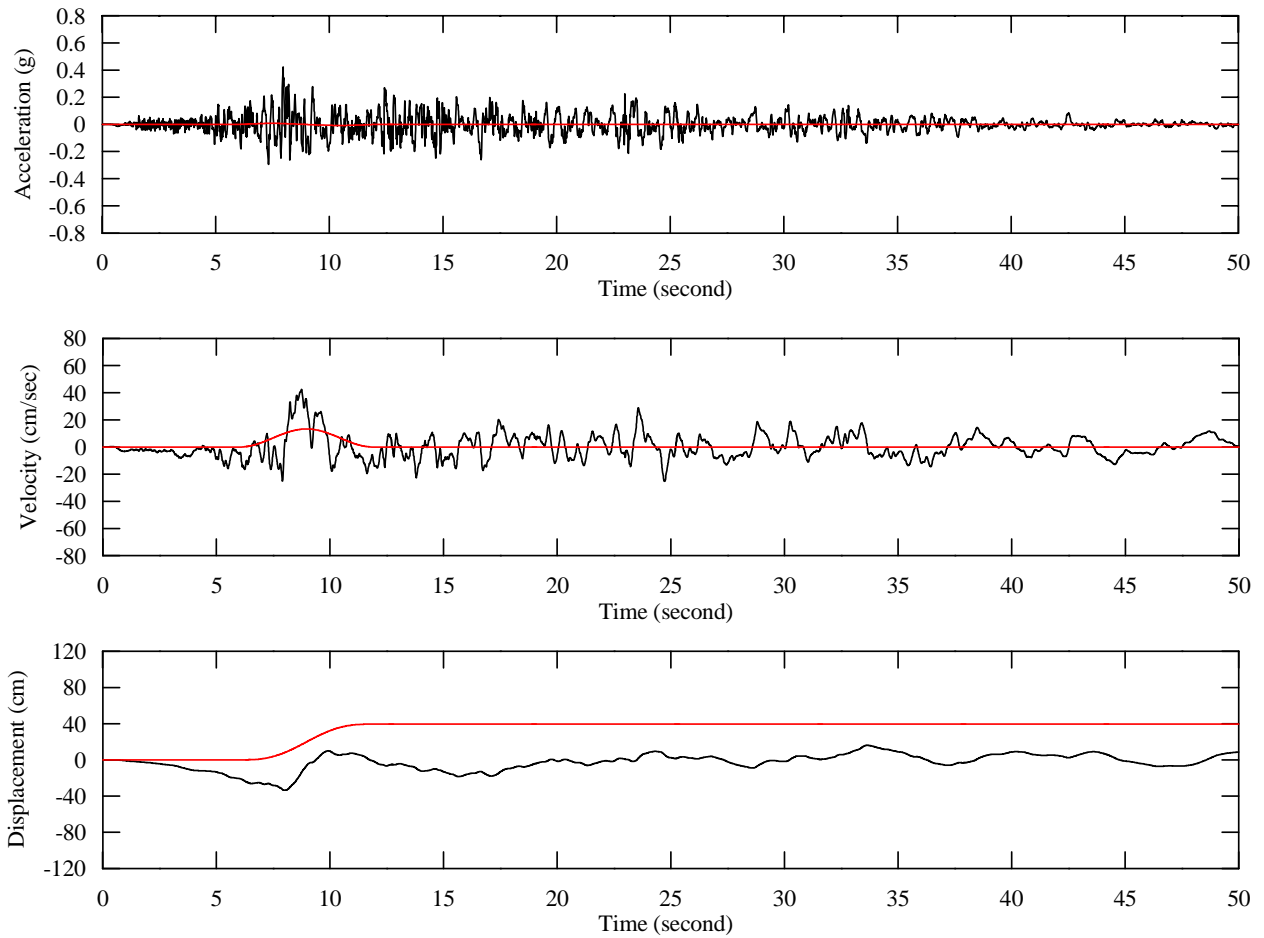


**Figure 96: Fault parallel time histories and fling time histories, 1999 Chi-Chi Earthquake, SEE scenario,  $V_{S30} = 5000$  ft/sec.**

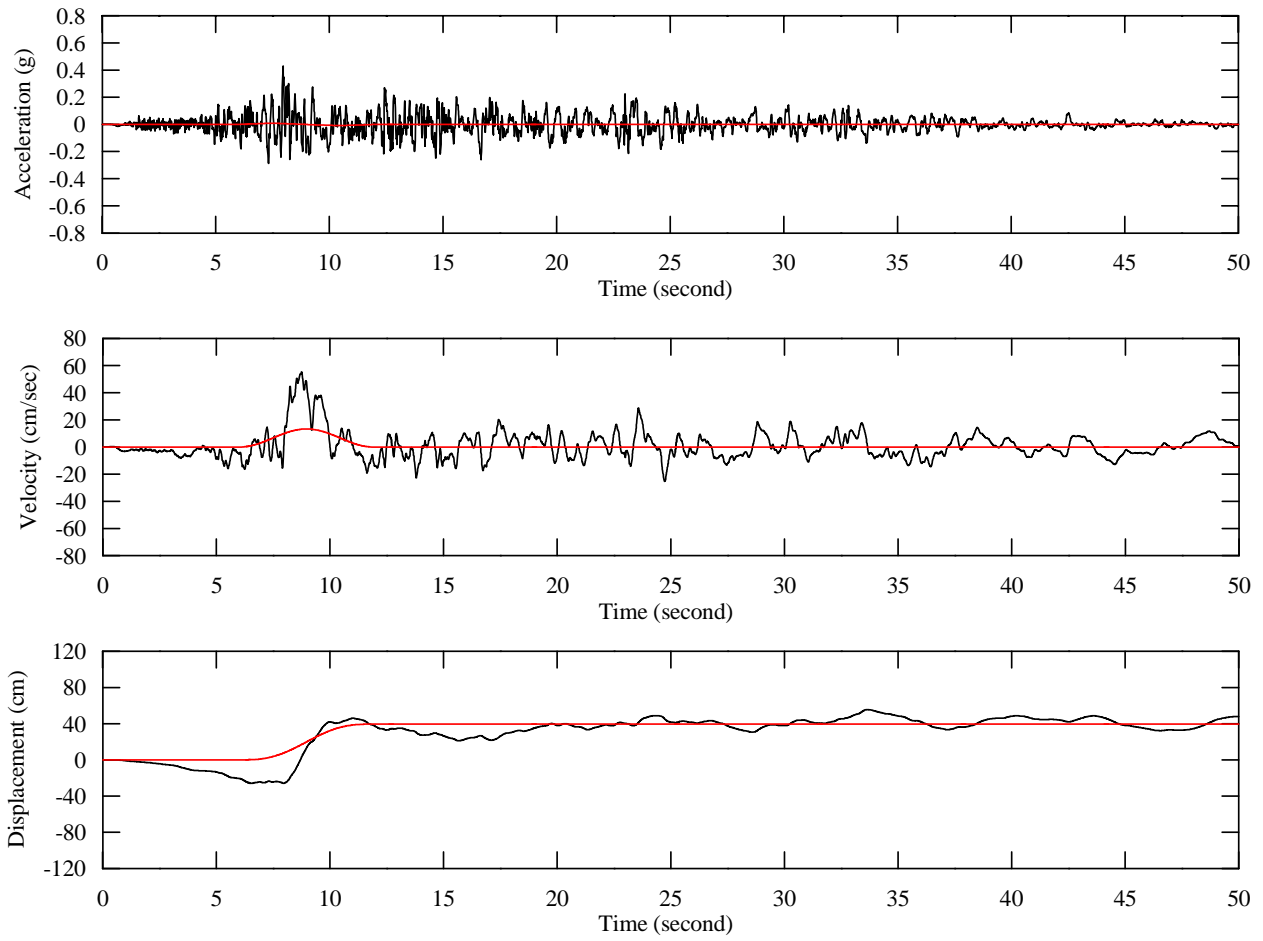


**Figure 97: Fault parallel time histories including fling, 1999 Chi-Chi Earthquake, SEE scenario,  $V_{S30} = 5000$  ft/sec.**

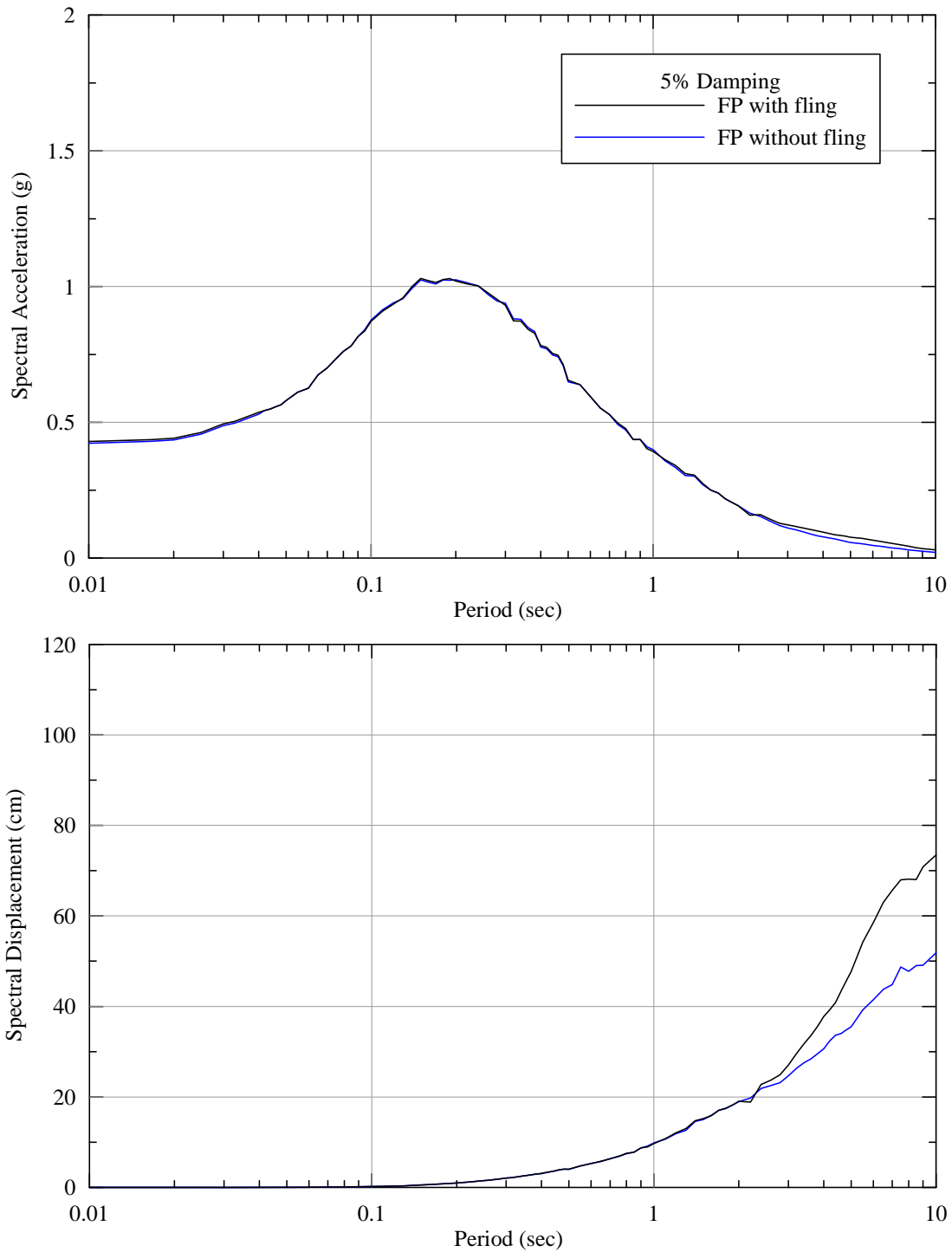


**Figure 98: Comparison of acceleration and displacement response spectra between the original and modified (with fling) time histories, 1999 Chi-Chi Earthquake, SEE scenario,  $V_{S30} = 5000$  ft/sec.**



---

**APPENDIX A**

Ground Motions for the Doyle Drive Replacement Project by  
Norman A. Abrahamson, Inc.

**GROUND MOTIONS FOR DOYLE DRIVE REPLACEMENT PROJECT**

**Norman A. Abrahamson, Inc.**

Piedmont, CA

December 15, 2008

# CONTENTS

<b>1</b>	<b>INTRODUCTION..</b> .....	<b>1</b>
<b>2</b>	<b>SOURCE CHARACTERIZATION..</b> .....	<b>2</b>
	2.1 Introduction.....	2
	2.2 Fault Parameters.....	2
	2.1 Magnitude Density Function .....	3
	2.1 Rupture Dimension Relations.....	3
	2.1.1 Point Source Model .....	2
<b>3</b>	<b>GROUND MOTION MODELS..</b> .....	<b>8</b>
	3.1 Base Attenuation Relations .....	8
	3.2 Directivity Models .....	8
	3.3 Vertical Ground Motions .....	9
<b>4</b>	<b>SEISMIC HAZARD ANALYSIS.....</b>	<b>13</b>
	4.1 Deterministic Ground Motions .....	13
	4.2 Probabilistic Seismic Hazard Results .....	13
	4.2.1 Deaggregation .....	13
	4.3 SEE Ground Motions .....	14
	4.4 FEE Ground Motions .....	15
	4.2 Probabilistic Seismic Hazard Results.....	13
<b>5</b>	<b>TIME HISTORIES.....</b>	<b>34</b>
	5.1 Approach to Time History Selection .....	34
	5.2 SEE Time Histories .....	34
	5.3 FEE Time Histories.....	35
	5.4 Guidelines for PGV Values.....	36
	<b>REFERENCES .....</b>	<b>42</b>
	<b>APPENDIX A: Candidate Time Histories .....</b>	<b>43</b>

# 1 INTRODUCTION

This report develops ground motions for the Doyle Drive Replacement Project based on Caltrans criteria. The ground motions are developed for two levels: the Safety Evaluation Earthquake (SEE) and the Functional Evaluation Earthquake (FEE). The SEE is defined as the larger of either the median ground motion from the maximum credible earthquake or the ground motion with a 1000-year return period. The Functional Evaluation Earthquake (FEE) is defined as the ground motion with a 50% chance of being exceeded in 75 years (108-year return period).

In addition to the response spectra, reference time histories are recommended for use in developing spectrum compatible time histories for the SEE and the FEE. Three sets of reference time histories are given for each design level.

A single site location (122.462W, 37.801N) is used for computing the rock hazard for the entire Doyle Drive corridor. To capture the different rock conditions along the corridor, the rock motion spectra are developed for two rock  $V_{S30}$  values: 3000 ft/sec and 5000 ft/sec.

## 2 SOURCE CHARACTERIZATION

### 2.1 INTRODUCTION

The location of the Doyle Drive project site relative to the major faults in the Bay Area region is shown in Figure 2-1. The site is located about 9 km east of the San Andreas Fault, 14 km east of the San Gregorio Fault, and 20 km west of the Hayward Fault.

### 2.2 FAULT PARAMETERS

For the major faults in northern California, the seismic source characterization is based on the 2003 USGS Working Group on Earthquake Probabilities in Northern California (WG, 2003). The 2003 WG report gives the probabilities of large earthquakes during the next 30 years on seven fault systems in Northern California: San Andreas, Hayward/Rodgers Creek, Calaveras, San Gregorio, Concord, Greenville, and Mt. Diablo. All of the faults except for the Mt Diablo fault have segmentation alternatives. The WG model includes Poisson and non-Poisson models of the earthquake recurrence.

The 2003 WG model allows for the fault segments to rupture separately or together. The 30-year probabilities of rupture of the individual segments and of all possible multiple segment ruptures are presented in the 2003 WG report. All of the combinations of ruptures given in the 2003 WG report are considered in the PSHA. The mean characteristic magnitudes and 30-year probabilities for the alternative rupture scenarios are listed in Table 2-1.

The 30-year probabilities given in the 2003 WG report are converted to equivalent recurrence intervals for use in the PSHA computer program. The equivalent recurrence interval is just the inverse of the equivalent annual rate assuming a Poisson recurrence:

$$\textit{Equivalent Recurrence Interval} = \frac{30}{-\ln(1 - P_{30})} \quad (2-1)$$

where  $P_{30}$  is the 30-year probability given in Table 2-1.

Other faults have been identified in the greater Bay Area region, but because of their insignificant contribution to the overall seismic hazard at the Doyle Drive site, they were not considered in the PSHA.

### **2.3 MAGNITUDE DENSITY FUNCTION**

The magnitude density function describes how the fault slip-rate is distributed in different size earthquakes. In this study, the characteristic model developed by Youngs and Coppersmith (1985) is used. This model is very similar to the 2003WG model; it has about 95% of the seismic moment in the characteristic part and about 5% of the seismic moment in the exponential tail, whereas the 2003 WG model has 6% of the moment in the exponential tail. The truncated exponential model is not considered because, when it is used for faults for which the activity rate is computed from the slip-rate, it leads to a large over-prediction of the historical rate of moderate magnitude earthquakes.

The minimum magnitude used in the hazard calculation is magnitude 5.0.

### **2.4 RUPTURE DIMENSION RELATIONS**

The rupture dimension is modeled using the relations for fault area and fault width developed by Wells and Coppersmith (1994) for all source types. The rupture length is computed by dividing the area by the width.

**Table 2-1.** Seismic sources and source parameters based on the 2003 USGS Working Group Model. Weights for variable parameter values are indicated in parentheses.

<b>Fault</b>	<b>Segment</b>	<b>Width (km)</b>	<b>Mean Characteristic Magnitude</b>	<b>30-Year Probability</b>
<b>Mechanism</b>	<b>Dip</b>	<b>Top (km)</b>		
San Andreas SS	SCZ 90.0	15.0 0.0	6.84 (0.2)	0.026 (0.6)
			7.03 (0.6)	0.0 (0.2)
			7.22 (0.2)	0.108 (0.2)
San Andreas SS	PN 90.0	13.0 0.0	6.95 (0.2)	0.044 (0.6)
			7.15 (0.6)	0.0 (0.2)
			7.32 (0.2)	0.172 (0.2)
San Andreas SS	NCS 90.0	11.0 0.0	7.28 (0.2)	0.009 (0.6)
			7.45 (0.6)	0.00 (0.2)
			7.61 (0.2)	0.037 (0.2)
San Andreas SS	NCN 90.0	11.0 0.0	7.12 (0.2)	0.009 (0.6)
			7.29 (0.6)	0.0 (0.2)
			7.44 (0.2)	0.043 (0.2)
San Andreas SS	SCZ +PN 90.0	14.0 0.0	7.26 (0.2)	0.035 (0.6)
			7.42 (0.6)	0.001 (0.2)
			7.56 (0.2)	0.102 (0.2)
San Andreas SS	NCS + NCN 90.0	11.0 0.0	7.53 (0.2)	0.034 (0.6)
			7.70 (0.6)	0.001 (0.2)
			7.86 (0.2)	0.106 (0.2)
San Andreas SS	SCZ + PN + NCS 90.0	13.0 0.0	7.59 (0.2)	0.001 (0.6)
			7.76 (0.6)	0.0(0.2)
			7.92 (0.2)	0.003 (0.2)
San Andreas SS	PN + NCS + NCN 90.0	11.7 0.0	7.65 (0.2)	0.002 (0.6)
			7.83 (0.6)	0.0 (0.2)
			8.01 (0.2)	0.011 (0.2)
San Andreas SS	SCZ + PN + NCS + NCN 90.0	12.5 0.0	7.72 (0.2)	0.047 (0.6)
			7.90 (0.6)	0.003 (0.2)
			8.10 (0.2)	0.138 (0.2)
San Andreas SS	floating 90.0	12.5 0.0	6.90 (0.2)	0.071 (0.6)
			6.90 (0.6)	0.004 (0.2)
			6.90 (0.2)	0.264 (0.2)
Hayward SS	SH 90.0	12.0 0.0	6.36 (0.2)	0.113 (0.6)
			6.67 (0.6)	0.022 (0.2)
			6.93 (0.2)	0.319 (0.2)
Hayward SS	NH 90.0	12.0 0.0	6.18 (0.2)	0.123 (0.6)
			6.49 (0.6)	0.023 (0.2)
			6.78 (0.2)	0.360 (0.2)
Hayward SS	SH + NH 90.0	12.0 0.0	6.68 (0.2)	0.085 (0.6)
			6.91 (0.6)	0.019 (0.2)
			7.12 (0.2)	0.232 (0.2)
Hayward SS	RC 90.0	12.0 0.0	6.81 (0.2)	0.152 (0.6)
			6.98 (0.6)	0.041 (0.2)
			7.14 (0.2)	0.414 (0.2)

**Table 1. (Cont'd)**

<b>Fault</b>	<b>Segment</b>	<b>Width (km)</b>	<b>Mean</b>	<b>30-Year</b>
<b>Mechanism</b>	<b>Dip</b>	<b>Top (km)</b>	<b>Characteristic</b>	<b>Probability</b>
			<b>Magnitude</b>	
Hayward	NH + RC	12.0	6.94 (0.2)	0.018 (0.6)
SS	90.0	0.0	7.11 (0.6)	0.0 (0.2)
			7.28 (0.2)	0.066 (0.2)
Hayward	SH + NH + RC	12.0	7.09 (0.2)	0.010 (0.6)
SS	90.0	0.0	7.26 (0.6)	0.001 (0.2)
			7.42 (0.2)	0.033 (0.2)
Hayward	floating	12.0	6.90 (0.2)	0.007 (0.6)
SS	90.0	0.0	6.90 (0.6)	0.003 (0.2)
			6.90 (0.2)	0.016 (0.2)
Calaveras	SC	11.0	5.00 (0.2)	0.213 (0.6)
SS	90.0	0.0	5.79 (0.6)	0.0 (0.2)
			6.14 (0.2)	0.538 (0.2)
Calaveras	CC	11.0	5.75 (0.2)	0.138 (0.6)
SS	90.0	0.0	6.23 (0.6)	0.039 (0.2)
			6.68 (0.2)	0.297 (0.2)
Calaveras	SC + CC	11.0	5.87 (0.2)	0.050 (0.6)
SS	90.0	0.0	6.36 (0.6)	0.0 (0.2)
			6.75 (0.2)	0.203 (0.2)
Calaveras	NC	12.0	6.58 (0.2)	0.124 (0.6)
SS	90.0	0.0	6.78 (0.6)	0.030 (0.2)
			6.97 (0.2)	0.356 (0.2)
Calaveras	CC + NC	11.5	6.68 (0.2)	0.003 (0.6)
SS	90.0	0.0	6.90 (0.6)	0.0 (0.2)
			7.11 (0.2)	0.036 (0.2)
Calaveras	SC + CC + NC	11.3	6.72 (0.2)	0.020 (0.6)
SS	90.0	0.0	6.93 (0.6)	0.0 (0.2)
			7.14 (0.2)	0.079 (0.2)
Calaveras	floating	11.3	6.20 (0.2)	0.074 (0.6)
SS	90.0	0.0	6.20 (0.6)	0.017 (0.2)
			6.20 (0.2)	0.195 (0.2)
Calaveras	floating SC + CC	11.0	6.20 (0.2)	0.251 (0.6)
SS	90.0	0.0	6.20 (0.6)	0.051 (0.2)
			6.20 (0.2)	0.560 (0.2)
Concord/GV	CON	16.0	5.75 (0.2)	0.050 (0.6)
SS	90.0	0.0	6.25 (0.6)	0.003 (0.2)
			6.67 (0.2)	0.182 (0.2)
Concord/GV	SGV	14.0	5.75 (0.2)	0.023 (0.6)
SS	90.0	0.0	6.24 (0.6)	0.001 (0.2)
			6.65 (0.2)	0.087 (0.2)
Concord/GV	CON + SGV	15.0	6.13 (0.2)	0.016 (0.6)
SS	90.0	0.0	6.58 (0.6)	0.001 (0.2)
			6.91 (0.2)	0.067 (0.2)

**Table 1. (Cont'd)**

<b>Fault</b>	<b>Segment</b>	<b>Width (km)</b>	<b>Mean Characteristic Magnitude</b>	<b>30-Year Probability</b>
<b>Mechanism</b>	<b>Dip</b>	<b>Top (km)</b>		
Concord/GV	NGV	14.0	5.45 (0.2)	0.061 (0.6)
SS	90.0	0.0	6.02 (0.6)	0.004 (0.2)
			6.49 (0.2)	0.219 (0.2)
Concord/GV	SGV +NGV	14.0	6.03 (0.2)	0.032 (0.6)
SS	90.0	0.0	6.48 (0.6)	0.002 (0.2)
			6.81 (0.2)	0.115 (0.2)
Concord/GV	CON +SGV +NGV	14.7	6.34 (0.2)	0.060 (0.6)
SS	90.0	0.0	6.71 (0.6)	0.007 (0.2)
			7.00 (0.2)	0.222 (0.2)
Concord/GV	floating	14.7	6.20 (0.2)	0.062 (0.6)
SS	90.0	0.0	6.20 (0.6)	0.002 (0.2)
			6.20 (0.2)	0.296 (0.2)
San Gregorio	SGS	12.0	6.75 (0.2)	0.023 (0.6)
SS	90.0	0.0	6.96 (0.6)	0.0 (0.2)
			7.17 (0.2)	0.115 (0.2)
San Gregorio	SGN	13.0	7.04 (0.2)	0.039 (0.6)
SS	90.0	0.0	7.23 (0.6)	0.0 (0.2)
			7.41 (0.2)	0.175 (0.2)
San Gregorio	SGS +SGN	12.5	7.27 (0.2)	0.026 (0.6)
SS	90.0	0.0	7.44 (0.6)	0.0 (0.2)
			7.58 (0.2)	0.101 (0.2)
San Gregorio	floating	12.5	6.90 (0.2)	0.021 (0.6)
SS	90.0	0.0	6.90 (0.6)	0.008 (0.2)
			6.90 (0.2)	0.039 (0.2)
Greenville	SG	15.0	6.37 (0.2)	0.031 (0.6)
SS	90.0	0.0	6.60 (0.6)	0.0 (0.2)
			6.83 (0.2)	0.107 (0.2)
Greenville	NG	15.0	6.41 (0.2)	0.029 (0.6)
SS	90.0	0.0	6.66 (0.6)	0.0 (0.2)
			6.88 (0.2)	0.107 (0.2)
Greenville	SG +NG	15.0	6.74 (0.2)	0.015 (0.6)
SS	90.0	0.0	6.94 (0.6)	0.001 (0.2)
			7.13 (0.2)	0.047 (0.2)
Greenville	floating	15.0	6.20 (0.2)	0.004 (0.6)
SS	90.0	0.0	6.20 (0.6)	0.001 (0.2)
			6.20 (0.2)	0.009 (0.2)
Mt Diablo	MTD	14.2	6.42 (0.2)	0.075 (0.6)
RV	27.4	4.0	6.65 (0.6)	0.005 (0.2)
			6.89 (0.2)	0.241 (0.2)

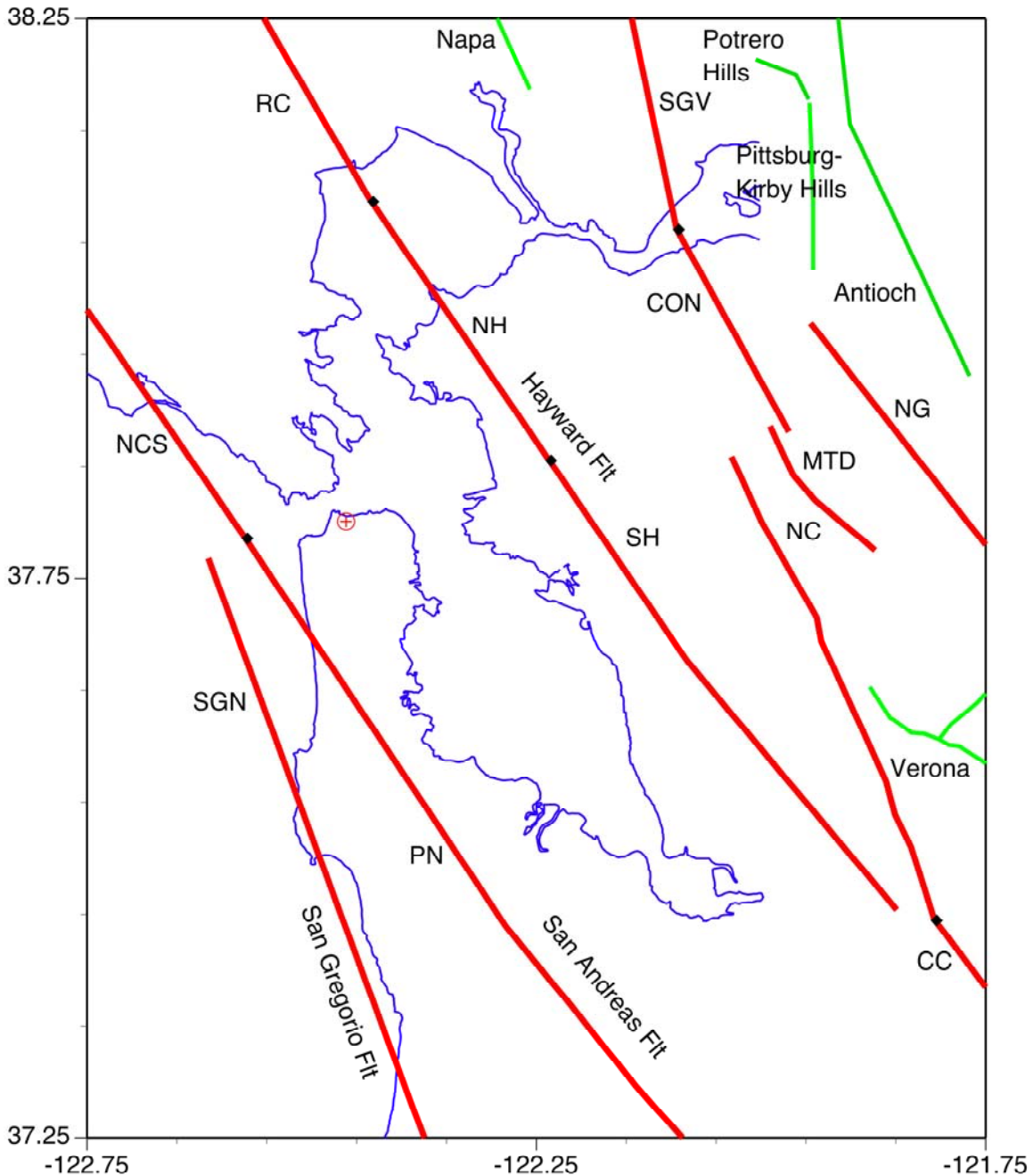


Figure 2-1. Map showing the location of the Doyle Drive Project Site (cross with circle) and the faults using in the PSHA. Fault shown in red are characterized following the USGS WG03 model. Faults shown in green were not used in the analysis

## 3 GROUND MOTION MODELS

### 3.1 BASE ATTENUATION RELATIONS

The five recently developed attenuation relationships as part of the PEER Next Generation Attenuation program are used. These empirical attenuation relationships were developed by five separate modeling teams: Abrahamson and Silva (2008), Boore and Atkinson (2008), Campbell and Bozorgnia (2008), Chiu and Youngs (2008) and Idriss (2008). These newly developed models represent updates to the previously published attenuation models: Abrahamson and Silva (1997), Boore et al. (1997), Campbell and Bozorgnia (2003), Sadigh et al. (1997), and Idriss (1991,1994ab) which have typically been used for ground motion studies. A key parameter used in four of the five NGA models is an average shear wave velocity in the top 30 m for the estimation of site effects on the predicted ground motion. The Idriss model is defined for a range of average shear wave velocity between 450 – 900 m/s rather than a specific shear wave value.

For the 3000 ft/s (914 m/s)  $V_{S30}$  case, all five NGA models are used with equal weight. For the 5000 ft/s (1524 m/s)  $V_{S30}$  case, the four NGA relations (excluding the Idriss model) based on  $V_{S30}$  are used to develop a scale factor from 3000 ft/s to 5000 ft/s. This factor is then applied to the  $V_{S30}=3000$  ft/s spectrum. This scale factor listed in Table 3-1.

### 3.2 DIRECTIVITY MODELS

The five attenuation relations listed above describe the attenuation of the average of the two horizontal components of ground motion. These attenuation relations were adjusted to account for near-fault directivity effects using a modified form of the Somerville et al. (1997) fault-rupture directivity model from Abrahamson (2000). Somerville et al. (1997) developed an empirically-based model quantifying the effects of rupture directivity on horizontal response spectra that can be used to scale the average horizontal component computed from attenuation relations. The Somerville et al. (1997) model comprises two period-dependent scaling factors that may be applied to any ground motion attenuation relationship. One of the factors accounts for the increase in shaking intensity in the average horizontal component of motion due to near-fault rupture directivity effects. The second factor reflects the directional nature of the shaking intensity using two ratios: fault normal (FN) and fault parallel (FP) versus the average (FA) component ratios. The fault normal component is taken as the major principal axis resulting in

an FN/FA ratio larger than 1 and the fault parallel component is taken as the minor principal axis with an FP/FA ratio smaller than 1. The two scaling factors depend on whether fault rupture is in the forward or backward direction, and also the length of fault rupturing toward the site.

Rupture directivity is only applied to the major faults (shown in red in Figure 2-1).

### **3.3 VERTICAL GROUND MOTIONS**

Vertical spectra were developed by applying a vertical to horizontal spectra ratio (V/H) to the horizontal spectra. Updated vertical ground motion models have not been developed yet as part of the NGA project. Therefore, the V/H ratio was estimated based on the Abrahamson and Silva (1997) and Sadigh et al. (1997) attenuation models.

The V/H ratios are computed for the earthquakes corresponding to the FEE and SEE (see Section 4). For the FEE, a magnitude 7.2 at a distance of 22 km is used. For the SEE, a magnitude 7.6 at a distance of 11 km is used. The V/H ratios for the FEE and SEE are shown in Figures 3-1 and 3-2, respectively. Smoothed V/H ratios are also shown in these figures. The smoothed values are listed in Table 3-2.

**Table 3.1** Scale factor used to compute the ground motion for  $V_{S30}=5000$  ft/s  
from the ground motion for  $V_{S30}=3000$  ft/s.

Period (Sec)	Scale Factor
0.01	0.910
0.02	0.920
0.03	0.925
0.05	0.930
0.075	0.930
0.1	0.930
0.12	0.920
0.15	0.910
0.17	0.905
0.2	0.900
0.24	0.900
0.3	0.900
0.4	0.900
0.5	0.900
0.75	0.900
1	0.900
1.5	0.900
2	0.895
3	0.890
4	0.885
5	0.880
6	0.878
7.5	0.875
10	0.870

**Table 3-2. V/H Ratio for the FEE and SEE**

Period (Sec)	V/H for FEE	V/H for SEE
0.01	0.736	0.873
0.02	0.736	0.873
0.03	0.810	0.995
0.05	0.890	1.160
0.075	0.890	1.161
0.1	0.806	1.015
0.12	0.740	0.900
0.15	0.650	0.770
0.17	0.590	0.696
0.2	0.537	0.615
0.24	0.500	0.560
0.3	0.462	0.509
0.4	0.435	0.478
0.5	0.439	0.468
0.75	0.460	0.491
1	0.484	0.507
1.5	0.506	0.540
2	0.556	0.592
3	0.645	0.687
4	0.729	0.755
5	0.776	0.808
6	0.811	0.830
7.5	0.846	0.886
10	0.906	1.000

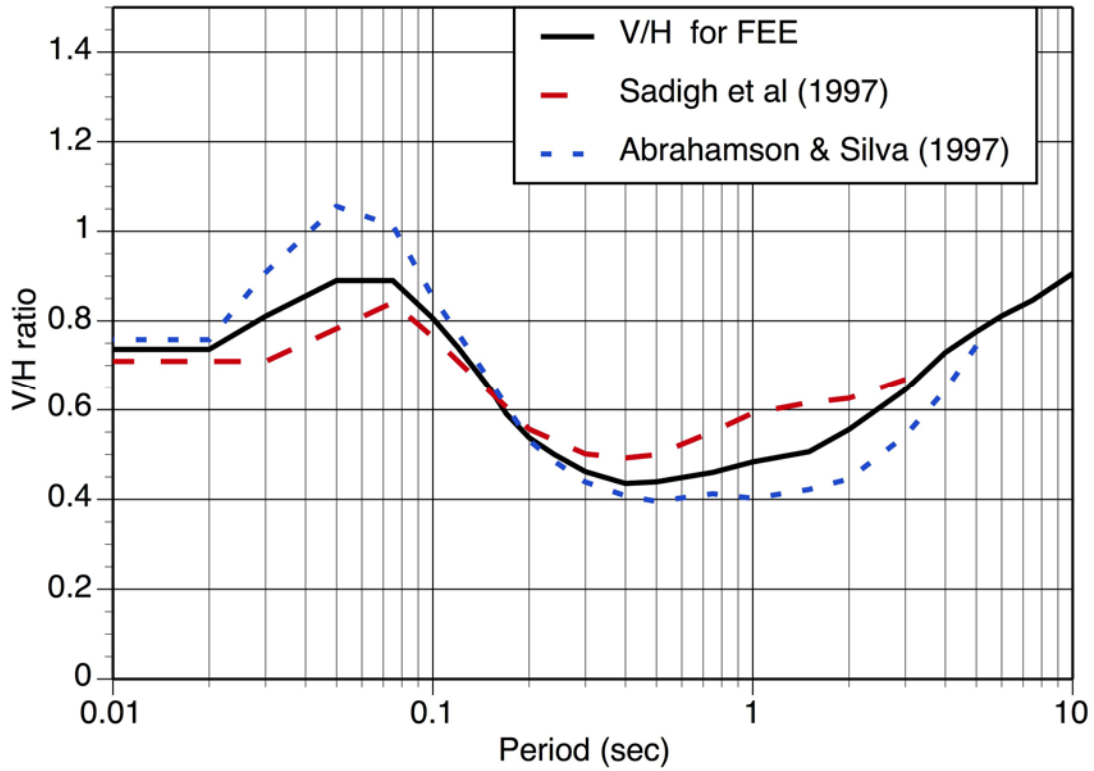


Figure 3-1. V/H ratio for the FEE.

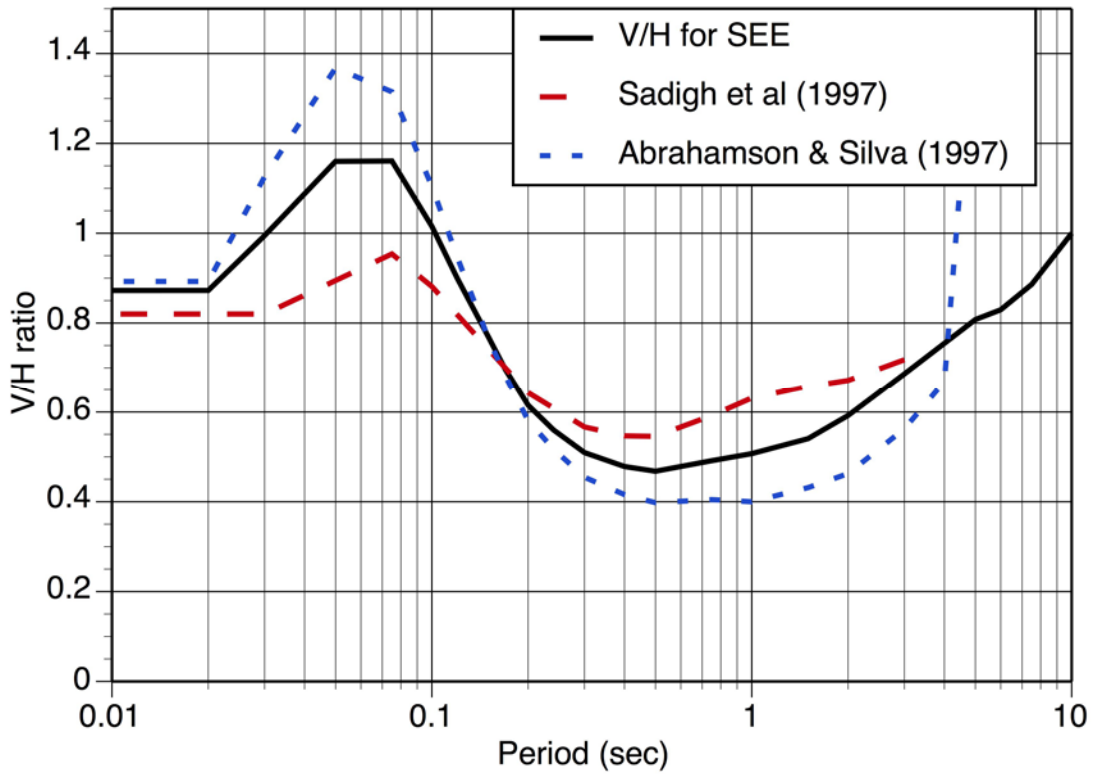


Figure 3-2. V/H ratio for the SEE

## **4 SEISMIC HAZARD ANALYSIS**

### **4.1 DETERMINISTIC GROUND MOTIONS**

The San Andreas, San Gregorio, and Hayward faults are considered for the deterministic ground motions. The magnitudes and distances for the three faults are listed in Table 4-1. The average of the median spectra from the five NGA models was computed and is shown in Figure 4-1. Due to the short distance, the San Andreas Fault leads to the largest deterministic spectrum.

Directivity effects are applied to the median deterministic ground motion for the San Andreas Fault using only the FN/ave and FP/ave scaling for a magnitude 8 earthquake at a distance of 9.1 km. Since the median ground motion is used, the effects of directivity on the average horizontal component are not applied to the deterministic case. The deterministic spectra for this case are listed in Table 4.2 and are plotted in Figure 4-2.

### **4.2 PROBABILISTIC SEISMIC HAZARD RESULTS**

The mean hazard is shown in Figures 4-3a to 4-3d for PGA, and spectral periods of 0.3, 1.0 and 3.0 seconds for the average horizontal component. The contributions from each fault to the total hazard are also shown in these figures. The return periods greater than 200 years, the San Andreas Fault is the dominant contributor to the hazard. At shorter return periods, the Hayward fault is dominant due to the higher probability of an earthquake occurring on this source. Uniform hazard spectra are computed for return periods of 108 and 1,000 years and are shown in Figure 4-4.

#### **4.2.1 Deaggregation**

The hazard curve gives the combined effect of all magnitudes and distances on the probability of exceeding a given ground motion level. Since all of the sources, magnitudes, and distances are mixed together, it is difficult to get an intuitive understanding of what is controlling the hazard from the hazard curve by itself. To provide insight into what events (magnitude, distance, epsilon) are the most important for the hazard at a given ground motion level, the hazard curve

is broken down into its contributions from different earthquake scenarios. This process is called deaggregation (e.g. Bazzurro and Cornell, 1999).

The common way of showing the deaggregation is to plot the contribution of magnitude-distance pairs to the hazard at a given return period. The magnitude-distance deaggregation for a 100-year return period for PGA and  $T=1$  second spectral acceleration are shown in Figures 4-5a and 4-5b. The deaggregation plots for a 1000-year return period are shown in Figure 4-6a and 4-6b.

Using the joint distribution of the magnitude and distance avoids the potential problems with the mean values, but the results are not as easily summarized as are the mean values. The deaggregations can also be displayed by plotting the mean parameters as a function of the return period. Figure 4-7 shows the mean magnitude, distance, and epsilon for PGA and spectral periods of 0.3, 1.0, 3.0 and 10 sec. For a 1000-year return period, the mean magnitude is shown as a function of spectral period in Figure 4-8.

The PSHA was also computed including the effects of directivity. For the probabilistic analysis, both the effect on the average horizontal and the effect on FN/FP components are included. For each scenario, the hypocenter location is randomized over the rupture plane and the associated directivity effects are incorporated in the PSHA. Figure 4-9 shows the hazard for  $T=3$  seconds for the average horizontal without directivity and for the FN and FP components. The FP component is similar to the average horizontal without directivity, indicating that the increase due to forward rupture is offset by the decrease for the FP component. The FN component becomes much larger for the longer return periods, since the longer return periods lead to more severe rupture directivity effects.

### **4.3 SEE GROUND MOTIONS**

The SEE ground motion defined as the larger of the median deterministic ground motion and the UHS with a 1000-year return period. The deterministic spectrum from the San Andreas fault is compared to the 1000-year UHS in Figure 4-10. The 1000-year UHS exceeded the median deterministic ground motion at all periods. Based on the results of the deaggregation (Figure 4-8), the earthquake magnitude for the SEE corresponds to  $M 7.4$  for  $T < 0.5$  sec,  $M 7.5$  for  $0.75 < T < 3$  sec, and  $M 7.6$  for  $T > 4$  sec.

To account for directivity effects, the SEE horizontal spectra are developed using the 1000-year UHS for the fault normal (FN) and for the fault parallel (FP) components. The resulting SEE spectra for the FN and FP components are shown in Figure 4-11 and are listed in Table 4-4.

The vertical component for the SEE is computed by scaling the UHS for average horizontal component by the V/H ratio listed in Table 3-2. The vertical SEE is listed in Table 4-4 and is plotted in Figure 4-11.

#### 4.4 FEE GROUND MOTIONS

The FEE ground motion defined as the UHS with a 108-year return period. The spectra for the FEE are listed in Table 4-5 and plotted in Figure 4-12. For the FEE, the FN and FP components are similar to each other, indicating that there is not a significant directivity effect for this short return period.

**Table 4.1** Deterministic Magnitude and Distance Values for the Largest Nearby Faults.

<b>Fault</b>	<b>Magnitude</b>	<b>Style-of-Faulting</b>	<b>Closest Distance: <math>R_{rup}</math> (km)</b>	<b>Closest Distance: <math>R_{JB}</math> (km)</b>	<b>Depth to Top of Rupture (km)</b>
San Andreas	8.0	SS	9.1	9.1	0
Hayward/ Rodgers Creek	7.3	SS	19.9	19.9	0
San Gregorio	7.4	SS	13.9	13.9	0

**Table 4-2.** Deterministic Median Horizontal Spectra (5% damping, g's).

period (sec)	3000 ft/s				5000 ft/s			
	Ave Horiz	Z	FN	FP	Ave Horiz	Z	FN	FP
0.01	0.3322	0.2446	0.3322	0.3322	0.3022	0.2225	0.3022	0.3022
0.02	0.3378	0.2488	0.3378	0.3378	0.3107	0.2288	0.3107	0.3107
0.03	0.3615	0.2929	0.3615	0.3615	0.3344	0.2710	0.3344	0.3344
0.05	0.4232	0.3766	0.4232	0.4232	0.3935	0.3502	0.3935	0.3935
0.075	0.5223	0.4209	0.5223	0.5223	0.4858	0.3914	0.4858	0.4858
0.1	0.6147	0.4549	0.6147	0.6147	0.5656	0.4186	0.5656	0.5656
0.15	0.7207	0.4685	0.7207	0.7207	0.6559	0.4264	0.6559	0.6559
0.2	0.7291	0.3919	0.7291	0.7291	0.6562	0.3527	0.6562	0.6562
0.25	0.6975	0.3486	0.6975	0.6975	0.6277	0.3137	0.6277	0.6277
0.3	0.6434	0.2970	0.6434	0.6434	0.5791	0.2674	0.5791	0.5791
0.4	0.5590	0.2433	0.5589	0.5589	0.5031	0.2191	0.5031	0.5031
0.5	0.4836	0.2123	0.4836	0.4836	0.4351	0.1911	0.4351	0.4351
0.75	0.3531	0.1624	<b>0.3683</b>	0.3385	0.3177	0.1462	0.3315	0.3046
1	0.2881	0.1393	0.3068	0.2705	0.2593	0.1253	0.2762	0.2434
1.5	0.2015	0.1020	0.2196	0.1849	0.1813	0.0918	0.1976	0.1664
2	0.1470	0.0817	0.1632	0.1325	0.1315	0.0731	0.1460	0.1185
3	0.0967	0.0624	0.1159	0.0806	0.0860	0.0555	0.1032	0.0718
4	0.0684	0.0499	0.0883	0.0530	0.0605	0.0441	0.0782	0.0469
5	0.0519	0.0403	0.0713	0.0377	0.0456	0.0354	0.0626	0.0331
7.5	0.0339	0.0287	0.0457	0.0251	0.0297	0.0251	0.0401	0.0220
10	0.0202	0.0182	0.0263	0.0155	0.0175	0.0158	0.0228	0.0135

**Table 4-3.** Uniform Hazard Spectra (5% damping, g's) for a Rock Site with  $V_{S30}=3000$  ft/sec.

per	108-Year Return Period			1000-year Return Period		
	Ave Horiz	FN	FP	Ave Horiz	FN	FP
0.01	0.1718	0.1718	0.1718	0.4622	0.4622	0.4622
0.02	0.1753	0.1753	0.1753	0.4726	0.4726	0.4726
0.03	0.1867	0.1867	0.1867	0.5116	0.5116	0.5116
0.05	0.2221	0.2221	0.2221	0.6135	0.6135	0.6135
0.075	0.2853	0.2853	0.2853	0.7784	0.7784	0.7784
0.10	0.3356	0.3356	0.3356	0.9308	0.9308	0.9308
0.15	0.3943	0.3943	0.3943	1.0899	1.0899	1.0899
0.20	0.4010	0.401	0.401	1.1099	1.1099	1.1099
0.24	0.3795	0.3795	0.3795	1.0690	1.0690	1.0690
0.30	0.3457	0.3457	0.3457	0.9888	0.9888	0.9888
0.40	0.2981	0.2981	0.2981	0.8582	0.8582	0.8582
0.50	0.2462	0.2462	0.2462	0.7393	0.7393	0.7393
0.75	0.1717	0.1728	0.1715	0.5440	0.5543	0.5417
1.00	0.1336	0.1355	0.1334	0.4268	0.4486	0.4277
1.50	0.0874	0.0904	0.0877	0.2936	0.3277	0.2953
2.00	0.0596	0.0634	0.0599	0.2032	0.2531	0.2099
3.00	0.0344	0.0378	0.0344	0.1281	0.1752	0.1260
4.00	0.0224	0.0259	0.0229	0.0882	0.1370	0.0881
5.00	0.0164	0.0194	0.0165	0.0682	0.1089	0.0666
7.50	0.0091	0.0094	0.0091	0.0395	0.0550	0.0395
10.00	0.0053	0.0053	0.0053	0.0241	0.0280	0.0241

**Table 4-4.** SEE Spectra (5% damping, g's) for Rock Sites.

Period (s)	3000 ft/s			5000 ft/s		
	FN	FP	V	FN	FP	V
0.01	0.4622	0.4622	0.4033	0.4206	0.4206	0.3670
0.02	0.4726	0.4726	0.4124	0.4348	0.4348	0.3794
0.03	0.5116	0.5116	0.5089	0.4758	0.4758	0.4733
0.05	0.6135	0.6135	0.7117	0.5767	0.5767	0.6690
0.075	0.7784	0.7784	0.9036	0.7317	0.7317	0.8494
0.1	0.9308	0.9308	0.9451	0.8750	0.8750	0.8884
0.12	1.0000	1.0000	0.9000	0.9350	0.9350	0.8415
0.15	1.0899	1.0899	0.8392	1.0136	1.0136	0.7805
0.17	1.1000	1.1000	0.7652	1.0175	1.0175	0.7078
0.2	1.1099	1.1099	0.6827	1.0211	1.0211	0.6281
0.24	1.0690	1.0690	0.5986	0.9835	0.9835	0.5507
0.3	0.9888	0.9888	0.5037	0.9097	0.9097	0.4634
0.4	0.8582	0.8582	0.4106	0.7895	0.7895	0.3778
0.5	0.7393	0.7393	0.3459	0.6802	0.6802	0.3182
0.75	0.5543	0.5417	0.2662	0.5100	0.4984	0.2449
1	0.4486	0.4277	0.2169	0.4127	0.3935	0.1995
1.5	0.3277	0.2953	0.1596	0.3015	0.2717	0.1468
2	0.2531	0.2099	0.1243	0.2316	0.1921	0.1137
3	0.1752	0.1260	0.0865	0.1577	0.1134	0.0779
4	0.1370	0.0881	0.0665	0.1212	0.0780	0.0589
5	0.1089	0.0666	0.0538	0.0958	0.0586	0.0473
6	0.0844	0.0534	0.0443	0.0741	0.0469	0.0389
7.5	0.0550	0.0395	0.0350	0.0481	0.0346	0.0306
10	0.0280	0.0241	0.0241	0.0244	0.0210	0.0210

**Table 4-5.** FEE Spectra (5% damping, g's) for Rock Sites.

Period (s)	3000 ft/s			5000 ft/s		
	FN	FP	V	FN	FP	V
0.01	0.1718	0.1718	0.1265	0.1563	0.1563	0.1151
0.02	0.1753	0.1753	0.1291	0.1613	0.1613	0.1188
0.03	0.1867	0.1867	0.1513	0.1727	0.1727	0.1400
0.05	0.2221	0.2221	0.1977	0.2066	0.2066	0.1839
0.075	0.2853	0.2853	0.2539	0.2653	0.2653	0.2361
0.1	0.3356	0.3356	0.2704	0.3121	0.3121	0.2515
0.12	0.3640	0.3640	0.2694	0.3349	0.3349	0.2478
0.15	0.3943	0.3943	0.2563	0.3588	0.3588	0.2332
0.17	0.3980	0.3980	0.2348	0.3602	0.3602	0.2125
0.2	0.4010	0.4010	0.2155	0.3609	0.3609	0.1940
0.24	0.3795	0.3795	0.1897	0.3416	0.3416	0.1707
0.3	0.3457	0.3457	0.1596	0.3111	0.3111	0.1436
0.4	0.2981	0.2981	0.1298	0.2683	0.2683	0.1168
0.5	0.2462	0.2462	0.1081	0.2216	0.2216	0.0973
0.75	0.1728	0.1715	0.0789	0.1555	0.1544	0.0710
1	0.1355	0.1334	0.0645	0.1220	0.1201	0.0581
1.5	0.0904	0.0877	0.0444	0.0814	0.0789	0.0400
2	0.0634	0.0599	0.0333	0.0567	0.0536	0.0298
3	0.0378	0.0344	0.0222	0.0336	0.0306	0.0198
4	0.0259	0.0229	0.0167	0.0229	0.0203	0.0148
5	0.0194	0.0165	0.0128	0.0171	0.0145	0.0113
6	0.0145	0.0127	0.0103	0.0127	0.0112	0.0090
7.5	0.0094	0.0091	0.0077	0.0082	0.0080	0.0067
10	0.0053	0.0053	0.0048	0.0046	0.0046	0.0042

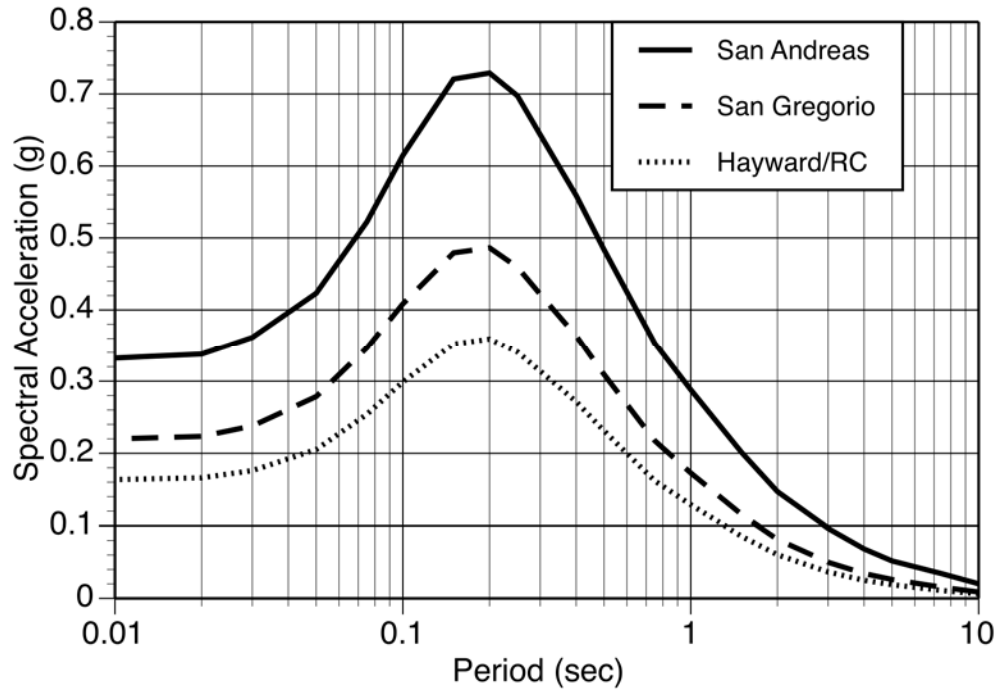


Figure 4-1. Deterministic spectra (5% damping) for the median ground motion from the Maximum Credible Earthquake for  $V_{S30}=3000$  ft/s.

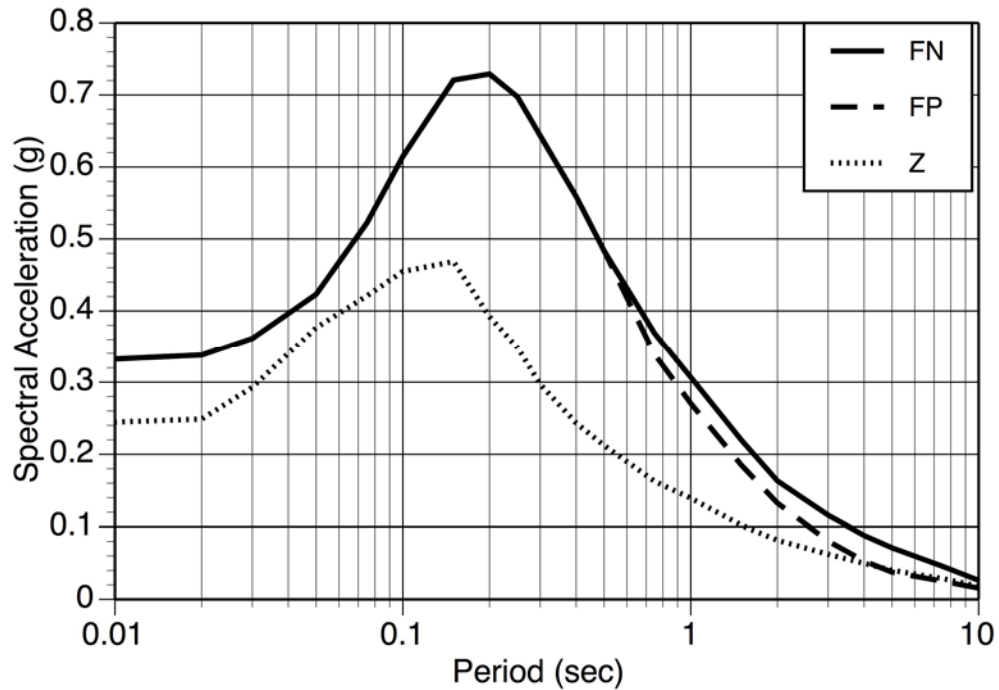


Figure 4-2. Deterministic spectra (5% damping) including directivity effects for  $V_{S30}=3000$  ft/s

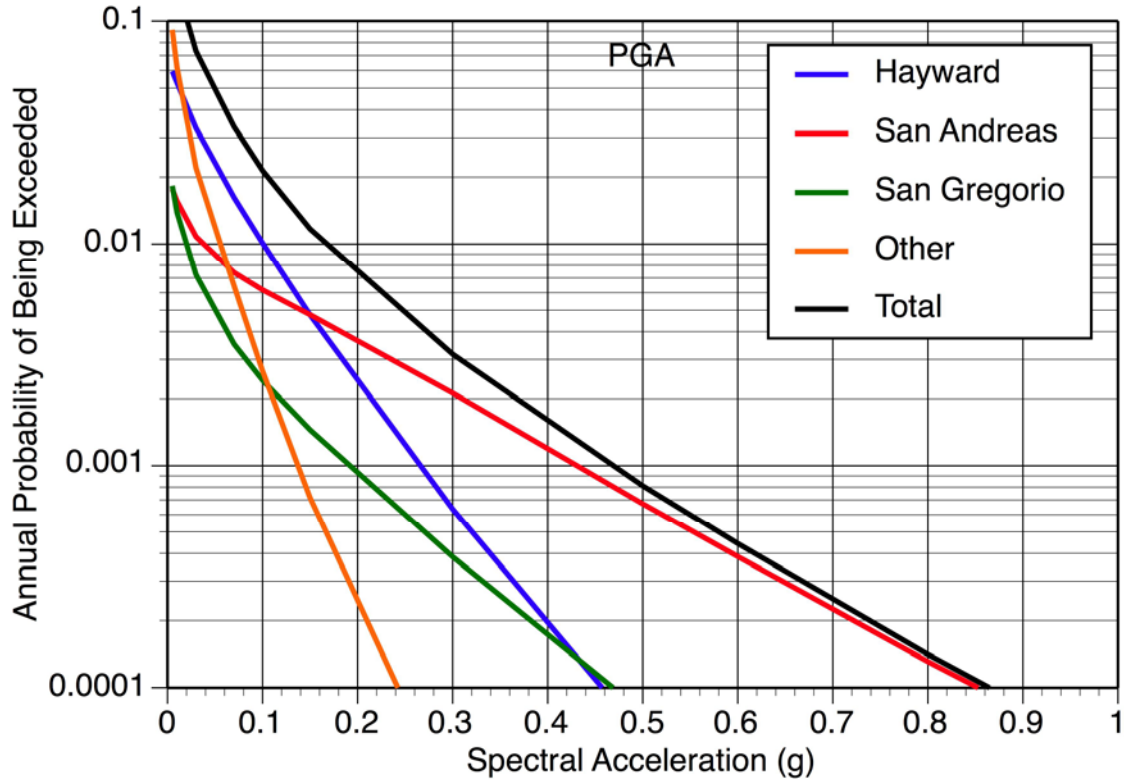


Figure 4-3a. Mean PGA hazard for  $V_{S30}=3000$  ft/sec.

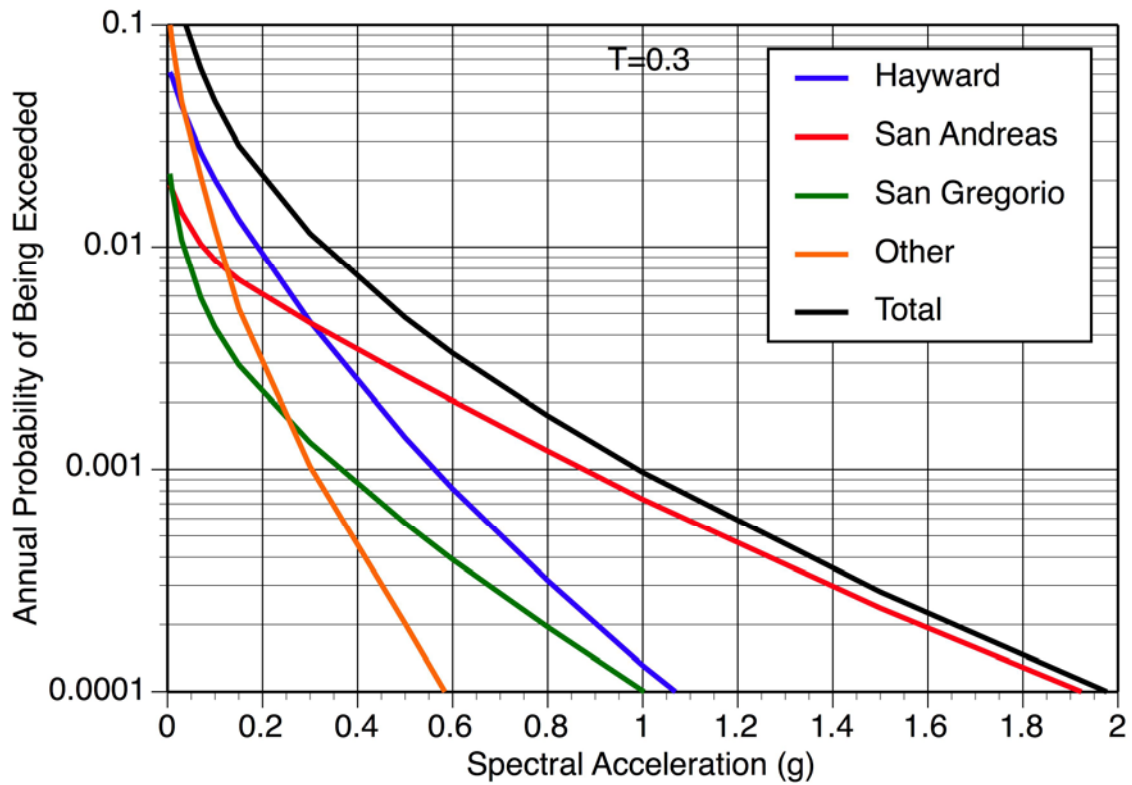


Figure 4-3b. Mean T=0.3 sec hazard for  $V_{S30}=3000$  ft/sec.

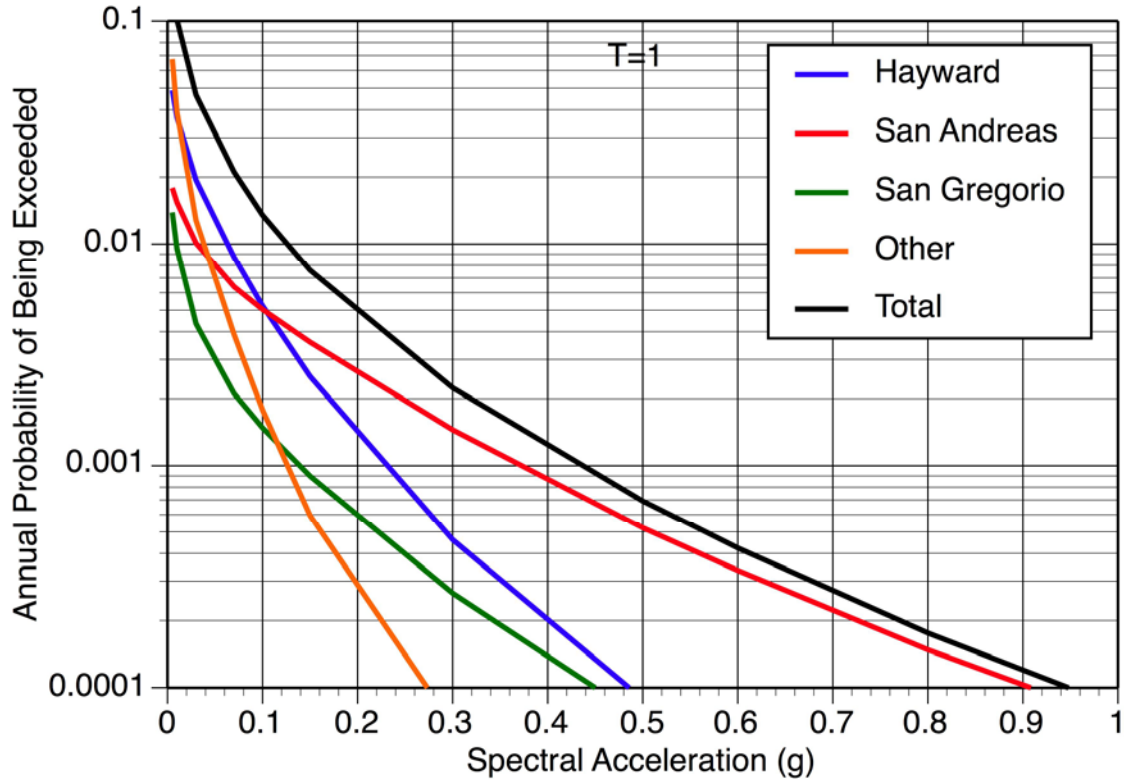


Figure 4-3c. Mean T=1 sec hazard for  $V_{S30}=3000$  ft/sec.

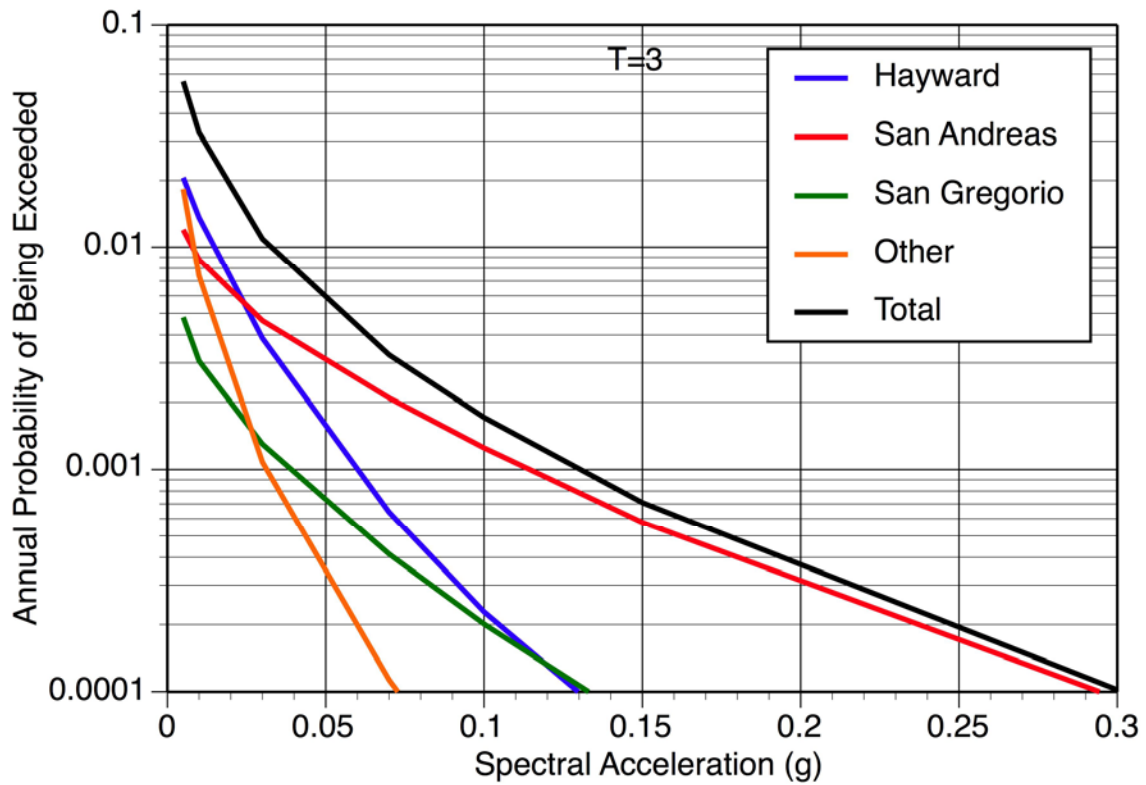


Figure 4-3d. Mean T=3 sec hazard for  $V_{S30}=3000$  ft/sec.

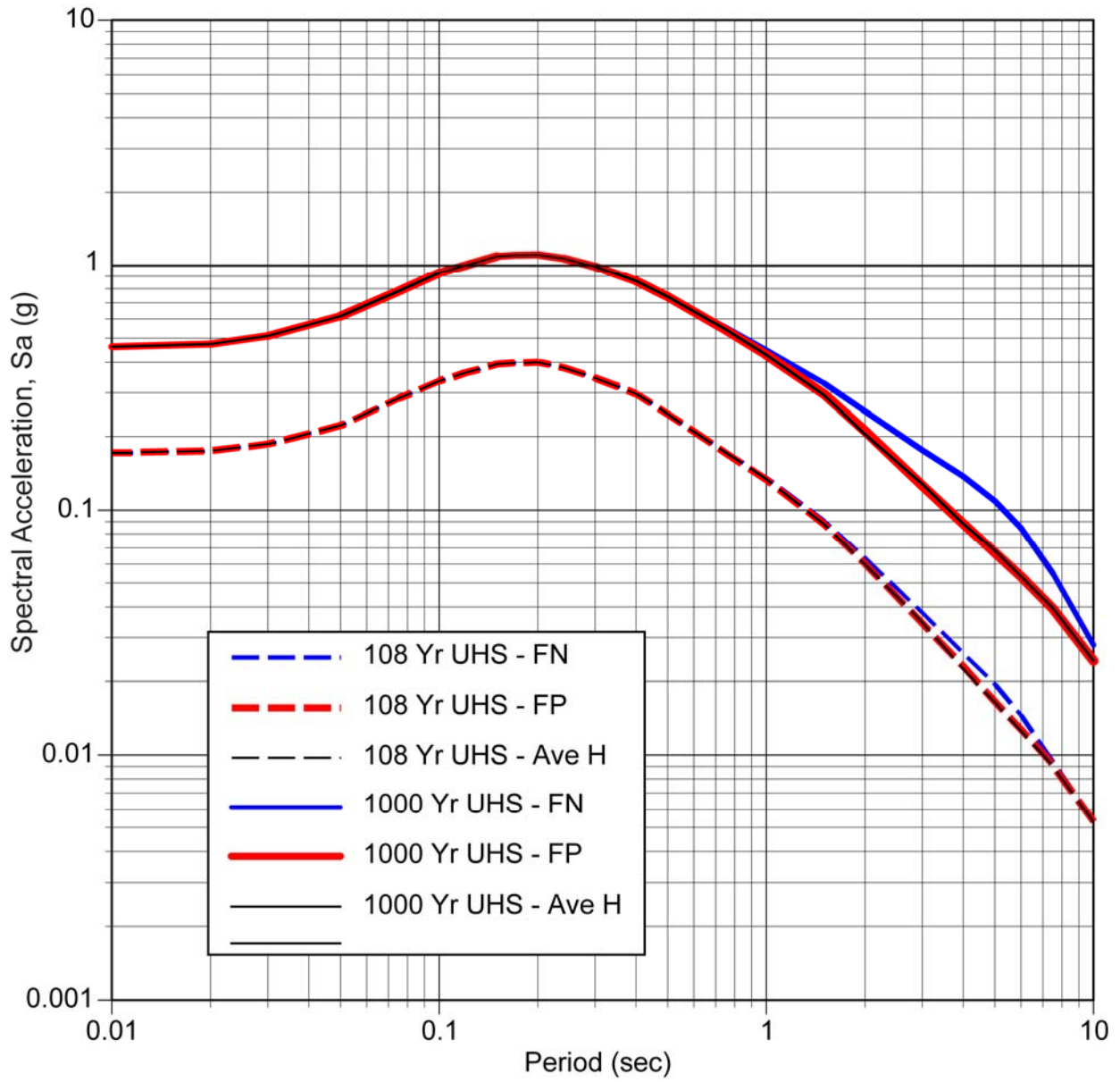


Figure 4-4. UHS (5% damping) for a rock site with  $V_{s30}=3000$  ft/s

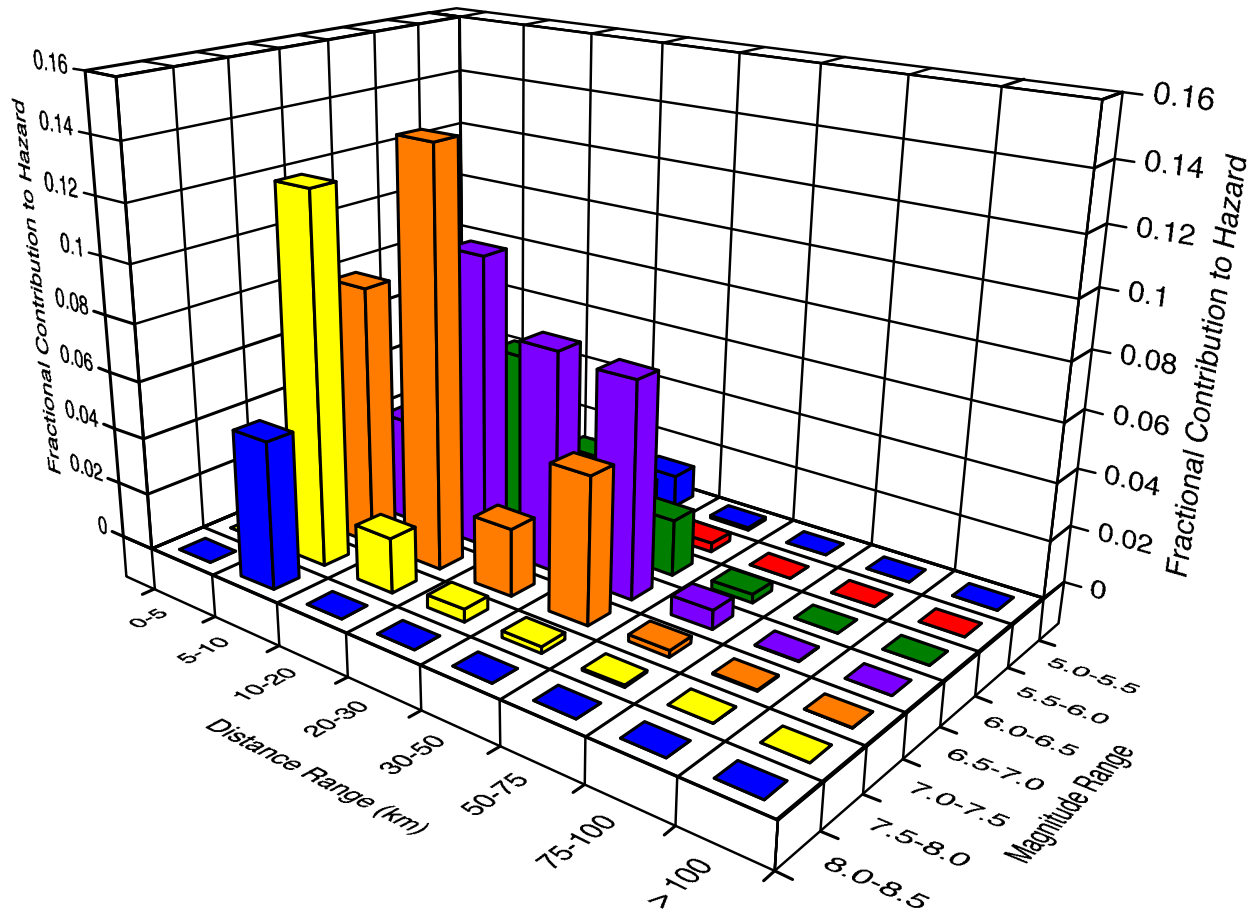


Figure 4-5a. Deaggregation for 108-Yr return period: PGA

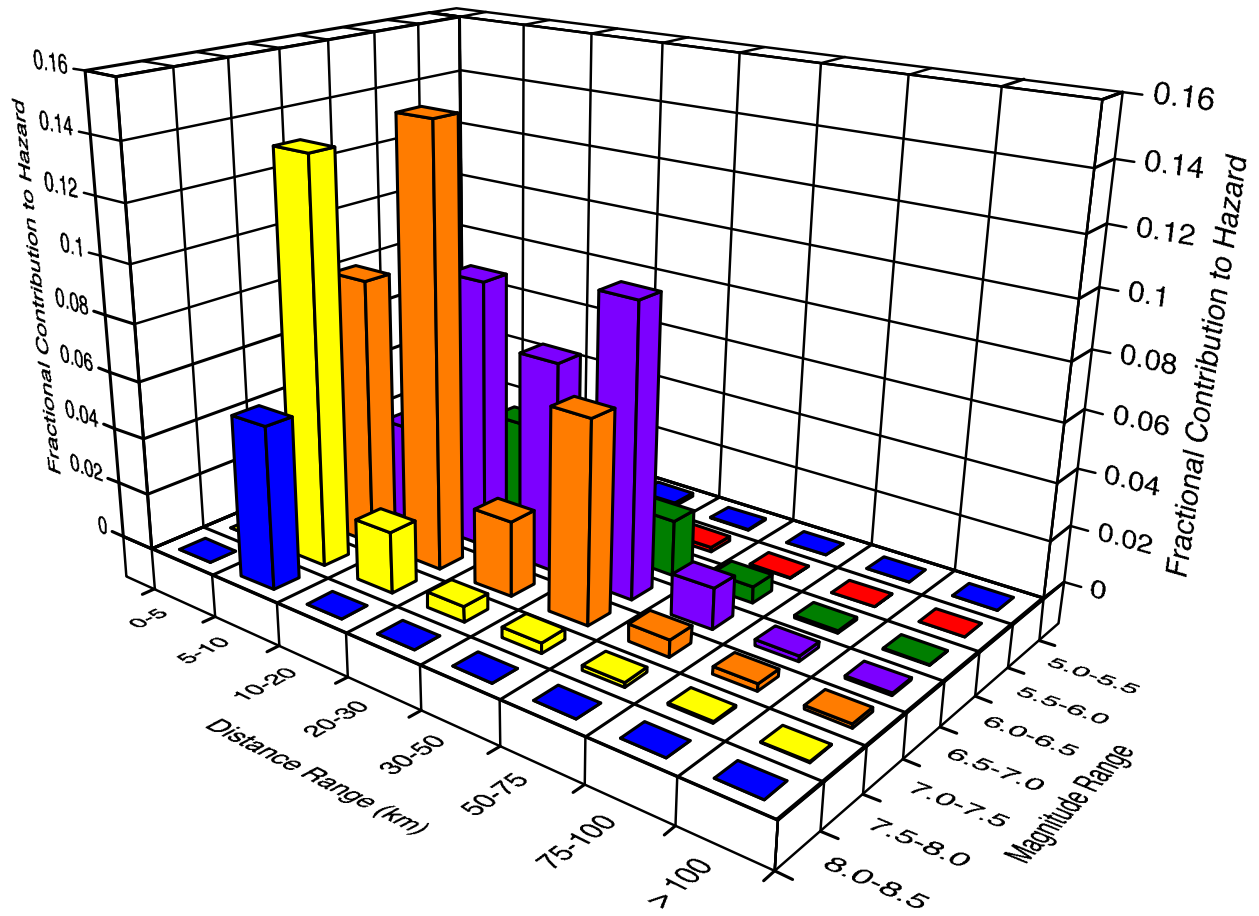


Figure 4-5b. Deaggregation for 108-Yr return period: T=1 sec

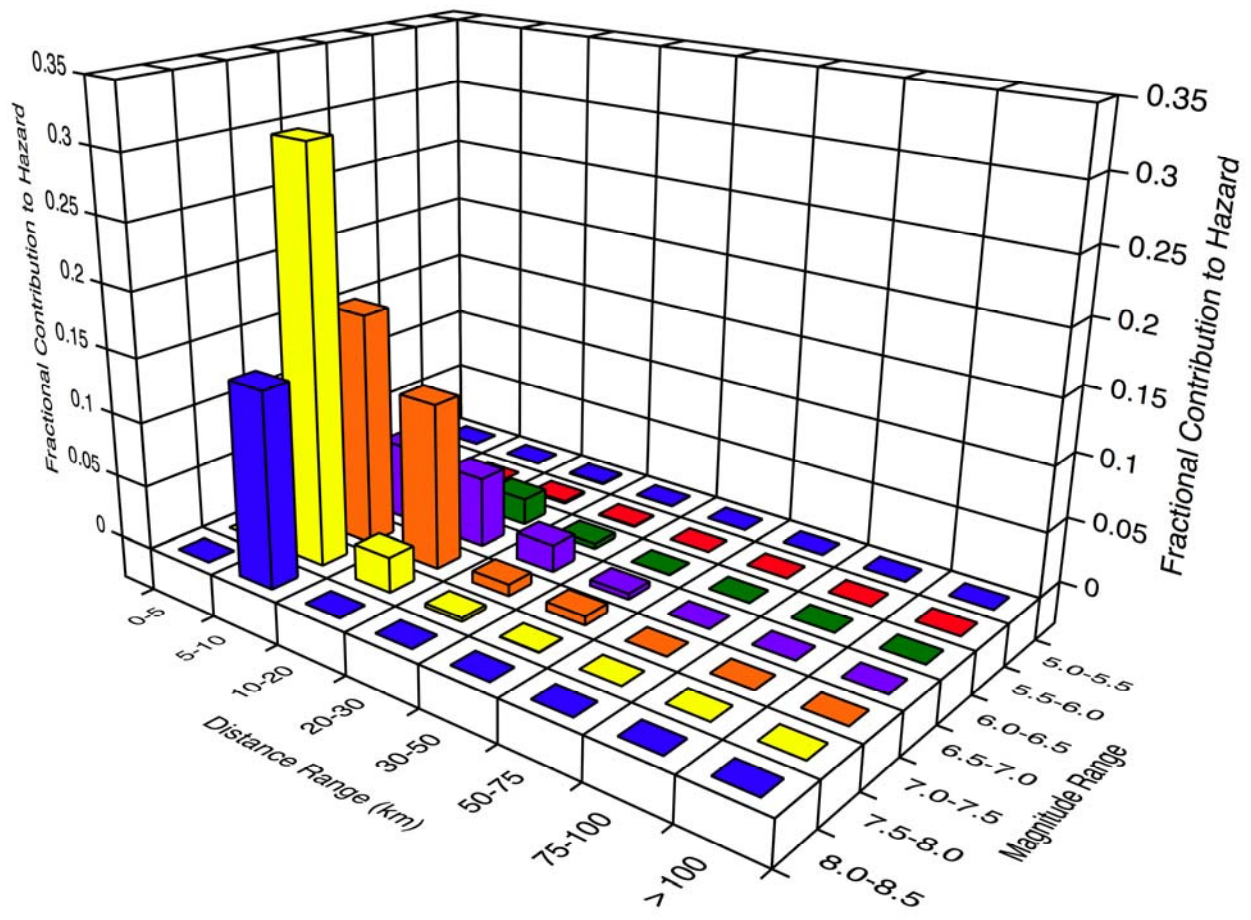


Figure 4-6a. Deaggregation for 1000-Yr return period: PGA

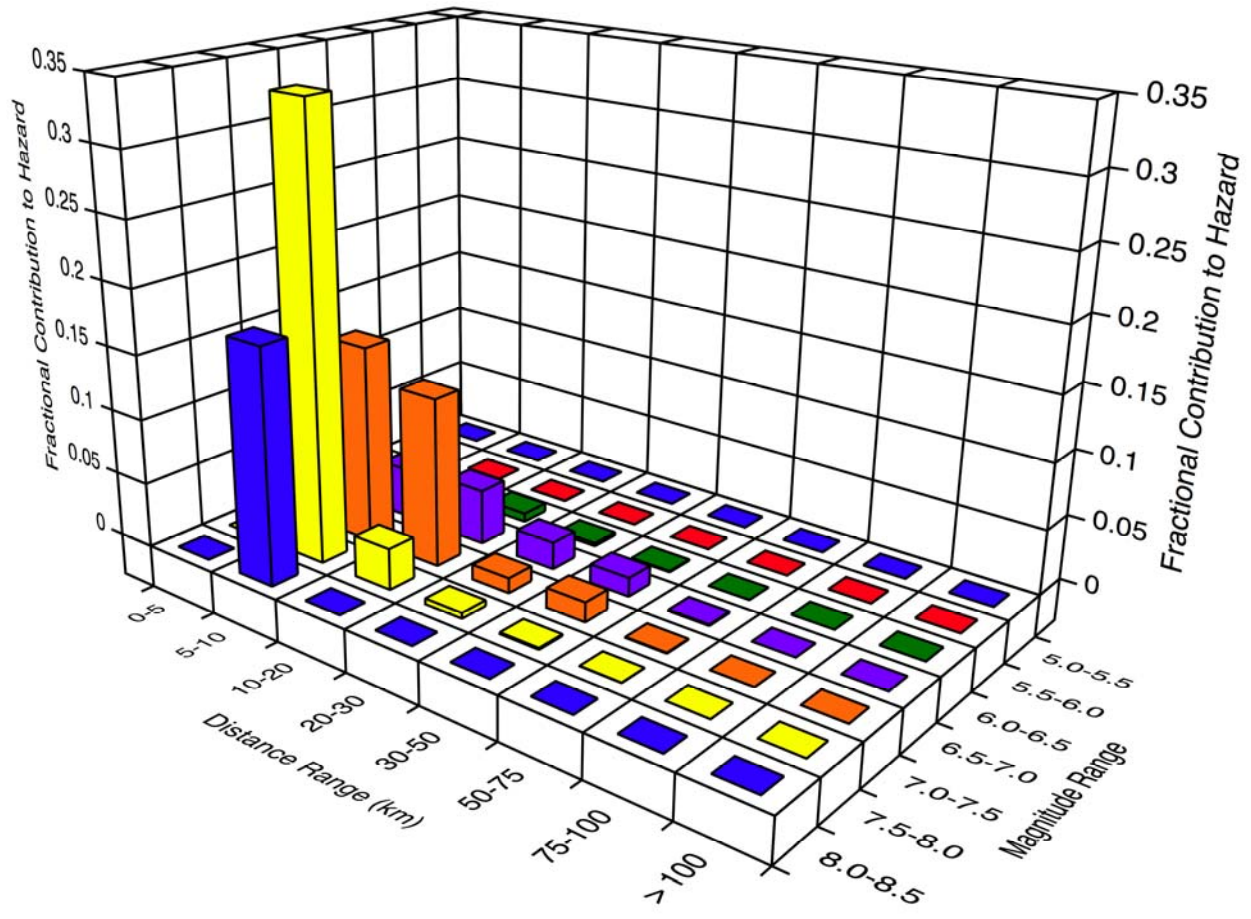


Figure 4-6b. Deaggregation for 1000-Yr Return Period: T=1 sec

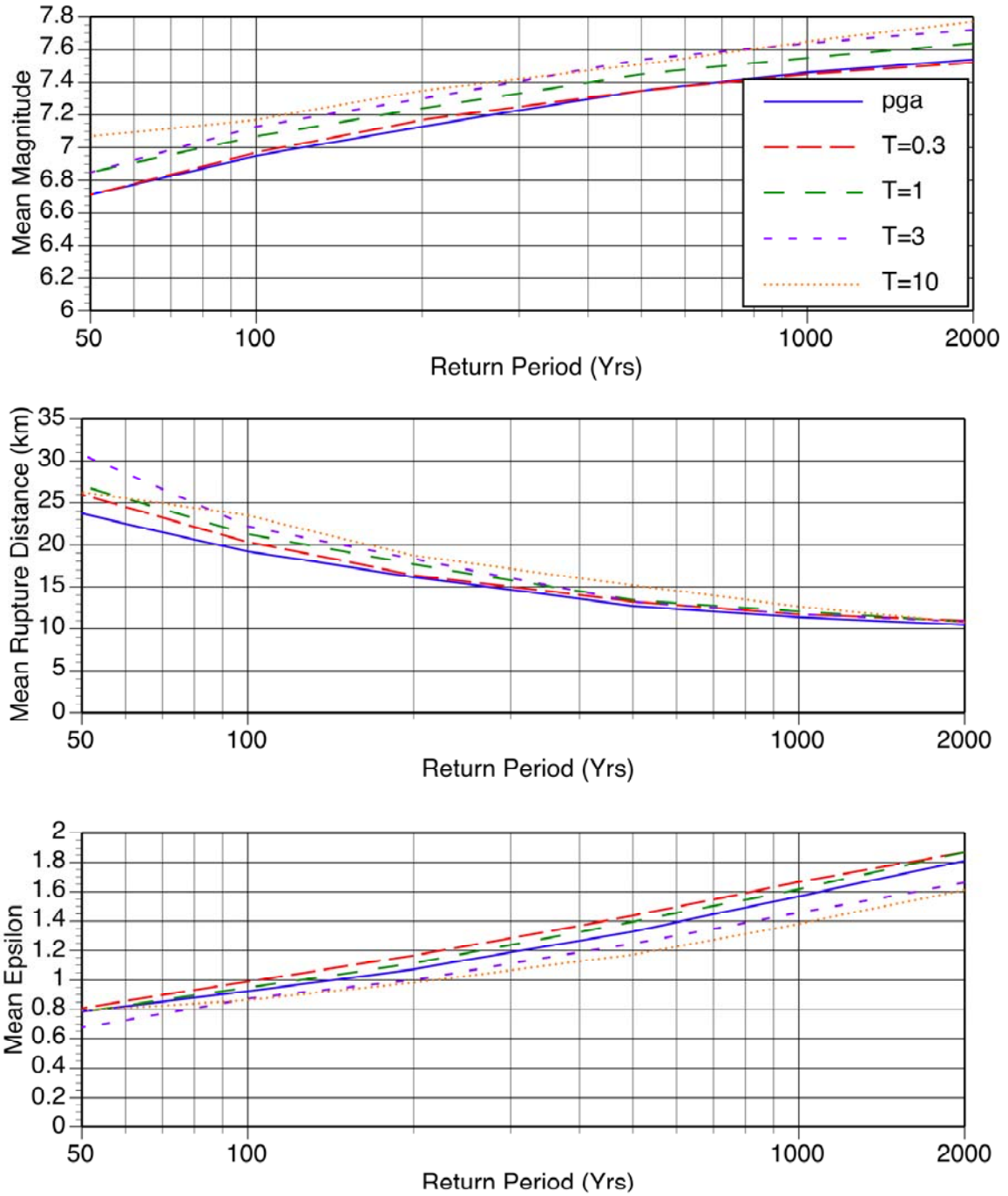


Figure 4-7. Mean magnitude, distance, and epsilon for the average horizontal component.

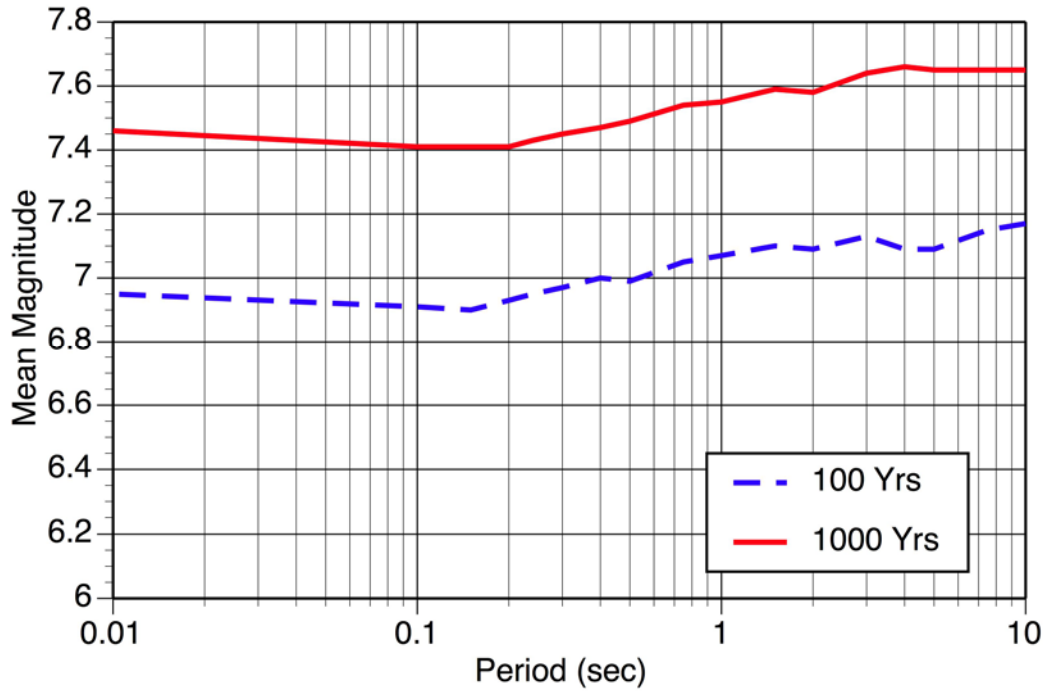


Figure 4-8. Mean magnitude for the average horizontal component.

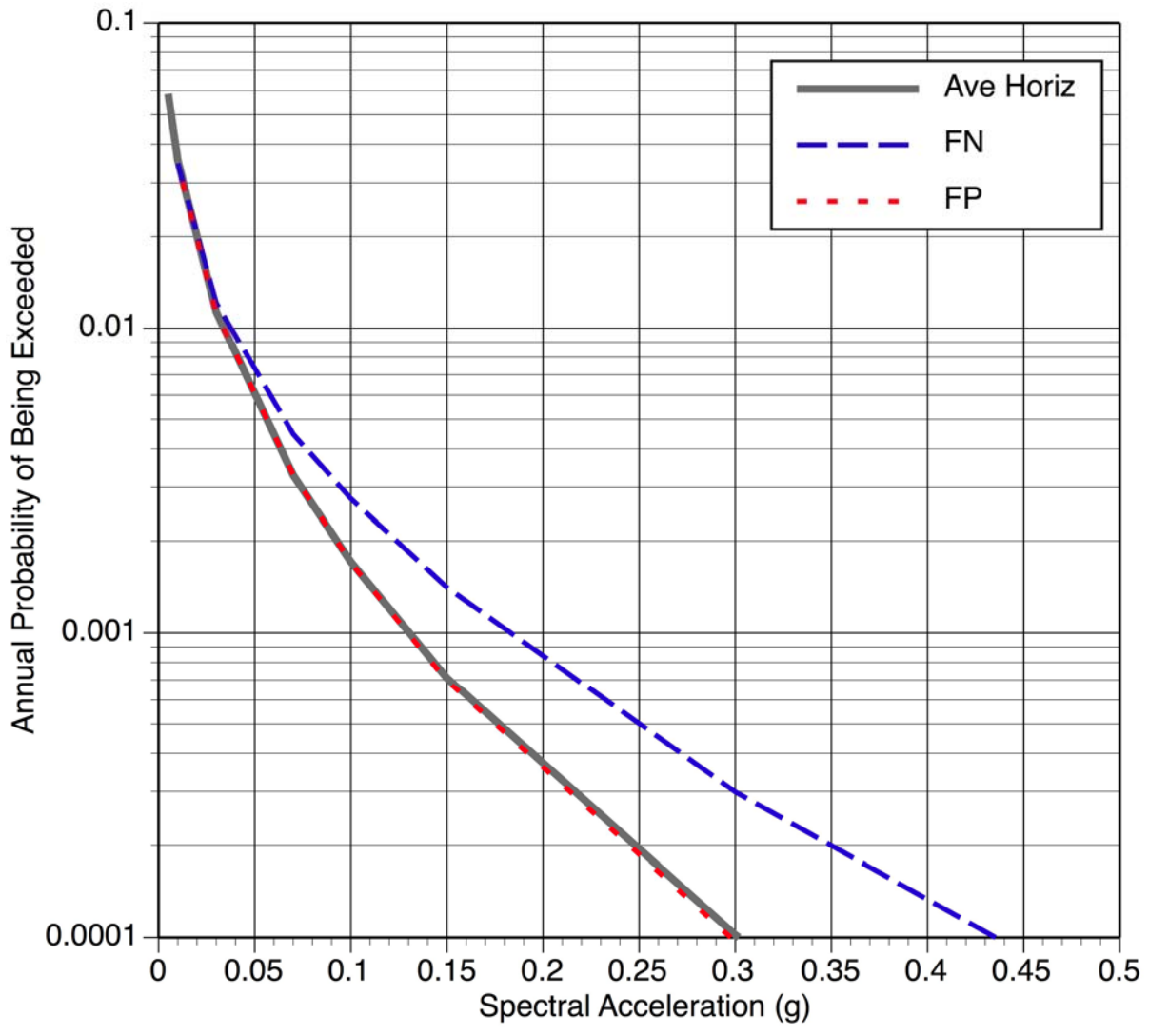


Figure 4-9. T=3 second hazard including directivity effects

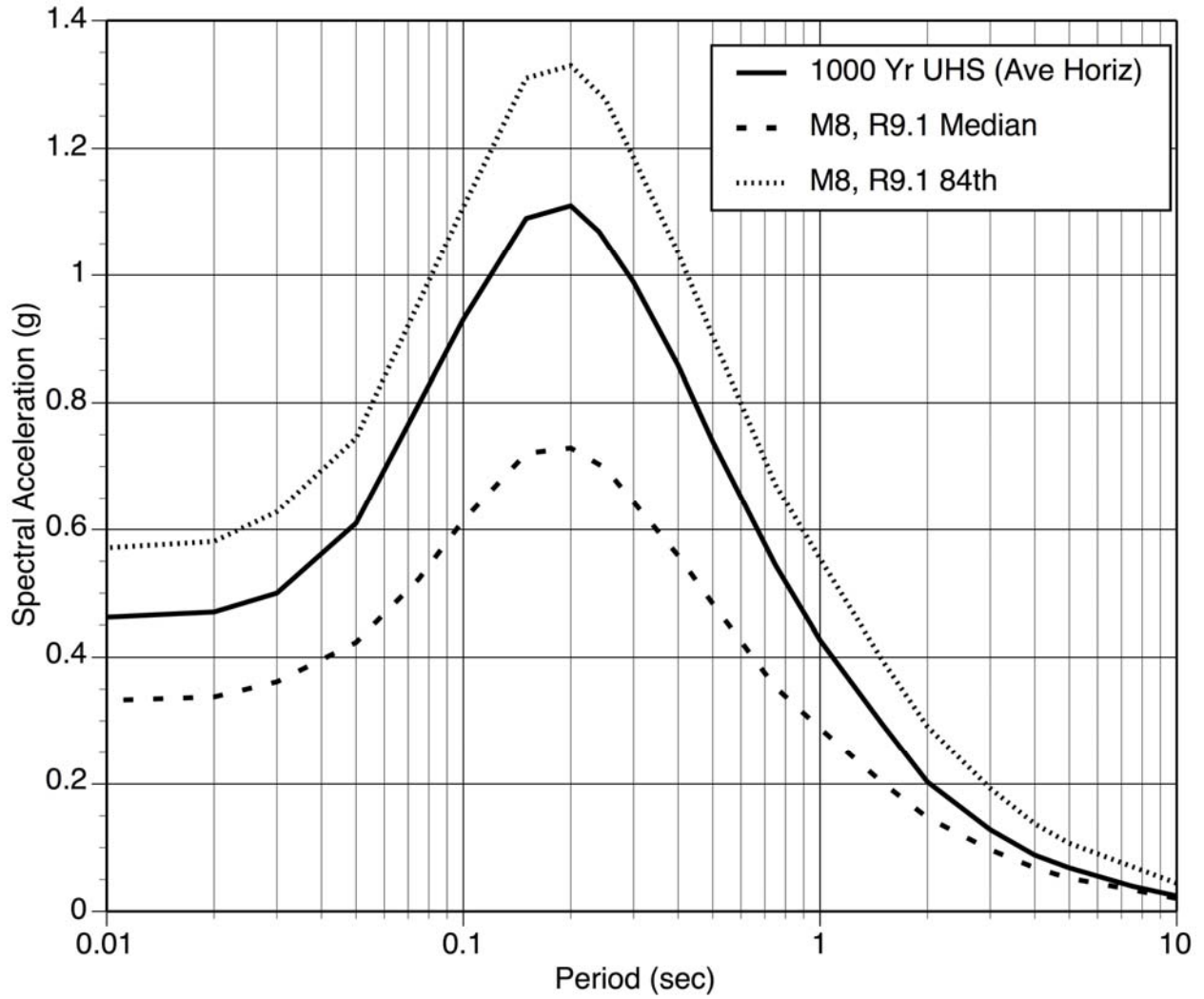


Figure 4-10. Comparison of the deterministic ground motion and the probabilistic ground motion used to define the SEE (5% damping).

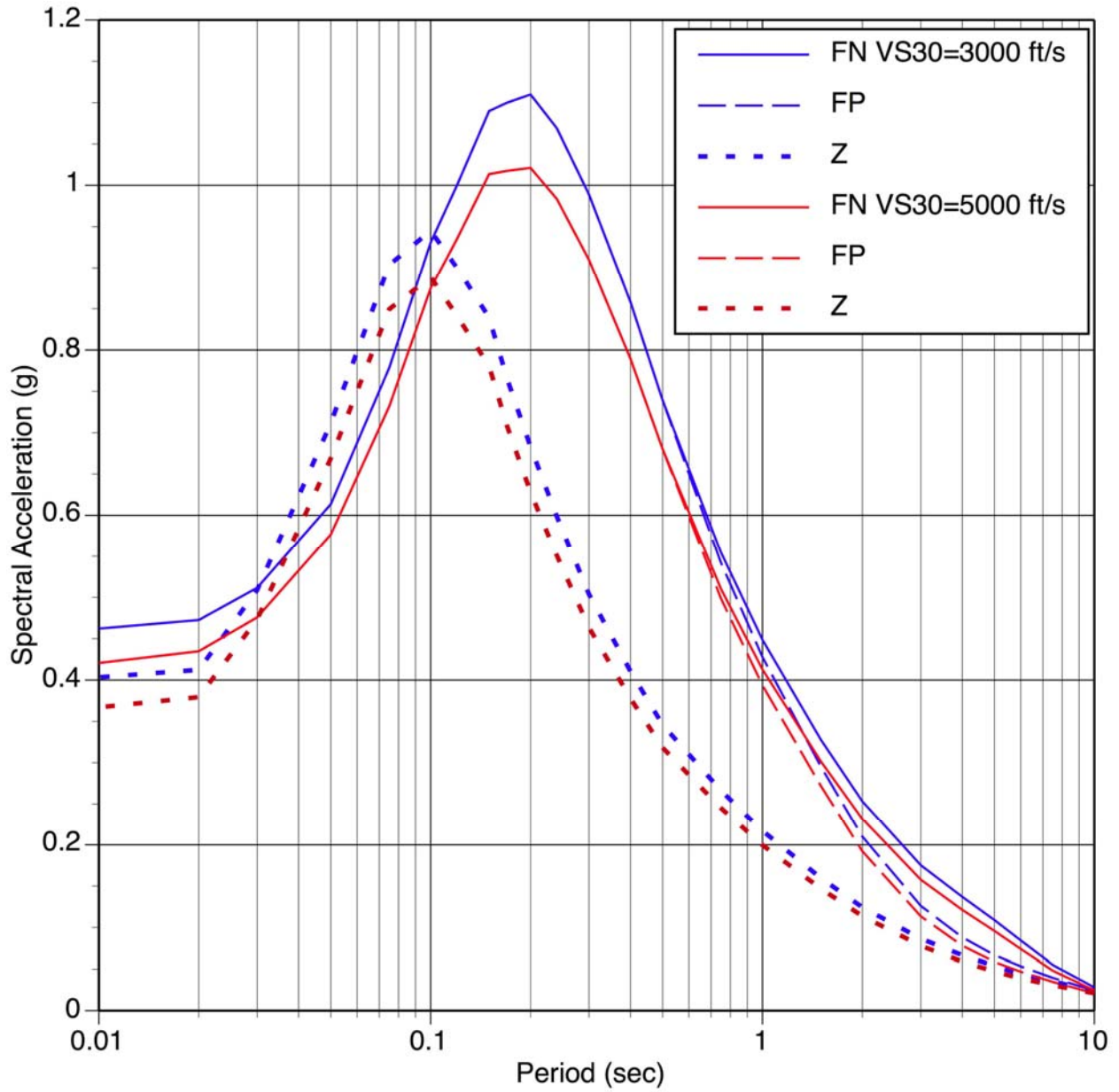


Figure 4-11. SEE spectra (5% damping) for two rock sites conditions:  $V_{S30}=3000$  ft/sec (blue) and  $V_{S30}=5000$  ft/sec (red).

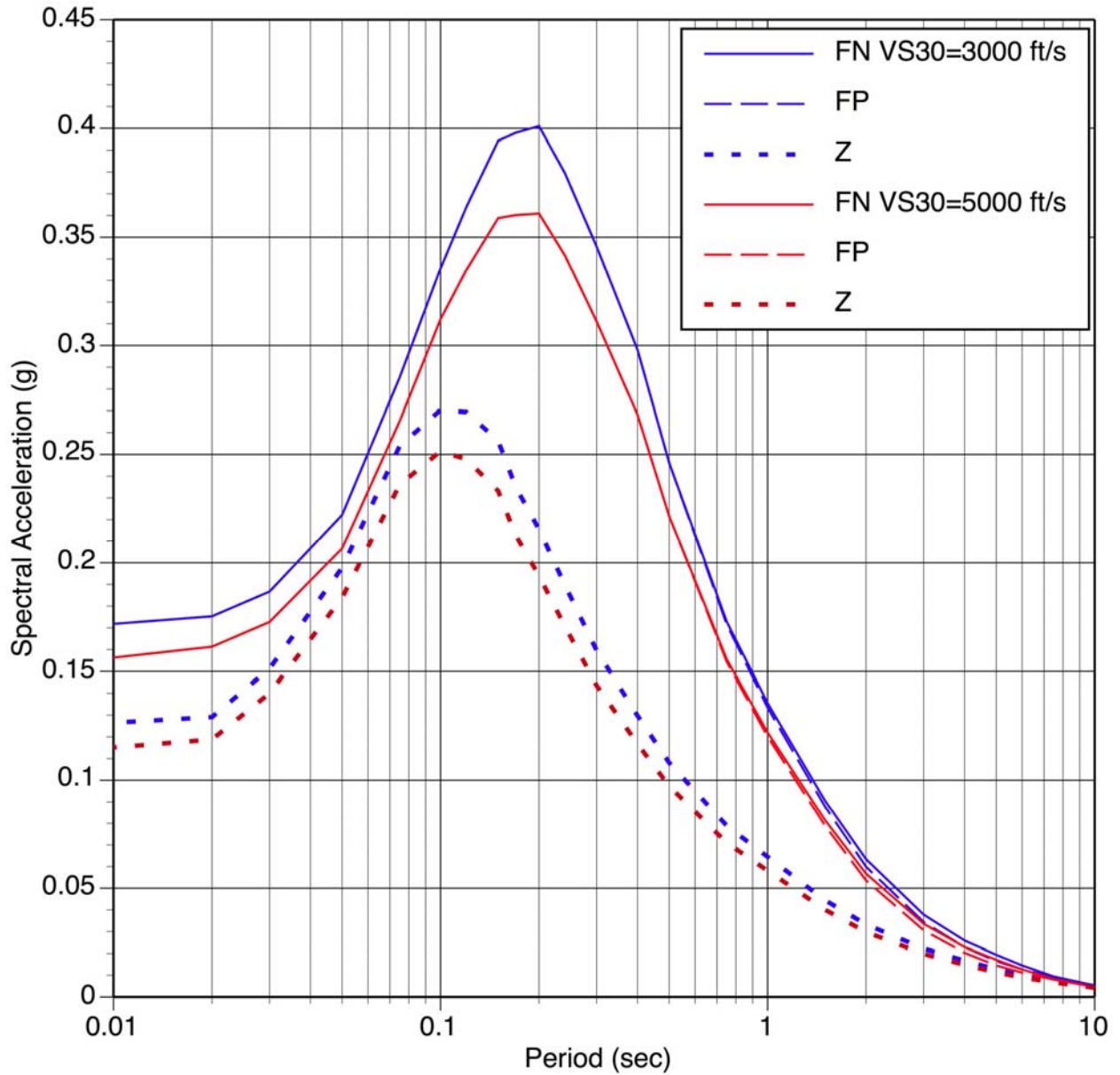


Figure 4-12. FEE spectra (5% damping) for two rock sites conditions:  $V_{S30}=3000$  ft/sec (blue) and  $V_{S30}=5000$  ft/sec (red).

## **5 TIME HISTORIES**

### **5.1 APPROACH**

The reference time histories are selected from a suite of candidate recorded ground motions with magnitudes and distances similar to the design earthquake. The style-of-faulting is not considered in the selection since past experience has shown that style-of-faulting does not have a significant effect on the non-stationary characteristics of the time histories. Both soil and rock sites are considered because the spectral matching step, to be applied in a later study, will adjust for the frequency content differences. The scale factor required to scale the recorded time history to the design spectrum level is not considered in the selection process because recent studies have shown that scale factor is not a useful parameter for selecting appropriate time histories.

Given the set of candidate recordings, three sets are selected based on the similarity of the horizontal spectral shape with the shape of the design spectrum and based on a qualitative review of the acceleration, velocity, and displacement waveforms for all three components.

### **5.2 SEE TIME HISTORIES**

The SEE corresponds to a magnitude 7.5 earthquake at a distance of 10 km. The PEER NGA data set was used to select candidate recordings with magnitudes in the range of 7.3 to 7.9 and with distances in the range of 0 to 20 km. The full set of candidate recordings is listed in Appendix A.

The selected recordings are listed in Table 5-1. This table also indicates which should be used for the FN and FP components. The horizontal spectral shapes of the selected recordings are compared to the SEE spectral shape in Figures 5-1a to 5-1c.

### **5.3 FEE TIME HISTORIES**

The FEE corresponds to a magnitude 7 earthquake at a distance of about 20 km. The PEER NGA data set was used to select candidate recordings with magnitudes in the range of 6.7 to 7.0 and with distances in the range of 10 to 30 km. The full set of candidate recordings is listed in Appendix A.

The selected recordings are listed in Table 5-2. This table also indicates which should be used for the FN and FP components. The horizontal spectral shapes of the selected recordings are compared to the SEE spectral shape in Figure 5-2a to 5-2c.

### **5.4 GUIDELINES FOR PGV VALUES**

The spectral matching described in the main body of the report will result in time histories with spectra similar to the design spectra. As an additional check, guidelines on the PGV are developed and presented in Table 5-3 that can be used to evaluate the spectral matching.

Table 5-1. Selected Reference Time Histories for the SEE

Set	Earthquake	Station	Mag	Rupture Distance (km)	Comp for FN	Comp for FP
1	Manjil	Abbar	7.4	12.6	T	L
2	1999 Koceali	Izmit	7.5	7.2	090	180
3	1999 Chi-Chi	TCU076	7.6	2.8	E	N

Table 5-2. Selected Reference Time Histories for the FEE

Set	Earthquake	Station	Mag	Rupture Distance (km)	Comp for FN	Comp for FP
1	1989 Loma Prieta	Gilroy 6	6.9	18.3	000	090
2	1999 Duzce	1061	7.1	11.5	N	E
3	2000 Hector Mine	Hector Mine	7.1	11.7	090	000

Table 5-3. Peak Ground Velocity Guidelines for Time Histories

	VS30	FN	FP	Z
SEE	3000 ft/s	62 (42-93) cm/s	59 (40-89) cm/s	30 (20-45) cm/s
SEE	5000 ft/s	57 (39-86) cm/s	55 (37-82) cm/s	28 (19-41) cm/s
FEE	3000 ft/s	15 (10-23) cm/s	15 (10-23) cm/s	7.3 (4.9-10.9) cm/s
FEE	5000 ft/s	14 (9-21) cm/s	14 (9-20) cm/s	6.6 (4.4-9.8) cm/s

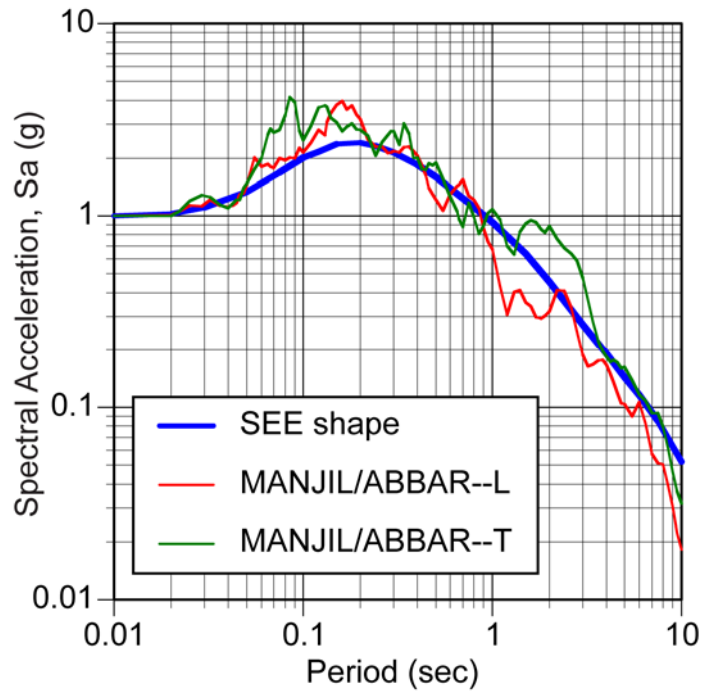


Figure 5-1a. Comparison of the SEE spectral shape and SEE set 1 spectral shape.

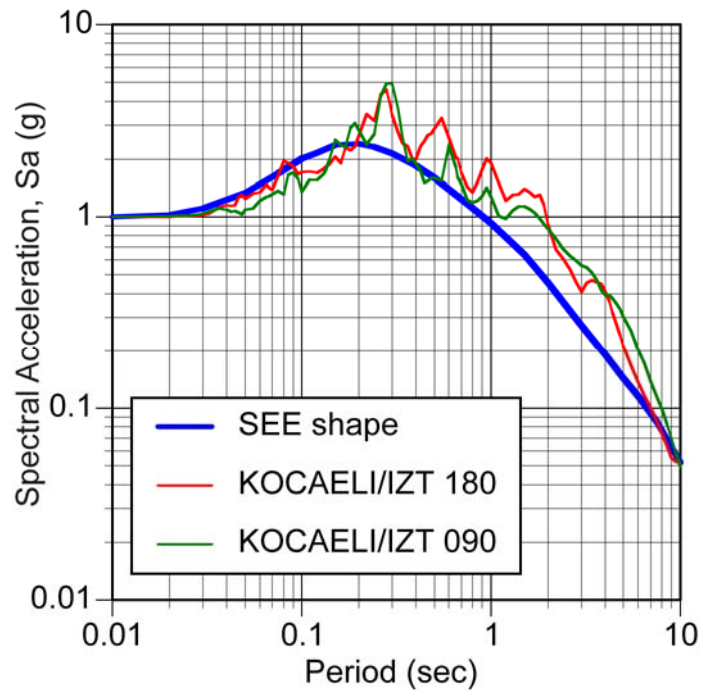


Figure 5-1b. Comparison of the SEE spectral shape and SEE set 2 spectral shape.

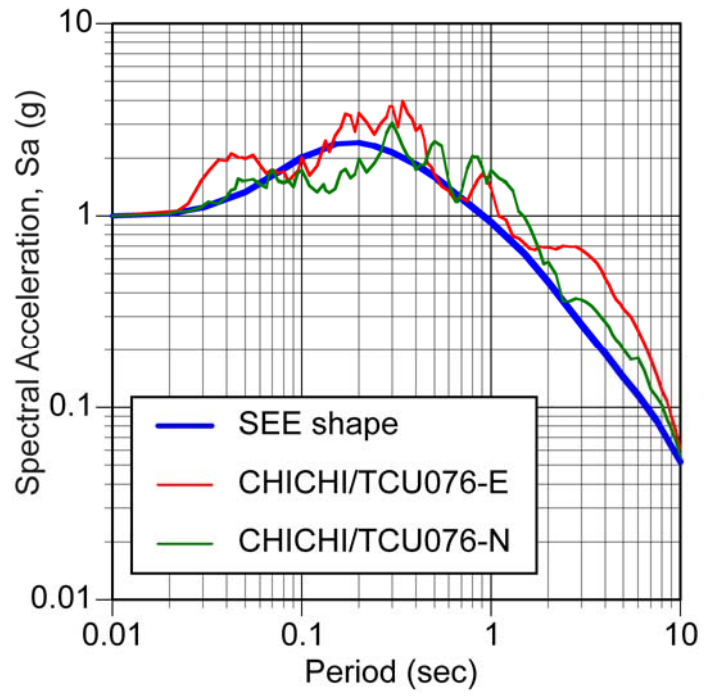


Figure 5-1c. Comparison of the SEE spectral shape and SEE set 3 spectral shape.

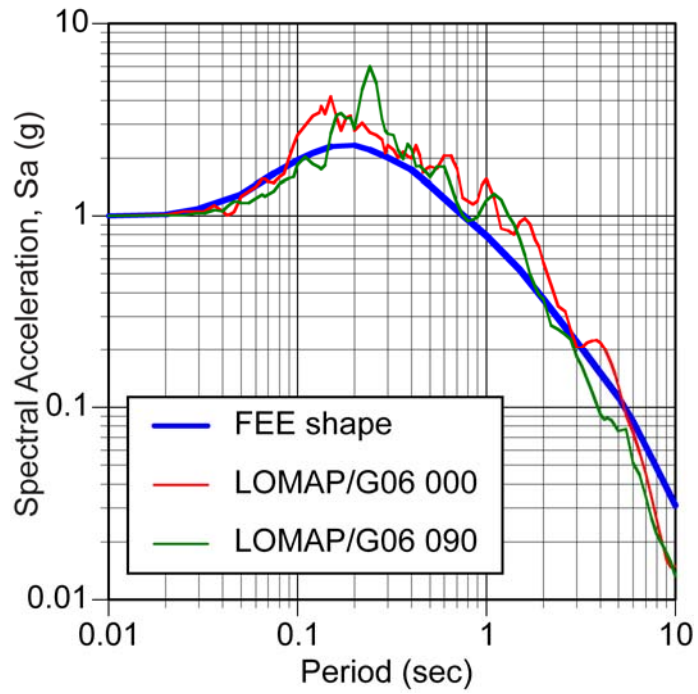


Figure 5-2a. Comparison of the FEE spectral shape and FEE set 1 spectral shape.

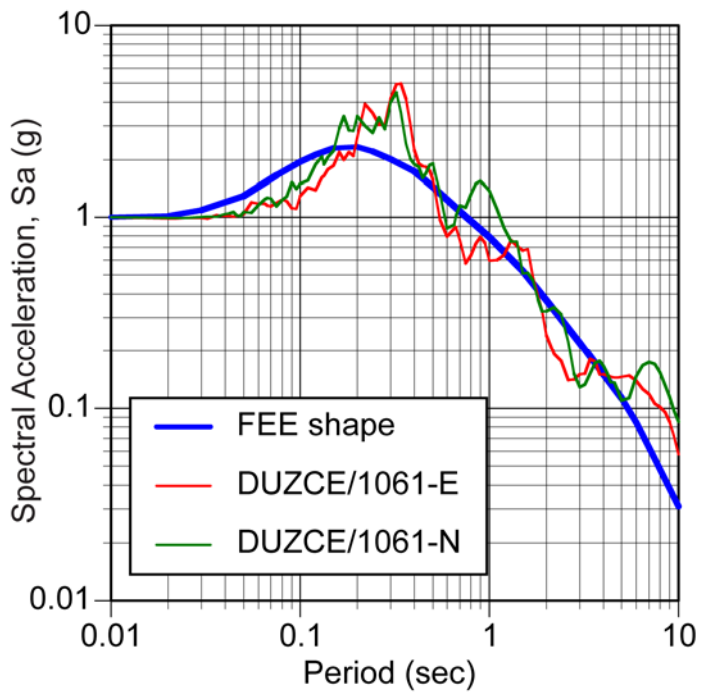


Figure 5-2b. Comparison of the FEE spectral shape and FEE set 2 spectral shape.

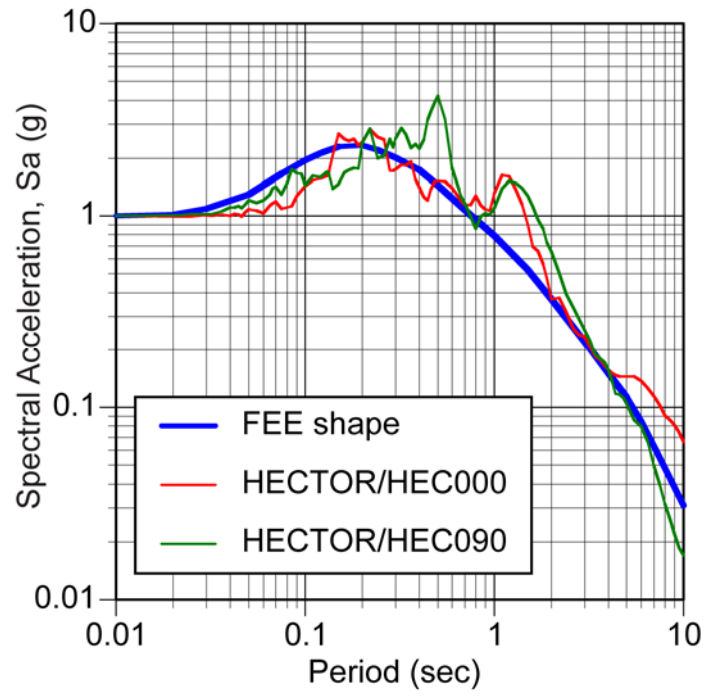


Figure 5-2c. Comparison of the FEE spectral shape and FEE set 3 spectral shape.

## 6 REFERENCES

- Abrahamson, N. A. and W. J. Silva (2008). Summary of the Abrahamson & Silva NGA Ground-Motion Relations, *Earthquake Spectra*, Vol. 24, No. 1, 67 – 98.
- Abrahamson, N. A. (2000). Effects of rupture directivity on probabilistic seismic hazard analysis, Proc. Sixth International Conference on Seismic Zonation, Palm Springs, CA. November 12-15, 2000.
- Abrahamson, N. A. and W. Silva (1997). Empirical Response Spectral Attenuation Relations for Shallow Crustal Earthquakes, *Seis. Res. Letters*, Vol. 68, No. 1, 94-127.
- Baker, J.W., and C.A. Cornell (2006). Correlation of response spectral values for multicomponent ground motions, *Bull. Seism. Soc. Am.*, Vol. 96, No. 1, 215-227.
- Boore, D. M. and G. M. Atkinson (2008). Ground-Motion Prediction Equations for the Average Horizontal Component of PGA, PGV, PGD and 5%-Damped PSA at Spectral Periods between 0.01 s and 10.0 s, *Earthquake Spectra*, Vol. 24, No. 1, 67 – 138.
- Boore, D. M., W. B. Joyner, and T. E. Fumal (1997). Equations for Estimating Horizontal Response Spectra and Peak Acceleration from Western North American Earthquakes: A Summary of Recent Work, *Seis. Res. Letters*, Vol. 68, No. 1, 128-153.
- Bazzurro, P. and C.A. Cornell (1999). Disaggregation of Seismic Hazard: *Bull. Seism. Soc. Am.*, Vol. 89, No. 2, 501-520.
- Campbell, K. W. and Y. Bozorgnia (2008). NGA Ground Motion Model for the Geometric Mean Horizontal Component of PGA, PGV, PGD and 5% Damped Linear Elastic Response Spectra for Periods Ranging from 0.01 to 10 s, *Earthquake Spectra*, Vol. 24, No. 1, 139 – 172.
- Campbell, K. W. (1997). Empirical near-source attenuation relationships for horizontal and vertical components of peak ground acceleration, peak ground velocity, and pseudo-absolute acceleration response spectra, *Seism. Res. Let.*, vol. 68, 154-179.
- Chiou, B. S-J and R. R. Youngs (2008). An NGA Model for the Average Horizontal Component of Peak Ground Motion and Response Spectra, *Earthquake Spectra*, Vol. 24, No. 1, 173 – 216.
- Idriss, I. M. (2008). An NGA Empirical Model for Estimating the Horizontal Spectral Values Generated By Shallow Crustal Earthquakes, *Earthquake Spectra*, Vol. 24, No. 1, 217 – 242.
- Idriss, I.M. (1991). Procedures for Selecting Earthquake Ground Motions at Rock Sites, Report to National Institute of Standards and Technology, Univ. of California at Davis, Dept. of Civil and Environmental Engineering, Center for Geotechnical Modeling, revised March 1993.
- Idriss, I.M. (1994a). Subject: standard error terms, FAX to Phalkun Tan at Woodward-Clyde Consultants, dated April 17, 1994.
- Idriss, I.M. (1994b). Subject: Attenuation relationship for peak horizontal accelerations at rock sites, FAX to Abrahamson and others, dated Sept. 1, 1994.

Peterson, M., W. Bryant, C. Cramer, T. Cao, M. Reichle, A. Frankel, J. Lienkaemper, P. McCrory, and D. Schwartz (1996). Probabilistic seismic hazard assessment for the State of California, California Department of Conservation, Div. Mines and Geology, OFR 96-08, USGS OFR 96-706.

Sadigh, K., C-Y Chang, J. A. Egan, F. Makdisi, and R. R. Youngs (1997). Attenuation relationships for shallow crustal earthquakes based on California strong motion data, *Seism. Res. Let.*, Vol 68, 180-189.

Somerville, P. G., N. F. Smith, R. W. Graves. And N. A. Abrahamson (1997). Modification of empirical strong ground motion attenuation relations to include the amplitude and duration effects of rupture directivity, *Seism. Res. Let.*, Vol. 68, 199-222.

Wells, D. and K. Coppersmith (1994). Updated empirical relationships among magnitude, rupture length, rupture area, and surface displacement, *Bull Seism. Soc. Am.*, Vol. 84, 974-1002.

Working Group on California Earthquake Probabilities (2003). Earthquake Probabilities in the San Francisco Bay Region: 2002-2031, U.S. Geological Society Open File Report 03-214.

Youngs, R. R. and K. Coppersmith (1985). Implications for fault slip rates and earthquake recurrence models to probabilistic seismic hazard estimates, *Bull. Seism. Soc. Am.*, Vol. 75, 939-964.

## APPENDIX A: Candidate Time Histories

Table A-1. Candidate Time Histories Considered for the SEE

YEAR	Earthquake Name	Earthquake Magnitude	Station Name	Rupture Distance (km)
1978	Tabas, Iran	7.35	Dayhook	13.94
1978	Tabas, Iran	7.35	Tabas	2.05
1992	Landers	7.28	Coolwater	19.74
1992	Landers	7.28	Joshua Tree	11.03
1992	Landers	7.28	Lucerne	2.19
1992	Landers	7.28	Morongo Valley	17.32
1999	Kocaeli, Turkey	7.51	Arcelik	13.49
1999	Kocaeli, Turkey	7.51	Duzce	15.37
1999	Kocaeli, Turkey	7.51	Gebze	10.92
1999	Kocaeli, Turkey	7.51	Izmit	7.21
1999	Kocaeli, Turkey	7.51	Yarimca	4.83
1999	Chi-Chi, Taiwan	7.62	ALS	10.80
1999	Chi-Chi, Taiwan	7.62	CHY006	9.77
1999	Chi-Chi, Taiwan	7.62	CHY010	19.96
1999	Chi-Chi, Taiwan	7.62	CHY024	9.64
1999	Chi-Chi, Taiwan	7.62	CHY025	19.09
1999	Chi-Chi, Taiwan	7.62	CHY028	3.14
1999	Chi-Chi, Taiwan	7.62	CHY029	10.97
1999	Chi-Chi, Taiwan	7.62	CHY034	14.82
1999	Chi-Chi, Taiwan	7.62	CHY035	12.65
1999	Chi-Chi, Taiwan	7.62	CHY036	16.06
1999	Chi-Chi, Taiwan	7.62	CHY041	19.83
1999	Chi-Chi, Taiwan	7.62	CHY074	10.80
1999	Chi-Chi, Taiwan	7.62	CHY080	2.69

1999	Chi-Chi, Taiwan	7.62	CHY101	9.96
1999	Chi-Chi, Taiwan	7.62	CHY104	18.04
1999	Chi-Chi, Taiwan	7.62	NSY	13.15
1999	Chi-Chi, Taiwan	7.62	TCU	5.18
1999	Chi-Chi, Taiwan	7.62	TCU036	19.84
1999	Chi-Chi, Taiwan	7.62	TCU039	19.90
1999	Chi-Chi, Taiwan	7.62	TCU046	16.74
1999	Chi-Chi, Taiwan	7.62	TCU048	13.55
1999	Chi-Chi, Taiwan	7.62	TCU049	3.78
1999	Chi-Chi, Taiwan	7.62	TCU050	9.51
1999	Chi-Chi, Taiwan	7.62	TCU051	7.66
1999	Chi-Chi, Taiwan	7.62	TCU052	0.66
1999	Chi-Chi, Taiwan	7.62	TCU053	5.97
1999	Chi-Chi, Taiwan	7.62	TCU054	5.30
1999	Chi-Chi, Taiwan	7.62	TCU055	6.36
1999	Chi-Chi, Taiwan	7.62	TCU056	10.50
1999	Chi-Chi, Taiwan	7.62	TCU057	11.84
1999	Chi-Chi, Taiwan	7.62	TCU059	17.13
1999	Chi-Chi, Taiwan	7.62	TCU060	8.53
1999	Chi-Chi, Taiwan	7.62	TCU061	17.19
1999	Chi-Chi, Taiwan	7.62	TCU063	9.80
1999	Chi-Chi, Taiwan	7.62	TCU064	16.62

Table A-1 (cont). Candidate Time Histories Considered for the SEE

YEAR	Earthquake Name	Earthquake Magnitude	Station Name	Rupture Distance (km)
1999	Chi-Chi, Taiwan	7.62	TCU065	0.59
1999	Chi-Chi, Taiwan	7.62	TCU067	0.64
1999	Chi-Chi, Taiwan	7.62	TCU068	0.32
1999	Chi-Chi, Taiwan	7.62	TCU070	19.02
1999	Chi-Chi, Taiwan	7.62	TCU071	5.31
1999	Chi-Chi, Taiwan	7.62	TCU072	7.03
1999	Chi-Chi, Taiwan	7.62	TCU074	13.46
1999	Chi-Chi, Taiwan	7.62	TCU075	0.91
1999	Chi-Chi, Taiwan	7.62	TCU076	2.76
1999	Chi-Chi, Taiwan	7.62	TCU078	8.20
1999	Chi-Chi, Taiwan	7.62	TCU079	10.97
1999	Chi-Chi, Taiwan	7.62	TCU082	5.18
1999	Chi-Chi, Taiwan	7.62	TCU084	11.24
1999	Chi-Chi, Taiwan	7.62	TCU087	7.00
1999	Chi-Chi, Taiwan	7.62	TCU088	18.16
1999	Chi-Chi, Taiwan	7.62	TCU089	8.88
1999	Chi-Chi, Taiwan	7.62	TCU100	11.39
1999	Chi-Chi, Taiwan	7.62	TCU101	2.13
1999	Chi-Chi, Taiwan	7.62	TCU102	1.51
1999	Chi-Chi, Taiwan	7.62	TCU103	6.10
1999	Chi-Chi, Taiwan	7.62	TCU104	12.89
1999	Chi-Chi, Taiwan	7.62	TCU105	17.18
1999	Chi-Chi, Taiwan	7.62	TCU106	14.99
1999	Chi-Chi, Taiwan	7.62	TCU107	16.01

1999	Chi-Chi, Taiwan	7.62	TCU109	13.08
1999	Chi-Chi, Taiwan	7.62	TCU110	11.60
1999	Chi-Chi, Taiwan	7.62	TCU116	12.40
1999	Chi-Chi, Taiwan	7.62	TCU120	7.41
1999	Chi-Chi, Taiwan	7.62	TCU122	9.35
1999	Chi-Chi, Taiwan	7.62	TCU123	14.93
1999	Chi-Chi, Taiwan	7.62	TCU128	13.15
1999	Chi-Chi, Taiwan	7.62	TCU129	1.84
1999	Chi-Chi, Taiwan	7.62	TCU136	8.29
1999	Chi-Chi, Taiwan	7.62	TCU138	9.79
1999	Chi-Chi, Taiwan	7.62	WGK	9.96
1999	Chi-Chi, Taiwan	7.62	WNT	1.84
1990	Manjil, Iran	7.37	Abbar	12.56
2002	Denali, Alaska	7.90	Pump Station #10	2.74

Table A-2. Candidate Time Histories Considered for the FEE

YEAR	Earthquake Name	Earthquake Magnitude	Station Name	Rupture Distance (km)
1980	Irpinia, Italy-01	6.90	Sturno	10.84
1980	Irpinia, Italy-01	6.90	Calitri	17.64
1980	Irpinia, Italy-01	6.90	Bisaccia	21.26
1980	Irpinia, Italy-01	6.90	Brienza	22.56
1980	Irpinia, Italy-01	6.90	Mercato San Severino	29.80
1989	Loma Prieta	6.93	BRAN	10.72
1989	Loma Prieta	6.93	Gilroy - Historic Bldg.	10.97
1989	Loma Prieta	6.93	Gilroy Array #2	11.07
1989	Loma Prieta	6.93	Gilroy Array #3	12.82
1989	Loma Prieta	6.93	Gilroy Array #4	14.34
1989	Loma Prieta	6.93	San Jose - Santa Teresa Hills	14.69
1989	Loma Prieta	6.93	Capitola	15.23
1989	Loma Prieta	6.93	WAHO	17.47
1989	Loma Prieta	6.93	Gilroy Array #6	18.33
1989	Loma Prieta	6.93	UCSC Lick Observatory	18.41
1989	Loma Prieta	6.93	UCSC	18.51
1989	Loma Prieta	6.93	Anderson Dam (Downstream)	20.26
1989	Loma Prieta	6.93	Anderson Dam (L Abut)	20.26
1989	Loma Prieta	6.93	Coyote Lake Dam (SW Abut)	20.34
1989	Loma Prieta	6.93	Coyote Lake Dam (Downst)	20.80
1989	Loma Prieta	6.93	Gilroy Array #7	22.68
1989	Loma Prieta	6.93	Sunnyvale - Colton Ave.	24.23
1989	Loma Prieta	6.93	Agnews State Hospital	24.57
1989	Loma Prieta	6.93	Hollister Diff. Array	24.82
1989	Loma Prieta	6.93	Hollister City Hall	27.60
1989	Loma Prieta	6.93	Hollister - South & Pine	27.93
1992	Cape Mendocino	7.01	Rio Dell Overpass - FF	14.33
1992	Cape Mendocino	7.01	Fortuna - Fortuna Blvd	19.95
1992	Cape Mendocino	7.01	Shelter Cove Airport	28.78
1994	Northridge-01	6.69	Sun Valley - Roscoe Blvd	10.05

1994	Northridge-01	6.69	Northridge - 17645 Saticoy St	12.09
1994	Northridge-01	6.69	Canyon Country - W Lost Cany	12.44
1994	Northridge-01	6.69	N Hollywood - Coldwater Can	12.51
1994	Northridge-01	6.69	Sunland - Mt Gleason Ave	13.35
1994	Northridge-01	6.69	Simi Valley - Katherine Rd	13.42
1994	Northridge-01	6.69	Canoga Park - Topanga Can	14.70
1994	Northridge-01	6.69	Tarzana - Cedar Hill A	15.60
1994	Northridge-01	6.69	Santa Susana Ground	16.74
1994	Northridge-01	6.69	Burbank - Howard Rd.	16.88
1994	Northridge-01	6.69	Beverly Hills - 14145 Mulhol	17.15
1994	Northridge-01	6.69	Beverly Hills - 12520 Mulhol	18.36

1994	Northridge-01	6.69	La Crescenta - New York	18.50
1994	Northridge-01	6.69	LA 00	19.07
1994	Northridge-01	6.69	Stone Canyon	19.07
1994	Northridge-01	6.69	Big Tujunga, Angeles Nat F	19.74
1994	Northridge-01	6.69	LA - Wonderland Ave	20.30
1994	Northridge-01	6.69	LA - Chalon Rd	20.45
1994	Northridge-01	6.69	Castaic - Old Ridge Route	20.72
1994	Northridge-01	6.69	LA - N Faring Rd	20.81
1994	Northridge-01	6.69	Lake Hughes #12A	21.36
1994	Northridge-01	6.69	Glendale - Las Palmas	22.21
1994	Northridge-01	6.69	Topanga - Fire Sta	22.28
1994	Northridge-01	6.69	LA - UCLA Grounds	22.49
1994	Northridge-01	6.69	LA - Brentwood VA Hospital	22.50
1994	Northridge-01	6.69	Hollywood - Willoughby Ave	23.07

1994	Northridge-01	6.69	LA - Century City CC North	23.41
1994	Northridge-01	6.69	LA - Wadsworth VA Hospital North	23.60
1994	Northridge-01	6.69	LA - Wadsworth VA Hospital South	23.60
1994	Northridge-01	6.69	Vasquez Rocks Park	23.64
1994	Northridge-01	6.69	LA - Griffith Park Observatory	23.77
1994	Northridge-01	6.69	LA - Hollywood Stor FF	24.03
1994	Northridge-01	6.69	Pacific Palisades - Sunset	24.08
1994	Northridge-01	6.69	Moorpark - Fire Sta	24.76
1994	Northridge-01	6.69	Lake Hughes #9	25.36
1994	Northridge-01	6.69	Monte Nido Fire Station	25.59
1994	Northridge-01	6.69	Santa Monica City Hall	26.45
1994	Northridge-01	6.69	LA - N Westmoreland	26.73
1994	Northridge-01	6.69	LA - Saturn St	27.01
1994	Northridge-01	6.69	LA - Fletcher Dr	27.26
1994	Northridge-01	6.69	LA - Centinela St	28.30
1994	Northridge-01	6.69	LA - W 15th St	29.74
1994	Northridge-01	6.69	LA - Baldwin Hills	29.88
1995	Kobe, Japan	6.90	Amagasaki	11.34
1995	Kobe, Japan	6.90	Fukushima	17.85
1995	Kobe, Japan	6.90	Shin-Osaka	19.15
1995	Kobe, Japan	6.90	OSAJ	21.35
1995	Kobe, Japan	6.90	Kakogawa	22.50
1995	Kobe, Japan	6.90	Morigawachi	24.78
1995	Kobe, Japan	6.90	Abeno	24.85
1995	Kobe, Japan	6.90	Yae	27.77
1995	Kobe, Japan	6.90	Sakai	28.08
1999	Duzce, Turkey	7.14	Lamont 1061	11.46
1999	Duzce, Turkey	7.14	Bolu	12.04
1999	Duzce, Turkey	7.14	Lamont 362	23.41
1999	Duzce, Turkey	7.14	Lamont 1060	25.88
1999	Hector Mine	7.13	Hector	11.66